The University of Nottingham

UNITED KINGDOM · CHINA · MALAYSIA

Studying Brown Fat in the Thermoneutral Animal

Peter Aldiss (BSc)

Thesis submitted to the University of Nottingham for

the degree of Doctor of Philosophy

August 2019

Declaration

Work in this thesis was carried out at the Department of Child Health, Obstetrics and Gynaecology, Queens Medical Centre, University of Nottingham between October 2015 and August 2019. Adipose tissue proteomics were carried out by Prof. David Boocock and Dr. Amanda Miles of the Clinical Proteomics Group, Nottingham Trent University. As such, this thesis is and accurate representation of my own work conducted under the supervision of Professors Michael Symonds and Helen Budge at the University of Nottingham.

Peter Aldiss

August 2019

Acknowledgements

First, I'd like to thank the British Heart Foundation for supporting my research and allowing me to complete a PhD and Professor Michael Symonds for the opportunity to write the grant in the first place. I'd also like to thank Professor Symonds for his support and advice throughout and for happily talking about anything other than work, mainly football, when needed and to Professor Budge for her support and meticulous eye when finalising papers. Thank you to Dr. David Boocock at Nottingham Trent University for all his (ongoing) help with completing the adipose tissue proteomics. Thanks to Fran for use of metabolic cages and valuable input for papers.

I would like to thank everyone at Nottingham who made my time there more than bearable. Thank you to my friends Ian, Lara, Caz, Mark and Anaid in particular for keeping me sane and providing endless laughs. Thanks to Graeme who has always been there for advice. Thanks to Kat for invaluable support and friendship. And last but not least a huge thanks to Jo, from support with metabolic cages to writing papers and job applications and for all the good times at conferences.

Finally, thanks to all my other friends and family for their love and support throughout. Thanks to Teddy and Wills for being a daily reminder that there are more important things in life and, that often, work can wait. I dedicate this thesis to them, and to their sister Eliza. I hope I've made them proud.

Abstract

In recent years it has become clear that the modelling of human disease in pre-clinical research is confounded by the temperature at which animals are routinely raised and housed. Typically housed at ~20-22°C, a temperature well below their thermoneutral zone (~28-33°C), these animals are hyper metabolic and hyperphagic whilst the mechanisms driving various pathologies (i.e. non-alcoholic fatty liver disease) differ at standard housing compared to thermoneutrality. This sub-thermoneutral housing temperature is of particular importance where adaptive thermogenesis is concerned. Brown adipose tissue (BAT), the main organ responsible for adaptive thermogenesis, utilises glucose and lipid to produce heat via the uncoupling protein (UCP) 1. However, housing animals at sub-thermoneutral temperatures mean BAT is hyperactive unlike humans who typically reside closer to thermoneutrality and it has recently been suggested that housing animals at thermoneutrality is a critical step in closer mimicking human physiology.

At standard housing temperatures BAT plays a key role in regulating nutrient metabolism. However, I hypothesised that when BAT is inactive at thermoneutrality even short exposure to an obesogenic diet would induce a dysfunctional phenotype. Further, I hypothesised that despite interscapular (IBAT) and perivascular adipose tissue (PVAT) being phenotypically similar they would respond differently to nutrient surplus due to their distinct anatomical locations and developmental origins.

First, I show that animals are susceptible to weight gain with just 72h exposure to a high-fat diet (HFD). This is associated with an upregulation of genes governing insulin signalling and white adipose tissue (AT) in IBAT and a pronounced down-regulation

of multiple metabolic pathways in PVAT. Further, utilising adipose tissue proteomics I show that 72h HFD is associated with an enrichment of proteins governing lipid and cholesterol related processes and functions in BAT in addition to perturbed glucagon and PPAR signalling pathways. In PVAT, however, there was an increased abundance of proteins involved in apoptosis and toll-like receptor signalling and an enrichment of DNA-related processes and functions and perturbed RNA degradation and cell adhesion pathways. Importantly, these changes occur prior to changes in individual tissue mass and highlight early adaptations to short-term nutrient excess.

Exercise training has been shown to drive a) the whitening of BAT and b) the induction of thermogenic genes ('browning') in subcutaneous white AT (WAT). In my second study I show that exercise training increases BAT mass of obese animals and, by examining the adipose tissue proteome show that this is associated with an upregulation of multiple proteins involved in skeletal muscle physiology. These alterations in BAT occur alongside an upregulation of proteins involved in carbon metabolism, oxidation phosphorylation and ATP synthesis suggesting that whilst there is no impact on UCP1, the metabolic rate of BAT has nevertheless increased. Further, I show that the typical induction of UCP1 mRNA seen in the inguinal subcutaneous AT (IWAT) of exercise-trained animals is absent and in fact, UCP1 is undetectable in animals raised at thermoneutrality. Again, by analysing the AT proteome I show that exercise training downregulated apoptotic proteins in IWAT in addition to large numbers of proteins involved in pre-mRNA synthesis and in RNA metabolism.

In a third study, I show obese animals raised at thermoneutrality gain weight and accumulate both BAT and subcutaneous adipose WAT when subsequently exposed to mild-cold. Importantly, this effect is not seen with chronic administration of a highly-selective β3-agonist (Mirabegron) suggesting the accumulation of subcutaneous fat is being driven by changes in ambient temperature. Further analysis shows there was no induction of thermogenic genes in subcutaneous IWAT. This increase in IWAT was associated with alterations in proteins involved in retinol metabolism (i.e. retinol saturase) and an increase in proteins involved in NAD+ binding. There was no upregulation of key thermogenic genes in either iBAT or PVAT however, in the latter, cold induced key genes governing mitochondrial biogenesis (i.e. PGC1a), glycolysis (i.e. CS, HK2 and PDK), fatty acid oxidation (i.e. PPARA, ACACA and ACACB) and insulin signalling (i.e. INSr and IRS1) suggesting that the metabolic activity of these two, distinct, thermogenic tissues are uncoupled from each other. Analysis of the BAT proteome in cold-exposed animals highlighted an upregulation of proteins involved in redox state and the pentose phosphate pathway and an enrichment of DNA-related processes and functions. Further, the glycosaminoglycan degradation, glycosphingolipid and botch signalling pathways were perturbed in BAT of cold-exposed animals.

Finally, I identified key hub, and interacting proteins in BAT and WAT of exercise trained and cold-exposed animals. These networks could help elucidate novel signalling pathways through which exercise and cold regulate AT function.

Overall, this work shows for the first time how obese adipose tissue responds to common dietary and thermogenic stimuli in the basal state and is an important step in our understanding of rodent AT biology at thermoneutrality.

List of papers

1. **Aldiss, P**., G. Davies, R. Woods, H. Budge, H. S. Sacks and M. E. Symonds (2017). 'Browning' the cardiac and peri-vascular adipose tissues to modulate cardiovascular risk. Interntional Journal of Cardiology 228: 265-274. **(Web of Science 'Highly cited paper' award)**

2. **Aldiss, P**., N. Dellschaft, H.S. Sacks, H. Budge and M. E. Symonds (2017). Beyond obesity – Thermogenic adipocytes and cardiometabolic health. Hormone Molecular Biology and Clinical Investigation, 31(2).

3. **Aldiss, P**., Betts, J., Sale, C., Pope, M., Budge, H. & Symonds, M. E. (2018). Exercise-induced 'browning' of adipose tissues. Metabolism 81, 63-70.

4. Symonds, M. E., **Aldiss, P**., Pope, M and Budge (2018). Recent advances in our understanding of brown/beige adipose tissue – the good fat that keeps you healthy. F1000Research, 7 (F1000 Faculty Rev):1129

5. **Aldiss, P**.; Lewis, J.E.; Boocock, D.J.; Miles, A.K.; Bloor, I.; Ebling, F.J.P.; Budge, H; Symonds, M.E. (2019) Interscapular and Perivascular Brown Adipose Tissue Respond Differently to a Short-Term High-Fat Diet. *Nutrients*, *11*, 1065.

6. **Aldiss, P**.; Lewis, J.E.; Lupini, I.; Boocock, D.J.; Miles, A.K.; Bloor, I.; Ebling, F.J.P.; Budge, H; Symonds, M.E. (2019). Exercise does not induce browning of

white adipose tissue at thermoneutrality and induces an oxidative, myogenic signature in brown adipose tissue. bioRxiv 649061.

7. **Aldiss, P**.; Lewis, J.E.; Lupini, I.; Boocock, D.J.; Miles, A.K.; Bloor, I.; Ebling, F.J.P.; Budge, H; Symonds, M.E. (2019). Standard housing temperature but not Mirabegron drives weight-gain and adipose tissue deposition in rats following dietary induced obesity at thermoneutrality. ***In prep.***

Appendix

1. **Aldiss, P**., H. Budge and M. E. Symonds (2016). Is a reduction in brown adipose thermogenesis responsible for the change in core body temperature at menopause?"Cardiovascular Endocrinology 5(4): 155-156.

2. Symonds, M. E., **Aldiss, P**., Dellschaft, N., Law, J., Fainberg, H., Pope, M., Sacks, H. and Budge, H. (2018). Brown adipose tissue development and function and its impact on reproduction, Journal of Endocrinology, 238(1), R53-R62.

3. Symonds, M. E., Farhat, G., **Aldiss, P**., Pope, M & Budge, H (2018). Brown adipose tissue and glucose homeostasis – the link between climate change and the global rise in obesity and diabetes, Adipocyte, 8:1, 46-50.

Contents

Contents

Chapter 1

Introduction

1.1 Foreword

This chapter will be presented as four separate but complementary, peer-reviewed review papers. In the first review (1.2), an edited version of which was published in 'Hormone Molecular Biology and Clinical Investigation' [1] I discuss the concept that the therapeutic activation of BAT and the 'browning' of WAT may be of more clinical relevance to the amelioration of cardiometabolic disease that obesity per se. I then introduce the concept of 'browning' (or're-browning') the adipose tissues surrounding the heart and vasculature to reduce the cardiovascular risk of obesity. This topic is then discussed at length in the second review (1.3) which was published in the 'International Journal of Cardiology' [2]. It covers the physiological and pathophysiological roles of cardiac and vascular adipose tissues and discusses how they can be targeted by environmental/pharmacological approaches, In addition, it assesses whether the benefits of exercise training are in part down to phenotypic changes seen in these tissues. The mechanisms governing sympathetic activation of BAT and 'browning' of WAT are conserved from mouse to man and are covered in these first two reviews. There is, however, much debate as to whether the 'browning' seen in rodent models of exercise training apply to humans. The third review (1.4) [3] discusses the mechanisms by which 'browning' occurs in response to exercise and what other factors may contribute to this effect in animal models. In addition the potential translation of these results and issues with detecting 'browning' in humans is considered. Finally, the fourth review (1.5) [4] presents an overview of our current understanding of the role of BAT and beige adipocytes in glucose homeostasis.

1.2 Beyond obesity - Thermogenic adipocytes and cardiometabolic health

Peter Aldiss[1] / Neele Dellschaft[1] / Harold Sacks[2] / Helen Budge[1] / Michael E. Symonds[3]

Beyond obesity – thermogenic adipocytes and cardiometabolic health

[1] The Early Life Research Unit, Division of Child Health, Obstetrics and Gynaecology, and School of Medicine, University Hospital, University of Nottingham, Nottingham, NG7 2UH, UK
[2] Endocrinology and Diabetes Division, VA Greater Los Angeles Healthcare System, Department of Medicine, University of California, David Geffen School of Medicine, Los Angeles, CA, USA
[3] The Early Life Research Unit, Division of Child Health, Obstetrics and Gynaecology, and Nottingham Digestive Disease Centre and Biomedical Research Unit, School of Medicine, University Hospital, University of Nottingham, Nottingham, NG7 2UH, UK, Phone: +44 115 82 30625, E-mail: michael.symonds@nottingham.ac.uk

Abstract:
The global prevalence of obesity and related cardiometabolic disease continues to increase through the 21st century. Whilst multi-factorial, obesity is ultimately caused by chronic caloric excess. However, despite numerous interventions focussing on reducing caloric intake these either fail or only elicit short-term changes in body mass. There is now a focus on increasing energy expenditure instead which has stemmed from the recent 're-discovery' of cold-activated brown adipose tissue (BAT) in adult humans and inducible 'beige' adipocytes. Through the unique mitochondrial uncoupling protein 1 (UCP1), these thermogenic adipocytes are capable of combusting large amounts of chemical energy as heat and in animal models can prevent obesity and cardiometabolic disease. At present, human data does not point to a role for thermogenic adipocytes in regulating body weight or fat mass but points to a pivotal role in regulating metabolic health by improving insulin resistance as well as glucose and lipid homeostasis. This review will therefore focus on the metabolic benefits of BAT activation and the mechanisms and signalling pathways by which these could occur including improvements in insulin signalling in peripheral tissues, systemic lipid and cholesterol metabolism and cardiac and vascular function.

Keywords: brown adipose tissue, cardiometabolic health, glucose metabolism, insulin signalling, lipid metabolism

DOI: 10.1515/hmbci-2017-0007

Received: March 14, 2017; **Accepted:** March 22, 2017

Introduction

Our current knowledge of adipose tissue (AT) physiology has grown exponentially this century and it is now understood that there are at least three types of AT namely white, brown and beige which differ in their embryological origin, function, molecular characterisation and anatomical distribution [1], [2], [3]. White adipose tissue (WAT), traditionally viewed as an energy storage vessel is now considered to be potentially the body's largest endocrine organ. In addition to regulating the storage and release of triglycerides (TGs) in response to changes in energy demand, WAT modulates an array of physiological processes through the secretion of growth factors, cytokines, peptides and adipokines [4], [5]. Brown adipose tissue (BAT), in contrast, is characterised by the possession of the functionally thermogenic mitochondrial uncoupling protein UCP1. It was traditionally thought to be present primarily in the human neonate where activation at birth acted to defend against hypothermia to the cold extra uterine environment [6]. Seminal work had previously demonstrated the presence of brown adipocytes in adult autopsies [7]; however, the discovery in 2009 that BAT could be activated pharmacologically and environmentally, was associated inversely with body mass index, with age and metabolic health led to it being heralded as a possible anti-obesity target [8], [9], [10], [11], [12], [13] (Figure 1). Furthermore, the discovery of inducible 'beige' adipocytes in classical WAT depots which are not only thermogenic in vitro [14] but improve metabolic health in vivo [14], [15], [16], [17] has led to further interest on 'browning' WAT.

Michael E. Symonds is the corresponding author.

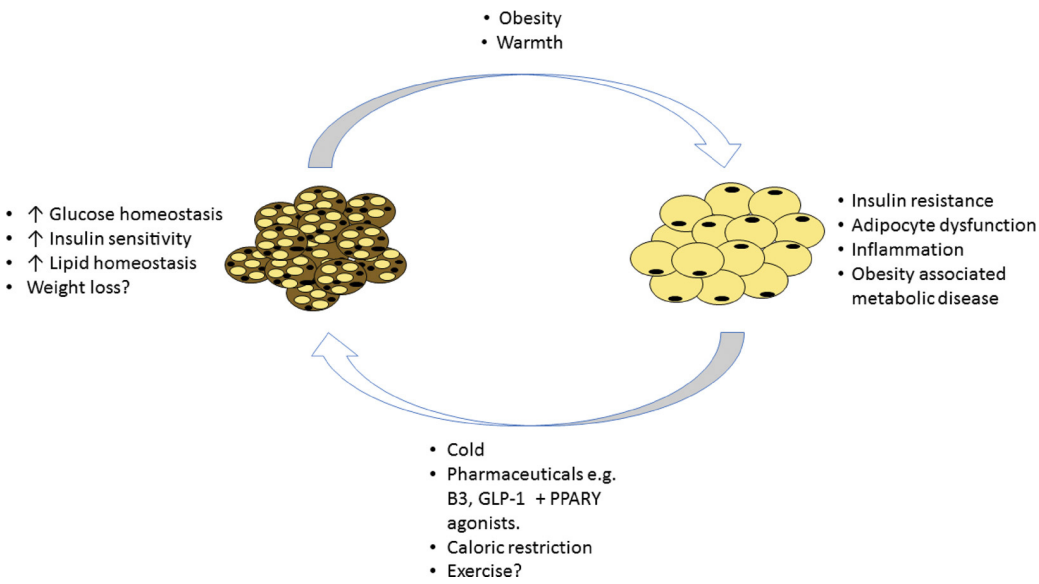

Figure 1: Overview of brown-to-white adipocyte transition, associated metabolic alterations and regulatory factors.

There is now a wealth of data from animal models suggesting that the activation of thermogenic adipocytes either environmentally or pharmacologically can elicit substantial reductions in adiposity [18]. However, these studies are typically done in chronically cold-acclimated rodents exhibiting large and active BAT depots which does not mimic human physiology [19]. Moreover, it is also important that the total amount of UCP1 is determined in each depot, and the tissues relative state of differentiation/expansion are also measured [20]. These factors therefore not only impact on classical brown fat but also beige adipocytes and the elusive search for a stimulus that can provide a greater stimulus than cold to promote UCP1 and the beiging process [20]. Evidence in humans certainly suggests that BAT activation increases energy expenditure, however, there is little to suggest a role of thermogenic adipocytes in combating obesity. In fact, long-term cold exposure [19 °C over 1 month] improved glucose homeostasis without an effect on body weight in healthy young men though adiposity was not studied. At present the role of thermogenic adipocytes in humans suggests a potential role in regulating cardiometabolic health in the absence of changes in weight and therefore these cardiometabolic alterations will be the focus of the current review.

BAT, hyperglycemia and insulin resistance

The dysregulation of insulin signalling and onset of insulin resistance and hyperglycemia is a key feature in obesity and related metabolic syndrome. The mechanisms by which insulin signalling becomes dysregulated is however both complex and tissue specific as the effects of insulin on glucose homeostasis is reliant on numerous downstream intracellular signalling events [21]. Typically, the binding of insulin to the α-subunit of the insulin receptor (IR) induces the rapid phosphorylation of its β subunit and the subsequent activation of tyrosine kinase which in turn allows phosphorylation of IR substrates-1 (IRS-1) and -2 (IRS-2). Phosphorylation of IRS-1 and IRS-2 and subsequent activation of phosphoinositide-3-kinase (PI3K) is key and affects numerous downstream signalling pathways by generating phosphatidyl-inositol-3, 4, 5-triphosphosphate (PIP3), a lipid second messenger. Of these downstream pathways, the Akt/PkB (protein kinase B) is key and its phosphorylation at the serine 407 and threonine 308 residues is pivotal in driving the metabolic actions of insulin in target tissues.

Importantly, and in the context of this review, recent evidence points to an important role for brown adipocytes in regulating systemic glucose homeostasis with BAT described as a 'glucose sink' [22]. It is essential therefore to understand the mechanisms by which glucose uptake occurs in thermogenic adipocytes (Figure 2). Glucose uptake in brown adipocytes was described as far back as 1985 [23] and this early in-vivo work in mice demonstrated that the uptake of 2-[1-14C]-deoxyglucose (2-DG) into BAT was

a. greater than in both the brain and heart as well as other peripheral tissues (WAT and skeletal muscle) following insulin administration and

b. greater than in the heart following norepinephrine (NE) administration suggestive that there may be divergent, stimulus specific mechanisms by which glucose uptake occurs.

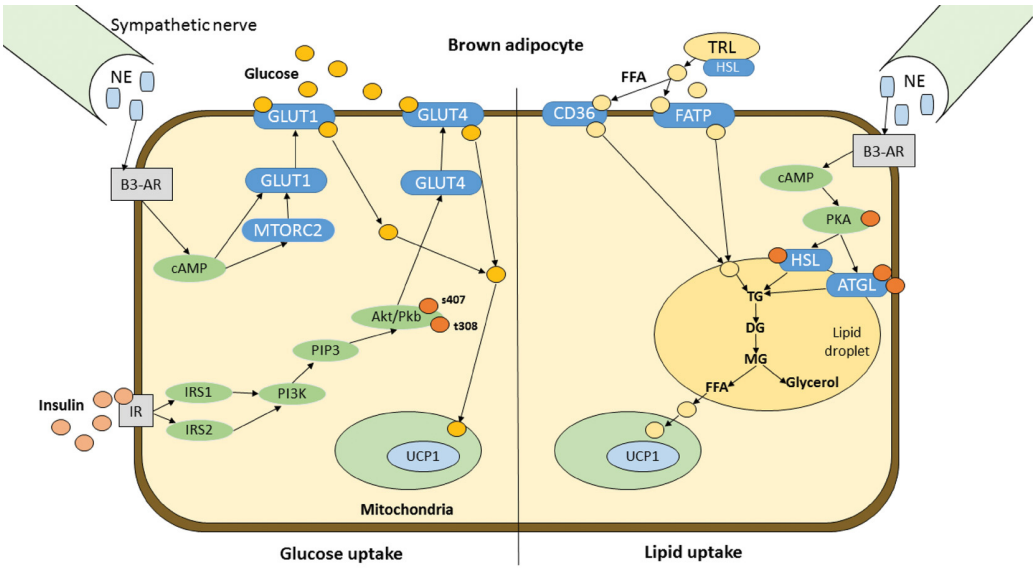

Figure 2: Overview of mechanisms regulating glucose and lipid metabolism in brown adipocytes. Discussed in detail in text.

Insulin stimulated glucose uptake in brown adipocytes is now well understood, occurring by the PI3K-Akt pathway and glucose transporter (GLUT) 4 translocation to the plasma membrane as it does in both WAT and skeletal muscle [24]. The mechanisms governing adrenergic stimulation of glucose uptake into brown adipocytes were traditionally less well described. Early in-vitro work demonstrated that glucose uptake in brown adipocytes exposed to NE occurs independently of insulin whilst conversely, insulin mediated glucose uptake into brown adipocytes was dependent on NE concentration [25]. It was suggested at the time that the effects of NE were likely to be mediated by adenosine 3′,5′-cyclic monophosphate (cAMP) and we now know that the increased glucose uptake in response to sympathetic activation occurs independently of GLUT4 translocation [26], [27]. This is largely due to both rapid de novo synthesis of the insulin independent GLUT1 in the plasma membrane by cAMP and also the translocation of GLUT1, promoted by mechanistic target of rapamycin (mTOR) complex 2 [26], [27]. Whilst both insulin, and NE-mediated glucose uptake initially occur by different mechanisms adrenergic stimulation ultimately activates the cAMP/protein kinase A (PKA) pathway recruiting PI3K and stimulating multiple protein kinase c (PKCs). This suggests that NE also acts through similar downstream mechanisms as the classic insulin signalling pathway [28] and it is these mechanisms that underpin the potential for BAT to modulate glucose homeostasis.

2-Deoxy-2-[18F]-fluoro-d-glucose (18F-FDG) was typically used during positron emission tomography (PET)/computed tomography (CT) scans to quantify metabolic activity of tumours in cancer patients. However, since the discovery that 18F-FDG positron emission tomography-computed tomography (PET-CT) can be used to quantify both the presence and activity of BAT its use in healthy populations has increased. In fasted humans undergoing 18F-FDG PET-CT scans cold exposure increases resting energy expenditure, an effect fuelled by oxidation of plasma glucose and free fatty acids [29]. Furthermore, cold exposure shifts glucose disposal to active BAT and away from the heart as earlier described [23], [29]. This increase in glucose utilisation by BAT improves whole body insulin stimulated glucose uptake and insulin sensitivity, changes which are potentially mediated by upregulation of GLUT 1/GLUT 4 or the numerous other genes and enzymes that regulate glucose uptake, glycogen turnover and glycolytic flux as discovered by transcriptomic profiling of sympathetically activated BAT [28], [30].

It is these BAT associated changes in glucose homeostasis in humans which have led to the hypothesis that its activation could be a therapeutic target for diabetes.

Long-term, intermittent reductions of ambient temperature from 24 °C to 19 °C for 10 h/night for a 1-month period yield no change in body composition but increase diet induced thermogenesis and post prandial insulin sensitivity in association with reduced leptin and increased adiponectin and GLUT4 expression in subcutaneous AT [31]. Short-term cold acclimation over 10 days elicits increases of 18F-FDG uptake into BAT concomitant with a ~1.4 fold increase in peripheral insulin sensitivity in type 2 diabetic patients. Given the role of skeletal muscle in regulating glucose homeostasis it is important to note that these effects may be due to the increased translocation of GLUT4 in skeletal muscle which occurred in the absence of changes in insulin signalling and thermogenic genes in WAT [32], [33]. Even so, it would seem that BAT regulates glucose-induced thermogenesis during an oral glucose tolerance test and that BAT thermogenesis exhibits a diurnal rhythm which is glucose responsive [34]. This may be functionally relevant as humans spend a large amount of time

in the post-prandial state and should be taken into account when considering dietary interventions that are targeted on response of BAT to nutrient excess. Animal studies allude to numerous other benefits of BAT activation. For instance, in models of type 1 diabetes, BAT transplantation can restore euglycaemia independently of insulin through insulin-like growth factor 1 stimulated adipogenesis [35]. The formation of healthy WAT and the secretion of hypoglycaemic adipokines are thought to underlie the effects of transplantation on glycaemia, however, the improvements in metabolic homeostasis are reportedly lost in the absence of interleukin-6 (IL6) suggestive that this pleiotropic cytokine has a pivotal role [36]. Whilst the mechanisms governing improvements in glucose homeostasis are not completely understood BAT appears to have a major role in regulating glucose metabolism.

It is feasible that the therapeutic activation of thermogenic adipocytes may be a future treatment for diabetes and related endocrine disorders whilst a number of drugs in use clinically or in development may improve insulin sensitivity in part through their effects on brown and beige adipocytes [37].

Metformin

Metformin is a biguanide drug commonly used, alone or in combination with insulin, in the treatment of diabetes. It primarily decreases circulating glucose by inhibiting hepatic gluconeogenesis and by increasing GLUT4-dependent glucose uptake into muscle and WAT through the activation of AMPK and both novel and conventional PKCs [38], [39], [40]. There is little evidence to date that the improved metabolic homeostasis and modest reductions in body weight occurring with metformin treatment are due to increased BAT thermogenesis. Indeed, whilst metformin may increase UCP1 in BAT of lean rats, treatment of both Zucker obese rats and brown adipocytes did not increase BAT UCP1 expression, guanosine diphosphate (GDP) binding or cellular respiration, respectively, and importantly no increase in resting energy expenditure is seen in humans [41], [42], [43], [44], [45].

Metformin may have a clearer significance in a perinatal setting where administration during early life may be critical in maintaining BAT function in pups overfed during lactation [46]. Despite increased size and adiposity, pups exposed to a caloric surplus during lactation had greater basal UCP1 expression in BAT, likely due to increased PPARα activation but were less responsive to cold exposure. After weaning to chow mice exhibited greater body mass, adiposity and insulin resistance at 16 weeks of age concomitant with a reduction in BAT UCP1 and the thermogenic response to both cold and a β3-agonist. Importantly, when pups were given daily metformin injections throughout lactation the adverse effects on BAT function were reversed at 4 weeks of age despite having similar body weight [46]. Long-term effects of this early postnatal life treatment and how this intervention may relate to a clinical situation warrant further research.

FGF21

Fibroblast growth factor (FGF) 21 is an autocrine and endocrine protein secreted primarily from the liver during fasting and starvation, increasing gluconeogenesis and ketogenesis and acting on numerous target tissues including WAT and BAT [47]. In addition to having endocrine functions FGF21 can act in an autocrine/paracrine manner. Peroxisome proliferator-activated receptor gamma (PPARγ) induced FGF21 production in WAT does not enter circulation but instead acts on WAT directly activating PPARγ from its inactive, sumoylated, form and, with that, enabling stimulation of adipogenesis, GLUT1 expression, glucose uptake and thermogenesis through browning [48], [49]. FGF21 also acts centrally, activating the sympathetic nervous system whereby subsequent NE production directly stimulates UCP1 expression in both BAT and WAT [50]. Additionally, in recent years it has been recognised as a potential 'BATokine' as its expression is increased in BAT following cold exposure though the functional relevance of BAT secreted FGF21 and its contribution to circulating concentrations are not yet understood [51].

Obesity increases expression of FGF21 in liver and WAT as well as circulating FGF21 which may be due to reduced function of its receptor and FGF21 resistance [52], [53], [54]. As FGF21 expression is controlled by PPARα and PPARγ, stimulation of these transcription factors through antidiabetic drugs like the fibrate class of hypolipidemic drugs and thiazolidinediones, respectively, will induce FGF21 [55], [56]. Direct administration of FGF21 improves glucose tolerance by decreasing both glucose and insulin concentrations, and lowers body weight, plasma TGs and non-esterified fatty acids, in both obese humans and mice, an adaptation partly be mediated by increased non-activity energy expenditure alluding to potential increases in BAT thermogenesis [56], [57], [58]. Indeed, in mice with diet-induced obesity, FGF21 administration induces UCP1 expression and glucose uptake into brown fat, and also promotes a substantial increase in WAT UCP1 [59], [60], [61]. Furthermore, cultured brown adipocytes directly stimulated with FGF21 also exhibit an upregulation of UCP1 gene expression together with increased oxygen and glucose consumption [62]. Data from UCP1 knockout mice suggests

the benefits of FG21 are not entirely due to increased thermogenic activity but also possibly due to reduced energy intake [63]. Nevertheless, development and optimisation of recombinant forms of FGF21 to be used in therapy of metabolic diseases such as diabetes are still in progress [56], [64].

GLP-1 receptor agonists

Glucagon-like peptide 1 (GLP-1) is a hormone postprandially released from ileum and colon L-cells. GLP-1 stimulates insulin secretion and inhibits glucagon secretion in a glucose-dependent manner, therefore not leading to hypoglycaemia in addition to slowing gastric emptying thus reducing appetite and body weight [65], [66]. Endogenous GLP-1 is cleaved by the protease dipeptidyl peptidase 4 (DPP4) within minutes and cleared through the kidney. Synthetic analogues which stimulate the GLP-1 receptor are designed to be resistant to DPP4 degradation and range from short-acting, which are administered twice a day, including liraglutide, to long-acting forms, administered once a week, including albiglutide [67]. These analogues are currently in clinical use for the management of hyperglycaemia in type 2 diabetes. In mice it has recently been shown that the metabolic benefits of GLP-1 agonists may occur in part through the activation of BAT and the browning of WAT depots [41], [68], [69]. When delivered through intracerebroventricular injection, GLP-1 [68] and its analogue exendin-4 [69] increase BAT thermogenesis via an increased uptake of TG-derived fatty acids and plasma glucose in addition to browning WAT, effects which may occur by activation of hypothalamic AMPK [41]. Similar results have been demonstrated when GLP-1 agonists have been administered peripherally [70], [71], [72] with the browning of WAT suggested to occur via upregulation of Sirtuin 1 (SIRT1) [73]. Whilst these effects remain to be confirmed in humans it is feasible that GLP-1 agonists could be suitable candidates to induce browning of visceral ATs.

Thermogenic adipocytes regulate lipid and cholesterol metabolism

Alterations in systemic lipid and cholesterol metabolism during obesity play a major role in the onset of associated cardiometabolic disease. Insulin and the classical insulin signalling pathways regulate lipid metabolism in both organs and peripheral tissues and dysregulation of insulin signalling effects WAT lipolysis, free fatty acid (FFA) and TG synthesis and lipid uptake from blood in addition to both hepatic cholesterol synthesis and very-low-density lipoprotein (vLDL) formation [74]. Whilst changes in lipid metabolism following BAT activation may relate to improvements in the insulin signalling, BAT utilises lipids as a fuel source stimulating whole body metabolism (Figure 2) [75]. During sympathetic stimulation the release of NE from sympathetic nerves results in the activation of adenylyl cyclase and production of cyclic AMP which in turn activates protein kinase A (PKA). PKA then phosphorylates adipose triglyceride lipase (ATGL) and hormone sensitive lipase (HSL), triggering lipolysis and the release of FFA from intracellular lipid droplets. These FFA enter the mitochondria and activate UCP1 uncoupling oxidative phosphorylation from adenosine triphosphate (ATP) synthesis to result in the dissipation of heat [76]. Ongoing stimulation of BAT requires a replenishment of intracellular lipid, a process mediated by both de novo lipogenesis [77] and the uptake of FA from TG-rich lipoproteins by lipoprotein lipase (LPL) and CD36 [78]. Other regulators of lipid mobilisation in BAT exist. For example, angiopoietin-like 4 (ANGPTL4), a regulator of LPL activity during both fasting and exercise was recently shown to modulate lipid shuttling in BAT during cold exposure preferentially driving uptake of TG-rich lipoprotein derived FFA, an effect which is regulated by AMP-activated protein kinase (AMPK) [79].

The use of animal models to determine how BAT regulates lipid metabolism has been invaluable. They have been used to demonstrate that activation of BAT, through the above mechanisms can correct hypercholesterolemia and attenuate atherosclerosis [75], [80]. In contrast, it has also been suggested that BAT activation may be involved in the progression of atherosclerosis due to cold-induced alterations in lipid profile [81]. However, it is important to note that the adverse effects of BAT activation are limited to apolipoprotein E K/o (ApoE −/−) and low-density lipoprotein receptor K/o (Ldlr −/−) mice, which both lack a functional ApoE-Ldlr pathway, a requirement for the physiological regulation of lipid metabolism and hepatic clearance of lipoprotein remnants such as LDL and VLDL [80]. When exposed to cold the increased metabolic activity of BAT and upregulation of thermogenic genes in WAT of these animals leads to unfavourable changes in total cholesterol, LDLc, intermediate LDL and in particular VLDL in addition to enhanced atherosclerotic lesions and plaque instability [81]. This, however, contrasts with the effects of BAT activation seen in APOE*3-Leiden.CETP mice. These mice have the human cholesterol ester transfer protein knocked-in and thus have a functional ApoE-Ldlr pathway and 'human-like' lipid metabolism [82]. In these animals' administration of the β3-adrenergic receptor agonist CL316-243 to activate BAT markedly reduces plasma TG, total cholesterol and VLDL concomitant with increased hepatic clearance of lipoprotein remnants and attenuation of atherosclerosis [80]. Whilst common murine models of atherosclerosis closely resemble human pathology their use for studies investigating

BAT physiology is limited, in this case the APOE*3-Leiden.CETP mice have a greater translational value and suggest BAT may be a therapeutic target combating CAD in humans [83].

Relative to glucose metabolism there is less evidence for a role of BAT in human lipid metabolism primarily due to the routine use of FDG tracer uptake in PET-CT studies. Individuals with higher amounts of active BAT, however, exhibit lower fasting TG and higher HDL whilst the expression of LPL and the acetyl-CoA dehydrogenase family of enzymes in UCP-1 containing epicardial AT is correlated with both circulating TG and HDL [84], [85]. Using the FFA tracer 18F-fluoro-thiaheptadecanoic acid (18FTHA) acute cold exposure (2 h) increased both fractional uptake of 18FTHA and uptake of FFA in BAT compared to subcutaneous AT and muscle [86]. In BAT positive subjects (based on 18F-FDG disposal) during fasting and acute cold, prolonged cold exposure (5–8 h) increases FFA oxidation and contributes to ~70% of the increase in resting energy expenditure. This is likely due to induction of UCP1, together with type 2 deiodenase, β3-adrenoreceptor and peroxisome proliferator-activated receptor gamma coactivator 1-alpha (PGC1α) which have been shown in rodent studies to be essential for BAT thermogenesis [29]. BAT activity also correlates with cold-induced lipolysis and whilst glucose uptake is reduced, cold-induced increases in FFA uptake are not impaired in individuals with type 2 diabetes or age-matched controls [87]. This suggests that cold exposure may be able to modulate lipid metabolism independent of ageing and insulin resistance. More recently BAT activation was shown to correlate with cold-induced changes in whole body FFA oxidation, lipolysis and TG-FFA cycling with BAT demonstrating a 45-fold higher respiration rate (e.g. 45 fold higher capacity for heat generation) compared to WAT [88]. Interestingly, whilst cold did not affect plasma TG, cholesterol or lipoproteins reductions in TG and VLDL were seen the following day suggestive that lipid metabolism may be modified after the cessation of cold exposure. These systemic effects are likely to be mediated by cold-induced increases in the expression of genes involved in both thermogenesis and lipid metabolism.

Despite the suggested benefits of cold adaptation [89], [90], FFA uptake into BAT during acute cold exposure accounts for less than 1% of total FFA turnover whilst there is no change in circulating TG [86]. This points to a minimal role for BAT in the acute regulation of lipid metabolism though increased hepatic VLDL-TAG secretion may confound studies over such a short time-frame [91]. It has long been speculated since the seminal work of Rothwell and Stock that BAT activation may play a role in diet-induced thermogenesis [92]. Whilst there is data to suggest both diet and dietary factors play a role in a compensatory activation of thermogenic tissues, evidence for this in humans is sparse as human BAT studies using PET-CT are typically done in the fasted state [93]. Importantly, glucose uptake is impaired following prolonged fasting suggestive that the general fasting state may not be appropriate for assessing the ability of BAT to regulate systemic metabolism [94], although uptake by BAT as measured using PET-CT is much lower than in skeletal muscle after feeding [95]. There is now increasing evidence that BAT function is stimulated by feeding.

Following 8 weeks of overfeeding in humans there is no increase in BAT thermal activity as measured by taking only two thermal images before feet immersion into cold water, and then two more 2 min later [96]. Not surprisingly given the acute nature of this test there was no correlation between thermal activity and metabolic adaptation or body weight [96]. It is important to note that instead of using a subscapular reference point, the reference region used includes the background area behind the torso which is cooler than skin temperature and so the results may not be indicative of BAT function. Furthermore, the use of 18FTHA pre and post cold acclimation demonstrates that despite a 2.6-fold increase in BAT oxidative capacity there is no increase in the uptake of dietary fatty acids in the post-prandial state [97]. Furthermore, dietary fatty acid uptake by BAT was comparable to abdominal WAT and skeletal muscle and significantly lower than both the heart (~55%) and liver (~83%) accounting in total for only ~0.3% dietary fatty acid uptake. It is important to note here however that the post-prandial cold-exposure period of 240 min may not have been sufficient to deplete intracellular lipid in BAT. These stores must normally be depleted before replenishment from circulating lipids can take place with a longer 5–8 h protocol speculated to be required [88]. Methodological differences between the various studies make it difficult to reach a definite conclusion on the potential for BAT to modulate lipid metabolism and in particular this may be negligible in short exposure periods. More studies with increased exposure time are needed to determine if the positive effects of BAT activation on lipid metabolism can be replicated [88].

Vascular brown adipocytes and atherosclerosis

Whilst the main focus in rodents has been on interscapular BAT and 'browning' in recent years there has also been an increased recognition of the physiological relevance of thermogenic adipocytes elsewhere, especially located around the heart (epicardial) and vasculature (perivascular) [98], [99]. This is because their contiguity with the myocardium and major vessels, respectively, implies they might be capable of regulating cardiomyocyte and vascular function in a paracrine and/or endocrine fashion [100]. Epicardial AT (EAT) originates from

the splanchnic mesoderm and/or the epicardium [101], [102] and is primarily located between the myocardium and visceral pericardium where it sits along the myocardium, the atrio- and inter-ventricular grooves and is vascularised by the coronary arteries. EAT provides mechanical protection to the coronary vasculature during contraction [98], [103], modulates coronary vascular tone through the secretion of numerous bioactive peptides (e.g. nitric oxide [104] and angiotensinogen 1–7 [105]) and perhaps protects the myocardium from lipotoxicity through the uptake of intravascular FFA [106], [107]. Importantly, EAT has also been proposed to protect the myocardium by acting as a source of heat during hypothermia [108] however, to date there is no direct evidence to suggest that the UCP1 expressing cells in this depot are thermogenically active. Similar to EAT, perivascular AT (PVAT) is the AT located around the major vasculature with its main role being to maintain and regulate vascular tone/remodelling and endothelial function/dysfunction [109], [110]. It is important to note that these tissues are characteristically similar to BAT at birth and also, to some degree throughout adulthood and that the transition from BAT to white-like AT may be due primarily to maternal and early life factors such as under/over-nutrition and diet composition [100], [111], [112].

With ageing and overnutrition adipocytes accumulate excess lipid, becoming hypertrophic and hypoxic and, after outstripping the vasculature, the hypoxic and inflammatory microenvironment drives the downregulation of mitochondrial function and adrenergic signalling with insulin resistance and atherogenesis ensuing [113], [114], [115]. It has also been demonstrated in mice that the thermogenic properties of PVAT are essential to optimal cardiovascular health. The complete ablation of PVAT in PDGRFα k/o mice renders animals hypertriglyceridemic [116] suggesting a major role of PVAT in lipid homeostasis. Mice lacking PVAT are also unable to regulate intravascular temperature suggestive that the thermogenic properties of this depot are essential to maintenance of adequate core temperature [116]. The role of PVAT in regulating lipid homeostasis is evident in humans where the association between UCP1 expression in human EAT and circulating HDL and TGs suggests that this depot plays a role in systemic lipid metabolism [85].

Given the role of dyslipidaemia in atherosclerosis the ability for cardiac and vascular adipocytes to regulate intravascular lipid metabolism may be a clinically significant [117]. Current evidence also suggests that the brown-to-white transition can modulate redox state [118] with this supported by human data demonstrating excess reactive oxygen species in CAD patients with reduced expression of thermogenic genes [119]. Given that components of the mitochondrial electron transport chain in PVAT are critical regulators of vascular tone it would suggest that the adipocytes present in EAT and PVAT may modulate vascular and myocardial redox state [112] and that 'whitening' of these may drive disease partly through excess reactive oxygen species. In fact, BAT regulates vascular function through production of the anti-contractile factor hydrogen peroxide which is regulated by NADPH oxidase 4 and alters vascular contractility through activation of protein-kinase G1α [120]. Importantly, mechanisms regulating contractiliy differ in mesenteric PVAT (which resembles WAT) and browning this depot increases the anti-contractile effect through hydrogen peroxide dependant mechanisms in a manner similar to BAT. Thus, the anti-contractile effects of BAT may be lost in the transition to WAT that occurs with ageing and obesity but may be restored in the presence of browning. Whilst manipulating the phenotype of adipocytes local to the vasculature is clinically challenging they offer a novel target to alleviate obesity associated vascular disease and it is clear that cross-talk between these adipocytes, the myocardium and vascular wall are of great importance.

Conclusion and outlook

It is clear that activating BAT is an attractive target for the prevention of metabolic and cardiovascular disease. To date there is clear evidence that BAT can improve glucose and insulin homeostasis through insulin-dependent and independent mechanisms [90]. Furthermore, BAT activation may be a means of manipulating systemic lipid metabolism in humans but will require further work to validate the promising results shown in rodents [80], [88]. Future work will no doubt further target the manipulation of thermogenic adipocytes by pharmacological and environmental means whilst the development of new tracers and imaging methods will greatly enhance our understanding of both BAT and 'beige' adipocyte biology.

Highlights

- Rodent data provides clear evidence of a role for BAT in reducing adiposity.
- To date no human study has shown that activating BAT leads to reductions in adiposity.
- Active BAT plays a key role in glucose and insulin homeostasis in humans.

- Activation of BAT may play a key role in human triglyceride metabolism but further studies are needed.
- Brown adipocytes surrounding the heart and vasculature may play a key role in attenuating atherosclerosis.

Funding

P. Aldiss is funded by the British Heart Foundation (Grant number – FS/15/4/31184).

Author Statement

Conflict of interest: Authors state no conflict of interest.

Informed consent: Informed consent is not applicable.

Ethical approval: The conducted research is not related to either human or animals use.

References

1. Cinti S. The adipose organ at a glance. Dis Model Mech. 2012;5:588–94.
2. Sanchez-Gurmaches J, Guertin DA. Adipocyte lineages: tracing back the origins of fat. Biochim Biophys Acta. 2014;1842:340–51.
3. de Jong JM, Larsson O, Cannon B, Nedergaard J. A stringent validation of mouse adipose tissue identity markers. Am J Physiol Endocrinol Metab. 2015;308:E1085–105.
4. Grant RW, Dixit VD. Adipose tissue as an immunological organ. Obesity (Silver Spring). 2015;23:512–8.
5. Kershaw EE, Flier JS. Adipose tissue as an endocrine organ. J Clin Endocrinol Metab. 2004;89:2548–56.
6. Symonds ME, Pope M, Budge H. The ontogeny of brown adipose tissue. Annu Rev Nutr. 2015;35:295–320.
7. Heaton JM. The distribution of brown adipose tissue in the human. J Anat. 1972;112(Pt 1):35–9.
8. Cypess AM, White AP, Vernochet C, Schulz TJ, Xue R, Sass CA, et al. Anatomical localization, gene expression profiling and functional characterization of adult human neck brown fat. Nat Med. 2013;19:635–9.
9. Cypess AM, Lehman S, Williams G, Tal I, Rodman D, Goldfine AB, et al. Identification and importance of brown adipose tissue in adult humans. N Engl J Med. 2009;360:1509–17.
10. Robinson L, Ojha S, Symonds ME, Budge H. Body mass index as a determinant of brown adipose tissue function in healthy children. J Pediatr. 2014;e1164:318–22.
11. Symonds ME, Henderson K, Elvidge L, Bosman C, Sharkey D, Perkins AC, et al. Thermal imaging to assess age-related changes of skin temperature within the supraclavicular region co-locating with brown adipose tissue in healthy children. J Pediatr. 2012;161:892–8.
12. Ouellet V, Routhier-Labadie A, Bellemare W, Lakhal-Chaieb L, Turcotte E, Carpentier AC, et al. Outdoor temperature, age, sex, body mass index, and diabetic status determine the prevalence, mass, and glucose-uptake activity of 18F-FDG-detected BAT in humans. J Clin Endocrinol Metab. 2011;96:192–9.
13. Yoneshiro T, Aita S, Matsushita M, Okamatsu-Ogura Y, Kameya T, Kawai Y, et al. Age-related decrease in cold-activated brown adipose tissue and accumulation of body fat in healthy humans. Obesity (Silver Spring). 2011;19:1755–60.
14. Wu J, Bostrom P, Sparks LM, Ye L, Choi JH, Giang AH, et al. Beige adipocytes are a distinct type of thermogenic fat cell in mouse and human. Cell. 2012;150:366–76.
15. De Matteis R, Lucertini F, Guescini M, Polidori E, Zeppa S, Stocchi V, et al. Exercise as a new physiological stimulus for brown adipose tissue activity. Nutr Metab Cardiovasc Dis. 2013;23:582–90.
16. Sidossis LS, Porter C, Saraf MK, Borsheim E, Radhakrishnan RS, Chao T, et al. Browning of subcutaneous white adipose tissue in humans after severe adrenergic stress. Cell Metab. 2015;22:219–27.
17. Shabalina IG, Petrovic N, de Jong JM, Kalinovich AV, Cannon B, Nedergaard J. UCP1 in brite/beige adipose tissue mitochondria is functionally thermogenic. Cell Rep. 2013;5:1196–203.
18. Poekes L, Lanthier N, Leclercq IA. Brown adipose tissue: a potential target in the fight against obesity and the metabolic syndrome. Clin Sci (Lond). 2015;129:933–49.
19. Maloney SK, Fuller A, Mitchell D, Gordon C, Overton JM. Translating animal model research: does it matter that our rodents are cold?. Physiology (Bethesda). 2014;29:413–20.
20. Kalinovich AV, de Jong JM, Cannon B, Nedergaard J. UCP1 in adipose tissues: two steps to full browning. Biochimie. 2017;134:127–37.
21. Cantley J. The control of insulin secretion by adipokines: current evidence for adipocyte-beta cell endocrine signalling in metabolic homeostasis. Mamm Genome. 2014;25:442–54.
22. Villarroya F, Vidal-Puig A. Beyond the sympathetic tone: the new brown fat activators. Cell Metab. 2013;17:638–43.
23. Cooney GJ, Caterson ID, Newsholme EA. The effect of insulin and noradrenaline on the uptake of 2-[1-14C]deoxyglucose in vivo by brown adipose tissue and other glucose-utilising tissues of the mouse. FEBS Lett. 1985;188:257–61.
24. Zaid H, Antonescu CN, Randhawa VK, Klip A. Insulin action on glucose transporters through molecular switches, tracks and tethers. Biochem J. 2008;413:201–15.

25. Marette A, Bukowiecki LJ. Stimulation of glucose transport by insulin and norepinephrine in isolated rat brown adipocytes. Am J Physiol. 1989;257(4 Pt 1):C714–21.
26. Dallner OS, Chernogubova E, Brolinson KA, Bengtsson T. Beta3-adrenergic receptors stimulate glucose uptake in brown adipocytes by two mechanisms independently of glucose transporter 4 translocation. Endocrinology. 2006;147:5730–9.
27. Olsen JM, Sato M, Dallner OS, Sandstrom AL, Pisani DF, Chambard JC, et al. Glucose uptake in brown fat cells is dependent on mTOR complex 2-promoted GLUT1 translocation. J Cell Biol. 2014;207:365–74.
28. Chernogubova E, Cannon B, Bengtsson T. Norepinephrine increases glucose transport in brown adipocytes via beta3-adrenoceptors through a cAMP, PKA, and PI3-kinase-dependent pathway stimulating conventional and novel PKCs. Endocrinology. 2004;145:269–80.
29. Chondronikola M, Volpi E, Borsheim E, Porter C, Annamalai P, Enerback S, et al. Brown adipose tissue improves whole-body glucose homeostasis and insulin sensitivity in humans. Diabetes. 2014;63:4089–99.
30. Hao Q, Yadav R, Basse AL, Petersen S, Sonne SB, Rasmussen S, et al. Transcriptome profiling of brown adipose tissue during cold exposure reveals extensive regulation of glucose metabolism. Am J Physiol Endocrinol Metab. 2015;308:E380–92.
31. Lee P, Smith S, Linderman J, Courville AB, Brychta RJ, Dieckmann W, et al. Temperature-acclimated brown adipose tissue modulates insulin sensitivity in humans. Diabetes. 2014;63:3686–98.
32. Blondin DP, Labbe SM, Phoenix S, Guerin B, Turcotte EE, Richard D, et al. Contributions of white and brown adipose tissues and skeletal muscles to acute cold-induced metabolic responses in healthy men. J Physiol. 2015;593:701–14.
33. Hanssen MJ, Hoeks J, Brans B, van der Lans AA, Schaart G, van den Driessche JJ, et al. Short-term cold acclimation improves insulin sensitivity in patients with type 2 diabetes mellitus. Nat Med. 2015;21:863–5.
34. Lee P, Bova R, Schofield L, Bryant W, Dieckmann W, Slattery A, et al. Brown adipose tissue exhibits a glucose-responsive thermogenic biorhythm in humans. Cell Metab. 2016;23:602–9.
35. Gunawardana SC, Piston DW. Insulin-independent reversal of type 1 diabetes in nonobese diabetic mice with brown adipose tissue transplant. Am J Physiol Endocrinol Metab. 2015;308:E1043–55.
36. Stanford KI, Middelbeek RJ, Townsend KL, An D, Nygaard EB, Hitchcox KM, et al. Brown adipose tissue regulates glucose homeostasis and insulin sensitivity. J Clin Invest. 2013;123:215–23.
37. Yuan X, Hu T, Zhao H, Huang Y, Ye R, Lin J, et al. Brown adipose tissue transplantation ameliorates polycystic ovary syndrome. Proc Natl Acad Sci U S A. 2016;113:2708–13.
38. Turban S, Stretton C, Drouin O, Green CJ, Watson ML, Gray A, et al. Defining the contribution of AMP-activated protein kinase (AMPK) and protein kinase C (PKC) in regulation of glucose uptake by metformin in skeletal muscle cells. J Biol Chem. 2012;287:20088–99.
39. Zhou G, Myers R, Li Y, Chen Y, Shen X, Fenyk-Melody J, et al. Role of AMP-activated protein kinase in mechanism of metformin action. J Clin Invest. 2001;108:1167–74.
40. Hundal RS, Krssak M, Dufour S, Laurent D, Lebon V, Chandramouli V, et al. Mechanism by which metformin reduces glucose production in type 2 diabetes. Diabetes. 2000;49:2063–9.
41. Beiroa D, Imbernon M, Gallego R, Senra A, Herranz D, Villarroya F, et al. GLP-1 agonism stimulates brown adipose tissue thermogenesis and browning through hypothalamic AMPK. Diabetes. 2014;63:3346–58.
42. Tokubuchi I, Tajiri Y, Iwata S, Hara K, Wada N, Hashinaga T, et al. Beneficial effects of metformin on energy metabolism and visceral fat volume through a possible mechanism of fatty acid oxidation in human subjects and rats. PLoS One. 2017;12:e0171293.
43. Keates AC, Bailey CJ. Metformin does not increase energy expenditure of brown fat. Biochem Pharmacol. 1993;45:971–3.
44. Rouru J, Isaksson K, Santti E, Huupponen R, Koulu M. Metformin and brown adipose tissue thermogenetic activity in genetically obese Zucker rats. Eur J Pharmacol. 1993;246:67–71.
45. Savontaus E, Rouru J, Boss O, Huupponen R, Koulu M. Differential regulation of uncoupling proteins by chronic treatments with beta 3-adrenergic agonist BRL 35135 and metformin in obese fa/fa Zucker rats. Biochem Biophys Res Commun. 1998;246:899–904.
46. Liang X, Yang Q, Zhang L, Maricelli JW, Rodgers BD, Zhu MJ, et al. Maternal high-fat diet during lactation impairs thermogenic function of brown adipose tissue in offspring mice. Sci Rep. 2016;6:34345.
47. Giralt M, Gavalda-Navarro A, Villarroya F. Fibroblast growth factor-21, energy balance and obesity. Mol Cell Endocrinol. 2015;418(Pt 1):66–73.
48. Dutchak PA, Katafuchi T, Bookout AL, Choi JH, Yu RT, Mangelsdorf DJ, et al. Fibroblast growth factor-21 regulates PPARgamma activity and the antidiabetic actions of thiazolidinediones. Cell. 2012;148:556–67.
49. Moyers JS, Shiyanova TL, Mehrbod F, Dunbar JD, Noblitt TW, Otto KA, et al. Molecular determinants of FGF-21 activity-synergy and cross-talk with PPARgamma signaling. J Cell Physiol. 2007;210:1–6.
50. Douris N, Stevanovic DM, Fisher FM, Cisu TI, Chee MJ, Nguyen NL, et al. Central fibroblast growth factor 21 browns white fat via sympathetic action in male mice. Endocrinology. 2015;156:2470–81.
51. Hondares E, Iglesias R, Giralt A, Gonzalez FJ, Giralt M, Mampel T, et al. Thermogenic activation induces FGF21 expression and release in brown adipose tissue. J Biol Chem. 2011;286:12983–90.
52. Tan BK, Hallschmid M, Adya R, Kern W, Lehnert H, Randeva HS. Fibroblast growth factor 21 (FGF21) in human cerebrospinal fluid: relationship with plasma FGF21 and body adiposity. Diabetes. 2011;60:2758–62.
53. Fisher FM, Chui PC, Antonellis PJ, Bina HA, Kharitonenkov A, Flier JS, et al. Obesity is a fibroblast growth factor 21 (FGF21)-resistant state. Diabetes. 2010;59:2781–9.
54. Hale C, Chen MM, Stanislaus S, Chinookoswong N, Hager T, Wang M, et al. Lack of overt FGF21 resistance in two mouse models of obesity and insulin resistance. Endocrinology. 2012;153:69–80.
55. Badman MK, Pissios P, Kennedy AR, Koukos G, Flier JS, Maratos-Flier E. Hepatic fibroblast growth factor 21 is regulated by PPARalpha and is a key mediator of hepatic lipid metabolism in ketotic states. Cell Metab. 2007;5:426–37.
56. Gaich G, Chien JY, Fu H, Glass LC, Deeg MA, Holland WL, et al. The effects of LY2405319, an FGF21 analog, in obese human subjects with type 2 diabetes. Cell Metab. 2013;18:333–40.
57. Kharitonenkov A, Shanafelt AB. FGF21: a novel prospect for the treatment of metabolic diseases. Curr Opin Investig Drugs. 2009;10:359–64.

58. Xu J, Lloyd DJ, Hale C, Stanislaus S, Chen M, Sivits G, et al. Fibroblast growth factor 21 reverses hepatic steatosis, increases energy expenditure, and improves insulin sensitivity in diet-induced obese mice. Diabetes. 2009;58:250–9.
59. Bernardo B, Lu M, Bandyopadhyay G, Li P, Zhou Y, Huang J, et al. FGF21 does not require interscapular brown adipose tissue and improves liver metabolic profile in animal models of obesity and insulin-resistance. Sci Rep. 2015;5:11382.
60. Coskun T, Bina HA, Schneider MA, Dunbar JD, Hu CC, Chen Y, et al. Fibroblast growth factor 21 corrects obesity in mice. Endocrinology. 2008;149:6018–27.
61. Camporez JP, Jornayvaz FR, Petersen MC, Pesta D, Guigni BA, Serr J, et al. Cellular mechanisms by which FGF21 improves insulin sensitivity in male mice. Endocrinology. 2013;154:3099–109.
62. Hondares E, Rosell M, Gonzalez FJ, Giralt M, Iglesias R, Villarroya F. Hepatic FGF21 expression is induced at birth via PPARalpha in response to milk intake and contributes to thermogenic activation of neonatal brown fat. Cell Metab. 2010;11:206–12.
63. Samms RJ, Smith DP, Cheng CC, Antonellis PP, Perfield JW, Kharitonenkov A, et al. Discrete aspects of FGF21 in vivo pharmacology do not require UCP1. Cell Rep. 2015;11:991–9.
64. Dong JQ, Rossulek M, Somayaji VR, Baltrukonis D, Liang Y, Hudson K, et al. Pharmacokinetics and pharmacodynamics of PF-05231023, a novel long-acting FGF21 mimetic, in a first-in-human study. Br J Clin Pharmacol. 2015;80:1051–63.
65. Dockray GJ. Enteroendocrine cell signalling via the vagus nerve. Curr Opin Pharmacol. 2013;13:954–8.
66. Sisley S, Gutierrez-Aguilar R, Scott M, D'Alessio DA, Sandoval DA, Seeley RJ. Neuronal GLP1R mediates liraglutide's anorectic but not glucose-lowering effect. J Clin Invest. 2014;124:2456–63.
67. Matthews JE, Stewart MW, De Boever EH, Dobbins RL, Hodge RJ, Walker SE, et al. Pharmacodynamics, pharmacokinetics, safety, and tolerability of albiglutide, a long-acting glucagon-like peptide-1 mimetic, in patients with type 2 diabetes. J Clin Endocrinol Metab. 2008;93:4810–7.
68. Lockie SH, Heppner KM, Chaudhary N, Chabenne JR, Morgan DA, Veyrat-Durebex C, et al. Direct control of brown adipose tissue thermogenesis by central nervous system glucagon-like peptide-1 receptor signaling. Diabetes. 2012;61:2753–62.
69. Kooijman S, Wang Y, Parlevliet ET, Boon MR, Edelschaap D, Snaterse G, et al. Central GLP-1 receptor signalling accelerates plasma clearance of triacylglycerol and glucose by activating brown adipose tissue in mice. Diabetologia. 2015;58:2637–46.
70. Heppner KM, Marks S, Holland J, Ottaway N, Smiley D, Dimarchi R, et al. Contribution of brown adipose tissue activity to the control of energy balance by GLP-1 receptor signalling in mice. Diabetologia. 2015;58:2124–32.
71. Tomas E, Stanojevic V, McManus K, Khatri A, Everill P, Bachovchin WW, et al. GLP-1(32–36)amide pentapeptide increases basal energy expenditure and inhibits weight gain in obese mice. Diabetes. 2015;64:2409–19.
72. Wei Q, Li L, Chen JA, Wang SH, Sun ZL. Exendin-4 improves thermogenic capacity by regulating fat metabolism on brown adipose tissue in mice with diet-induced obesity. Ann Clin Lab Sci. 2015;45:158–65.
73. Xu F, Lin B, Zheng X, Chen Z, Cao H, Xu H, et al. GLP-1 receptor agonist promotes brown remodelling in mouse white adipose tissue through SIRT1. Diabetologia. 2016;59:1059–69.
74. Dimitriadis G, Mitrou P, Lambadiari V, Maratou E, Raptis SA. Insulin effects in muscle and adipose tissue. Diabetes Res Clin Pract. 2011;93(Suppl 1):S52–9.
75. Bartelt A, Bruns OT, Reimer R, Hohenberg H, Ittrich H, Peldschus K, et al. Brown adipose tissue activity controls triglyceride clearance. Nat Med. 2011;17:200–5.
76. Cannon B, Nedergaard J. Brown adipose tissue: function and physiological significance. Physiol Rev. 2004;84:277–359.
77. Mottillo EP, Balasubramanian P, Lee YH, Weng C, Kershaw EE, Granneman JG. Coupling of lipolysis and de novo lipogenesis in brown, beige, and white adipose tissues during chronic beta3-adrenergic receptor activation. J Lipid Res. 2014;55:2276–86.
78. Laplante M, Festuccia WT, Soucy G, Blanchard PG, Renaud A, Berger JP, et al. Tissue-specific postprandial clearance is the major determinant of PPARgamma-induced triglyceride lowering in the rat. Am J Physiol Regul Integr Comp Physiol. 2009;296:R57–66.
79. Dijk W, Heine M, Vergnes L, Boon MR, Schaart G, Hesselink MK, et al. ANGPTL4 mediates shuttling of lipid fuel to brown adipose tissue during sustained cold exposure. Elife. 2015;e084284.
80. Berbee JF, Boon MR, Khedoe PP, Bartelt A, Schlein C, Worthmann A, et al. Brown fat activation reduces hypercholesterolaemia and protects from atherosclerosis development. Nat Commun. 2015;6:6356.
81. Dong M, Yang X, Lim S, Cao Z, Honek J, Lu H, et al. Cold exposure promotes atherosclerotic plaque growth and instability via UCP1-dependent lipolysis. Cell Metab. 2013;18:118–29.
82. Zadelaar S, Kleemann R, Verschuren L, de Vries-Van der Weij J, van der Hoorn J, Princen HM, et al. Mouse models for atherosclerosis and pharmaceutical modifiers. Arterioscler Thromb Vasc Biol. 2007;27:1706–21.
83. von Scheidt M, Zhao Y, Kurt Z, Pan C, Zeng L, Yang X, et al. Applications and limitations of mouse models for understanding human atherosclerosis. Cell Metab. 2017;25:248–61.
84. Wang Q, Zhang M, Xu M, Gu W, Xi Y, Qi L, et al. Brown adipose tissue activation is inversely related to central obesity and metabolic parameters in adult human. PLoS One. 2015;10:e0123795.
85. Chechi K, Blanchard PG, Mathieu P, Deshaies Y, Richard D. Brown fat like gene expression in the epicardial fat depot correlates with circulating HDL-cholesterol and triglycerides in patients with coronary artery disease. Int J Cardiol. 2013;167:2264–70.
86. Ouellet V, Labbe SM, Blondin DP, Phoenix S, Guerin B, Haman F, et al. Brown adipose tissue oxidative metabolism contributes to energy expenditure during acute cold exposure in humans. J Clin Invest. 2012;122:545–52.
87. Blondin DP, Labbe SM, Noll C, Kunach M, Phoenix S, Guerin B, et al. Selective impairment of glucose but not fatty acid or oxidative metabolism in brown adipose tissue of subjects with type 2 diabetes. Diabetes. 2015;64:2388–97.
88. Chondronikola M, Volpi E, Borsheim E, Porter C, Saraf MK, Annamalai P, et al. Brown adipose tissue activation is linked to distinct systemic effects on lipid metabolism in humans. Cell Metab. 2016;23:1200–6.
89. Johnson F, Mavrogianni A, Ucci M, Vidal-Puig A, Wardle J. Could increased time spent in a thermal comfort zone contribute to population increases in obesity?. Obes Rev. 2011;12:543–51.
90. Betz MJ, Enerback S. Human brown adipose tissue: what we have learned so far. Diabetes. 2015;64:2352–60.

91. Hoeke G, Kooijman S, Boon MR, Rensen PC, Berbee JF. Role of brown fat in lipoprotein metabolism and atherosclerosis. Circ Res. 2016;118:173–82.
92. Rothwell NJ, Stock MJ. Luxuskonsumption, diet-induced thermogenesis and brown fat: the case in favour. Clin Sci (Lond). 1983;64:19–23.
93. Fromme T, Klingenspor M. Uncoupling protein 1 expression and high-fat diets. Am J Physiol Regul Integr Comp Physiol. 2011;300:R1–8.
94. Hanssen MJ, Wierts R, Hoeks J, Gemmink A, Brans B, Mottaghy FM, et al. Glucose uptake in human brown adipose tissue is impaired upon fasting-induced insulin resistance. Diabetologia. 2015;58:586–95.
95. Vosselman MJ, Brans B, van der Lans AA, Wierts R, van Baak MA, Mottaghy FM, et al. Brown adipose tissue activity after a high-calorie meal in humans. Am J Clin Nutr. 2013;98:57–64.
96. Peterson CM, Orooji M, Johnson DN, Naraghi-Pour M, Ravussin E. Brown adipose tissue does not seem to mediate metabolic adaptation to overfeeding in men. Obesity (Silver Spring). 2017;25:502–5.
97. Blondin DP, Tingelstad HC, Noll C, Frisch F, Phoenix S, Guerin B, et al. Dietary fatty acid metabolism of brown adipose tissue in cold-acclimated men. Nat Commun. 2017;8:14146.
98. Iacobellis G. Local and systemic effects of the multifaceted epicardial adipose tissue depot. Nat Rev Endocrinol. 2015;11:363–71.
99. Gil-Ortega M, Somoza B, Huang Y, Gollasch M, Fernandez-Alfonso MS. Regional differences in perivascular adipose tissue impacting vascular homeostasis. Trends Endocrinol Metab. 2015;26:367–75.
100. Aldiss P, Davies G, Woods R, Budge H, Sacks HS, Symonds ME. 'Browning' the cardiac and peri-vascular adipose tissues to modulate cardiovascular risk. Int J Cardiol. 2017;228:265–74.
101. Yamaguchi Y, Cavallero S, Patterson M, Shen H, Xu J, Kumar SR, et al. Adipogenesis and epicardial adipose tissue: a novel fate of the epicardium induced by mesenchymal transformation and PPARgamma activation. Proc Natl Acad Sci U S A. 2015;112:2070–5.
102. Sacks HS, Fain JN. Human epicardial adipose tissue: a review. Am Heart J. 2007;153:907–17.
103. Szasz T, Webb RC. Perivascular adipose tissue: more than just structural support. Clin Sci (Lond). 2012;122:1–12.
104. Gao YJ, Lu C, Su LY, Sharma AM, Lee RM. Modulation of vascular function by perivascular adipose tissue: the role of endothelium and hydrogen peroxide. Br J Pharmacol. 2007;151:323–31.
105. Lee RM, Lu C, Su LY, Gao YJ. Endothelium-dependent relaxation factor released by perivascular adipose tissue. J Hypertens. 2009;27:782–90.
106. Marchington JM, Mattacks CA, Pond CM. Adipose tissue in the mammalian heart and pericardium: structure, foetal development and biochemical properties. Comp Biochem Physiol B. 1989;94:225–32.
107. Marchington JM, Pond CM. Site-specific properties of pericardial and epicardial adipose tissue: the effects of insulin and high-fat feeding on lipogenesis and the incorporation of fatty acids in vitro. Int J Obes. 1990;14:1013–22.
108. Sacks HS, Fain JN, Holman B, Cheema P, Chary A, Parks F, et al. Uncoupling protein-1 and related messenger ribonucleic acids in human epicardial and other adipose tissues: epicardial fat functioning as brown fat. J Clin Endocrinol Metab. 2009;94:3611–5.
109. Szasz T, Bomfim GF, Webb RC. The influence of perivascular adipose tissue on vascular homeostasis. Vasc Health Risk Manag. 2013;9:105–16.
110. Ozen G, Daci A, Norel X, Topal G. Human perivascular adipose tissue dysfunction as a cause of vascular disease: Focus on vascular tone and wall remodeling. Eur J Pharmacol. 2015;766:16–24.
111. Ojha S, Fainberg HP, Wilson V, Pelella G, Castellanos M, May ST, et al. Gene pathway development in human epicardial adipose tissue during early life. JCI Insight. 2016;1:e87460.
112. Sacks HS, Fain JN, Bahouth SW, Ojha S, Frontini A, Budge H, et al. Adult epicardial fat exhibits beige features. J Clin Endocrinol Metab. 2013;98:E1448–55.
113. Shimizu I, Aprahamian T, Kikuchi R, Shimizu A, Papanicolaou KN, MacLauchlan S, et al. Vascular rarefaction mediates whitening of brown fat in obesity. J Clin Invest. 2014;124:2099–112.
114. Shimizu I, Walsh K. The whitening of brown fat and its implications for weight management in obesity. Curr Obes Rep. 2015;4:224–9.
115. Roberts-Toler C, O'Neill BT, Cypess AM. Diet-induced obesity causes insulin resistance in mouse brown adipose tissue. Obesity (Silver Spring). 2015;23:1765–70.
116. Chang L, Villacorta L, Li R, Hamblin M, Xu W, Dou C, et al. Loss of perivascular adipose tissue on peroxisome proliferator-activated receptor-gamma deletion in smooth muscle cells impairs intravascular thermoregulation and enhances atherosclerosis. Circulation. 2012;126:1067–78.
117. Buckley ML, Ramji DP. The influence of dysfunctional signaling and lipid homeostasis in mediating the inflammatory responses during atherosclerosis. Biochim Biophys Acta. 2015;1852:1498–510.
118. Carriere A, Jeanson Y, Berger-Muller S, Andre M, Chenouard V, Arnaud E, et al. Browning of white adipose cells by intermediate metabolites: an adaptive mechanism to alleviate redox pressure. Diabetes. 2014;63:3253–65.
119. Dozio E, Vianello E, Briganti S, Fink B, Malavazos AE, Scognamiglio ET, et al. Increased reactive oxygen species production in epicardial adipose tissues from coronary artery disease patients is associated with brown-to-white adipocyte trans-differentiation. Int J Cardiol. 2014;174:413–4.
120. Friederich-Persson M, Nguyen Dinh Cat A, Persson P, Montezano AC, Touyz RM. Brown adipose tissue regulates small artery function through NADPH oxidase 4-derived hydrogen peroxide and redox-sensitive protein kinase G-1alpha. Arterioscler Thromb Vasc Biol. 2017;37:455–65.

1.3 ‘Browning’ the cardiac and peri-vascular adipose tissues to modulate cardiovascular risk

International Journal of Cardiology 228 (2017) 265–274

Contents lists available at ScienceDirect

International Journal of Cardiology

journal homepage: www.elsevier.com/locate/ijcard

Review

'Browning' the cardiac and peri-vascular adipose tissues to modulate cardiovascular risk

Peter Aldiss [a,1], Graeme Davies [a,1], Rachel Woods [a], Helen Budge [a], Harold S. Sacks [b], Michael E. Symonds [a,*]

[a] The Early Life Research Unit, Division of Child Health, Obstetrics and Gynaecology, School of Medicine, University Hospital, University of Nottingham, Nottingham, UK, NG7 2UH
[b] VA Greater Los Angeles Healthcare System, Endocrinology and Diabetes Division, and Department of Medicine David Geffen School of Medicine, Los Angeles, CA 90073, USA

ARTICLE INFO

Article history:
Received 14 July 2016
Accepted 5 November 2016
Available online 9 November 2016

Keywords:
Epicardial adipose tissue
Perivascular adipose tissue
Brown adipose tissue
CVD

ABSTRACT

Excess visceral adiposity, in particular that located adjacent to the heart and coronary arteries is associated with increased cardiovascular risk. In the pathophysiological state, dysfunctional adipose tissue secretes an array of factors modulating vascular function and driving atherogenesis. Conversely, brown and beige adipose tissues utilise glucose and lipids to generate heat and are associated with improved cardiometabolic health. The cardiac and thoracic perivascular adipose tissues are now understood to be composed of brown adipose tissue in the healthy state and undergo a brown-to-white transition i.e. during obesity which may be a driving factor of cardiovascular disease. In this review we discuss the risks of excess cardiac and vascular adiposity and potential mechanisms by which restoring the brown phenotype i.e. "re-browning" could potentially be achieved in clinically relevant populations.

1. Introduction

Excess adiposity is a major independent risk factor for cardiovascular disease (CVD) [1,2] and the associated metabolic syndrome. Pathological changes in white adipose tissue with obesity directly contribute to both metabolic abnormalities and the atherosclerotic process [3,4]. Visceral adiposity, compared to subcutaneous fat accumulation, is recognised to have a greater impact on cardiovascular disease (CVD) which may be due in part to its close proximity to the heart. In contrast, brown adipose tissue (BAT) is a thermogenic organ that expresses the unique uncoupling protein (UCP)1 on the inner mitochondrial membrane, enabling it to circumvent ATP production and dissipate chemical energy as heat [5]. In humans reduced BAT function is closely associated with obesity, compromised metabolic health and cardiovascular risk [6–8]. The activation of existing BAT, through the recruitment of brown adipocytes or the 'browning' of white adipocytes to 'beige' cells could be a new therapeutic target for combating cardiometabolic disease.

The purpose of this review will be to a) give an overview of the health risks of excess cardiac and vascular adipose tissues b) discuss how this may be related to a transformation from brown to white adipose tissue ("whitening") and c) highlight potential interventions to 'brown' these depots with the specific intent of improving cardiovascular health.

2. Defining the cardiac adipose tissues

Terms to describe cardiac adipose tissue vary in the literature and are used interchangeably. It is therefore important to clarify the specific anatomical location and origin of each fat depot as despite their close proximity they have distinct differences in embryological origin [9] (Fig. 1).

2.1. Paracardial adipose tissue

Often termed intra-thoracic [10], mediastinal [11] or pericardial, is situated on the external surface of the fibrous layer of the pericardium, vascularised by non-coronary arteries and consists of adipocytes originating from the thoracic mesenchyme [9].

2.2. Epicardial adipose tissue (EAT)

EAT is considered to originate from the splanchnic mesoderm, however, recently it is shown to be derived from mesenchymal transformation of cells in the epicardium [12,13]. It is vascularised by branches of the coronary arteries. EAT is located between the myocardium and the visceral layer of the pericardium [12] accounting for ~20% of total heart weight [14], covering 80% of the cardiac surfaces [15] and present in the atrioventricular and interventricular

* Corresponding author at: Division of Child Health, Obstetrics and Gynaecology, School of Medicine, University Hospital, University of Nottingham, Nottingham NG7 2UH, UK.
E-mail address: michael.symonds@nottingham.ac.uk (M.E. Symonds).
[1] Contributed equally.

http://dx.doi.org/10.1016/j.ijcard.2016.11.074

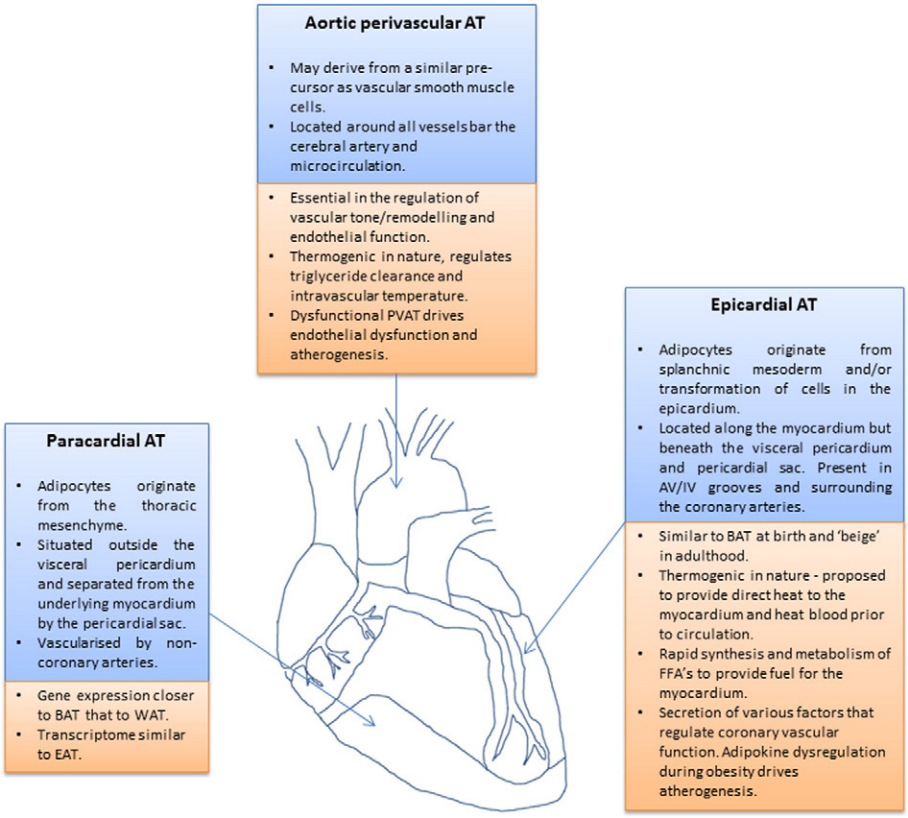

Fig. 1. Anatomical location, physiological and pathological roles of paracardial, epicardial and perivascular adipose tissues.

grooves, within and along the myocardium and surrounding the coronary arteries [14,16]. Importantly, there is no fibrous layer separating EAT from the underlying myocardium and coronary vessels hence the theory that EAT locally modulates CVD risk by secreting factors acting in a paracrine fashion on both cardiomyocytes and the vasculature.

2.3. Pericardial adipose tissue

Pericardial adipose tissue is a broad term used when referring to the total mass of both epicardial and paracardial adipose tissues.

2.4. Intramyocardial adipose tissue

This term is given to the adipocytes located within the myocardium itself. Classically these have been hypothesised to spill over into the myocardium from the adjacent hypertrophic EAT due to the absence of muscle fascia putatively contributing to lipotoxicity in adjacent cardiomyocytes [17]. More recently however it has been shown that intramyocardial lipid accumulation occurs when adipocytes are generated both from the developing endocardium [18] and by the differentiation of atrial cardiac mesenchymal progenitors [19].

2.5. Perivascular adipose tissue (PVAT)

PVAT is defined as the adipose tissue situated outside the blood vessels being structurally distinct from the adventitia and also not separated from it by a fibrous layer. Present in varying amounts around all arteries bar the cerebral artery and microcirculation [20].

3. Physiological roles of the cardiac and vascular adipose depots

3.1. Paracardial adipose tissue

Little is known about its precise role with most studies predominantly focussed on either perivascular or EAT due to their close proximity to the vasculature. Its gene expression profile is closer to that of BAT than subcutaneous adipose tissue [11] and its transcriptome is also similar to EAT [21] in men with CVD. Paracardial adipose tissue expresses a pathogenic profile characterised by increased expression of glucocorticoids and macrophage infiltration during CAD [22,23]. Hypothetically, it may be both thermogenic and a metabolically active endocrine organ capable of contributing to systemic inflammatory processes modulating CVD progression.

3.2. EAT

It serves a multitude of roles essential to both survival and cardiovascular function. As the depot of fat that surrounds the coronary arteries, EAT acts in a similar fashion to PVAT providing mechanical protection during the contraction from neighbouring tissues [9,24] such as the myocardium. Similarly, as a perivascular depot EAT plays a key role in modulating coronary vascular tone and function through the secretion of numerous vasoactive factors such as leptin [25,26], adiponectin [27], nitric oxide [28] and angiotensin (1–7) [29] among others [20]. Metabolically, EAT has the highest rate of lipogenesis and free fatty acid (FFA) metabolism of all fat depots [30], although this was observed in adult guinea pigs and has not been replicated in other animal models or humans. EAT is hypothesised to store intravascular FFA to protect cardiomyocytes from excess exposure when raised in plasma, but also releases them to provide energy for the myocardium [30,31]. The storage hypothesis of excess FFAs as a protective function against myocardial lipotoxicity has not been rigorously tested because this

would require the coronary arteries to perfuse EAT before they penetrate the myocardium as distinct vessels which is not normally the case. Physiologically the propensity to rapidly synthesise and metabolise FFA is vital given that in humans they are the primary fuel of the myocardium [32]. EAT expresses thermogenic genes typically associated with BAT and beige adipose tissue [33,34]. It has been proposed to provide direct heat to the myocardium conferring a survival advantage by protecting the heart during hypothermia, ischaemia or hypoxia [34]. There is no direct evidence however to suggest that these adipocytes produce heat and given their location adjacent to the contracting myocardium it is feasible they may function in non-thermogenic roles such as to alter myocardial and/or vascular redox state [33], a hypothesis supported by evidence that the 'browning' process modulates redox state [35] and also by the recent finding that components of the mitochondrial electron transport chain in PVAT are essential to vascular function [36]. Expression of thermogenic genes in this depot however are associated with systemic lipid homeostasis [37] and EAT may also contribute to the uptake of intravascular FFA and protect the coronary vasculature from hypertriglyceridemia associated damage. Furthermore the distribution of putatively thermogenic EAT around the coronary arteries suggest the possibility that it might be involved in maintaining myocardial temperature by heating blood in the coronaries en route to the heart [38].

3.3. PVAT

In healthy adults the secretory profile of PVAT is essential in the regulation and maintenance of vascular tone, remodelling and endothelial function [39]. Under pathophysiological conditions such as obesity PVAT becomes dysfunctional and compared to subcutaneous and other visceral depots expresses a higher inflammatory profile [40], releasing angiogenic factors [41] and inducing the proliferation of vascular smooth muscle cells [42] leading to endothelial dysfunction and atherosclerosis [39]. Similar to both paracardial and EAT, PVAT is phenotypically brown though their appearance depends on anatomical location such that PVAT surrounding the thoracic aorta exhibits brown characteristics and PVAT surrounding the abdominal aorta is a mixture of brown and white [43–45]. Interestingly, the ablation of PVAT in mice and the subsequent loss of its thermogenic properties impairs triglyceride clearance rendering them unable to regulate intravascular temperature [44] implicating PVAT as a key player in the maintenance of thermal homeostasis.

4. Excess cardiac and vascular adiposity and CVD risk

Despite Mazur et al. [46] stating in 2010 that EAT is not an independent predictor of metabolic syndrome in children and adolescents and that the prognostic value of this tissue may differ comparative to the adult population, cross-sectional epidemiological imaging data using echocardiography demonstrates a clear direct relationship between EAT and CVD risk. In obese adolescents with metabolic syndrome EAT thickness (EATT) was raised and positively correlated with fasting plasma glucose and triglycerides, HOMA-IR, carotid IMT and a range of parameters of cardiac dysfunction including left ventricular mass and myocardial performance index [47]. Similar results between lean and obese adolescents were shown by Boyraz et al. [48] who further divided the obese group into mild–moderate and severe obesity where EAT was only positively correlated with the majority of metabolic and clinical parameters in the latter group. Conversely, in both overweight and obese adolescents, EAT was significantly correlated with parameters of lipid metabolism i.e. triglycerides, HDL-C and ApoB in addition to uric acid and alanine aminotransferase indicative of a possible link between increased EAT and non-alcoholic fatty liver disease [49]. The accumulation of excess EAT has a clear association with cardiometabolic parameters in obese children and adolescents and as such makes this depot a particularly attractive target as interventions that can reduce or prevent excess cardiac adiposity in early life may be more relevant in modulating cardiovascular risk in adulthood.

The association between EAT or volume continues through to adulthood where it becomes even more pronounced and is strongly correlated with the progression and severity of CAD [50–53]. The most common method to quantify EATT has traditionally been echocardiography which has some major limitations in its accuracy. For instance, typical measurements include quantifying EATT over the just one location i.e. the anterior right ventricle [50–52] or the thickness of extra-pericardial and EAT combined [53] and therefore do not constitute a true representation of the association of coronary EAT and cardiovascular risk and/or coronary atherosclerosis. Multi-detector computed tomography (MDCT) however, by way of a higher resolution and 3D views is able to accurately quantify the exact amount of EAT in various locations based on tissue density and has the ability to specify the tissue directly around the coronary arteries [10]. Similar to echocardiography studies, peri-coronary EAT (pc-EAT) is increased in CAD patients [54] and is also associated with other risk factors such as coronary artery calcium, hypertension and diabetes [55]. More detailed analysis demonstrates that vessels with coronary plaque show increased pc-EAT and that is further increased in vessels containing mixed plaques supporting the relationship of excess EAT to the atherosclerotic process. Similarly, after calculating the average thickness of pc-EAT surrounding all three coronary arteries it was shown to be thicker in those vessels with obstructive atherosclerosis [56]. These human cross-sectional studies do not prove a causal role for EAT in the pathogenesis of CAD. However, evidence for causality was generated in a pig model of coronary atherosclerosis, in which the resection of EAT from the anterior descending coronary artery ameliorated atherosclerotic plaque progression within the vessel but only at the site of adipectomy [57].

5. Cardiac and vascular adipose tissue dysfunction

It is hypothesised that pathological changes occurring in cardiac and vascular adipose tissues as they become hypertrophic from positive energy balance cause their association with CVD risk. During both ageing and chronic overnutrition, white adipose tissues expand by hypertrophy of existing adipocytes and hyperplasia of adipocyte pre-cursors [58,59] with the concomitant recruitment of immune cells, activation of inflammatory signalling pathways, leading to adipose tissue dysfunction and a pro-inflammatory phenotype [60]. Similar to white adipocytes with the onset of obesity, multilocular lipid droplets in BAT accumulate lipid becoming hypertrophic and outstrip the vascular supply. This creates a hypoxic microenvironment leading to diminished mitochondrial function, adrenergic signalling, increased inflammation and insulin resistance [61–63]. Data from rodents [43], sheep [64,65] and humans [11] indicate that the cardiac and vascular adipose tissues are phenotypically brown during the early stages of life and despite whitening with age retain brown characteristics in adulthood [11,21,33]. It could be hypothesised that further whitening of cardiac and vascular adipose tissues in obesity and the subsequent dysfunction that occurs could drive a hypoxic, inflammatory microenvironment affecting the vasculature and driving coronary atherosclerosis (Fig. 2). In support of this theory is evidence that the EAT of individuals with CAD is associated with a brown-to-white trans-differentiation characterised by significant decreases in thermogenic genes and upregulation of white adipogenesis [66]. This brown-to-white phenotype is associated with a significant increase in EAT reactive oxygen species production [66] whilst the EAT transcriptome is also characterised by markers of inflammation [67]. Furthermore, the association between EAT expression of UCP1 and circulating HDL/triglycerides suggests that functional brown adipocytes in this depot could modulate lipid metabolism in humans [37]. Given dyslipidaemia is a major contributor to atherogenesis this may be another mechanism whereby the brown-

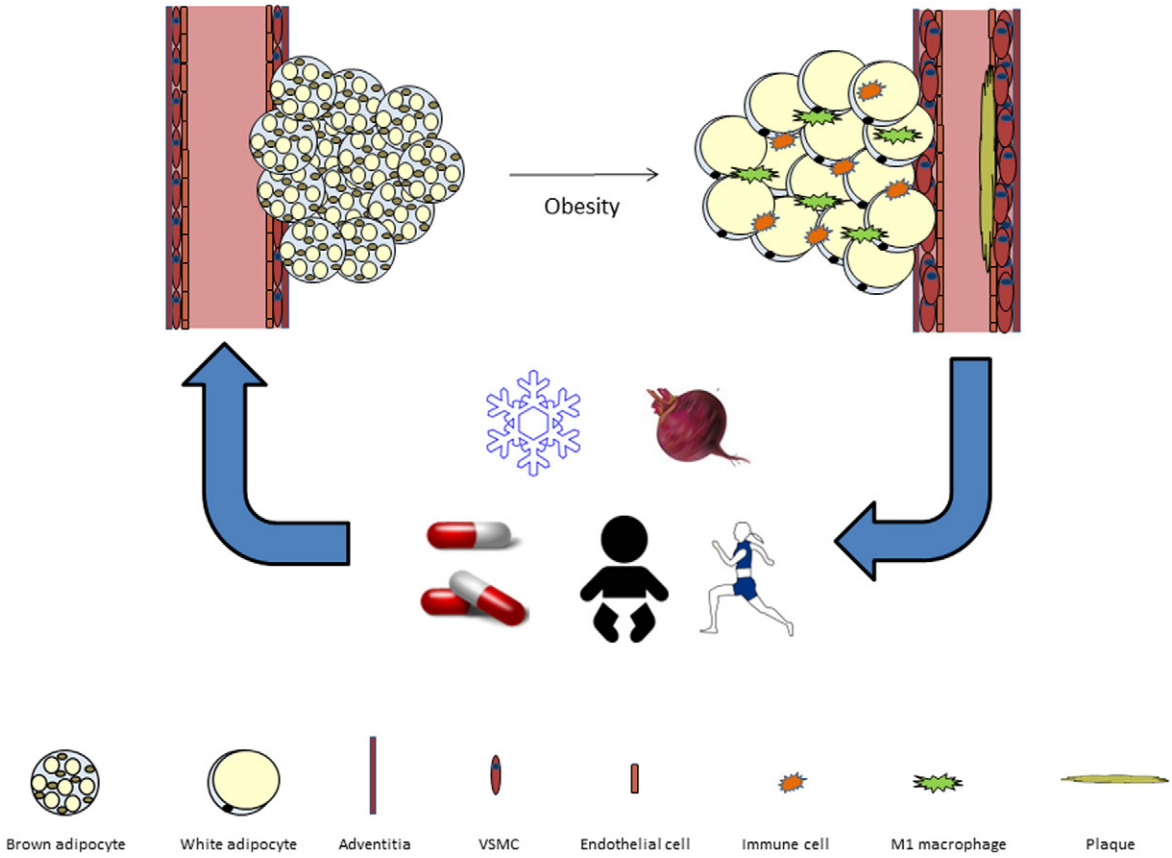

Fig. 2. Summary figure. In the healthy state cardiac and vascular adipose tissues resemble BAT. During obesity these tissues become hypertrophic, inflammatory and dysfunctional driving endothelial dysfunction and atherogenesis. Maternal and early life (intra/extra-uterine environment), Cold exposure (SNS mediated norepinephrine release), exercise (myokine/cardiomyokine secretion), Pharmacological activation (β3 agonists and GLP1 receptor agonists) and dietary factors (nitrates/fatty acids) may modulate cardiovascular health by restoring the brown phenotype in these tissues.

to-white switch in cardiac and vascular adipose tissues drives disease progression.

Brown and beige adipose tissues have generated significant scientific interest due to their unique ability to oxidise large amounts of glucose and lipids during UCP1 mediated thermogenesis. It is now postulated that increasing brown and/or beige adipose mass and activity is a feasible target to prevent obesity and related cardiometabolic disease [68,69]. Adult humans retain significant amounts of metabolically active BAT which is inversely associated with BMI, age and metabolic health and importantly can be activated by either cold exposure or a B3-agonist administration [6,70–74]. BAT can modulate glucose and lipid homeostasis in addition to insulin stimulated glucose disposal, insulin sensitivity and diet induced thermogenesis [75–78] with substantial benefits seen in the insulin sensitivity of Type 2 diabetics [79] thus highlighting its potential clinical importance. Further evidence for a beneficial role of BAT from rodent studies demonstrates that its activation corrects hyperlipidemia [80], reduces hypercholesterolemia and protects from the development of atherosclerosis [81]. Transplantation of BAT apparently, improves not only whole body metabolism but the function of the heart and other WAT depots [82,83]. Meanwhile beige adipocytes are functionally thermogenic and their induction is also associated with metabolic benefits [84,85] suggestive that 'browning' white depots may promote similar cardiometabolic benefits.

6. 'Browning' cardiac and vascular adipose tissues to reduce cardiovascular risk

Modulation of the cardiac and vascular adipose tissue to increase the proportion of thermogenic brown or beige adipocytes could be a feasible way to improve local inflammation and reduce cardiovascular risk. However whilst there are an array of methods to 'brown' fat in rodents, few of these are at a stage where they could be translated to the human population, thus we will discuss only those that may have an immediate clinical application.

6.1. Pregnancy and early life

It is now understood that both maternal health and factors during early life have a direct influence on the phenotype of offspring adipose tissues [86,87]. We have recently shown (in press) that EAT of the human neonate (0–29 days age) is phenotypically brown consisting of multilocular, UCP1 positive adipocytes. During the progression to infancy (1–12 months) and childhood (1–8 years) EAT undergoes a transition to primarily unilocular, UCP1 negative adipocytes with only a subset in these older age-groups having discrete islands of UCP1 positive cells. Interestingly, and similar to anorexic individuals who exhibit a reduction in the thermogenic activity of BAT [88,89] subjects underperforming in growth scores exhibited a downregulation of thermogenic gene expression in EAT. This suggests that where nutrient availability is compromised the thermogenic machinery is reduced to maintain metabolic homeostasis. Whilst it is important to remain cautious when extrapolating results from children with various comorbidities the brown-to-white transition in early life and regulation of tissue composition during nutrient scarcity supports our previous work in sheep.

Similar to humans sheep are born with maximal, fully functional BAT to defend against hypothermia at birth making them an ideal large animal model to study the development of brown adipose tissues in early life [90]. Similar to the human neonate a clear morphological

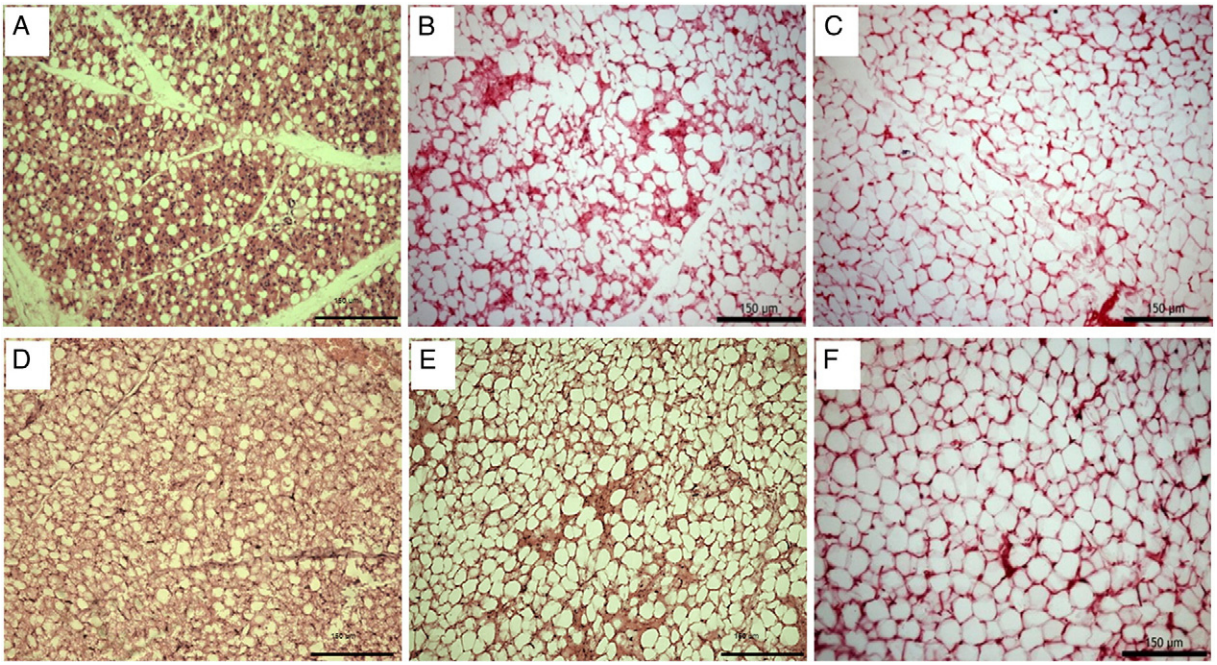

Fig. 3. Histological brown-to-white transition of ovine paracardial adipose tissue at 1(A), 7 (B)and 28 (C) days after birth and epicardial adipose tissue at 1 (D), 7 (E) and 28 (F) days after birth. Scale bar = 150 μm

transition can be seen to occur in epicardial and paracardial AT of sheep where it resembles BAT at birth but is WAT by 28 days of age (Fig. 3). The adverse effects of the intra uterine environment during undernutrition and concomitant low birth weight have long been hypothesised to result in an increased risk of CVD [91]. Maternal nutrient restriction during late gestation in the sheep [64] down regulates the expression of thermogenic, adrenergic and mitochondrial genes in paracardial AT suggestive that reduced nutrient availability to the growing foetus compromises the thermogenic capacity of the cardiac adipose tissues. Interestingly, nutrient restriction earlier in pregnancy followed by ad-libitum feeding upregulates both UCP1 and genes involved in both white (i.e. *C/EBP*a and HoxC9) and brown (i.e. BMP7) adipogenesis [65] in pericardial AT. In rodents, the offspring of obese dams demonstrates that there is a diminished anti-contractile effect of PVAT occurring prior to both obesity and hypertension [92]. These studies highlight the importance of maternal nutrient status as it has the ability alter the thermogenic and adipogenic potential of cardiac adipose tissues whilst also programming offspring for hypertension in the absence of measureable changes in adiposity or blood pressure. Further investigations in both small and large mammals and children with CVD should be conducted to investigate the influence of maternal and early life factors on the function of these tissues. From a clinical and public health perspective it is essential to work to improve maternal and offspring health to prevent deleterious effects to the cardiac and vascular adipose tissues early in life.

6.2. Cold exposure

Cold exposure is the most well established activator of BAT and the browning of WAT [93,94], which in mice also increases lipid clearance from the circulation [95] and ameliorates hyperlipidaemia [96]. Cold exposure improves the lipid profile of humans; for example, patients with hypercholesterolaemia exposed to 14 °C water over a period of 90 days had decreased LDL and total cholesterol [97]. In young healthy human volunteers undergoing controlled overnight exposure at 19 °C, improvements were seen in insulin sensitivity concomitant with an increase in BAT abundance [78].

These beneficial effects of cold exposure and BAT activation are, however, in contrast to the increased incidence of acute myocardial infarction (AMI) mortality reported in the winter months in European countries [98] and the USA [99]. Elderly individuals exposed to cold are most at risk [100] and also may lack BAT which could have a role in increased sensitivity to cold. Paradoxically increased winter mortality from AMI has also been reported in countries such as Portugal where the temperature shows relatively little seasonal variation but has higher winter AMI mortality compared to those in Northern Europe [98], indicating that factors other than temperature may also be involved. For example, it is also known that respiratory infections are increased in winter and can increase the risk of AMI [101]. Due to possible confounding factors it is difficult to elucidate the mechanism between cold exposure and possible adverse or beneficial effects on CVD risk in epidemiological studies.

Associations between cold exposure, BAT activity and atherosclerosis have been examined in controlled conditions using animal models but have reported conflicting results. A possible mechanism for cold exposure and increased AMI was proposed by Dong et al. who reported that in ApoE −/− Ldlr −/− mice exposed to 4 °C, atherosclerotic plaque growth and instability increased but was not observed with UCP1 deletion [102]. However these mice lack functional hepatic lipid clearance and cold exposure improves lipid profile in APOE*3-Leiden·CETP mice where hepatic lipid clearance is conserved [81]. A more recent study has reported however that ApoE −/− mice have increased atherosclerosis at thermoneutrality (30 °C) compared to 22 °C [103]. This raises interesting questions about the severity of cold challenge and CVD risk. It is known that mild cold exposure is sufficient to activate human BAT [78] and could therefore be activated without possible adverse effects occurring in severe cold. Therefore the beneficial adaptations to cold challenge with BAT activation still remain topics that warrant further investigation and particular caution in clinical populations with manifest CVD.

6.3. Pharmacological activation

Very few of the pharmacological agents used in pre-clinical research to induce browning are at a stage where they could be used in clinical

studies. Fortunately, however, there exist two which are in use clinically at present and have recently been shown to induce a brown phenotype in WAT. The first of these is a new selective β3-agonist (Mirabegron) developed using cloned human β3 receptors that is currently licenced in the UK for the treatment of incontinence [104]. Previous β3-agonists mimic the effects of cold-exposure and activate beige adipocytes [93,105] in animal models but only produce short-term improvements in heat production, insulin sensitivity and fat oxidation in humans [106–109]. These discrepancies between efficacy are due to differences in receptors, pharmacokinetic properties and bioavailability between species [110] with various undesirable off-target effects on the cardiovascular system reported [111]. When given to BAT-positive healthy males Mirabegron acutely activates BAT thermogenesis and increases resting metabolic rate [112] though the dose used was four times (200 mg vs. 50 mg) that recommended for alleviating symptoms of overactive bladder and was associated with increased heart rate and both systolic and diastolic blood pressure. Efficacy of this agent at lower doses and during chronic administration still needs to be determined. Should a safe dose be established that can 'brown' adipose tissues it would become a good candidate to induce browning of cardiac and vascular adipose tissues by pharmacological means.

Glucagon-like peptide 1 (GLP-1) agonists Exenatide and Liraglitude are currently in clinical use for the management of hyperglycaemia in type 2 diabetes. They have been shown in both animal studies and during post-hoc analysis of phase-3 studies, as well as in the randomised double-blinded prospective Leader trial [113] to have benefits on the cardiovascular system and, in the Leader trial, major adverse cardiac events. In mice it has recently been shown that the metabolic benefits of GLP-1 agonists may occur in part through the activation of BAT and the 'browning' of WAT depots [114–116]. When delivered through intracerebroventricular injection, GLP-1 [114] and its analogue exendin-4 [115] increase BAT thermogenesis, mediated via an increased uptake of TG-derived FA's and plasma glucose in addition to browning WAT, effects which may occur by activation of hypothalamic AMPK [116]. Similar results have been demonstrated when GLP-1 agonists have been administered peripherally [117–119] with the browning of WAT suggested to occur via upregulation of SIRT1 [120]. Whilst these effects remain to be confirmed in humans it is feasible that GLP-1 agonists could be suitable candidates to induce browning of visceral adipose tissues.

6.4. Exercise

Exercise is a key modulator of cardiometabolic health [121] and elicits a number of benefits on adipose tissues including a reduction in cell number/size and inflammation [122], upregulated angiogenesis [123] and mitochondrial biogenesis [124]. In recent years it has emerged that another mechanism by which exercise improves metabolic health in rodents is by the browning of WAT whereby myokines, produced during muscular contractions, are secreted into the circulation and act in an endocrine manner on adipose tissues [125,126]. A number of these factors are also secreted from cardiomyocytes and we speculate that these 'cardiomyokines' act on local cardiac and vascular adipose tissues to induce 'browning' and modulate cardiovascular health. Of these secreted factors, FGF21 is understood to be a potent 'browning' agent in rodents though its significance in humans is a topic of much debate [127]. FGF21 however is induced following exercise [127], secreted by cardiomyocytes [128] and regulates cardiac physiology [129]. It is therefore feasible that this cardiomyokine acts in a paracrine manner on EAT to induce a brown phenotype and modulate cardiovascular health. Similarly, though the subject of much debate, irisin [130] is an exercise induced PGC1-α dependent myokine that induces the browning of WAT [126,131] whilst meteorin1, a PGC1-α4 regulated myokine induces a brown phenotype in WAT by promoting IL4/IL13 production from eosinophils and alternative M2 macrophage activation [125]. Interestingly both irisin and meteorin1 are produced by cardiac tissue and the pericardial connective tissue [132,133]. If these are further upregulated post-exercise it is feasible that they could modulate the phenotype of the local adipose depots. Natriuretic peptides are classically secreted cardiac factors well known for their role in modulating cardiovascular homeostasis and browning adipose tissues [134] which are also upregulated post-exercise [135,136]. The existence of a paracrine axis between beige EAT as the target and natriuretic peptides released from the atria and ventricles into the ventricular blood and then the aorta and coronary arteries seems possible but remains to be proven. Other factors that may play a role include IL-6 [137] and the metabolite lactate which is significantly increased during exercise and has recently been postulated to brown WAT to modulate tissue redox state [35]. In summary, there are an array of factors postulated to induce browning which are secreted from cardiac tissues and may act on the local adipose tissues to improve their phenotype. The effect of increasing physical activity prior to cardiac surgeries on the function of these adipose depots should be investigated in future clinical studies.

6.5. Nutritional intervention

Diet induced thermogenesis was initially reported by Rothwell and Stock where an upregulation of UCP1, increased BAT mass and reduced energy cost of weight gain occurred in rats fed a cafeteria diet [138]. Although diet induced thermogenesis is more controversial than cold induced thermogenesis [139] there have been several reports of nutrients and dietary compounds capable of BAT activation. Interestingly, some of these are also known to have cardio-protective effects that could be speculated to involve the browning of vascular adipose tissue depots.

Dietary nitrates, found in green leafy vegetables and beetroot have been found to have beneficial effects on lowering blood pressure and improving endothelial function in several human intervention studies [140,141]. This is thought to be through the metabolism of nitrates to nitric oxide which is known to cause vasodilation of resistance vessels [140]. At least in some humans, dietary nitrates have also been found to increase platelet cyclic GMP [142], a signalling molecule involved in brown adipocyte thermogenesis and mitochondrial biogenesis [143,144]. A recent study has found that feeding nitrates to rats and mice results in the upregulation of thermogenic and beta oxidation genes and UCP1 abundance in both white and brown adipose tissues through the cyclic GMP/protein kinase G pathway [145]. These browning effects were augmented in hypoxic conditions, similar to those in adipose tissue of obese individuals [145], which provides further promise for beneficial effects of dietary nitrate. This evidence provides the rationale for studies in humans to assess BAT activation with dietary nitrate which to date have not been conducted.

Conjugated Linoleic Acid (CLA) exists as a group of isomers of linoleic acid (C18:2n − 6), of which the two main biologically active isomers are the *cis*-9, *trans*-11 and the *trans*-10, *cis*-12. The *cis*-9, *trans*-11 isomer is naturally the most abundant (up to ~90% of total CLA [146]) and is found in ruminant dairy and meat products, where the *trans*-10, *cis*-12 isomer makes up a small percentage (~0.03–1.5% of total CLA [146]). These isomers are also commercially available as a supplement, where the isomers are generally mixed in varying levels.

Animal and, to a lesser extent, human studies have shown promising results for CLA supplementation in the prevention of atherosclerotic plaque development and improvements in lipid profile [147,148]. There have also been several studies suggesting that CLA supplementation in humans can favourably alter body composition, by reducing body fat percentage [149–151], however, other studies have not observed this [152,153]. Clear mechanisms for these cardioprotective and body compositional effects of CLA are yet to be fully identified, and there is potential that BAT could be involved in both although there are no human studies that indicate that browning can be induced by CLA. In mice the *trans*-10, *cis*-12 isomer increases energy expenditure, which correlated with increases in UCP1 mRNA [154,155],

with other studies finding that the *trans*-10, *cis*-12 isomer alone, or as a mixed isomer with *cis*-9, *trans*-11 causes browning of WAT and increased UCP1 [156], however other studies have failed to show this [157]. Work in our laboratory has shown that suckling sheep receiving milk from a mother supplemented with dietary fatty acids, which increased concentrations of total and *cis*-9, *trans*-11 CLA, exhibited an increase in UCP1 [158]. It is possible that the observed increase in UCP1 could be caused by an increase in noradrenaline, which has been reported in mice fed a mixed CLA supplement [159] and is a known activator of UCP1 [160].

There have been some negative side effects of CLA supplementation including low grade inflammation [156], however a longer term trial in humans showed no difference in adverse events between CLA supplemented and placebo groups [151]. The variable results seen between studies could be explained by the differing concentrations and doses of individual CLA isomers administered in each study. These variations make comparisons difficult and conclusions as to the role of CLA are hard to draw. More studies using a pure isomer supplementation are needed to establish causation, and whether CLA promotes adipose tissue browning in humans.

Diets rich in omega 3 polyunsaturated fatty acids, particularly long chain eicosapentaenoic acid (C20:5 n − 3, EPA) and docosahexaenoic acid (C22:6 n − 3, DHA) from marine sources or fish oil supplementation have been shown to reduce the risk of cardiovascular disease in human epidemiological studies [161] and have beneficial effects on decreasing blood pressure [162], inhibiting the progression of atherosclerosis [163], lowering plasma triglycerides and de novo lipogenesis [164]. A recent study has found that feeding mice fish oil enriched in either DHA (DHA 25%, EPA 8%) or EPA (EPA 28%, DHA 12%) induces UCP1 in both BAT and WAT through TRPV1, although browning of vascular adipose tissues in particular was not investigated. The beige marker Tbx1 and thermogenic genes such as FGF21 were also upregulated in the inguinal WAT depot [165]. An earlier report in mice however suggested that dietary supplementation with EPA/DHA to a high fat diet decreased visceral AT mass but no change in UCP1 [166]. These differing results may be, at least in part, due to the different dietary macronutrient compositions and varying amounts of EPA and DHA fed to the mice as Kim et al. used DHA (25%, EPA 8%) or EPA (EPA 28%, DHA 12%) and Janovska et al. used 46% DHA, 14% EPA. Ambient temperature also differed between the studies as Kim et al. utilised a temperature of 23 °C whereas Janovska et al. adopted thermoneutrality (30 °C) which may affect brown adipose activation. The optimum dose of EPA/DHA and conditions to promote browning in rodents is still unknown.

A recent in vitro study has shown promising results in human primary pre-adipocytes, where treatment with EPA but not DHA caused pronounced upregulation of UCP1 and mitochondrial function in pre-adipocytes and mature adipocytes [167]. Interestingly, arachidonic acid (C20:4, n − 6) treatment upregulated the white adipocyte marker TCF21. A low dietary omega 3:6 fatty acid ratio has been associated with increased CVD risk [168], it can be speculated that an increased white adipogenesis with impaired browning due to lack of omega 3 fatty acids may play a role. The effects of these fatty acids on adipose tissue browning have not yet been determined in vivo and require further investigation.

7. Summary

Human cardiac and perivascular adipose tissues are phenotypically brown early in life but whiten with age and obesity, becoming dysfunctional and contributing to atherogenesis in the local vasculature. Whilst active BAT may offer protection from metabolic disease, re-inducing a brown phenotype in the cardiac and vascular adipose tissues i.e. “re-browning” may be a more direct way of reducing cardiovascular risk as it likely reduces local inflammation and hypoxia adjacent to the vascular wall thus attenuating endothelial dysfunction and the atherogenic process.

This re-browning of cardiac and vascular adipose tissues may be achieved using a variety of dietary, environmental and pharmacological strategies. Future clinical trials should be considered to investigate the effects of the most appropriate interventions on the adipose tissues prior to cardiac surgeries as has been done previously when determining the effect of various treatments on vascular and myocardial tissues [169–172]. If the brown phenotype can be induced in these tissues in clinical populations it will facilitate longer studies to determine if they can attenuate the atherosclerotic process. Future pre-clinical work could be directed at a) investigating the precise role each of these depots play in driving atherogenesis and other cardiovascular diseases b) determining how manipulation of the intrauterine and early life environment affects long-term function of these depots and c) develop new methods to brown these depots in adulthood.

Conflict of interest statement

The authors report no relationships that could be construed as a conflict of interest.

Acknowledgements

P. Aldiss is funded by the British Heart Foundation (FS/15/4/31184), G. Davies is funded by University of Nottingham and Cardiometabolic Research Foundation, Los Angeles (CRFLAPhD2012) and R. Woods is funded by the BBSRC (BBSRCBB/I016015/1).

References

[1] H.B. Hubert, M. Feinleib, P.M. McNamara, W.P. Castelli, Obesity as an independent risk factor for cardiovascular disease: a 26-year follow-up of participants in the Framingham Heart Study, Circulation 67 (1983) 968–977.
[2] J.M. Hughes-Austin, B.A. Larsen, M.A. Allison, Visceral adipose tissue and cardiovascular disease risk, Curr. Cardiovasc. Risk Rep. 7 (2013) 95–101.
[3] F. Maresca, et al., Adipokines, vascular wall, and cardiovascular disease: a focused overview of the role of adipokines in the pathophysiology of cardiovascular disease, Angiology 66 (2015) 8–24.
[4] K. Nakamura, J.J. Fuster, K. Walsh, Adipokines: a link between obesity and cardiovascular disease, J. Cardiol. 63 (2014) 250–259.
[5] B. Cannon, J. Nedergaard, Brown adipose tissue: function and physiological significance, Physiol. Rev. 84 (2004) 277–359.
[6] A.M. Cypess, et al., Identification and importance of brown adipose tissue in adult humans, N. Engl. J. Med. 360 (2009) 1509–1517.
[7] R. Takx, et al., Supraclavicular Brown adipose tissue FDG uptake and cardiovascular disease, J. Nucl. Med. 57 (8) (2016) 1221–1225.
[8] W.D. van Marken Lichtenbelt, et al., Cold-activated brown adipose tissue in healthy men, N. Engl. J. Med. 360 (2009) 1500–1508.
[9] G. Iacobellis, Local and systemic effects of the multifaceted epicardial adipose tissue depot, Nat. Rev. Endocrinol. 11 (2015) 363–371.
[10] D. Dey, R. Nakazato, D. Li, D.S. Berman, Epicardial and thoracic fat - noninvasive measurement and clinical implications, Cardiovasc. Diagn. Ther. 2 (2012) 85–93.
[11] L. Cheung, et al., Human mediastinal adipose tissue displays certain characteristics of brown fat, Nutr. Diabetes 3 (2013), e66.
[12] Y. Yamaguchi, et al., Adipogenesis and epicardial adipose tissue: a novel fate of the epicardium induced by mesenchymal transformation and PPARgamma activation, Proc. Natl. Acad. Sci. U. S. A. 112 (2015) 2070–2075.
[13] H.S. Sacks, J.N. Fain, Human epicardial adipose tissue: a review, Am. Heart J. 153 (2007) 907–917.
[14] D. Corradi, et al., The ventricular epicardial fat is related to the myocardial mass in normal, ischemic and hypertrophic hearts, Cardiovasc. Pathol. 13 (2004) 313–316.
[15] J. Shirani, K. Berezowski, W.C. Roberts, Quantitative measurement of normal and excessive (cor adiposum) subepicardial adipose tissue, its clinical significance, and its effect on electrocardiographic QRS voltage, Am. J. Cardiol. 76 (1995) 414–418.
[16] J.M. Company, et al., Epicardial fat gene expression after aerobic exercise training in pigs with coronary atherosclerosis: relationship to visceral and subcutaneous fat, J. Appl. Physiol. (1985) 109 (2010) 1904–1912.
[17] K. Selthofer-Relatic, I. Bosnjak, Myocardial fat as a part of cardiac visceral adipose tissue: physiological and pathophysiological view, J. Endocrinol. Investig. 38 (2015) 933–939.
[18] H. Zhang, et al., Endocardium contributes to cardiac fat, Circ. Res. 118 (2) (2016) 254–265.
[19] D. Kami, T. Kitani, T. Kawasaki, S. Gojo, Cardiac mesenchymal progenitors differentiate into adipocytes via Klf4 and c-Myc, Cell Death Dis. 7 (2016), e2190.
[20] T. Szasz, G.F. Bomfim, R.C. Webb, The influence of perivascular adipose tissue on vascular homeostasis, Vasc. Health Risk Manag. 9 (2013) 105–116.

[21] S. Guauque-Olarte, et al., The transcriptome of human epicardial, mediastinal and subcutaneous adipose tissues in men with coronary artery disease, PLoS One 6 (2011), e19908.
[22] F. Atalar, et al., Mediastinal adipose tissue expresses a pathogenic profile of 11 beta-hydroxysteroid dehydrogenase type 1, glucocorticoid receptor, and CD68 in patients with coronary artery disease, Cardiovasc. Pathol. 22 (2013) 183–188.
[23] F. Atalar, et al., The role of mediastinal adipose tissue 11beta-hydroxysteroid d ehydrogenase type 1 and glucocorticoid expression in the development of coronary atherosclerosis in obese patients with ischemic heart disease, Cardiovasc. Diabetol. 11 (2012) 115.
[24] T. Szasz, R.C. Webb, Perivascular adipose tissue: more than just structural support, Clin. Sci. (Lond.) 122 (2012) 1–12.
[25] K. Nakagawa, et al., Leptin causes vasodilation in humans, Hypertens. Res. 25 (2002) 161–165.
[26] K. Matsuda, et al., Leptin causes nitric-oxide independent coronary artery vasodilation in humans, Hypertens. Res. 26 (2003) 147–152.
[27] G. Fesus, et al., Adiponectin is a novel humoral vasodilator, Cardiovasc. Res. 75 (2007) 719–727.
[28] Y.J. Gao, C. Lu, L.Y. Su, A.M. Sharma, R.M. Lee, Modulation of vascular function by perivascular adipose tissue: the role of endothelium and hydrogen peroxide, Br. J. Pharmacol. 151 (2007) 323–331.
[29] R.M. Lee, C. Lu, L.Y. Su, Y.J. Gao, Endothelium-dependent relaxation factor released by perivascular adipose tissue, J. Hypertens. 27 (2009) 782–790.
[30] J.M. Marchington, C.M. Pond, Site-specific properties of pericardial and epicardial adipose tissue: the effects of insulin and high-fat feeding on lipogenesis and the incorporation of fatty acids in vitro, Int. J. Obes. 14 (1990) 1013–1022.
[31] J.M. Marchington, C.A. Mattacks, C.M. Pond, Adipose tissue in the mammalian heart and pericardium: structure, foetal development and biochemical properties, Comp. Biochem. Physiol. B 94 (1989) 225–232.
[32] J.A. Wisneski, E.W. Gertz, R.A. Neese, M. Mayr, Myocardial metabolism of free fatty acids. Studies with 14C-labeled substrates in humans, J. Clin. Invest. 79 (1987) 359–366.
[33] H.S. Sacks, et al., Adult epicardial fat exhibits beige features, J. Clin. Endocrinol. Metab. 98 (2013) E1448–E1455.
[34] H.S. Sacks, et al., Uncoupling protein-1 and related messenger ribonucleic acids in human epicardial and other adipose tissues: epicardial fat functioning as brown fat, J. Clin. Endocrinol. Metab. 94 (2009) 3611–3615.
[35] A. Carriere, et al., Browning of white adipose cells by intermediate metabolites: an adaptive mechanism to alleviate redox pressure, Diabetes 63 (2014) 3253–3265.
[36] R.M. Costa, et al., H2O2 generated from mitochondrial electron transport chain in thoracic perivascular adipose tissue is crucial for modulation of vascular smooth muscle contraction, Vasc. Pharmacol. 84 (2016) 28–37.
[37] K. Chechi, P.G. Blanchard, P. Mathieu, Y. Deshaies, D. Richard, Brown fat like gene expression in the epicardial fat depot correlates with circulating HDL-cholesterol and triglycerides in patients with coronary artery disease, Int. J. Cardiol. 167 (2013) 2264–2270.
[38] H. Sacks, M.E. Symonds, Anatomical locations of human brown adipose tissue: functional relevance and implications in obesity and type 2 diabetes, Diabetes 62 (2013) 1783–1790.
[39] G. Ozen, A. Daci, X. Norel, G. Topal, Human perivascular adipose tissue dysfunction as a cause of vascular disease: focus on vascular tone and wall remodeling, Eur. J. Pharmacol. 766 (2015) 16–24.
[40] A. Omar, T.K. Chatterjee, Y. Tang, D.Y. Hui, N.L. Weintraub, Proinflammatory phenotype of perivascular adipocytes, Arterioscler. Thromb. Vasc. Biol. 34 (2014) 1631–1636.
[41] K. Rittig, et al., The secretion pattern of perivascular fat cells is different from that of subcutaneous and visceral fat cells, Diabetologia 55 (2012) 1514–1525.
[42] R. Schlich, et al., VEGF in the crosstalk between human adipocytes and smooth muscle cells: depot-specific release from visceral and perivascular adipose tissue, Mediat. Inflamm. 2013 (2013) 982458.
[43] N.K. Brown, et al., Perivascular adipose tissue in vascular function and disease: a review of current research and animal models, Arterioscler. Thromb. Vasc. Biol. 34 (2014) 1621–1630.
[44] L. Chang, et al., Loss of perivascular adipose tissue on peroxisome proliferator-activated receptor-gamma deletion in smooth muscle cells impairs intravascular thermoregulation and enhances atherosclerosis, Circulation 126 (2012) 1067–1078.
[45] T.P. Fitzgibbons, et al., Similarity of mouse perivascular and brown adipose tissues and their resistance to diet-induced inflammation, Am. J. Physiol. Heart Circ. Physiol. 301 (2011) H1425–H1437.
[46] A. Mazur, M. Ostanski, G. Telega, E. Malecka-Tendera, Is epicardial fat tissue a marker of metabolic syndrome in obese children? Atherosclerosis 211 (2010) 596–600.
[47] B. Akyol, M. Boyraz, C. Aysoy, Relationship of epicardial adipose tissue thickness with early indicators of atherosclerosis and cardiac functional changes in obese adolescents with metabolic syndrome, J. Clin. Res. Pediatr. Endocrinol. 5 (2013) 156–163.
[48] M. Boyraz, et al., Importance of epicardial adipose tissue thickness measurement in obese adolescents, its relationship with carotid intima-media thickness, and echocardiographic findings, Eur. Rev. Med. Pharmacol. Sci. 17 (2013) 3309–3317.
[49] I. Schusterova, F.H. Leenen, A. Jurko, F. Sabol, J. Takacova, Epicardial adipose tissue and cardiometabolic risk factors in overweight and obese children and adolescents, Pediatr. Obes. 9 (2014) 63–70.
[50] G. Iacobellis, et al., Echocardiographic epicardial adipose tissue is related to anthropometric and clinical parameters of metabolic syndrome: a new indicator of cardiovascular risk, J. Clin. Endocrinol. Metab. 88 (2003) 5163–5168.
[51] G. Iacobellis, et al., Epicardial fat from echocardiography: a new method for visceral adipose tissue prediction, Obes. Res. 11 (2003) 304–310.
[52] G. Iacobellis, F. Leonetti, Epicardial adipose tissue and insulin resistance in obese subjects, J. Clin. Endocrinol. Metab. 90 (2005) 6300–6302.
[53] R. Taguchi, et al., Pericardial fat accumulation in men as a risk factor for coronary artery disease, Atherosclerosis 157 (2001) 203–209.
[54] P. Maurovich-Horvat, et al., Influence of pericoronary adipose tissue on local coronary atherosclerosis as assessed by a novel MDCT volumetric method, Atherosclerosis 219 (2011) 151–157.
[55] A.M. Aydin, A. Kayali, A.K. Poyraz, K. Aydin, The relationship between coronary artery disease and pericoronary epicardial adipose tissue thickness, J. Int. Med. Res. 43 (2015) 17–25.
[56] M.B. Demircelik, et al., Epicardial adipose tissue and pericoronary fat thickness measured with 64-multidetector computed tomography: potential predictors of the severity of coronary artery disease, Clinics 69 (2014) 388–392.
[57] M.L. McKenney, et al., Epicardial adipose excision slows the progression of porcine coronary atherosclerosis, J. Cardiothorac. Surg. 9 (2014) 2.
[58] M.T. Hyvonen, K.L. Spalding, Maintenance of white adipose tissue in man, Int. J. Biochem. Cell Biol. 56 (2014) 123–132.
[59] T. Tchkonia, et al., Fat tissue, aging, and cellular senescence, Aging Cell 9 (2010) 667–684.
[60] F.M. Wensveen, S. Valentic, M. Sestan, T. Turk Wensveen, B. Polic, The "big bang" in obese fat: events initiating obesity-induced adipose tissue inflammation, Eur. J. Immunol. 45 (2015) 2446–2456.
[61] I. Shimizu, et al., Vascular rarefaction mediates whitening of brown fat in obesity, J. Clin. Invest. 124 (2014) 2099–2112.
[62] I. Shimizu, K. Walsh, The whitening of brown fat and its implications for weight management in obesity, Curr. Obes. Rep. 4 (2015) 224–229.
[63] C. Roberts-Toler, B.T. O'Neill, A.M. Cypess, Diet-induced obesity causes insulin resistance in mouse brown adipose tissue, Obesity (Silver Spring) 23 (2015) 1765–1770.
[64] S. Ojha, L. Robinson, M. Yazdani, M.E. Symonds, H. Budge, Brown adipose tissue genes in pericardial adipose tissue of newborn sheep are downregulated by maternal nutrient restriction in late gestation, Pediatr. Res. 74 (2013) 246–251.
[65] S. Ojha, M.E. Symonds, H. Budge, Suboptimal maternal nutrition during early-to-mid gestation in the sheep enhances pericardial adiposity in the near-term fetus, Reprod. Fertil. Dev. 27 (8) (2015) 1205–1212.
[66] E. Dozio, et al., Increased reactive oxygen species production in epicardial adipose tissues from coronary artery disease patients is associated with brown-to-white adipocyte trans-differentiation, Int. J. Cardiol. 174 (2014) 413–414.
[67] E.A. McAninch, et al., Epicardial adipose tissue has a unique transcriptome modified in severe coronary artery disease, Obesity (Silver Spring) 23 (2015) 1267–1278.
[68] S. Kajimura, B.M. Spiegelman, P. Seale, Brown and beige fat: physiological roles beyond heat generation, Cell Metab. 22 (2015) 546–559.
[69] K. Townsend, Y.H. Tseng, Brown adipose tissue: recent insights into development, metabolic function and therapeutic potential, Adipocyte 1 (2012) 13–24.
[70] A.M. Cypess, et al., Anatomical localization, gene expression profiling and functional characterization of adult human neck brown fat, Nat. Med. 19 (2013) 635–639.
[71] L. Robinson, S. Ojha, M.E. Symonds, H. Budge, Body mass index as a determinant of brown adipose tissue function in healthy children, J. Pediatr. 164 (2014) 318–322, e311.
[72] M.E. Symonds, et al., Thermal imaging to assess age-related changes of skin temperature within the supraclavicular region co-locating with brown adipose tissue in healthy children, J. Pediatr. 161 (2012) 892–898.
[73] V. Ouellet, et al., Outdoor temperature, age, sex, body mass index, and diabetic status determine the prevalence, mass, and glucose-uptake activity of 18F-FDG-detected BAT in humans, J. Clin. Endocrinol. Metab. 96 (2011) 192–199.
[74] T. Yoneshiro, et al., Age-related decrease in cold-activated brown adipose tissue and accumulation of body fat in healthy humans, Obesity (Silver Spring) 19 (2011) 1755–1760.
[75] J. Orava, et al., Different metabolic responses of human brown adipose tissue to activation by cold and insulin, Cell Metab. 14 (2011) 272–279.
[76] V. Ouellet, et al., Brown adipose tissue oxidative metabolism contributes to energy expenditure during acute cold exposure in humans, J. Clin. Invest. 122 (2012) 545–552.
[77] M. Chondronikola, et al., Brown adipose tissue improves whole-body glucose homeostasis and insulin sensitivity in humans, Diabetes 63 (2014) 4089–4099.
[78] P. Lee, et al., Temperature-acclimated brown adipose tissue modulates insulin sensitivity in humans, Diabetes 63 (2014) 3686–3698.
[79] M.J. Hanssen, et al., Short-term cold acclimation improves insulin sensitivity in patients with type 2 diabetes mellitus, Nat. Med. 21 (2015) 863–865.
[80] A. Bartelt, J. Heeren, Adipose tissue browning and metabolic health, Nat. Rev. Endocrinol. 10 (2014) 24–36.
[81] J.F. Berbee, et al., Brown fat activation reduces hypercholesterolaemia and protects from atherosclerosis development, Nat. Commun. 6 (2015) 6356.
[82] K.I. Stanford, et al., Brown adipose tissue regulates glucose homeostasis and insulin sensitivity, J. Clin. Invest. 123 (2013) 215–223.
[83] S.C. Gunawardana, D.W. Piston, Insulin-independent reversal of type 1 diabetes in nonobese diabetic mice with brown adipose tissue transplant, Am. J. Physiol. Endocrinol. Metab. 308 (2015) E1043–E1055.

[84] I.G. Shabalina, et al., UCP1 in brite/beige adipose tissue mitochondria is functionally thermogenic, Cell Rep. 5 (2013) 1196–1203.
[85] Y. Okamatsu-Ogura, et al., Thermogenic ability of uncoupling protein 1 in beige adipocytes in mice, PLoS One 8 (2013), e84229.
[86] M.E. Symonds, M. Pope, D. Sharkey, H. Budge, Adipose tissue and fetal programming, Diabetologia 55 (2012) 1597–1606.
[87] M.E. Symonds, M. Pope, H. Budge, Adipose tissue development during early life: novel insights into energy balance from small and large mammals, Proc. Nutr. Soc. 71 (2012) 363–370.
[88] M.A. Bredella, P.K. Fazeli, B. Lecka-Czernik, C.J. Rosen, A. Klibanski, IGFBP-2 is a negative predictor of cold-induced brown fat and bone mineral density in young non-obese women, Bone 53 (2013) 336–339.
[89] F. Pasanisi, et al., Evidence of brown fat activity in constitutional leanness, J. Clin. Endocrinol. Metab. 98 (2013) 1214–1218.
[90] M.E. Symonds, M. Pope, H. Budge, The ontogeny of brown adipose tissue, Annu. Rev. Nutr. 35 (2015) 295–320.
[91] D.J. Barker, Fetal origins of coronary heart disease, Br. Heart J. 69 (1993) 195–196.
[92] K.E. Zaborska, M. Wareing, G. Edwards, C. Austin, Loss of anti-contractile effect of perivascular adipose tissue in offspring of obese rats, Int. J. Obes. 40 (8) (2016) 1205–1214.
[93] G. Barbatelli, et al., The emergence of cold-induced brown adipocytes in mouse white fat depots is determined predominantly by white to brown adipocyte transdifferentiation, Am. J. Physiol. Endocrinol. Metab. 298 (2010) E1244–E1253.
[94] B. Cannon, J. Nedergaard, Brown adipose tissue: function and physiological significance, Physiol. Rev. 84 (2004) 277–359.
[95] W. Dijk, et al., ANGPTL4 mediates shuttling of lipid fuel to brown adipose tissue during sustained cold exposure, 2015. Elife 4, http://dx.doi.org/10.7554/eLife.08428.
[96] A. Bartelt, et al., Brown adipose tissue activity controls triglyceride clearance, Nat. Med. 17 (2011) 200–U293.
[97] F. De Lorenzo, M. Mukherjee, Z. Kadziola, R. Sherwood, V.V. Kakkar, Central cooling effects in patients with hypercholesterolaemia, Clin. Sci. (Lond.) 95 (1998) 213–217.
[98] J.D. Healy, Excess winter mortality in Europe: a cross country analysis identifying key risk factors, J. Epidemiol. Community Health 57 (2003) 784–789.
[99] S. Gonseth, S. Nussle, P. Bovet, F. Panese, J.L. Wiemels, Excess winter deaths caused by cardiovascular diseases are associated with both mild winter temperature and socio-economic inequalities in the U.S. Int. J. Cardiol. 187 (2015) 642–644.
[100] C. Guest, K. W., A. Woodward, K. Hennessy, L. Kalkstein, C. Skinner, A.J. McMichael, Climate and mortality in Australia: retrospective study, 1979–1990, and predicted impacts in five major cities in 2030, Clim. Res. 13 (1999) 1–15.
[101] T.C. Clayton, M. Thompson, T.W. Meade, Recent respiratory infection and risk of cardiovascular disease: case–control study through a general practice database, Eur. Heart J. 29 (2008) 96–103.
[102] M. Dong, et al., Cold exposure promotes atherosclerotic plaque growth and instability via UCP1-dependent lipolysis, Cell Metab. 18 (2013) 118–129.
[103] X.Y. Tian, et al., Thermoneutral housing accelerates metabolic inflammation to potentiate atherosclerosis but not insulin resistance, Cell Metab. 23 (2016) 165–178.
[104] E. Sacco, et al., Discovery history and clinical development of mirabegron for the treatment of overactive bladder and urinary incontinence, Expert Opin. Drug Discovery 9 (2014) 433–448.
[105] J. Himms-Hagen, et al., Multilocular fat cells in WAT of CL-316243-treated rats derive directly from white adipocytes, Am. J. Physiol. Cell Physiol. 279 (2000) C670–C681.
[106] C. Weyer, P.A. Tataranni, S. Snitker, E. Danforth Jr., E. Ravussin, Increase in insulin action and fat oxidation after treatment with CL 316,243, a highly selective beta3-adrenoceptor agonist in humans, Diabetes 47 (1998) 1555–1561.
[107] M.A. van Baak, et al., Acute effect of L-796568, a novel beta 3-adrenergic receptor agonist, on energy expenditure in obese men, Clin. Pharmacol. Ther. 71 (2002) 272–279.
[108] T.M. Larsen, et al., Effect of a 28-d treatment with L-796568, a novel beta(3)-adrenergic receptor agonist, on energy expenditure and body composition in obese men, Am. J. Clin. Nutr. 76 (2002) 780–788.
[109] B. Buemann, S. Toubro, A. Astrup, Effects of the two beta3-agonists, ZD7114 and ZD2079 on 24 hour energy expenditure and respiratory quotient in obese subjects, Int. J. Obes. Relat. Metab. Disord. 24 (2000) 1553–1560.
[110] J.R. Arch, Beta(3)-adrenoceptor agonists: potential, pitfalls and progress, Eur. J. Pharmacol. 440 (2002) 99–107.
[111] J.R. Arch, Challenges in beta(3)-adrenoceptor agonist drug development, Ther. Adv. Endocrinol. Metab. 2 (2011) 59–64.
[112] A.M. Cypess, et al., Activation of human brown adipose tissue by a beta3-adrenergic receptor agonist, Cell Metab. 21 (2015) 33–38.
[113] S.P. Marso, et al., Liraglutide and cardiovascular outcomes in type 2 diabetes, 2016. N. Engl. J. Med., http://dx.doi.org/10.1056/NEJMoa1603827.
[114] S.H. Lockie, et al., Direct control of brown adipose tissue thermogenesis by central nervous system glucagon-like peptide-1 receptor signaling, Diabetes 61 (2012) 2753–2762.
[115] S. Kooijman, et al., Central GLP-1 receptor signalling accelerates plasma clearance of triacylglycerol and glucose by activating brown adipose tissue in mice, Diabetologia 58 (2015) 2637–2646.
[116] D. Beiroa, et al., GLP-1 agonism stimulates brown adipose tissue thermogenesis and browning through hypothalamic AMPK, Diabetes 63 (2014) 3346–3358.
[117] K.M. Heppner, et al., Contribution of brown adipose tissue activity to the control of energy balance by GLP-1 receptor signalling in mice, Diabetologia 58 (2015) 2124–2132.
[118] Q. Wei, L. Li, J.A. Chen, S.H. Wang, Z.L. Sun, Exendin-4 improves thermogenic capacity by regulating fat metabolism on brown adipose tissue in mice with diet-induced obesity, Ann. Clin. Lab. Sci. 45 (2015) 158–165.
[119] E. Tomas, et al., GLP-1(32-36)amide Pentapeptide increases basal energy expenditure and inhibits weight gain in obese mice, Diabetes 64 (2015) 2409–2419.
[120] F. Xu, et al., GLP-1 receptor agonist promotes brown remodelling in mouse white adipose tissue through SIRT1, Diabetologia 59 (2016) 1059–1069.
[121] M.J. Joyner, D.J. Green, Exercise protects the cardiovascular system: effects beyond traditional risk factors, J. Physiol. 587 (2009) 5551–5558.
[122] F. Haczeyni, et al., Exercise improves adipose function and inflammation and ameliorates fatty liver disease in obese diabetic mice, Obesity (Silver Spring) 23 (2015) 1845–1855.
[123] B.L. Disanzo, T. You, Effects of exercise training on indicators of adipose tissue angiogenesis and hypoxia in obese rats, Metabolism 63 (2014) 452–455.
[124] V.J. Vieira, R.J. Valentine, Mitochondrial biogenesis in adipose tissue: can exercise make fat cells 'fit'? J. Physiol. 587 (2009) 3427–3428.
[125] R.R. Rao, et al., Meteorin-like is a hormone that regulates immune-adipose interactions to increase beige fat thermogenesis, Cell 157 (2014) 1279–1291.
[126] P. Bostrom, et al., A PGC1-alpha-dependent myokine that drives brown-fat-like development of white fat and thermogenesis, Nature 481 (2012) 463–468.
[127] M. Giralt, A. Gavalda-Navarro, F. Villarroya, Fibroblast growth factor-21, energy balance and obesity, Mol. Cell. Endocrinol. 418 (Pt 1) (2015) 66–73.
[128] Y. Guo, Q. Liu, Y. Gui, C. Liao, D. Xu, Exercise promotes cardiac-specific fibroblast growth factor 21 expression, Int. J. Cardiol. 203 (2016) 532–533.
[129] A. Planavila, I. Redondo-Angulo, F. Villarroya, FGF21 and cardiac physiopathology, Front. Endocrinol. (Lausanne) 6 (2015) 133.
[130] E. Albrecht, et al., Irisin — a myth rather than an exercise-inducible myokine, Sci. Rep. 5 (2015) 8889.
[131] M.P. Jedrychowski, et al., Detection and quantitation of circulating human irisin by tandem mass spectrometry, Cell Metab. 22 (2015) 734–740.
[132] S. Aydin, et al., Cardiac, skeletal muscle and serum irisin responses to with or without water exercise in young and old male rats: cardiac muscle produces more irisin than skeletal muscle, Peptides 52 (2014) 68–73.
[133] Z.Y. Li, et al., Subfatin is a novel adipokine and unlike Meteorin in adipose and brain expression, CNS Neurosci. Ther. 20 (2014) 344–354.
[134] B.F. Palmer, D.J. Clegg, An emerging role of natriuretic peptides: igniting the fat furnace to fuel and warm the heart, Mayo Clin. Proc. 90 (2015) 1666–1678.
[135] S. Bordbar, M.A. Bigi, A. Aslani, E. Rahimi, N. Ahmadi, Effect of endurance and strength exercise on release of brain natriuretic peptide, J. Cardiovasc. Dis. Res. 3 (2012) 22–25.
[136] M. Follenius, G. Brandenberger, Increase in atrial natriuretic peptide in response to physical exercise, Eur. J. Appl. Physiol. Occup. Physiol. 57 (1988) 159–162.
[137] K.I. Stanford, R.J. Middelbeek, L.J. Goodyear, Exercise effects on white adipose tissue: Beiging and metabolic adaptations, Diabetes 64 (2015) 2361–2368.
[138] N.J. Rothwell, M.J. Stock, A role for brown adipose tissue in diet-induced thermogenesis, Nature 281 (1979) 31–35.
[139] L.P. Kozak, Brown fat and the myth of diet-induced thermogenesis, Cell Metab. 11 (2010) 263–267.
[140] A.J. Webb, et al., Acute blood pressure lowering, vasoprotective, and antiplatelet properties of dietary nitrate via bioconversion to nitrite, Hypertension 51 (2008) 784–790.
[141] M. Siervo, J. Lara, I. Ogbonmwan, J.C. Mathers, Inorganic nitrate and beetroot juice supplementation reduces blood pressure in adults: a systematic review and meta-analysis, J. Nutr. 143 (2013) 818–826.
[142] S. Velmurugan, et al., Antiplatelet effects of dietary nitrate in healthy volunteers: involvement of cGMP and influence of sex, Free Radic. Biol. Med. 65 (2013) 1521–1532.
[143] M.M. Mitschke, et al., Increased cGMP promotes healthy expansion and browning of white adipose tissue, FASEB J. 27 (2013) 1621–1630.
[144] B. Haas, et al., Protein kinase G controls brown fat cell differentiation and mitochondrial biogenesis, Sci. Signal. 2 (2009) ra78.
[145] L.D. Roberts, et al., Inorganic nitrate promotes the browning of white adipose tissue through the nitrate-nitrite-nitric oxide pathway, Diabetes 64 (2015) 471–484.
[146] A.L. Lock, D.E. Bauman, Modifying milk fat composition of dairy cows to enhance fatty acids beneficial to human health, Lipids 39 (2004) 1197–1206.
[147] P. Shokryzadan, et al., Conjugated linoleic acid: a potent fatty acid linked to animal and human health, 2015. Crit. Rev. Food Sci. Nutr., http://dx.doi.org/10.1080/10408398.2015.1060190.
[148] E.J. Noone, H.M. Roche, A.P. Nugent, M.J. Gibney, The effect of dietary supplementation using isomeric blends of conjugated linoleic acid on lipid metabolism in healthy human subjects, Br. J. Nutr. 88 (2002) 243–252.
[149] H. Blankson, et al., Conjugated linoleic acid reduces body fat mass in overweight and obese humans, J. Nutr. 130 (2000) 2943–2948.
[150] E. Thom, J. Wadstein, O. Gudmundsen, Conjugated linoleic acid reduces body fat in healthy exercising humans, J. Int. Med. Res. 29 (2001) 392–396.
[151] J.-M. Gaullier, et al., Conjugated linoleic acid supplementation for 1 y reduces body fat mass in healthy overweight humans, Am. J. Clin. Nutr. 79 (2004) 1118–1125.
[152] G. Berven, et al., Safety of conjugated linoleic acid (CLA) in overweight or obese human volunteers, Eur. J. Lipid Sci. Technol. 102 (2000) 455–462.
[153] K.L. Zambell, et al., Conjugated linoleic acid supplementation in humans: effects on body composition and energy expenditure, Lipids 35 (2000) 777–782.

[154] R.L. House, et al., Functional genomic characterization of delipidation elicited by trans-10, cis-12-conjugated linoleic acid (t10c12-CLA) in a polygenic obese line of mice, Physiol. Genomics 21 (2005) 351–361.
[155] P.C. LaRosa, et al., trans-10, cis-12 conjugated linoleic acid causes inflammation and delipidation of white adipose tissue in mice: a microarray and histological analysis, Physiol. Genomics 27 (2006) 282–294.
[156] W. Shen, et al., Conjugated linoleic acid reduces adiposity and increases markers of browning and inflammation in white adipose tissue of mice, J. Lipid Res. 54 (2013) 909–922.
[157] D.B. West, F.Y. Blohm, A.A. Truett, J.P. DeLany, Conjugated linoleic acid persistently increases total energy expenditure in AKR/J mice without increasing uncoupling protein gene expression, J. Nutr. 130 (2000) 2471–2477.
[158] R. Woods, in: Proceedings of Tthe Physiological Society, 2016 (The Physiological Society).
[159] K. Ohnuki, S. Haramizu, K. Oki, K. Ishihara, T. Fushiki, A single oral administration of conjugated linoleic acid enhanced energy metabolism in mice, Lipids 36 (2001) 583–587.
[160] F. Bouillaud, D. Ricquier, G. Mory, J. Thibault, Increased level of mRNA for the uncoupling protein in brown adipose tissue of rats during thermogenesis induced by cold exposure or norepinephrine infusion, J. Biol. Chem. 259 (1984) 11583–11586.
[161] P.E. Marik, J. Varon, Omega-3 dietary supplements and the risk of cardiovascular events: a systematic review, Clin. Cardiol. 32 (2009) 365–372.
[162] J.M. Geleijnse, E.J. Giltay, D.E. Grobbee, A.R. Donders, F.J. Kok, Blood pressure response to fish oil supplementation: metaregression analysis of randomized trials, J. Hypertens. 20 (2002) 1493–1499.
[163] M.R. Skilton, et al., Fetal growth, omega-3 (n−3) fatty acids, and progression of subclinical atherosclerosis: preventing fetal origins of disease? The cardiovascular risk in young Finns study, Am. J. Clin. Nutr. 97 (2013) 58–65.
[164] J. Breslow, L. n−3 fatty acids and cardiovascular disease, Am. J. Clin. Nutr. 83 (2006) 1477S–1482S.
[165] M. Kim, et al., Fish oil intake induces UCP1 upregulation in brown and white adipose tissue via the sympathetic nervous system, Sci. Rep. 5 (2015) 18013.
[166] P. Janovska, P. Flachs, L. Kazdova, J. Kopecky, Anti-obesity effect of n−3 polyunsaturated fatty acids in mice fed high-fat diet is independent of cold-induced thermogenesis, Physiol. Res. 62 (2013) 153–161.
[167] M. Fleckenstein-Elsen, et al., Eicosapentaenoic acid and arachidonic acid differentially regulate adipogenesis, acquisition of a brite phenotype and mitochondrial function in primary human adipocytes, Mol. Nutr. Food Res. 60 (9) (2016) 2065–2075.
[168] A.P. Simopoulos, The importance of the omega-6/omega-3 fatty acid ratio in cardiovascular disease and other chronic diseases, Exp. Biol. Med. (Maywood) 233 (2008) 674–688.
[169] C. Antoniades, et al., Myocardial redox state predicts in-hospital clinical outcome after cardiac surgery effects of short-term pre-operative statin treatment, J. Am. Coll. Cardiol. 59 (2012) 60–70.
[170] C. Antoniades, et al., Rapid, direct effects of statin treatment on arterial redox state and nitric oxide bioavailability in human atherosclerosis via tetrahydrobiopterin-mediated endothelial nitric oxide synthase coupling, Circulation 124 (2011) 335–345.
[171] C. Antoniades, et al., Induction of vascular GTP-cyclohydrolase I and endogenous tetrahydrobiopterin synthesis protect against inflammation-induced endothelial dysfunction in human atherosclerosis, Circulation 124 (2011) 1860–1870.
[172] C. Antoniades, et al., Preoperative atorvastatin treatment in CABG patients rapidly improves vein graft redox state by inhibition of Rac1 and NADPH-oxidase activity, Circulation 122 (2010) S66–S73.

1.4 Exercise-induced ‘browning’ of adipose tissues

METABOLISM CLINICAL AND EXPERIMENTAL 81 (2018) 63–70

Available online at www.sciencedirect.com

Metabolism

www.metabolismjournal.com

Exercise-induced 'browning' of adipose tissues

Peter Aldiss[a], James Betts[b], Craig Sale[c], Mark Pope[a], Helen Budge[a], Michael E. Symonds[a,d,*]

[a] The Early Life Research Unit, Division of Child Health, Obstetrics and Gynaecology, University Hospital, University of Nottingham, Nottingham NG7 2UH, UK
[b] Department for Health, University of Bath, Bath BA2 7AY, UK
[c] Musculoskeletal Physiology Research Group, Sport, Health and Performance Enhancement Research Centre, School of Science and Technology, Nottingham Trent University, Nottingham, UK
[d] Nottingham Digestive Disease Centre, Biomedical Research Centre School of Medicine, University Hospital, University of Nottingham, Nottingham NG7 2UH, UK

ARTICLE INFO

Article history:
Received 22 September 2017
Accepted 13 November 2017

Keywords:
Exercise
Brown adipose tissue
Browning
White adipose tissue

ABSTRACT

Global rates of obesity continue to rise and are necessarily the consequence of a long-term imbalance between energy intake and energy expenditure. This is the result of an expansion of adipose tissue due to both the hypertrophy of existing adipocytes and hyperplasia of adipocyte pre-cursors. Exercise elicits numerous physiological benefits on adipose tissue, which are likely to contribute to the associated cardiometabolic benefits. More recently it has been demonstrated that exercise, through a range of mechanisms, induces a phenotypic switch in adipose tissue from energy storing white adipocytes to thermogenic beige adipocytes. This has generated the hypothesis that the process of adipocyte 'browning' may partially underlie the improved cardiometabolic health in physically active populations. Interestingly, 'browning' also occurs in response to various stressors and could represent an adaptive response. In the context of exercise, it is not clear whether the appearance of beige adipocytes is metabolically beneficial or whether they occur as a transient adaptive process to exercise-induced stresses. The present review discusses the various mechanisms (e.g. fatty acid oxidation during exercise, decreased thermal insulation, stressors and angiogenesis) by which the exercise-induced 'browning' process may occur.

Contents

* *Corresponding author at:* Academic Division of Child Health Obstetrics & Gynaecology, School of Medicine, Queen's Medical Centre, The University of Nottingham, Nottingham NG7 2UH, UK.
E-mail address: michael.symonds@nottingham.ac.uk (M.E. Symonds).

https://doi.org/10.1016/j.metabol.2017.11.009

1. White, Brown and 'Beige' Adipose Tissue

Adipose tissue typically accounts for ~20–28% of total body mass in lean humans, with variance largely due to biological sex, and in the obese state can account for ~80% of body weight [1]. It is well understood that adipose tissues vary in their function and are dependent on both the type and anatomical location of the depot. Subcutaneous adipose tissue (ScAT), located under the skin, accounts for the majority of total white adipose tissue (WAT) in humans [2]. Visceral adipose tissue (VAT), located around the kidneys (perirenal), intestines (mesenteric and omental), vasculature (perivascular) and heart (epicardial/paracardial) normally accounts for much less but poses a far greater cardiometabolic risk following expansion [3]. Far from being "merely" energy storage depots, adipose tissues are potentially the largest endocrine organ in the body and, by the secretion of numerous factors, can regulate a range of physiological functions including metabolic homeostasis, appetite, angiogenesis, immunity and the cardiovascular system [4].

Conversely, brown adipose tissue (BAT) is located primarily in the supraclavicular region but also in smaller amounts around the kidneys, vasculature and heart [5]. BAT is responsible for adaptive thermogenesis, which preserves homeostasis in response to a thermal stimulus (e.g. temperature and/or energy balance); for example by uncoupling oxidative metabolism from ATP production in favour of heat production via uncoupling protein 1 (UCP1) [6]. The re-discovery of this tissue in adult humans [7] and its association with multiple parameters of metabolic health [8–10] and cardiovascular events [11] has led to huge interest in the potential to activate this tissue to combat obesity-associated cardiometabolic disease. More recently it has been shown that, following a stimulus (e.g. exercise), brown-like UCP1+ cells termed 'beige' adipocytes appear interspersed in what were previously classical white depots [12,13]. It has therefore been suggested that these beige adipocytes: a) are distinct in origin, deriving from a lineage not shared with brown or white adipocytes; b) appear due to the trans-differentiation of pre-existing white adipocytes; or c) arise from a combination of the above [14]. It is important to note, however, that the molecular signature of both brown and beige adipocytes differs between small animals and humans [15]. In rodents, brown and beige adipocytes are anatomically distinct and clearly distinguishable whereas in humans current evidence suggests BAT is a heterogeneous depot expressing markers of both brown and beige adipocytes [16,17]. As such, for the purpose of this review we will use the term 'browning' to describe the appearance of UCP1+ adipocytes. Species differences in molecular signature aside, the 'browning' of white adipose tissues has become an attractive therapeutic target due to mounting evidence suggesting that these 'beige' cells are metabolically active, contributing to both thermogenesis and metabolic health [17,18].

Exercise and physical activity play a key role in modulating many parameters of cardiometabolic health, eliciting several benefits on adipose tissues [19]. A reduction in adipocyte size can be seen with exercise training [20], although this effect seems to be sex-specific as females undergoing the same training regime as men exhibited no changes in body mass or adipocyte size [21]. Furthermore, exercise training elicits improvements in adipose tissue inflammation [22], vascularity [23] and mitochondrial biogenesis [24], increasing the supply of oxygen and nutrients to the tissue and improving their oxidative capacity. More recently it has emerged that factors produced during exercise by skeletal muscle, adipose tissue and potentially the liver act to induce the 'browning' of WAT in an endocrine and/or paracrine manner. Of these, irisin, a PPARγ coactivator-1α (PGC1α) dependent myokine [25], has generated the most interest as a browning agent, although there is major controversy surrounding the results and validity of this purported myokine [26]. Numerous other factors that promote 'browning' are also altered during or following exercise, such as interleukin-6 [27], B-aminoisobutyric acid [28], meteorin-like [29], fibroblast growth factor-21 [30], natriuretic peptides (NP's) [31–33] and lactate [34], leading many to suggest that the long-lasting metabolic effects of exercise may be due to the 'browning' of white adipose tissues (Summary Figure). However, many of these indices have only been validated in-vitro or in animal models and as such their role in 'browning' human WAT are currently unknown.

2. Regulation of Adipose Tissue Metabolism During Exercise

Despite the therapeutic potential of thermogenic 'beige' cells, it is not entirely clear why they appear during exercise, a time of heat production [35]. It has been suggested, however, that following the lipolytic response to exercise and subsequent increase in circulating non-esterified fatty acids (NEFA) there is a need for other areas of oxidation and that the browning of white adipocytes provides these sites in order to maintain NEFA flux [36]. Adipose tissue metabolism during exercise is regulated by multiple factors released both centrally and peripherally to modulate the rate of NEFA uptake and release. The major endocrine mechanism is increased plasma epinephrine which, acting through cyclic AMP (cAMP) and protein kinase A (PKA), phosphorylates adipose triglyceride lipase (ATGL) to stimulate lipolysis and maintain NEFA supply during exercise, a response that is abolished following the blockade of B-adrenoreceptors with propanalol [37,38]. Other lipolytic factors include norepinephrine (NE), glucagon, cortisol and NP's [37]. NE only contributes marginally to exercise-induced lipolysis [38], whilst glucagon and cortisol concentrations increase later in exercise and bind to stimulatory GTP-binding protein to activate ATGL through cAMP and PKA [37]. NP's are increased during exercise of moderate intensity and stimulate lipolysis through the activation of cGMP-dependent protein kinase I (cGKI) and subsequent phosphorylation of perilipin 1 and hormone-sensitive lipase (HSL) [39]. Altered concentrations of adenosine and insulin act against these signals to regulate lipolysis and prevent excess release of NEFA, which is apparent when the typical exercise-induced reduction in insulin is absent [40]. Post-exercise, lipolysis stabilises but remains higher compared to rest for up to 24 h, thus even a single bout of exercise can influence energy expenditure/balance over the next day [41] and modulate insulin sensitivity for up to 48 h [42]. Whilst exercise elicits substantial alterations in adipose tissue metabolism, whether the 'browning' that occurs following exercise training occurs

during an acute bout of exercise to facilitate the oxidation of excess NEFA as postulated by Virtanen et al. [36] remains to be determined. Intriguingly, two recent groups have demonstrated that BAT lipolysis is not essential for cold-induced thermogenesis whereas WAT lipolysis is crucial, fueling thermogenesis during fasting [43,44]. It would be interesting to know, in the context of the hypothesis by Virtanen et al. [36], whether WAT lipolysis is also essential for the 'browning' seen following exercise.

3. Is Exercise Induced 'Browning' a Consequence of Reduced Adiposity?

Regular exercise can improve body composition, including reduced adiposity and/or increased muscle mass. A particularly interesting recent finding was that the phenotypic switch towards thermogenic brown cells shown following exercise in rats primarily occurred in subcutaneous depots, which was concomitant with alterations in BAT morphology (i.e. whitening) and a decreased thermogenic capacity [45]. Exercise training reduced adiposity but the appearance of multilocular adipocytes, thermogenic genes and increase in oxidative capacity were only evident in the inguinal depot (visceral depots being resistant), suggesting depot-specificity. These inter-depot differences, also highlighted by De Jong et al. [46], are of particular interest as exercise does not induce browning in human WAT biopsies [47] and suggests a single biopsy is not an appropriate method to detect browning in humans (at least until we better understand how this process is regulated across both a single depot and between depots). Whilst challenging, future human studies should be designed to examine the response to exercise both at multiple sites in the same adipose depot and also across different depots.

The 'whitening' of BAT and reduced thermogenic capacity following exercise training was suggested to be a counter-regulatory mechanism whereby the ability of BAT to expend energy is reduced during times of increased energy expenditure [48–50]. However, the discovery that exercise induces browning of subcutaneous depots whilst simultaneously increasing lipid content in BAT has led to suggestions for other roles of exercise induced 'browning'. It is now postulated, in rodents, that a reduction in BAT occurs in response to regular increases in core body temperature, whilst the browning of subcutaneous WAT occurs due to a reduction in total mass and thus the degree of insulation conferred by this depot [45,51]. Whilst this theory is consistent with multiple findings that high-fat feeding and resultant excess subcutaneous adiposity decreases UCP1 content [52], recent evidence in mice suggests that adipose tissue does not confer any insulatory properties [53]. However, given that rodents are typically cold-exposed throughout life [54], the 'browning' seen in subcutaneous adipose tissues following exercise could be an adaptive mechanism to increase the thermal potential of reduced adiposity, thus offsetting any increased sensation of peripheral cold.

Interestingly, recent work by Peppler and colleagues demonstrated that removal of IWAT by lipectomy did not attenuate the metabolic benefits of wheel-running in mice and that a compensatory browning was not shown in epididymal WAT despite the reduction in adiposity [55]. However, compensatory browning in the face of reduced adiposity may be limited to ScAT. Had other ScAT depots, or in fact dermal AT been collected an induction of thermogenic genes may have been present. Whilst the authors note the limited clinical relevance of their model it suggests the importance of exercise-induced browning of IWAT may be negligible and is of particular relevance given that humans do not exhibit 'browning' following exercise but still exhibit numerous metabolic benefits [56–58]. Whilst human WAT biopsies may not be the most effective way to detect 'browning' due to the limited amount of tissue relative to depot mass, exercise does reduce BAT mass and activity in athletic humans [47,59]. This is consistent with rodent data and the notion that the thermogenic capacity of BAT may be reduced in the presence of regular increases in core body temperature. Given the inverse relationship between BAT mass and lean mass [23], it is possible that the recruitment of a large muscle mass during exercise training negates the need for BAT, given the potentially superior capacity for muscle to generate heat [60].

4. 'Browning' as an Adaptive Mechanism to Exercise-induced Stress?

There is a growing consensus that the 'browning' of adipose tissues occurs as an adaptive mechanism to certain stresses, aside from the atypical stress of a reduced ambient temperature. This stress-induced 'browning' has been shown in numerous clinical populations including those suffering burn injuries and pheocromocytoma [13,61]. The hypermetabolic state induced by burn injury is derived from a chronic increase in circulating catecholamines and IL-6 which induce the remodelling of subcutaneous adipose tissue [13,62]. This chronic stress increases mitochondrial mass in ScAT, expression of thermogenic markers such as UCP1 and Pgc1α in addition to whole body energy expenditure [63]. These factors that are thought to play a major role in the hypermetabolism evident in cancer patients, contributing to the cachexic state [64,65]. Regular physical exercise induces multiple physiological stressors such as regular chronic sympathetic activation leading to increases in catecholamine secretion and IL-6 after only 6 min of exercise [66], whilst 25-fold increases in IL-6 are seen during longer running protocols in humans and are maintained 2.5 h post-exercise [67]. Whether the effects of IL-6 on adipose tissue are due to its pro- or anti-inflammatory properties or due to the synergistic immune response following exercise which includes alterations in IL-1ra and IL-10 [68] for instance is unknown.

Rodent studies suggest that the metabolic benefits of both BAT and the exercise-induced browning of ScAT are dependent on the presence of IL-6, with no effect in IL-6k/o mice; again, whether this is simply an effect of IL-6 or due to the effect of its absence on other factors is unclear [69,70]. Accumulating evidence suggests that 'browning' is associated with reduced adipose tissue inflammation, so the 'browning' seen with exercise could be an adaptive response to increased inflammatory markers such as IL-6 [22]. There are other factors indicating a role for browning as an adaptive mechanism to exercise-

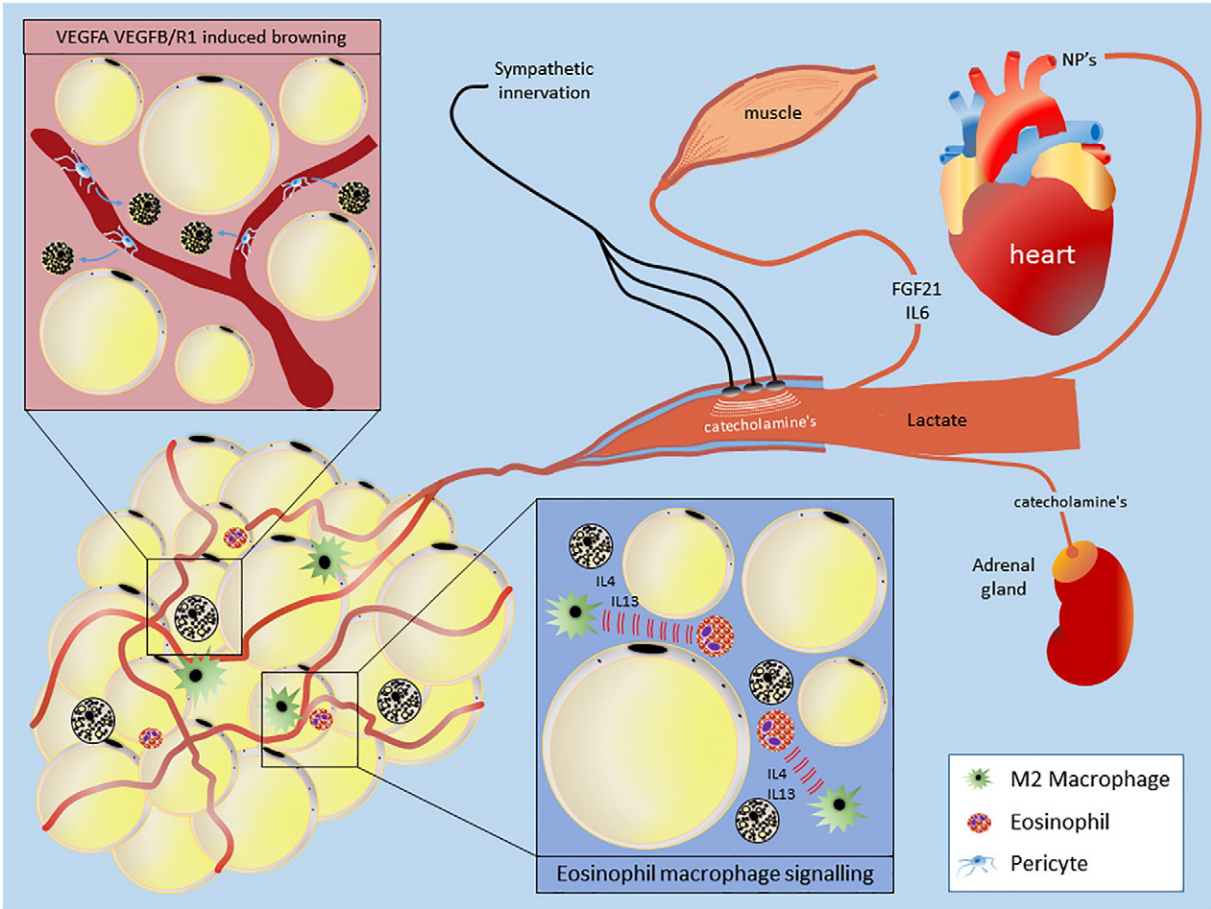

Summary Figure – Mechanisms of exercise-induced browning. Discussed in detail in-text.

induced stresses. In particular, the recent finding that lactate administration induces browning, thus maintaining intracellular redox state [34]. Whilst lactate was not reported in response to exercise in that study, both the treatment of murine and human adipocytes with lactate and its exogenous administration in-vivo induced UCP1 in a redox state dependent manner [34]. Physical exercise is a source of free radicals, occurring primarily during strenuous or prolonged exercise and whilst these free radicals can, depending on the state of antioxidant defence, cause cellular damage at high levels they are also important signalling molecules [71]. In the context of exercise, the increase in free radicals could modulate changes in the intracellular redox state of WAT, with lactate being an evolutionary mechanism to modulate redox state by inducing the brown phenotype. BAT has an abundance of antioxidant enzymes, including UCP1 (which itself plays a key role in regulating ROS production) [72,73] although, as discussed above, chronic exposure to a higher core temperature during exercise training may downregulate its activity. As such, 'browning' in other depots may be a compensatory mechanism for a reduction in BAT mitochondrial function.

Another mechanism by which "browning" could occur is through the increase in NP secreted from cardiac tissues in response to the increased stress and demands placed on the cardiac system during exercise [31]. Whilst NP induce browning in subcutaneous adipose tissues [31], it is feasible that their prime target is the local adipose tissues around heart and vasculature that modulate both myocardial [74] and vascular [75] redox state, in order to attenuate excess oxidative stress within the heart and vasculature.

5. Does Exercise-induced Angiogenesis Modulate the Expression of Beige Cells?

An increase in angiogenesis and vascularisation of tissues and organs, with raised oxygenation, blood flow and nutrient delivery is one of the mechanisms through which exercise improves cardiometabolic health [76]. Unlike classical BAT which shares origins with skeletal muscle, beige adipocytes were originally shown to originate from vascular smooth muscle cells and subsequently it was demonstrated that most, if not all beige adipocytes are derived from the vascular niche [77,78]. This is particularly interesting given that browning occurs in a distinct region of the inguinal depot along the main vasculature and suggests that angiogenesis and/or the proliferation of vascular smooth muscle cells into beige adipocytes may be key to this regional browning effect [79]. Further evidence to support a role of exercise-induced angiogenic mechanisms in the induction of the beige phenotypes comes from data demonstrating that adipose specific over-expression of vascular endothelial growth factor (VEGF;

a key regulator of angiogenesis) reproduces the browning that occurs in an enriched environment, effects which were negated with adipose specific VEGF k/o and VEGF blockade [80]. This suggests that VEGF and related angiogenic mechanisms are essential for the browning effect induced by exercise.

More recently it has been shown that expansion of the adipose vasculature by another member of the VEGF family, VEGFB (plus its receptor VEGFR1), prevents the occurrence of several aspects of obesity-induced metabolic dysfunction concomitant with increased vascularisation and thermogenic markers in WAT [81]. In the obese state the dysfunction of adipose tissues and the 'whitening' of BAT stems from the adipocytes becoming hypertrophic and outstripping the vasculature to become hypoxic [82,83]. Thus it is likely that the restoration of the vascular supply to these tissues can induce or restore the brown phenotype and, in the case of exercise, the induction of angiogenic genes will promote the vascular supply in WAT to induce 'browning'. Whether 'browning' is an essential end-product of this process or a simple by-product of an increased vascularisation and differentiation of pre-cursor cells from the vascular niche remains to be determined. Furthermore, it is worth noting the presence, location and relevance of the lymph node in relation to the regionalisation of 'browning' demonstrated by Barreau et al. [79].

Exercise training triggers multiple complex changes in immune function [84] and emerging evidence suggests that innate immune cells control brown and beige adipogenesis [85]. Meteorin-like is produced following resistance training via the induction of the PGC1 isoform PGC1α 4 and induces the browning of adipose tissues by stimulating IL-4 and IL-13 secretion from eosinophils and the activation of alternate M2 macrophages [29]. Whilst the role of catecholamine production from macrophages has recently been questioned, the use of bone-marrow derived macrophages and not tissue resident macrophages leaves such questions unanswered, particularly as the latter may play a local role in immune-adipose crosstalk. Just as UCP2 regulates immune cell metabolism, differentiation and survival, it is feasible UCP1 may play a similar role in adipose tissue [86,87]. Finally, immune cells produced post-exercise from the lymph node may have a local effect on neighbouring adipocytes leading to the region specific 'browning' seen by others [79].

6. Summary

Exercise, through various secreted factors and mechanisms induces a 'browning' of WAT. However, the physiological explanation for this process is unclear. From an evolutionary point of view the preservation of energy stores is vital. Why then would exercise cause the appearance of thermogenic adipocytes that can increase energy expenditure? It is plausible that our lean and active ancestors naturally possessed large quantities of brown or beige adipocytes. Our subsequent transition to a modern, largely sedentary population has meant these adipocytes have undergone a 'whitening' and the 'browning' that occurs in response to exercise is actually a transition back to their natural state. Despite a lack of understanding as to why exercise should elicit these effects on adipose tissue, it is worth noting Orgel's second law: "Evolution is cleverer than you are". Based on this rule there is likely a valid physiological explanation(s) for the 'browning' process that is yet to be discovered.

Whilst exercise induces a brown phenotype in rodent ScAT, it is not yet clear whether exercise elicits similar effects in humans though the available data suggests that, similar to rodents, exercise downregulates both the mass and activity of human BAT. Whether this is compensated for by browning of WAT or is due to the significant increases in muscle mass and therefore greater capacity for shivering thermogenesis remains to be established.

At present both rodent and human evidence is based on either sedentary or exercise-trained populations, with little attention given to the role of physical activity per se. Whether regular physical activity rather than exercise training potentiates any thermogenic effects on adipose tissues is unknown but, considering the effects of regular physical activity on adiposity and cardiometabolic health, is an area that merits investigation. Studies investigating regular physical activity would also not be confounded by increases in core body temperature and reductions in adiposity, so would rule out these hypothetical mechanisms.

Disclosure Statement

The authors report no relationships that could be construed as a conflict of interest.

Acknowledgements

This work was supported by the British Heart Foundation [grant number FS/15/4/31184].

REFERENCES

[1] Thompson D, Karpe F, Lafontan M, Frayn K. Physical activity and exercise in the regulation of human adipose tissue physiology. Physiol Rev 2012;92:157–91. https://doi.org/10.1152/physrev.00012.2011.
[2] Thomas EL, et al. Magnetic resonance imaging of total body fat. J Appl Physiol 1998;85(1985):1778–85.
[3] Despres JP. Is visceral obesity the cause of the metabolic syndrome? Ann Med 2006;38:52–63. https://doi.org/10.1080/07853890500383895.
[4] Coelho M, Oliveira T, Fernandes R. Biochemistry of adipose tissue: an endocrine organ. Arch Med Sci 2013;9:191–200. https://doi.org/10.5114/aoms.2013.33181.
[5] Sacks H, Symonds ME. Anatomical locations of human brown adipose tissue: functional relevance and implications in obesity and type 2 diabetes. Diabetes 2013;62:1783–90. https://doi.org/10.2337/db12-1430.
[6] Cannon B, Nedergaard J. Brown adipose tissue: function and physiological significance. Physiol Rev 2004;84:277–359. https://doi.org/10.1152/physrev.00015.2003.
[7] Cypess AM, et al. Identification and importance of brown adipose tissue in adult humans. N Engl J Med 2009;360:1509–17. https://doi.org/10.1056/NEJMoa0810780.

[8] van Marken Lichtenbelt WD, et al. Cold-activated brown adipose tissue in healthy men. N Engl J Med 2009;360:1500–8. https://doi.org/10.1056/NEJMoa0808718.
[9] Matsushita M, et al. Impact of brown adipose tissue on body fatness and glucose metabolism in healthy humans. Int J Obes (Lond) 2014;38:812–7. https://doi.org/10.1038/ijo.2013.206.
[10] Yoneshiro T, et al. Age-related decrease in cold-activated brown adipose tissue and accumulation of body fat in healthy humans. Obesity (Silver Spring) 2011;19:1755–60. https://doi.org/10.1038/oby.2011.125.
[11] Takx R, et al. Supraclavicular Brown adipose tissue FDG uptake and cardiovascular disease. J Nucl Med 2016. https://doi.org/10.2967/jnumed.115.166025.
[12] De Matteis R, et al. Exercise as a new physiological stimulus for brown adipose tissue activity. Nutr Metab Cardiovasc Dis 2013;23:582–90. https://doi.org/10.1016/j.numecd.2012.01.013.
[13] Sidossis LS, et al. Browning of subcutaneous white adipose tissue in humans after severe adrenergic stress. Cell Metab 2015;22:219–27. https://doi.org/10.1016/j.cmet.2015.06.022.
[14] Sanchez-Gurmaches J, Guertin DA. Adipocyte lineages: tracing back the origins of fat. Biochim Biophys Acta 2014;1842:340–51. https://doi.org/10.1016/j.bbadis.2013.05.027.
[15] Liu X, Cervantes C, Liu F. Common and distinct regulation of human and mouse brown and beige adipose tissues: a promising therapeutic target for obesity. Protein Cell 2017;8:446–54. https://doi.org/10.1007/s13238-017-0378-6.
[16] Jespersen NZ, et al. A classical brown adipose tissue mRNA signature partly overlaps with brite in the supraclavicular region of adult humans. Cell Metab 2013;17:798–805. https://doi.org/10.1016/j.cmet.2013.04.011.
[17] Wu J, et al. Beige adipocytes are a distinct type of thermogenic fat cell in mouse and human. Cell 2012;150:366–76. https://doi.org/10.1016/j.cell.2012.05.016.
[18] Shabalina IG, et al. UCP1 in brite/beige adipose tissue mitochondria is functionally thermogenic. Cell Rep 2013;5:1196–203. https://doi.org/10.1016/j.celrep.2013.10.044.
[19] Joyner MJ, Green DJ. Exercise protects the cardiovascular system: effects beyond traditional risk factors. J Physiol 2009;587:5551–8. https://doi.org/10.1113/jphysiol.2009.179432.
[20] Despres JP, Bouchard C, Savard R, Tremblay A, Allard C. Lack of relationship between changes in adiposity and plasma lipids following endurance training. Atherosclerosis 1985;54:135–43.
[21] Despres JP, et al. The effect of a 20-week endurance training program on adipose-tissue morphology and lipolysis in men and women. Metabolism 1984;33:235–9.
[22] Haczeyni F, et al. Exercise improves adipose function and inflammation and ameliorates fatty liver disease in obese diabetic mice. Obesity (Silver Spring) 2015;23:1845–55. https://doi.org/10.1002/oby.21170.
[23] Disanzo BL, You T. Effects of exercise training on indicators of adipose tissue angiogenesis and hypoxia in obese rats. Metabolism 2014;63:452–5. https://doi.org/10.1016/j.metabol.2013.12.004.
[24] Vieira VJ, Valentine RJ. Mitochondrial biogenesis in adipose tissue: can exercise make fat cells 'fit'? J Physiol 2009;587:3427–8. https://doi.org/10.1113/jphysiol.2009.175307.
[25] Bostrom P, et al. A PGC1-alpha-dependent myokine that drives brown-fat-like development of white fat and thermogenesis. Nature 2012;481:463–8. https://doi.org/10.1038/nature10777.
[26] Albrecht E, et al. Irisin - a myth rather than an exercise-inducible myokine. Sci Rep 2015;5:8889. https://doi.org/10.1038/srep08889.
[27] Ma Y, Gao M, Sun H, Liu D. Interleukin-6 gene transfer reverses body weight gain and fatty liver in obese mice. Biochim Biophys Acta 2015;1852:1001–11. https://doi.org/10.1016/j.bbadis.2015.01.017.
[28] Kammoun HL, Febbraio MA. Come on BAIBA light my fire. Cell Metab 2014;19:1–2. https://doi.org/10.1016/j.cmet.2013.12.007.
[29] Rao RR, et al. Meteorin-like is a hormone that regulates immune-adipose interactions to increase beige fat thermogenesis. Cell 2014;157:1279–91. https://doi.org/10.1016/j.cell.2014.03.065.
[30] Giralt M, Gavalda-Navarro A, Villarroya F. Fibroblast growth factor-21, energy balance and obesity. Mol Cell Endocrinol 2015;418(Pt 1):66–73. https://doi.org/10.1016/j.mce.2015.09.018.
[31] Palmer BF, Clegg DJ. An emerging role of natriuretic peptides: igniting the fat furnace to fuel and warm the heart. Mayo Clin Proc 2015;90:1666–78. https://doi.org/10.1016/j.mayocp.2015.08.006.
[32] Bordbar S, Bigi MA, Aslani A, Rahimi E, Ahmadi N. Effect of endurance and strength exercise on release of brain natriuretic peptide. J Cardiovasc Dis Res 2012;3:22–5. https://doi.org/10.4103/0975-3583.91599.
[33] Follenius M, Brandenberger G. Increase in atrial natriuretic peptide in response to physical exercise. Eur J Appl Physiol Occup Physiol 1988;57:159–62.
[34] Carriere A, et al. Browning of white adipose cells by intermediate metabolites: an adaptive mechanism to alleviate redox pressure. Diabetes 2014;63:3253–65. https://doi.org/10.2337/db13-1885.
[35] Gagnon D, Jay O, Lemire B, Kenny GP. Sex-related differences in evaporative heat loss: the importance of metabolic heat production. Eur J Appl Physiol 2008;104:821–9. https://doi.org/10.1007/s00421-008-0837-0.
[36] Virtanen KA. BAT thermogenesis: linking shivering to exercise. Cell Metab 2014;19:352–4. https://doi.org/10.1016/j.cmet.2014.02.013.
[37] Tsiloulis T, Watt MJ. Exercise and the regulation of adipose tissue metabolism. Prog Mol Biol Transl Sci 2015;135:175–201. https://doi.org/10.1016/bs.pmbts.2015.06.016.
[38] Arner P, Kriegholm E, Engfeldt P, Bolinder J. Adrenergic regulation of lipolysis in situ at rest and during exercise. J Clin Invest 1990;85:893–8. https://doi.org/10.1172/JCI114516.
[39] Sengenes C, et al. Involvement of a cGMP-dependent pathway in the natriuretic peptide-mediated hormone-sensitive lipase phosphorylation in human adipocytes. J Biol Chem 2003;278:48617–26. https://doi.org/10.1074/jbc.M303713200.
[40] Marker JC, et al. Catecholamines in prevention of hypoglycemia during exercise in humans. Am J Physiol 1991;260:E705-12.
[41] Magkos F, Mohammed BS, Patterson BW, Mittendorfer B. Free fatty acid kinetics in the late phase of postexercise recovery: importance of resting fatty acid metabolism and exercise-induced energy deficit. Metabolism 2009;58:1248–55. https://doi.org/10.1016/j.metabol.2009.03.023.
[42] Bogardus C, et al. Effect of muscle glycogen depletion on in vivo insulin action in man. J Clin Invest 1983;72:1605–10. https://doi.org/10.1172/JCI111119.
[43] Schreiber R, et al. Cold-induced thermogenesis depends on ATGL-mediated lipolysis in cardiac muscle, but not brown adipose tissue. Cell Metab 2017. https://doi.org/10.1016/j.cmet.2017.09.004.
[44] Shin H, et al. Lipolysis in brown adipocytes is not essential for cold-induced thermogenesis in mice. Cell Metab 2017. https://doi.org/10.1016/j.cmet.2017.09.002.
[45] Wu MV, Bikopoulos G, Hung S, Ceddia RB. Thermogenic capacity is antagonistically regulated in classical brown and white subcutaneous fat depots by high fat diet and endurance training in rats: impact on whole-body energy expenditure. J Biol Chem 2014;289:34129–40. https://doi.org/10.1074/jbc.M114.591008.
[46] de Jong JM, Larsson O, Cannon B, Nedergaard J. A stringent validation of mouse adipose tissue identity markers. Am J Physiol Endocrinol Metab 2015;308:E1085-105. https://doi.org/10.1152/ajpendo.00023.2015.
[47] Vosselman MJ, et al. Low brown adipose tissue activity in endurance-trained compared with lean sedentary men. Int J Obes (Lond) 2015. https://doi.org/10.1038/ijo.2015.130.

[48] Nozu T, Kikuchi K, Ogawa K, Kuroshima A. Effects of running training on in vitro brown adipose tissue thermogenesis in rats. Int J Biometeorol 1992;36:88–92.
[49] Larue-Achagiotis C, Rieth N, Goubern M, Laury MC, Louis-Sylvestre J. Exercise-training reduces BAT thermogenesis in rats. Physiol Behav 1995;57:1013–7.
[50] Yamashita H, et al. Effect of running training on uncoupling protein mRNA expression in rat brown adipose tissue. Int J Biometeorol 1993;37:61–4.
[51] Sepa-Kishi DM, Ceddia RB. Exercise-mediated effects on white and Brown adipose tissue plasticity and metabolism. Exerc Sport Sci Rev 2016;44:37–44. https://doi.org/10.1249/JES.0000000000000068.
[52] Fromme T, Klingenspor M. Uncoupling protein 1 expression and high-fat diets. Am J Physiol Regul Integr Comp Physiol 2011;300:R1-. https://doi.org/10.1152/ajpregu.00411.2010.
[53] Fischer AW, Csikasz R, von Essen G, Cannon B, Nedergaard J. No insulating effect of obesity. Am J Physiol Endocrinol Metab 2016. https://doi.org/10.1152/ajpendo.00093.2016 [ajpendo 00093 02016].
[54] Maloney SK, Fuller A, Mitchell D, Gordon C, Overton JM. Translating animal model research: does it matter that our rodents are cold? Physiology (Bethesda) 2014;29:413–20. https://doi.org/10.1152/physiol.00029.2014.
[55] Peppler WT, Townsend LK, Knuth CM, Foster MT, Wright DC. Subcutaneous inguinal white adipose tissue is responsive to, but dispensable for, the metabolic health benefits of exercise. Am J Physiol Endocrinol Metab 2017. https://doi.org/10.1152/ajpendo.00226.2017 [ajpendo 00226 02017].
[56] Nakhuda A, et al. Biomarkers of browning of white adipose tissue and their regulation during exercise- and diet-induced weight loss. Am J Clin Nutr 2016;104:557–65. https://doi.org/10.3945/ajcn.116.132563.
[57] Ronn T, et al. Extensive changes in the transcriptional profile of human adipose tissue including genes involved in oxidative phosphorylation after a 6-month exercise intervention. Acta Physiol (Oxf) 2014;211:188–200. https://doi.org/10.1111/apha.12247.
[58] Scheele C. Adipose adaptation to exercise training -increased metabolic rate but no signs of browning. Acta Physiol (Oxf) 2014;211:11–2. https://doi.org/10.1111/apha.12280.
[59] Singhal V, et al. Effect of chronic athletic activity on brown fat in young women. PLoS One 2016;11:e0156353. https://doi.org/10.1371/journal.pone.0156353.
[60] M, U. D., et al. Human brown adipose tissue [O]O PET imaging in the presence and absence of cold stimulus. Eur J Nucl Med Mol Imaging 2016. https://doi.org/10.1007/s00259-016-3364-y.
[61] Vergnes L, et al. Adipocyte Browning and Higher mitochondrial function in periadrenal but not SC fat in pheochromocytoma. J Clin Endocrinol Metab 2016;101:4440–8. https://doi.org/10.1210/jc.2016-2670.
[62] Patsouris D, et al. Burn induces browning of the subcutaneous white adipose tissue in mice and humans. Cell Rep 2015;13:1538–44. https://doi.org/10.1016/j.celrep.2015.10.028.
[63] Razzoli M, et al. Stress-induced activation of brown adipose tissue prevents obesity in conditions of low adaptive thermogenesis. Mol Metab 2016;5:19–33. https://doi.org/10.1016/j.molmet.2015.10.005.
[64] Hetzler KL, et al. Sex differences in the relationship of IL-6 signaling to cancer cachexia progression. Biochim Biophys Acta 2015;1852:816–25. https://doi.org/10.1016/j.bbadis.2014.12.015.
[65] Tsoli M, Swarbrick MM, Robertson GR. Lipolytic and thermogenic depletion of adipose tissue in cancer cachexia. Semin Cell Dev Biol 2015. https://doi.org/10.1016/j.semcdb.2015.10.039.
[66] Nielsen HB, Secher NH, Christensen NJ, Pedersen BK. Lymphocytes and NK cell activity during repeated bouts of maximal exercise. Am J Physiol 1996;271:R222-27.
[67] Ostrowski K, et al. A trauma-like elevation of plasma cytokines in humans in response to treadmill running. J Physiol 1998;513(Pt 3):889–94.
[68] Scott JP, et al. Effect of exercise intensity on the cytokine response to an acute bout of running. Med Sci Sports Exerc 2011;43:2297–306. https://doi.org/10.1249/MSS.0b013e31822113a9.
[69] Knudsen JG, et al. Role of IL-6 in exercise training- and cold-induced UCP1 expression in subcutaneous white adipose tissue. PLoS One 2014;9:e84910. https://doi.org/10.1371/journal.pone.0084910.
[70] Stanford KI, et al. Brown adipose tissue regulates glucose homeostasis and insulin sensitivity. J Clin Invest 2013;123:215–23. https://doi.org/10.1172/JCI62308.
[71] Powers SK, Jackson MJ. Exercise-induced oxidative stress: cellular mechanisms and impact on muscle force production. Physiol Rev 2008;88:1243–76. https://doi.org/10.1152/physrev.00031.2007.
[72] Oelkrug R, Goetze N, Meyer CW, Jastroch M. Antioxidant properties of UCP1 are evolutionarily conserved in mammals and buffer mitochondrial reactive oxygen species. Free Radic Biol Med 2014;77:210–6. https://doi.org/10.1016/j.freeradbiomed.2014.09.004.
[73] Kazak L, et al. UCP1 deficiency causes brown fat respiratory chain depletion and sensitizes mitochondria to calcium overload-induced dysfunction. Proc Natl Acad Sci U S A 2017. https://doi.org/10.1073/pnas.1705406114.
[74] Antonopoulos AS, et al. Mutual regulation of epicardial adipose tissue and myocardial redox state by PPAR-gamma/adiponectin signalling. Circ Res 2016;118:842–55. https://doi.org/10.1161/CIRCRESAHA.115.307856.
[75] Margaritis M, et al. Interactions between vascular wall and perivascular adipose tissue reveal novel roles for adiponectin in the regulation of eNOS function in human vessels. Circulation 2013. https://doi.org/10.1161/circulationaha.112.001133.
[76] Bloor CM. Angiogenesis during exercise and training. Angiogenesis 2005;8:263–71. https://doi.org/10.1007/s10456-005-9013-x.
[77] Berry DC, Jiang Y, Graff JM. Mouse strains to study cold-inducible beige progenitors and beige adipocyte formation and function. Nat Commun 2016;7:10184. https://doi.org/10.1038/ncomms10184.
[78] Long JZ, et al. A smooth muscle-like origin for beige adipocytes. Cell Metab 2014;19:810–20. https://doi.org/10.1016/j.cmet.2014.03.025.
[79] Barreau C, et al. Regionalization of browning revealed by whole subcutaneous adipose tissue imaging. Obesity (Silver Spring) 2016;24:1081–9. https://doi.org/10.1002/oby.21455.
[80] During MJ, et al. Adipose VEGF links the white-to-brown fat switch with environmental, genetic, and pharmacological stimuli in male mice. Endocrinology 2015;156:2059–73. https://doi.org/10.1210/en.2014-1905.
[81] Robciuc MR, et al. VEGFB/VEGFR1-induced expansion of adipose vasculature counteracts obesity and related metabolic complications. Cell Metab 2016;23:712–24. https://doi.org/10.1016/j.cmet.2016.03.004.
[82] Shimizu I, et al. Vascular rarefaction mediates whitening of brown fat in obesity. J Clin Invest 2014;124:2099–112. https://doi.org/10.1172/JCI71643.
[83] Trayhurn P, Alomar SY. Oxygen deprivation and the cellular response to hypoxia in adipocytes - perspectives on white and brown adipose tissues in obesity. Front Endocrinol (Lausanne) 2015;6:19. https://doi.org/10.3389/fendo.2015.00019.
[84] Woods JA, Vieira VJ, Keylock KT. Exercise, inflammation, and innate immunity. Immunol Allergy Clin North Am 2009;29:381–93. https://doi.org/10.1016/j.iac.2009.02.011.

[85] DiSpirito JR, Mathis D. Immunological contributions to adipose tissue homeostasis. Semin Immunol 2015. https://doi.org/10.1016/j.smim.2015.10.005.
[86] Chaudhuri L, Srivastava RK, Kos F, Shrikant PA. Uncoupling protein 2 regulates metabolic reprogramming and fate of antigen-stimulated CD8+ T cells. Cancer Immunol Immunother 2016;65:869–74. https://doi.org/10.1007/s00262-016-1851-4.
[87] Emre Y, Nubel T. Uncoupling protein UCP2: when mitochondrial activity meets immunity. FEBS Lett 2010;584:1437–42. https://doi.org/10.1016/j.febslet.2010.03.014.

1.5 Recent advances in our understanding of brown and beige adipose tissue: the good fat that keeps you healthy

Check for updates

REVIEW

Recent advances in our understanding of brown and beige adipose tissue: the good fat that keeps you healthy [version 1; referees: 2 approved]

Michael E. Symonds [1,2], Peter Aldiss[1], Mark Pope[1], Helen Budge[1]

[1]Early Life Research Unit, Division of Child Health, Obstetrics & Gynaecology, School of Medicine, University of Nottingham, Nottingham, UK
[2]Nottingham Digestive Disease Centre and Biomedical Research Centre, School of Medicine, University of Nottingham, Nottingham, NG7 2UH, UK

v1 **First published:** 24 Jul 2018, **7**(F1000 Faculty Rev):1129 (doi: 10.12688/f1000research.14585.1)
Latest published: 24 Jul 2018, **7**(F1000 Faculty Rev):1129 (doi: 10.12688/f1000research.14585.1)

Abstract
Brown adipose tissue (BAT) possesses a unique uncoupling protein (UCP1) which, when activated, enables the rapid generation of heat and the oxidation of lipids or glucose or both. It is present in small amounts (~15–350 mL) in adult humans. UCP1 is rapidly activated at birth and is essential in preventing hypothermia in newborns, who rapidly generate large amounts of heat through non-shivering thermogenesis. Since the "re-discovery" of BAT in adult humans about 10 years ago, there has been an exceptional amount of research interest. This has been accompanied by the establishment of beige fat, characterised as discrete areas of UCP1-containing cells dispersed within white adipocytes. Typically, the amount of UCP1 in these depots is around 10% of the amount found in classic BAT. The abundance of brown/beige fat is reduced with obesity, and the challenge is to prevent its loss with ageing or to reactivate existing depots or both. This is difficult, as the current gold standard for assessing BAT function in humans measures radio-labelled glucose uptake in the fasted state and is usually dependent on cold exposure and the same subject can be found to exhibit both positive and negative scans with repeated scanning. Rodent studies have identified multiple pathways that may modulate brown/beige fat function, but their direct relevance to humans is constrained, as these studies typically are undertaken in cool-adapted animals. BAT remains a challenging organ to study in humans and is able to swiftly adapt to changes in the thermal environment and thus enable rapid changes in heat production and glucose oxidation.

Keywords
Brown adipose tissue

Open Peer Review

Referee Status: ✔ ✔

	Invited Referees 1	2
version 1 published 24 Jul 2018	✔	✔

F1000 Faculty Reviews are commissioned from members of the prestigious F1000 Faculty. In order to make these reviews as comprehensive and accessible as possible, peer review takes place before publication; the referees are listed below, but their reports are not formally published.

1 **Francesc Villarroya**, University of Barcelona, Spain

2 **Shingo Kajimura**, University of California, USA

Discuss this article

Comments (0)

Corresponding author: Michael E. Symonds (Michael.Symonds@nottingham.ac.uk)

Author roles: Symonds ME: Conceptualization, Data Curation, Investigation, Methodology, Project Administration, Visualization, Writing – Original Draft Preparation; **Aldiss P**: Conceptualization, Writing – Review & Editing; **Pope M**: Visualization, Writing – Review & Editing; **Budge H**: Conceptualization, Writing – Review & Editing

Competing interests: No competing interests were disclosed.

Grant information: The author(s) declared that no grants were involved in supporting this work.

How to cite this article: Symonds ME, Aldiss P, Pope M and Budge H. **Recent advances in our understanding of brown and beige adipose tissue: the good fat that keeps you healthy [version 1; referees: 2 approved]** *F1000Research* 2018, **7**(F1000 Faculty Rev):1129 (doi: 10.12688/f1000research.14585.1)

First published: 24 Jul 2018, **7**(F1000 Faculty Rev):1129 (doi: 10.12688/f1000research.14585.1)

Introduction

The subject of brown adipose tissue (BAT) has become increasingly topical and controversial since its re-discovery in adult humans in 2007[1]. The simultaneous publication of three studies in the *New England Journal of Medicine* demonstrating the unequivocal detection of brown fat in adult humans[2–4] paved the way for an exponential rise in publications on this subject[5]. Brown fat is important because, though present in relatively small amounts in the body, it has the potential to rapidly produce large amounts of heat and thus impact on both energy balance and glucose and lipid homeostasis[6,7]. This is exemplified in the rapid activation of brown fat around the time of birth and the critical role it plays in the prevention of hypothermia[8]. The "re-discovery" of brown fat has been accompanied by the identification of beige adipocytes (that is, small clusters of brown-like white adipocytes within white fat depots)[9,10]. Furthermore, lineage-tracing experiments in mice indicated that classic brown adipocytes, characterised as possessing the unique mitochondrial uncoupling protein 1 (UCP1), have a common lineage with skeletal muscle and are very different from the cellular origins of beige and white adipocytes[8,11].

When UCP1 is stimulated, usually by the sympathetic nervous system, this results in the free flow of protons across the inner mitochondrial membrane[12], thereby bypassing the need to convert ADP to ATP, as occurs in the mitochondria of all other tissues. The primary stimulus for uncoupling remains contentious but is considered to be the release of fatty acids from lipid either within or surrounding brown adipocytes[13]. Brown fat has the potential to produce far more heat per unit mass than any other organ in the body[8]. Furthermore, the amount of UCP1 in classic brown fat is 10 times greater than that in the beige fat of rodents[14], meaning that the latter has a much smaller capacity to impact on whole-body energy balance. Beige fat, however, has the largest potential as a therapeutic target in the prevention of obesity or diabetes (or both) because it can be present in many white depots as clusters of pre-adipocytes that then can be recruited[14]. However, the capacity of beige fat to modulate metabolism (especially glucose oxidation) may be mediated in part by mechanisms that do not involve UCP1 and have been proposed to be non-canonical[15]. As summarised in Figure 1, the amount of activity of brown fat is reduced with raised white fat mass in obesity and its accompanying metabolically compromised endocrine environment.

Advances in our understanding of the amount and activity of brown fat in adult humans

The gold standard by which the activity of brown fat is assessed in adult humans is still positron emission tomography-computed tomography (PET-CT)[16]. This was the original method used to identify brown fat, and the same technique is used clinically around the world. It is a method that identifies brown fat from the uptake of radio-labelled glucose (fludeoxyglucose, or ^{18}FDG) and is measured relative to the amount of glucose uptake in other tissues[16]. However, to gain a significant signal within brown fat, the subject needs to be both fasted and cold-exposed[17]. A better tracer than glucose for assessing brown fat thermogenesis is acetate[18], which is converted into acetyl-CoA within the cell and then incorporated into components of the citric acid cycle (a reaction that does not occur for ^{18}FDG). Consequently, as brown fat rapidly turns over, the radio-labelled carbons in acetate are released as carbon dioxide and the amount of positron label lost is directly proportional to the metabolic activity of the tissue[19], which in the case of brown fat is substantial[18]. When brown fat is activated by cold exposure, lipids stored within the depot are mobilised and oxidised to release heat[19]. Acetate, however, is rarely used as a tracer, as it needs to be freshly prepared and, as it is not routinely used for cancer detection, such a facility is seldom available. This technical challenge means that our understanding of brown fat metabolism in humans remains constrained.

Quantification of brown fat in humans

It is now recognised that the amount of brown fat is under-assessed in most studies which use radio-labelled glucose in PET-CT and varies considerably between individuals, with current estimates now ranging from about 30 to 350 mL in healthy subjects[20,21]. PET-CT studies examining the impact of an intervention on brown fat function in humans have to subdivide participants into brown fat "positive/+ve" and "negative/−ve" sub-groups[22] or only study BAT+ve individuals[23]. This could be considered a rather arbitrary classification, as all adults have the potential to exhibit a brown fat+ve response when repeatedly assessed with PET-CT[21]. However, one small study has shown that a BAT+ve scan is associated with greater UCP1 within supraclavicular brown fat[24]. The same study demonstrated a large increase in UCP1 gene expression with cold exposure, although there was appreciable variation in response between individuals. Taken together, these findings indicate the rapid response of brown fat to cold thermal stimulation for which increased gene expression[24] could be a longer-term response that parallels the pronounced change in substrate uptake, compared with warm conditions, as recently indicated in human supraclavicular brown fat[23]. It has also been suggested, from PET-CT studies, that more brown fat is present in females than in males, although these results are more likely to reflect the greater sensitivity to cold by females[6].

The practical and health limitations of using PET-CT, which involves significant exposure to radiation, prevent its widespread use on healthy populations, meaning other methods of assessing brown fat function *in vivo* are required. These include thermal imaging for which a close correlation between brown fat function, as measured with PET-CT, has been established[25]. Furthermore, there are currently no reports of any individuals undergoing thermal imaging who do not have a hot spot that co-locates with the supraclavicular depot (that then increases in temperature with mild hand cooling)[17]. Thermal imaging has also demonstrated a marked responsiveness of supraclavicular brown fat to diet[26] and its contribution to dietary-induced thermogenesis. It is therefore able to provide novel insights into the impact of diet on brown fat that cannot be readily obtained from PET-CT studies.

Primary activators of brown fat

Reduced ambient temperature in humans remains the most potent stimulator of brown fat[27] and is not unexpected given that cold exposure to the extra-uterine environment is the primary

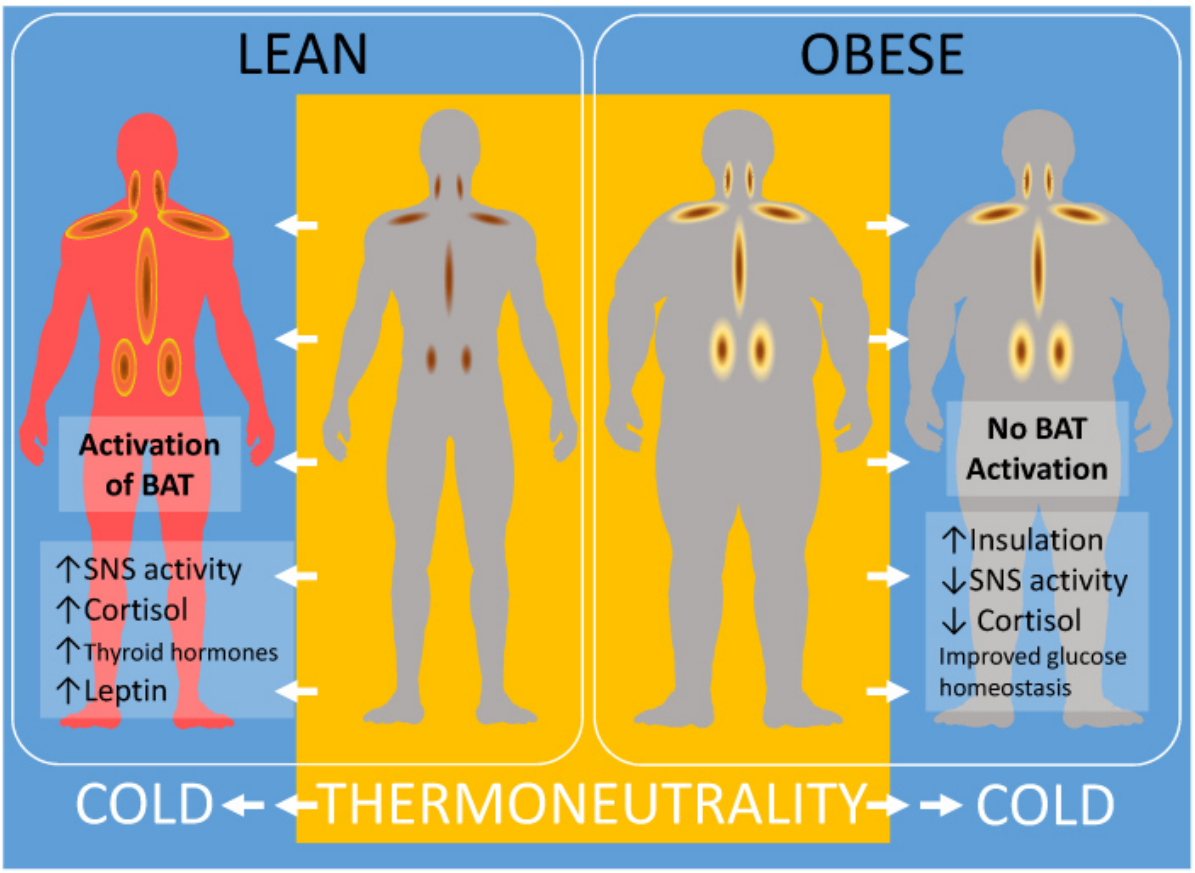

Figure 1. Summary of the impact of obesity on brown adipose tissue function and regulation in adult humans and the potential benefits of chronic cold exposure. ATGL, adipose triglyceride lipase; BAT, brown adipose tissue; FFA, free fatty acid; HSL, hormone-sensitive lipase; MGL, monoglyceride lipase; NEFA, non-esterified fatty acid; SNS, sympathetic nervous system; T, temperature; TG, triglyceride; WAT, white adipose tissue.

catalyst for the onset of non-shivering thermogenesis at birth[8]. This adaptation is accompanied by a rapid rise in a range of metabolic hormones, including catecholamines, thyroid hormones, cortisol, and leptin[7], with leptin co-locating onto the nucleus during cold induction of beige adipocytes[28]. The extent to which repeated cold challenges can be used to enhance brown fat function in adults remains an important milestone for current research.

Importantly, glucose uptake in supraclavicular brown fat increases substantially with cold exposure and is positively correlated with the magnitude of cold-induced thermogenesis[23]. Even in subjects who are classified as BAT−ve, an increase in mean glucose uptake is seen with cooling, although it is about 50% less than in those participants who are BAT+ve[24]. A comparable adaptation has been observed in individuals who are diabetic, in whom the only study conducted to date indicates an improvement in glucose homeostasis[29]. This was not fully explained, however, by the increase in glucose uptake within brown fat as measured by PET-CT[29]. These findings are important given the potentially large amounts of brownable fat (up to 1,500 mL) as indicated in young healthy obese adults[30].

The exact amount of glucose oxidised by brown fat remains to be fully established, and it has been conservatively calculated that 300 mL of brown fat could dispose of at least 9 g of glucose per day[20]. This value could be much greater on the basis of the threefold to fivefold increase in glucose uptake recently measured in supraclavicular fat with moderate cold exposure[23]. With the innovative developments in studying brown fat mitochondria, further refinements in these calculations are likely. This is because two types of mitochondria have now been identified within rodent interscapular brown fat—the peridroplet and cytoplasmic domains—the latter of which regulates lipid supply, whereas the cytoplasmic domain could be more important in regulating glucose oxidation[31]. Further adaptations as shown in beige fat of mice following cold exposure include the appearance of dense intra-adipose sympathetic arborisations[32], but have yet to be confirmed in humans. The capacity to predict which experimental models of browning are most relevant to humans could be further

enhanced by the systematic integration of transcriptional profiles using online resources that are now being developed[33]. The full extent to which changes in brown fat function can contribute to inadequate glucose homeostasis remains to be fully explored. It is noteworthy, however, that two recent studies have indicated that raised temperature is associated with increased risk of diabetes, either during pregnancy in Canada[34] or in all adults across the United States[35]. Taken together, these findings emphasise the impact of climate change on human health and the extent to which adverse effects may be dependent on the body's natural heat generator (that is, brown fat)[5].

Other targeted approaches to stimulate brown fat in humans have included the use of the β3-adrenoreceptor antagonist mirabegron (at a relatively high dose of 200 mg). Mirabegron promotes glucose uptake in a wide range of brown fat depots[36], as determined with PET-CT, as well as stimulating metabolic rate, although these two measures were not well correlated. Thus, it is possible that the effects of mirabegron are related more to effects on glucose metabolism in brown fat[37] rather than to heat production per se, but this needs further studying. Surprisingly, despite being published nearly 4 years ago, this study remains the only one of its kind. Both acute and chronic stimulation of the stress-sympathetic nervous system would appear to offer a route by which brown fat activity can be enhanced. For example, 24-hour infusion of hydrocortisone in adult males increases the temperature of the supraclavicular depot that co-locates with brown fat[26]. In children, the stress associated with severe burn injury promotes the appearance of UCP1 in subcutaneous fat after 4 weeks[38].

Limitation on our understanding of regulation of brown fat metabolism from rodent studies

The past 5 years have seen a prolific amount of research into brown fat, which suggests that it may have the capacity to improve metabolic homeostasis in adults, but such a goal will not be a straightforward outcome to achieve. This is, in part, because of the very different metabolic roles for brown fat in rodents and humans together with the divergence in experimental protocols used in animal studies[39] that do not readily compare with the human situation[5]. However, the potential for UCP1 to generate heat appears to be similar between species[40], although the exact range of mechanisms involved remains to be fully established[13]. It should be noted that laboratory rodents are typically maintained within a highly artificial environment, are usually fed a highly processed diet that is the same each day, experience no change in photoperiod (that is, fixed 12-hour day and 12-hour night) or ambient temperature, and have limited (if any) exposure to pathogens[41]. Furthermore, the main brown (or beige) fat depot in adult humans is located within the supraclavicular region[42], and although this is also present in rodents[43], it has seldom been examined, as the interscapular and inguinal depots are primarily investigated.

Thus, it is important that the results from the plethora of rodent-based investigations are considered in light of the depot examined and the relevance to human adipose tissue of the identified pathways.

Although the focus of most rodent studies has been on identifying novel pathways that could be targeted to promote brown fat function, these have had relatively little impact on enabling sustainable interventions in adult humans. This could be for a number of reasons that now are starting to gain more consideration across the scientific community. The main concern is the thermal environment in which rodents are maintained when brown fat is examined, as it is clear that 20–21 °C represents a substantial thermal stress and that thermoneutrality is approximately 28–30 °C[39]. Moreover, many rodent studies go on to examine the effect of further exposure to what, for laboratory mice, would be extreme cold (that is, about 6 °C), which results in maximal brown fat activation. This is rather an abrupt challenge and without a gradual decline in temperature, as would occur in the wild, is an unphysiological adaptation. In terms of susceptibility to metabolic-related disease, this is best illustrated in a mouse model of non-alcoholic fatty liver disease (NAFLD). Housing at thermoneutrality exacerbates the magnitude of NAFLD as well as removing any difference between sexes[44]. Not surprisingly, those mice housed at 30 °C are characterised as possessing less brown fat and have lower plasma corticosterone concentrations which, in humans, are known to positively impact on brown fat function in some[26,45] but not all[46] studies. Furthermore, thermoneutral housing accelerates atherosclerosis through increased metabolic inflammation, which surprisingly is uncoupled from insulin resistance[47]. The link among inflammation, obesity-induced insulin resistance, and atherosclerosis has been clear for decades[48]. It is likely, therefore, that these results in rodents have been confounded by chronic mild-cold stress and that better modelling of human physiology, especially with regard to the role of brown fat in metabolic disease, will be needed in future. The critical role of temperature has been highlighted *in vitro*[49], under which conditions the appearance of UCP1 also appears to be dependent on reduced ambient temperature[28].

Conclusions

The re-discovery of BAT in adults has led to the recognition that promoting its activity could be an effective new strategy to improve metabolic homeostasis in a sedentary world where obesity and diabetes are prevalent. Although to date most studies in humans have focused on promoting heat production in brown fat, given the recent findings on increased glucose metabolism, this could be a more promising area in future research.

Competing interests

The authors declare that they have no competing interests

Grant information

The author(s) declared that no grants were involved in supporting this work.

References

F F1000 recommended

1. Nedergaard J, Bengtsson T, Cannon B: **Unexpected evidence for active brown adipose tissue in adult humans.** *Am J Physiol Endocrinol Metab.* 2007; **293**(2): E444–52.
PubMed Abstract | Publisher Full Text

2. F Cypess AM, Lehman S, Williams G, *et al.*: **Identification and importance of brown adipose tissue in adult humans.** *N Engl J Med.* 2009; **360**(15): 1509–17.
PubMed Abstract | Publisher Full Text | Free Full Text | F1000 Recommendation

3. F van Marken Lichtenbelt WD, Vanhommerig JW, Smulders NM, *et al.*: **Cold-activated brown adipose tissue in healthy men.** *N Engl J Med.* 2009; **360**(15): 1500–8.
PubMed Abstract | Publisher Full Text | F1000 Recommendation

4. F Virtanen KA, Lidell ME, Orava J, *et al.*: **Functional brown adipose tissue in healthy adults.** *N Engl J Med.* 2009; **360**(15): 1518–25.
PubMed Abstract | Publisher Full Text | F1000 Recommendation

5. Symonds ME, Aldiss P, Dellschaft N, *et al.*: **Brown adipose tissue development and function and its impact on reproduction.** *J Endocrinol.* 2018; **238**(1): R53–R62.
PubMed Abstract | Publisher Full Text

6. F Cannon B, Nedergaard J: **Nonshivering thermogenesis and its adequate measurement in metabolic studies.** *J Exp Biol.* 2011; **214**(Pt 2): 242–53.
PubMed Abstract | Publisher Full Text | F1000 Recommendation

7. Symonds ME: **Brown adipose tissue growth and development.** *Scientifica (Cairo).* 2013; **2013**: 305763.
PubMed Abstract | Publisher Full Text | Free Full Text

8. Symonds ME, Pope M, Budge H: **The Ontogeny of Brown Adipose Tissue.** *Annu Rev Nutr.* 2015; **35**: 295–320.
PubMed Abstract | Publisher Full Text

9. F Timmons JA, Wennmalm K, Larsson O, *et al.*: **Myogenic gene expression signature establishes that brown and white adipocytes originate from distinct cell lineages.** *Proc Natl Acad Sci U S A.* 2007; **104**(11): 4401–6.
PubMed Abstract | Publisher Full Text | Free Full Text | F1000 Recommendation

10. Cannon B, Nedergaard J: **Cell biology: Neither brown nor white.** *Nature.* 2012; **488**(7411): 286–7.
PubMed Abstract | Publisher Full Text

11. F Seale P, Bjork B, Yang W, *et al.*: **PRDM16 controls a brown fat/skeletal muscle switch.** *Nature.* 2008; **454**(7207): 961–7.
PubMed Abstract | Publisher Full Text | Free Full Text | F1000 Recommendation

12. Cannon B, Nedergaard J: **Brown adipose tissue: function and physiological significance.** *Physiol Rev.* 2004; **84**(1): 277–359.
PubMed Abstract | Publisher Full Text

13. Cannon B, Nedergaard J: **What Ignites UCP1?** *Cell Metab.* 2017; **26**(5): 697–8.
PubMed Abstract | Publisher Full Text

14. F Nedergaard J, Cannon B: **UCP1 mRNA does not produce heat.** *Biochim Biophys Acta.* 2013; **1831**(5): 943–9.
PubMed Abstract | Publisher Full Text | F1000 Recommendation

15. F Ikeda K, Kang Q, Yoneshiro T, *et al.*: **UCP1-independent signaling involving SERCA2b-mediated calcium cycling regulates beige fat thermogenesis and systemic glucose homeostasis.** *Nat Med.* 2017; **23**(12): 1454–65.
PubMed Abstract | Publisher Full Text | Free Full Text | F1000 Recommendation

16. F Cypess AM, Haft CR, Laughlin MR, *et al.*: **Brown fat in humans: consensus points and experimental guidelines.** *Cell Metab.* 2014; **20**(3): 408–15.
PubMed Abstract | Publisher Full Text | Free Full Text | F1000 Recommendation

17. Law J, Chalmers J, Morris DE, *et al.*: **The use of infrared thermography in the measurement and characterization of brown adipose tissue activation.** *Temperature.* 2017; **5**(2): 147–61.
Publisher Full Text

18. F Ouellet V, Labbé SM, Blondin DP, *et al.*: **Brown adipose tissue oxidative metabolism contributes to energy expenditure during acute cold exposure in humans.** *J Clin Invest.* 2012; **122**(2): 545–52.
PubMed Abstract | Publisher Full Text | Free Full Text | F1000 Recommendation

19. Cannon B, Nedergaard J: **Yes, even human brown fat is on fire!** *J Clin Invest.* 2012; **122**(2): 486–9.
PubMed Abstract | Publisher Full Text | Free Full Text

20. F Gerngroß C, Schretter J, Klingenspor M, *et al.*: **Active Brown Fat During ^{18}F-FDG PET/CT Imaging Defines a Patient Group with Characteristic Traits and an Increased Probability of Brown Fat Redetection.** *J Nucl Med.* 2017; **58**(7): 1104–1110.
PubMed Abstract | Publisher Full Text | F1000 Recommendation

21. F Leitner BP, Huang S, Brychta RJ, *et al.*: **Mapping of human brown adipose tissue in lean and obese young men.** *Proc Natl Acad Sci U S A.* 2017; **114**(32): 8649–54.
PubMed Abstract | Publisher Full Text | Free Full Text | F1000 Recommendation

22. F Yoneshiro T, Matsushita M, Hibi M, *et al.*: **Tea catechin and caffeine activate brown adipose tissue and increase cold-induced thermogenic capacity in humans.** *Am J Clin Nutr.* 2017; **105**(4): 873–81.
PubMed Abstract | Publisher Full Text | F1000 Recommendation

23. F Weir G, Ramage LE, Akyol M, *et al.*: **Substantial Metabolic Activity of Human Brown Adipose Tissue during Warm Conditions and Cold-Induced Lipolysis of Local Triglycerides.** *Cell Metab.* 2018; **27**(6): 1348–1355.e4.
PubMed Abstract | Publisher Full Text | Free Full Text | F1000 Recommendation

24. F Chondronikola M, Volpi E, Børsheim E, *et al.*: **Brown adipose tissue improves whole-body glucose homeostasis and insulin sensitivity in humans.** *Diabetes.* 2014; **63**(12): 4089–99.
PubMed Abstract | Publisher Full Text | Free Full Text | F1000 Recommendation

25. Law J, Morris DE, Izzi-Engbeaya C, *et al.*: **Thermal Imaging Is a Noninvasive Alternative to PET/CT for Measurement of Brown Adipose Tissue Activity in Humans.** *J Nucl Med.* 2018; **59**(3): 516–22.
PubMed Abstract | Publisher Full Text | Free Full Text

26. Scotney H, Symonds ME, Law J, *et al.*: **Glucocorticoids modulate human brown adipose tissue thermogenesis *in vivo*.** *Metabolism.* 2017; **70**: 125–32.
PubMed Abstract | Publisher Full Text | Free Full Text

27. F Cypess AM, Chen YC, Sze C, *et al.*: **Cold but not sympathomimetics activates human brown adipose tissue *in vivo*.** *Proc Natl Acad Sci U S A.* 2012; **109**(25): 10001–5.
PubMed Abstract | Publisher Full Text | Free Full Text | F1000 Recommendation

28. Velickovic K, Lugo Leija HA, Bloor I, *et al.*: **Low temperature exposure induces browning of bone marrow stem cell derived adipocytes *in vitro*.** *Sci Rep.* 2018; **8**(1): 4974.
PubMed Abstract | Publisher Full Text | Free Full Text

29. F Hanssen MJ, Hoeks MJ, Brans B, *et al.*: **Short-term cold acclimation improves insulin sensitivity in patients with type 2 diabetes mellitus.** *Nat Med.* 2015; **21**(8): 863–5.
PubMed Abstract | Publisher Full Text | F1000 Recommendation

30. F Hanssen MJ, van der Lans AA, Brans B, *et al.*: **Short-term Cold Acclimation Recruits Brown Adipose Tissue in Obese Humans.** *Diabetes.* 2016; **65**(5): 1179–89.
PubMed Abstract | Publisher Full Text | F1000 Recommendation

31. F Benador IY, Veliova M, Mahdaviani K, *et al.*: **Mitochondria Bound to Lipid Droplets Have Unique Bioenergetics, Composition, and Dynamics that Support Lipid Droplet Expansion.** *Cell Metab.* 2018; **27**(4): 869–885.e6.
PubMed Abstract | Publisher Full Text | Free Full Text | F1000 Recommendation

32. F Jiang H, Ding X, Cao Y, *et al.*: **Dense Intra-adipose Sympathetic Arborizations Are Essential for Cold-Induced Beiging of Mouse White Adipose Tissue.** *Cell Metab.* 2017; **26**(4): 686–692.e3.
PubMed Abstract | Publisher Full Text | F1000 Recommendation

33. F Cheng Y, Jiang L, Keipert S, *et al.*: **Prediction of Adipose Browning Capacity by Systematic Integration of Transcriptional Profiles.** *Cell Rep.* 2018; **23**(10): 3112–25.
PubMed Abstract | Publisher Full Text | F1000 Recommendation

34. F Booth GL, Luo J, Park AL, *et al.*: **Influence of environmental temperature on risk of gestational diabetes.** *CMAJ.* 2017; **189**(19): E682–E689.
PubMed Abstract | Publisher Full Text | Free Full Text | F1000 Recommendation

35. F Blauw LL, Aziz NA, Tannemaat MR, *et al.*: **Diabetes incidence and glucose intolerance prevalence increase with higher outdoor temperature.** *BMJ Open Diabetes Res Care.* 2017; **5**(1): e000317.
PubMed Abstract | Publisher Full Text | Free Full Text | F1000 Recommendation

36. F Cypess AM, Weiner LS, Roberts-Toler C, *et al.*: **Activation of human brown adipose tissue by a β3-adrenergic receptor agonist.** *Cell Metab.* 2015; **21**(1): 33–8.
PubMed Abstract | Publisher Full Text | Free Full Text | F1000 Recommendation

37. Hainer V: **Beta3-adrenoreceptor agonist mirabegron - a potential antiobesity drug?** *Expert Opin Pharmacother.* 2016; **17**(16): 2125–7.
PubMed Abstract | Publisher Full Text

38. F Sidossis LS, Porter C, Saraf MK, *et al.*: **Browning of Subcutaneous White Adipose Tissue in Humans after Severe Adrenergic Stress.** *Cell Metab.* 2015; **22**(2): 219–27.
PubMed Abstract | Publisher Full Text | Free Full Text | F1000 Recommendation

39. F Maloney SK, Fuller A, Mitchell D, *et al.*: **Translating animal model research: does it matter that our rodents are cold?** *Physiology (Bethesda).* 2014; **29**(6): 413–20.
PubMed Abstract | Publisher Full Text | F1000 Recommendation

40. F Porter C, Herndon DN, Chondronikola M, *et al.*: **Human and Mouse Brown Adipose Tissue Mitochondria Have Comparable UCP1 Function.** *Cell Metab.* 2016; **24**(2): 246–55.
PubMed Abstract | Publisher Full Text | Free Full Text | F1000 Recommendation

41. Symonds ME, Sebert S, Budge H: **The obesity epidemic: from the environment to epigenetics - not simply a response to dietary manipulation in a thermoneutral environment.** *Front Genet.* 2011; **2**: 24.
PubMed Abstract | Publisher Full Text | Free Full Text

42. F Cypess AM, White AP, Vernochet C, *et al.*: **Anatomical localization, gene**

expression profiling and functional characterization of adult human neck brown fat. *Nat Med.* 2013; **19**(5): 635–9.
PubMed Abstract | Publisher Full Text | Free Full Text | F1000 Recommendation

43. F Mo Q, Salley J, Roshan T, *et al.*: **Identification and characterization of a supraclavicular brown adipose tissue in mice.** *JCI Insight.* 2017; **2**(11): pii: 93166.
PubMed Abstract | Publisher Full Text | Free Full Text | F1000 Recommendation

44. F Giles DA, Moreno-Fernandez ME, Stankiewicz TE, *et al.*: **Thermoneutral housing exacerbates nonalcoholic fatty liver disease in mice and allows for sex-independent disease modeling.** *Nat Med.* 2017; **23**(7): 829–38.
PubMed Abstract | Publisher Full Text | Free Full Text | F1000 Recommendation

45. Robinson LJ, Law JM, Symonds ME, *et al.*: **Brown adipose tissue activation as measured by infrared thermography by mild anticipatory psychological stress in lean healthy females.** *Exp Physiol.* 2016; **101**(4): 549–57.
PubMed Abstract | Publisher Full Text

46. Ramage LE, Akyol M, Fletcher AM, *et al.*: **Glucocorticoids Acutely Increase Brown Adipose Tissue Activity in Humans, Revealing Species-Specific Differences in UCP-1 Regulation.** *Cell Metab.* 2016; **24**(1): 130–41.
PubMed Abstract | Publisher Full Text | Free Full Text

47. F Tian XY, Ganeshan K, Hong C, *et al.*: **Thermoneutral Housing Accelerates Metabolic Inflammation to Potentiate Atherosclerosis but Not Insulin Resistance.** *Cell Metab.* 2016; **23**(1): 165–78.
PubMed Abstract | Publisher Full Text | Free Full Text | F1000 Recommendation

48. Osborn O, Olefsky JM: **The cellular and signaling networks linking the immune system and metabolism in disease.** *Nat Med.* 2012; **18**(3): 363–74.
PubMed Abstract | Publisher Full Text

49. F Ye L, Wu J, Cohen P, *et al.*: **Fat cells directly sense temperature to activate thermogenesis.** *Proc Natl Acad Sci U S A.* 2013; **110**(30): 12480–5.
PubMed Abstract | Publisher Full Text | Free Full Text | F1000 Recommendation

Open Peer Review

Current Referee Status: ✔ ✔

Editorial Note on the Review Process

F1000 Faculty Reviews are commissioned from members of the prestigious F1000 Faculty and are edited as a service to readers. In order to make these reviews as comprehensive and accessible as possible, the referees provide input before publication and only the final, revised version is published. The referees who approved the final version are listed with their names and affiliations but without their reports on earlier versions (any comments will already have been addressed in the published version).

The referees who approved this article are:

Version 1

1 **Shingo Kajimura** Diabetes Center, University of California, San Francisco, California, USA
Competing Interests: No competing interests were disclosed.

1 **Francesc Villarroya** Biochemistry and Molecular Biology, University of Barcelona, Barcelona, 08028, Spain
Competing Interests: No competing interests were disclosed.

Chapter 2

Interscapular And Perivascular Brown Adipose Tissue Respond Differently To a Short-Term High-Fat Diet

---

nutrients

MDPI

Article

Interscapular and Perivascular Brown Adipose Tissue Respond Differently to a Short-Term High-Fat Diet

Peter Aldiss [1], Michael E. Symonds [1,2,*], Jo E. Lewis [3], David J. Boocock [4], Amanda K. Miles [4], Ian Bloor [1], Francis J. P. Ebling [3] and Helen Budge [1]

[1] The Early Life Research Unit, Division of Child Health, Obstetrics and Gynaecology, School of Medicine, University of Nottingham NG7 2UH, UK; peter.aldiss@nottingham.ac.uk (P.A.); ian.bloor@nottingham.ac.uk (I.B.); helen.budge@nottingham.ac.uk (H.B.)

[2] Nottingham Digestive Disease Centre and Biomedical Research Unit, School of Medicine, University of Nottingham NG7 2UH, UK

[3] School of Life Sciences, Queen's Medical Centre, University of Nottingham, NG7 2UH; fran.ebling@nottingham.ac.uk; jl2033@medschl.cam.ac.uk

[4] John van Geest Cancer Research Centre, Nottingham Trent University, Nottingham NG11 8NS, UK; david.boocock@ntu.ac.uk (D.J.B.); amanda.miles@ntu.ac.uk (A.K.M.)

* Correspondence: michael.symonds@nottingham.ac.uk; Tel.: +44-115-8230625

Received: 20 February 2019; Accepted: 8 May 2019; Published: 13 May 2019

Abstract: Brown adipose tissue (BAT) function may depend on its anatomical location and developmental origin. Interscapular BAT (iBAT) regulates acute macronutrient metabolism, whilst perivascular BAT (PVAT) regulates vascular function. Although phenotypically similar, whether these depots respond differently to acute nutrient excess is unclear. Given their distinct anatomical locations and developmental origins and we hypothesised that iBAT and PVAT would respond differently to brief period of nutrient excess. Sprague-Dawley rats aged 12 weeks (n=12) were fed either a standard (10% fat, n=6) or high fat diet (HFD: 45% fat, n=6) for 72h and housed at thermoneutrality. Following an assessment of whole body physiology, fat was collected from both depots for analysis of gene expression and the proteome. HFD consumption for 72h induced rapid weight gain (c. 2.6%) and reduced serum non-esterified fatty acids (NEFA) with no change in either total adipose or depot mass. In iBAT, an upregulation of genes involved in insulin signalling and lipid metabolism was accompanied by enrichment of lipid-related processes and functions, plus glucagon and peroxisome proliferator-activated receptor (PPAR) signalling pathways. In PVAT, HFD induced a pronounced down-regulation of multiple metabolic pathways which was accompanied with increased abundance of proteins involved in apoptosis (e.g. Hdgf and Ywaq) and toll-like receptor signalling (Ube2n). There was also an enrichment of DNA-related processes and functions (e.g. nucleosome assembly and histone exchange) and RNA degradation and cell adhesion pathways. In conclusion, we show that iBAT and PVAT elicit divergent responses to short-term nutrient excess highlighting early adaptations in these depots before changes in fat mass.

Keywords: brown fat; white fat; proteome; nutrient excess

1. Introduction

Adipose tissue function differs with its anatomical location and developmental origin [1]. For instance, whilst interscapular brown adipose tissue (iBAT) shares its lineage with skeletal muscle (e.g. Myf5+), perivascular brown adipose tissue (PVAT) is thought to derive from vascular smooth muscle cells (e.g. SM22α+) [1,2]. iBAT can play a role in whole body glucose, and lipid homeostasis as well as thermoregulation through the activation of uncoupling protein 1 (UCP1) which dissipates chemical energy as heat bypassing the conversion of ADP to ATP [3–5]. Despite PVAT being

phenotypically similar to iBAT, i.e. abundant in UCP1 and other thermogenic genes, its primary physiological role is the regulation of vascular function rather than systemic metabolism per se [2]. Dysfunctional BAT may contribute to obesity and associated metabolic disease, whereas compromised PVAT may enhance the atherogenic processes due to its close proximity to and crosstalk with the endothelium [6,7].

The effect of diet-induced obesity on BAT is well established [8], but less is known on its response to brief periods of high-fat feeding. Central inflammation occurs after only 3-4 days of commencing a high-fat diet (HFD) that is accompanied with central and peripheral insulin resistance, adipose tissue inflammation and hepatic steatosis [9–16]. In humans, insulin resistance can be induced after 24h of a saturated-fatty acid (SFA) rich diet, with longer periods of overfeeding causing similar results to those seen in animal models [17]. Although both iBAT and PVAT contain abundant UCP1 and express glycolytic/lipolytic genes [18], their response to brief nutrient excess is unclear. Therefore, we determined whether iBAT and PVAT differ in their response to a short-term (i.e. 72h) caloric surplus. Given the evidence that ambient housing temperature is a critical factor in determining adipose tissue function [19,20], we determined the response to a HFD at thermoneutrality (Tn, 28-30°C) so as to mimic human physiology by studying BAT under basal conditions (i.e. when UCP1 is not active).

2. Materials and Methods

All studies were approved by the University of Nottingham Animal Welfare and Ethical Review Board, and were carried out in accordance with the UK Animals (Scientific Procedures) Act of 1986. Twelve male Sprague-Dawley rats aged 8 weeks were purchased from Charles River (Kent, UK). Animals were randomised (http://www.graphpad.com/quickcalcs/randomize1.cfm) to either the control or intervention group. The study was carried out at thermoneutrality (c. 28^{0}C) to negate any confounding effects of active BAT on the response to nutrient excess, and animals were acclimated to this environment for 4 weeks. Following the 4 week acclimation, all animals were weighed and received either the control diet (824050 SDS, Kent, UK) or a 45% high-fat (HFD, n=6) diet (824018 SDS, Kent, UK) for 72h. During this time, animals had ad libitum access to food and water and all procedures were carried out under a 12:12-hour reverse light-dark cycle (i.e. the during the active phase) so as to minimise animal stress and maximise data quality and translatability [21].

2.1. Metabolic cages

All animals were placed in an open-circuit calorimeter known as the 'comprehensive laboratory animal monitoring system' (CLAMS: Columbus Instruments, Linton Instrumentation, Diss, UK) for the last 48h of the study. Oxygen consumption (VO_2) and carbon dioxide production (VCO_2) were measured [22] and were then used to calculate energy expenditure (EE) and respiratory exchange ratio (RER) [23,24], as previously described. Measurements were taken at 9 minute intervals for the last 24h. At the end of the 24h period, all animals were weighed and fasted overnight prior to euthanasia by rising CO_2 gradient. Relevant tissues were then rapidly dissected, weighed, snap-frozen in liquid nitrogen and stored at -80°C for subsequent analysis. PVAT was dissected from the aortic arch down the thoracic aorta [25].

2.2. Gene expression analysis

Total RNA was extracted from iBAT and PVAT with the RNeasy Plus Micro extraction kit (Qiagen, West Sussex, UK) using an adapted version of the single step acidified phenol-chloroform method. RNA purity was subsequently quantified with the Nanodrop ND-100 (Nanodrop Technologies, Wilmington, USA) and all samples were normalised to 1 ng μL^{-1}. Reverse transcription was carried out using the High Capacity RNA-to-cDNA kit (Life Technologies, Paisley, UK) and cDNA was then amplified on a Touchgene Gradient thermocycler (Techne Inc, Bibby Scientific Limited, Staffordshire, UK). Genes regulating thermogenesis, insulin signalling and energy metabolism were analysed by quantitative PCR on the Step One Plus q-PCR system and v.2.2

software (Applied Biosciences) using either iTaq Universal SybrGreen mastermix (BioRad, Watford, UK) or Taqman universal mastermix (ThermoFisher, Loughborough, UK) with rat-specific oligonucleotide primers (Sigma, Gillingham, UK) or FAM-MGB Taqman probes (see Supp Table 1 and 2 for primer list). Gene expression was determined using the GeNorm algorithm against two selected reference genes: *YWHAZ* and *TBP* (stability value M = 0.18 in BAT and 0.25 in PVAT).

2.3. Targeted insulin resistance PCR arrays

We utilised the Insulin Resistance (SAB target list) PCR Array (BioRad) to screen for 86 genes involved in the onset of adipose tissue insulin resistance (n=3 per group). All procedures were carried out according to manufacturers' instructions. Validation of representative data is shown in Supplementary data (Supp Figure 2).

2.4. Serum analysis

Serum was thawed gently on ice with concentrations of glucose (GAGO-20, Sigma Aldrich, Gillingham, UK), triglycerides (LabAssay ™ Trigylceride, Wako, Neuss, Germany), non-esterified fatty acids (NEFA)-HR(2), (Wako) and insulin (80-INSRT-E01, Alpco, Salem, NH, USA) measured following manufacturer's instructions.

2.5. Protein Extraction, clean-up and trypsinization

Proteins were extracted by homogenisation of c. 50-100 mg of frozen tissue in 500 L CellLytic MT cell lysis buffer (Sigma, C3228) and 5 L of Halt Protease Inhibitor Cocktail (Thermo, 78430) with subsequent centrifugation at 20,000 x g for 10 min. The concentration of each supernatant was determined using the Pierce BCA Protein Assay Kit (Thermo, 23225) prior to storage at -80°C. Lipid and other contaminants were removed from 100 L of each protein lysate using the ReadyPrep 2D cleanup Kit (Biorad, 1632130) with the final protein pellet reconstituted in 100 L of 50 mM TEAB buffer (6 M Urea, pH 8.0). Following quantification of the post-clean up concentration each sample was normalised (50 ug) and 5 L of 200 mM DTT/50 mM TEAB (pH 8.0) was added to each for the reduction of proteins over a 1 h period. Following this, 20 L of 200 mM Iodoacetamide/50 mM TEAB (pH 8.0) was added for alkylation (1 h) and finally, 20 L of 200 mM DTT/50 mM TEAB (pH 8.0) to consume unreacted Iodoacetamide (1 h) with the latter two incubations carried out in the dark. 775 L of 50 mM TEAB was then added to reduce the urea concentration to c. 0.6 M and Sequencing Grade Modified Trypsin (Promega, V5113) solution was added in a final concentration of 1:20 (w:w trypsin/protein). All samples were gently vortexed and incubated overnight for 18 h at 37°C, following which 2.5 L of formic acid was added to reduce the pH and halt trypsin activity. All samples were then dried down at 60°C for 4 h and stored at 80°C before resuspending in liquid chromatography mass spectrometry (LCMS) grade 5% acetonitrile in 0.1% formic acid for subsequent analysis.

2.6. Mass spectrometry

Samples (4 L) were injected by Eksigent 425 LC system onto a trap column (Mobile Phase A; 0.1% formic acid, B; Acetonitrile with 0.1% formic acid; YMC Triart C_{18} guard column 0.3 x 5 mm, 300 m ID) at 10 L/min mobile phase A for 2 min before gradient elution onto the analytical column (YMC Triart C_{18} 150 x 0.3mm ID, 3 m) in line to a Sciex TripleTOF 6600 Duospray Source using a 50 m electrode, positive mode +5500V. Samples were analysed in both IDA (Information Dependent Acquisition, for the generation of a spectral library) and SWATH (Data Independent Acquisition, to generate quantitative data) modes. The following linear gradients were used: for IDA, mobile phase B increasing from 2% to 30% over 68 min; 40% B at 72 min followed by column wash at 80% B and re-equilibration (87 min total run time). For SWATH, 3-30% B over 38 min; 40% B at 43 min followed by wash and re-equilibration as before (57 min total run time). IDA acquisition mode was used with a top 30 ion fragmentation (TOFMS *m/z* 400-1250; product ion 100-1500) followed by 15 sec exclusion using rolling collision energy, 50 ms accumulation time; 1.8 s cycle. SWATH acquisition was using

100 variable windows (optimised on sample type) 25 ms accumulation time, 2.6 s cycle (*m*/*z* 400-1250). IDA data was searched together using ProteinPilot 5.0.2, iodoacetamide alkylation, thorough search with emphasis on biological modifications (Swissprot rat database June 2018). SWATH data was analysed using Sciex OneOmics software [26] extracted against the locally generated library with the parameters 12 peptides per protein, 6 transitions per peptide, XIC width 30 ppm, 5 min retention time window.

2.7. Statistical analysis

Statistical analysis was performed in GraphPad Prism version 8.0 (GraphPad Software, San Diego, CA). Data are expressed as Mean ± SEM and details of specific statistical tests are given in figure legends.

Functional analysis of the proteome was performed using the Advaita Bioinformatic iPathwayGuide software (www.advaitabio.com/ipathwayguide.html) with a fold change ± 0.5 and confidence score cut-off of 0.75. Significantly impacted biological processes, molecular interactions and pathways were analysed in the context of pathways obtained from the Kyoto Encyclopedia of Genes and Genomes (KEGG) database (Release 84.0+/10-26, Oct 17) [27] and the Gene Ontology Consortium database (2017-Nov) [28]. The Elim pruning method, which removes genes mapped to a significant gene ontology (GO) term from more general (higher level) GO terms, was used to overcome the limitation of errors introduced by considering genes multiple times [29].

3. Results

3.1. Short-term HFD downregulates genes involved in thermogenesis in PVAT only

As expected, the short period of consuming a HFD did not cause any difference in final body weight between groups (Figure 1A), or in total fat mass (Control: 22.87±3.31; HFD: 23.51±3.68 g) or the weight of individual fat depots (Supp. Table 3). Increased 24h energy intake (Figure 1B) led to a small but significant increase final body weight (Figure 1C) equal to c. 2.6% body weight. Whilst there was no change in ambulatory activity or energy expenditure (Figures 1D, 1F, Suppl. Figure 1) the reduction in RER (Figure 1E) reflects a shift towards fat as the major fuel substrate in the HFD group. Interestingly, despite this rapid weight gain, there were no differences in serum insulin, glucose or triglycerides, although NEFA was reduced (Figure 1G-J). Thermogenic genes in BAT were unaffected, whereas PVAT was more susceptible to the HFD (Figure 2A and C). Despite similar UCP1 messenger RNA (mRNA), there was a reduction in gene expression for β3AR, DIO2 and PRDM16 in PVAT. There were no differences with the HFD in PGC1α, CIDEA, FGF21, CITED1, SLC36a2 or P2RX5 in iBAT, whilst only SLC36a2 was reduced in PVAT. Markers of beige adipocytes, TBX1 and TMEM26, were expressed in both iBAT and PVAT and the HFD only reduced TMEM26 in iBAT. The white adipocyte specific cell-surface marker, ASC1 [30], was expressed in both iBAT and PVAT and reduced with HFD in the latter.

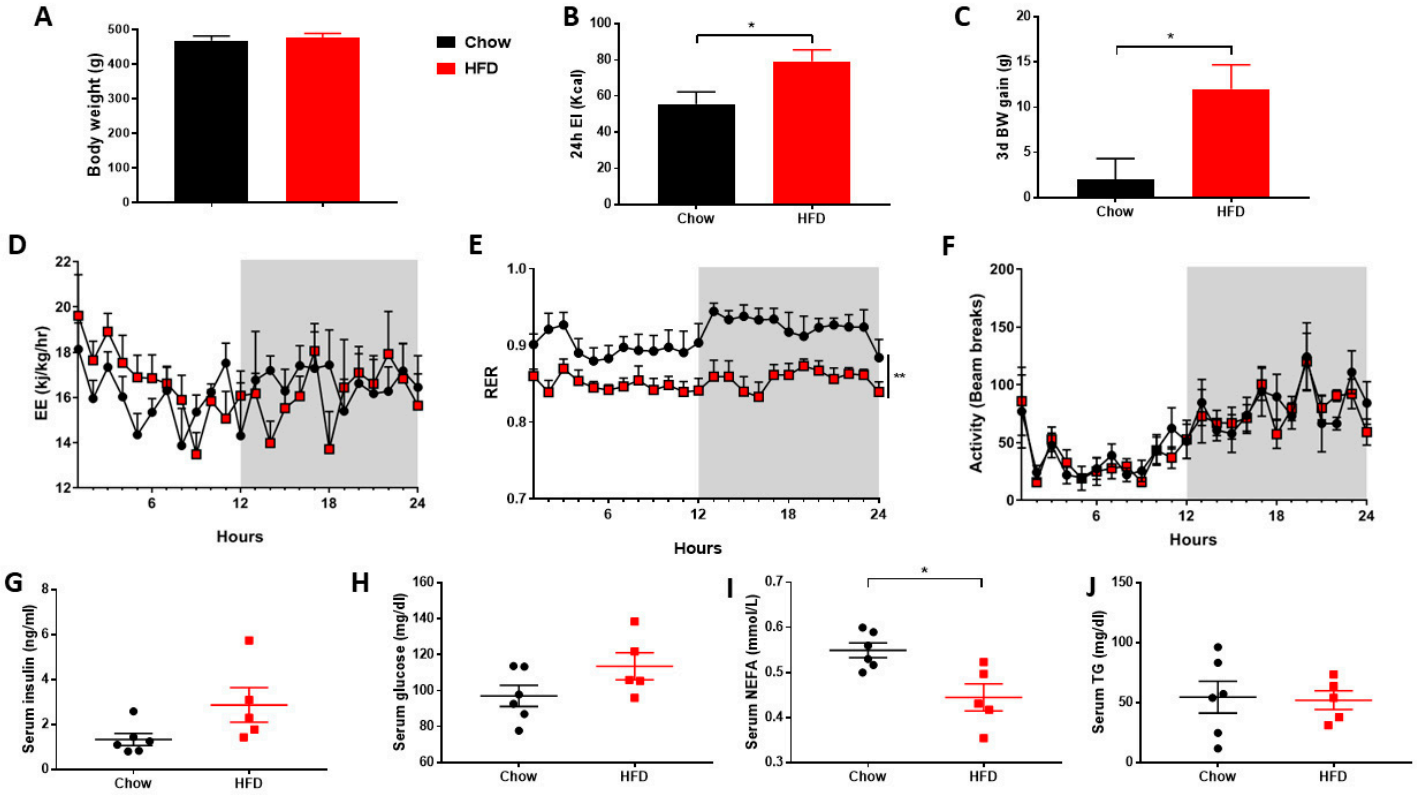

Figure 1. High fat diet (HFD) modified total energy balance but had no effect on insulin, glucose, triglycerides or non-esterified fatty acids. (A) Final body weight, (B) 24h energy intake, (C) 3 day weight gain, (D) 24h energy expenditure (EE), respiratory exchange ratio (RER) and ambulatory activity and (E) serum metabolites. Data expressed as mean ± SEM, n=6 per group. For comparison, data was analysed by either Students t-test (A-C, E) or two-way ANOVA (D) and Sidak post-hoc tests. Significance denoted as * < 0.05; ** < 0.01 or *** < 0.001.

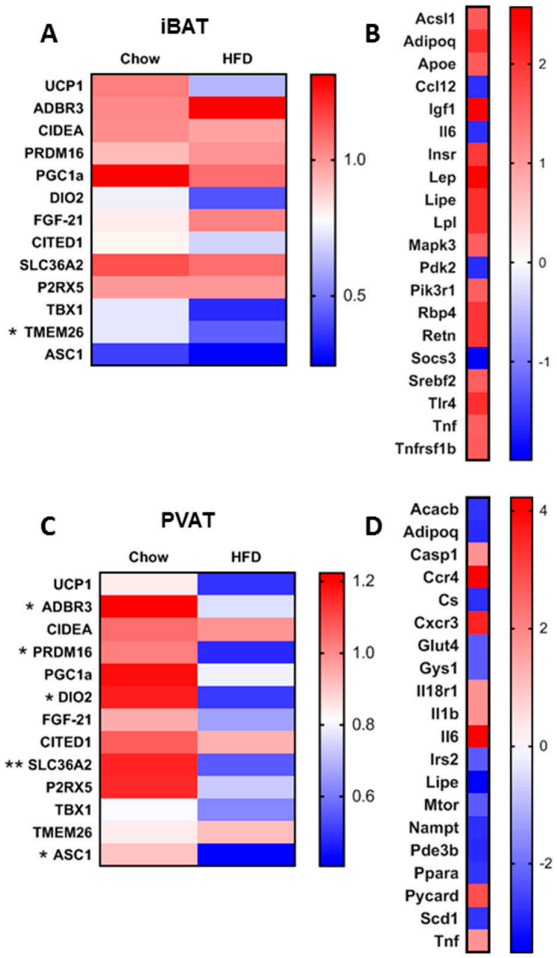

Figure 2. Summary of the effect of the HFD on differences in thermogenic genes involved in brown adipose tissue (BAT), beige and WAT adipocyte function in interscapular BAT (iBAT) (A) and perivascular BAT (PVAT) (C). Top 20 up/down-regulated genes involved in adipose tissue insulin resistance in iBAT (B) and PVAT (D). Data expressed as mean (A and C, n=5-6) or fold change (B and D, n=3). Data were analysed by Students t-test (A and C) with significance denoted as * < 0.05 or ** < 0.01.

3.2. Short-term HFD alters insulin signalling pathways in a depot-specific manner

Due to the marked reduction in thermogenic genes in PVAT in response to the HFD, a number of genes that regulate insulin signalling and energy metabolism were measured to determine if these were affected by short-term nutrient excess. Targeted array profiling demonstrated that genes involved in insulin signalling (i.e. Igf1, Insr, and Mapk3) and lipid metabolism (i.e. Hsl, Lpl, Acsl1 and Srebf2) were upregulated in iBAT (Figure 2B and D). iBAT also exhibited increased expression of genes associated with 'whitening' (i.e. Lep, Retn and Adipoq) and inflammation (i.e. Tlr4, Emr1 and Tnfrsf1b). Only four genes were down-regulated in iBAT including Pdk2 and Il6. PVAT exhibited a marked upregulation of Ccr4 and Cxcr3 which govern T-cell differentiation and infiltration. The HFD increased in markers of inflammasome activation, Pycard, Il1β and Casp1 in PVAT, concomitant with a down-regulation of genes governing lipid (i.e. Hsl, Pde3B, Acacb and Ppara) and glucose metabolism (i.e. Cs, Gys1, Irs2 and mTOR).

3.3. Short-term high fat feeding induces divergent alterations in the BAT and PVAT proteome

As the HFD induced clear differences in depot response, we analysed the proteome to identify novel proteins and pathways regulated by short-term high-fat feeding. A total of 107 proteins were differentially regulated in iBAT with those involved in the 20S core proteasome complex (Psma3l, ↑), endocytosis (Vps4a, ↓), calcium signalling (Camk2d, ↓) and glycolysis (Pkm, ↑) amongst the most significant (Table 1). In PVAT, 183 proteins were differentially regulated including those involved in glycolysis (Pfkp, ↓), apoptosis (Hdgf,↑; Ywhaq, ↑ and Ghitm, ↓), TLR signalling (Ube2n, ↑) and peroxisomal lipid metabolism (Acox1, ↓) (Table 2).

Table 1. Top 10 differentially regulated proteins in BAT.

Symbol	Gene name	Entrez	Logfc	Adjpv
Psma3l	Proteasome subunit alpha type-3	408248	**0.793509**	0.000116
Tmem126a	Transmembrane protein 126A	293113	**-1.83882**	0.000185
Ssr3	Signal Sequence Receptor Subunit 3	81784	**-1.61099**	0.0002
Ccdc51	Coiled-Coil Domain Containing 51	316008	**-0.693**	0.000763
Pkm	Pyruvate Kinase M1/2	25630	**0.7335**	0.00279
Vps4a	Vacuolar Protein Sorting 4 Homolog A	246772	**-0.71726**	0.003363
Apoa4	Apolipoprotein A4	25080	**-1.0162**	0.004051
Prss1	Serine Protease 1	24691	**0.827668**	0.005684
Serpina3n	Serpin Family A Member 3	24795	**-0.58665**	0.006792
Camk2d	Calcium/Calmodulin Dependent Protein Kinase II Delta	24246	**-2.55115**	0.007442

Entrez gene ID (Entrez), log fold change (Logfc) where minus symbol equals downregulation, adjusted *P* value (adjPval).

Table 2. Top 10 differentially regulated proteins in PVAT

Symbol	Gene name	Entrez	Logfc	Adjpv
Pfkp	Phosphofructokinase, Platelet	60416	**-1.38584**	0.000225
Hdgf	Heparin Binding Growth Factor	114499	**0.69362**	0.000445
Rbmxrtl	RNA-binding motif protein, X chromosome retrogene-like	307779	**1.91652**	0.001389
Ywhaq	14-3-3 Protein Theta	25577	**0.613265**	0.001405
Ghitm	Growth Hormone Inducible Transmembrane Protein	290596	**-0.71467**	0.001854
Capza1	Capping Actin Protein Of Muscle Z-Line Subunit Alpha 1	691149	**1.194102**	0.002081
Mtpn	Myotrophin	79215	**0.669685**	0.002234
Ube2n	Ubiquitin Conjugating Enzyme E2 N	116725	**0.80585**	0.002495
B2m	Beta-2-Microglobulin	24223	**0.809804**	0.002742
Acox1	Acyl-CoA Oxidase 1	50681	**-3.50641**	0.004222

Entrez gene ID (Entrez), log fold change (Logfc) where minus symbol equals downregulation, adjusted *P* value (adjPval).

Gene ontology (GO) analysis demonstrated the proteins in iBAT (Table 3) were significantly enriched for lipid-related processes and functions including *positive regulation of lipid catabolic process*, *high-density lipoprotein particle assembly*, *phosphatidylcholine-sterol O-acyltransferase activator activity* and *very-low-density lipoprotein particle*. In PVAT (Table 4), however, proteins were significantly enriched for nuclear and DNA-related processes and functions, including *nucleosome assembly*, *histone exchange*, *sequence-specific DNA binding* and *nuclear chromosomes*. Impact analysis, which combines classical overrepresentation analysis with the perturbation of a given pathway, demonstrated that *fat and digestion*, *glucagon signalling* and peroxisome proliferator-activated receptor (*PPAR) signalling* pathways were amongst those impacted in iBAT (Figure 3A-D) whilst *RNA degradation*, *cell adhesion molecules* and *ribosome* pathways were among those impacted in PVAT (Figure 3E-G).

Table 3. GO terms enriched in BAT.

GoId	GoName	CountDE	CountAll	Pv_elim
	Biological Process			
GO:0039536	negative regulation of RIG-I signaling pathway	3	3	0.0011
GO:0050996	positive regulation of lipid catabolic process	4	6	0.0014
GO:0046470	phosphatidylcholine metabolic process	5	7	0.0038
GO:0030300	regulation of intestinal cholesterol absorption	3	4	0.004
GO:0034380	high-density lipoprotein particle assembly	3	4	0.004
	Molecular Function			
GO:0031210	phosphatidylcholine binding	3	3	0.0011
GO:0060228	phosphatidylcholine-sterol O-acyltransferase activator activity	3	4	0.004
GO:0003713	transcription coactivator activity	4	8	0.0054
GO:0001047	core promoter binding	3	5	0.0091
GO:0017127	cholesterol transporter activity	3	5	0.0091
	Cellular Component			
GO:0034366	spherical high-density lipoprotein particle	3	4	0.0041
GO:0042627	chylomicron	3	4	0.0041
GO:0005667	transcription factor complex	3	6	0.0174
GO:0034361	very-low-density lipoprotein particle	3	6	0.0174

Table 4. GO terms enriched in PVAT.

GoId	GoName	CountDE	CountAll	Pv_elim
	Biological Process			
GO:0006334	nucleosome assembly	8	10	0.00023
GO:0017144	drug metabolic process	5	8	0.00287
GO:0043486	histone exchange	3	3	0.00343
GO:1901655	cellular response to ketone	8	21	0.00825
GO:0021766	hippocampus development	6	14	0.0116
	Molecular Function			
GO:0042393	histone binding	7	8	0.000011
GO:0003785	actin monomer binding	3	3	0.0033
GO:0043565	sequence-specific DNA binding	8	23	0.0143
GO:0035091	phosphatidylinositol binding	5	8	0.0219
GO:0005506	iron ion binding	6	16	0.0227
	Cellular Component			
GO:0000788	nuclear nucleosome	3	3	0.0035
GO:0000784	nuclear chromosome, telomeric region	3	4	0.0123
GO:0030054	cell junction	38	183	0.0174
GO:0071013	catalytic step 2 spliceosome	5	12	0.0246
GO:0001931	uropod	3	5	0.0273

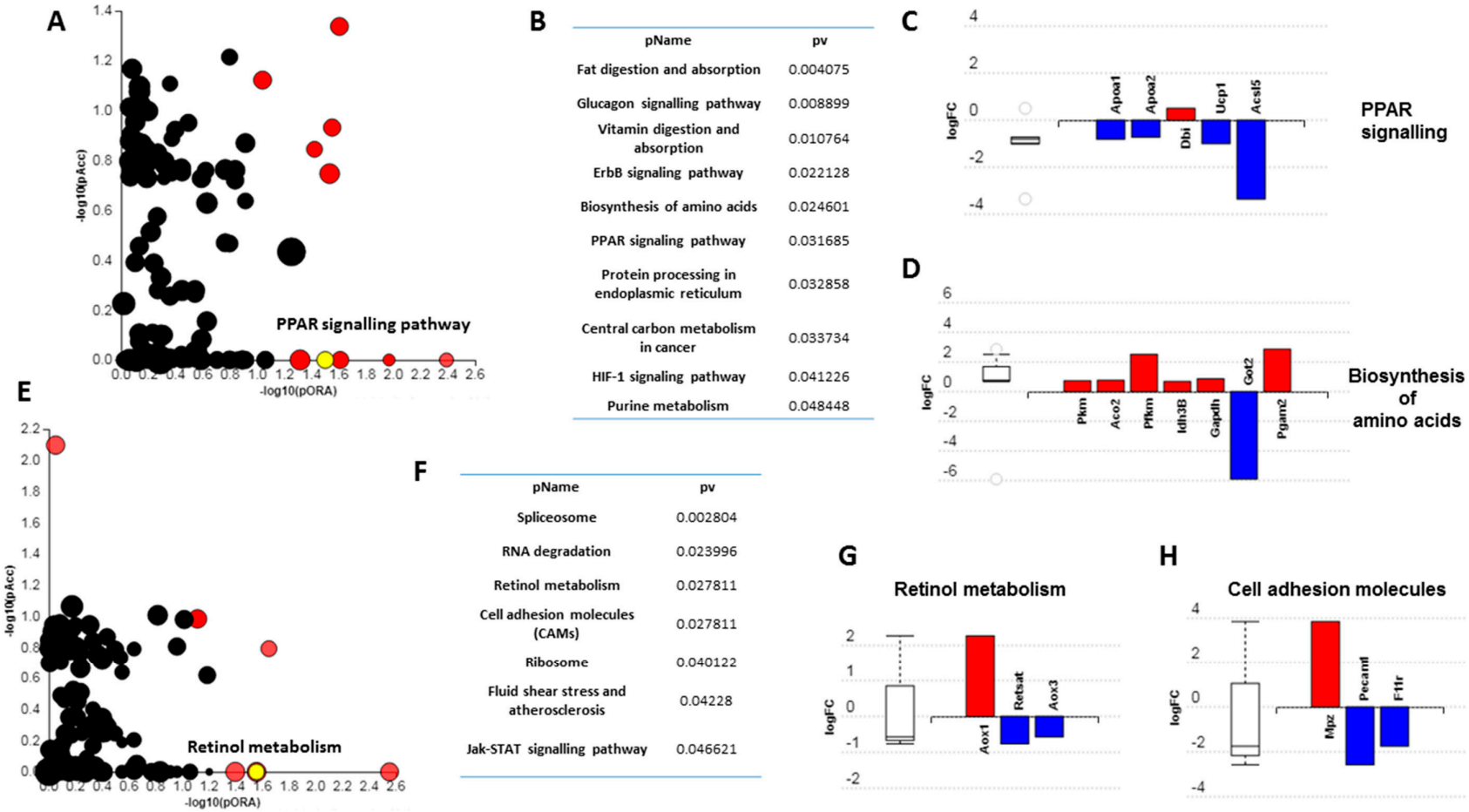

pName	pv
Fat digestion and absorption	0.004075
Glucagon signalling pathway	0.008899
Vitamin digestion and absorption	0.010764
ErbB signaling pathway	0.022128
Biosynthesis of amino acids	0.024601
PPAR signaling pathway	0.031685
Protein processing in endoplasmic reticulum	0.032858
Central carbon metabolism in cancer	0.033734
HIF-1 signaling pathway	0.041226
Purine metabolism	0.048448

pName	pv
Spliceosome	0.002804
RNA degradation	0.023996
Retinol metabolism	0.027811
Cell adhesion molecules (CAMs)	0.027811
Ribosome	0.040122
Fluid shear stress and atherosclerosis	0.04228
Jak-STAT signalling pathway	0.046621

Figure 3. Overview of alterations in the proteome of iBAT and PVAT following 72h of high fat feeding. Impact analysis: iBAT (A), PVAT (E); Most impacted pathways: iBAT (B), PVAT (F); Proteins altered in specified pathways: iBAT (C and D), PVAT (G and H).Figures created with Advaita Bio IPathwayGuide using only differentially altered proteins. Peroxisome proliferator-activated receptor (PPAR).

4. Discussion

Brown adipose tissue plays a major role in regulating whole body glucose and lipid homeostasis under cold conditions (i.e. when UCP1 is active) with apparent anti-obesity potential in rodents [8]. Here, we demonstrate that when animals are housed at thermoneutrality (i.e. when UCP1 is not active) short-term exposure to a HFD is sufficient to induce rapid whole-body weight gain which may be due to uptake of circulating NEFA. Furthermore, iBAT and PVAT, whilst phenotypically similar, differ in their response to this brief period of nutrient excess. This is the first study to investigate whether these anatomically and developmentally distinct depots [1,2] respond differently to a brief caloric surplus, and suggests that not all BAT is similar with regards to its potential to regulate nutrient metabolism.

An important aspect of our study is the finding that adaptations in iBAT and PVAT with rapid whole-body weight gain occur prior to increased fat mass and it is likely this weight gain is a consequence of lipid accumulation across all fat depots. The changes in iBAT and PVAT could, therefore, be early events in the transition from BAT to a whiter phenotype, the development of adipose tissue dysfunction and /or adaptations in response to caloric surplus. For instance, PSMA3, a component of the core 20S proteasome complex is upregulated in visceral adipose tissue of obese rats [31] and is seen here to be upregulated after only 72h of HFD suggesting a potential role in the acute and chronic adaptation to HFD in these tissues.

In BAT however, activation of the proteasome is essential for cold-induced thermogenesis with selective induction of proteostasis in BAT improving metabolic activity and body weight independent of insulin tolerance in diet-induced obesity [32]. In this study, downregulation of Transmembrane Protein 126a (TMEM126a) in iBAT is of particular interest. It is an inner-mitochondrial, cristae associated transmembrane protein strongly expressed in multiple tissues in adult humans and co-localises with ATP synthase F1 subunit alpha (ATP5A) [33,34]. Intriguingly, TMEM126 also co-localises with, and binds to, a CD137 ligand (CD137L) in macrophages to regulate reverse signaling [35,36]. CD137 is a common marker of beige adipocytes. Whether TMEM126a regulates mitochondrial function in iBAT or in the development of beige adipocytes is unknown. Another mitochondrial protein, Coiled-Coil Domain Containing 51 (CCDC51), has previously been shown to be a target of the transcription factor iroquois homeobox 3 (IRX3). In human obesity, IRX3 is a target of the FTO risk loci with allele carriers having increased IRX3 expression in early adipogenesis where it is proposed to regulate adipocyte function and browning through the modulation of mitochondrial genes [37].

Our finding that the response to brief nutrient excess differs in PVAT compared to iBAT may be explained, in part, by the proximity of PVAT to, and local interaction with, the vascular system. The downregulation of Phosphofructokinase, Platelet (PFKP), which catalyses fructose 6-phosphate to fructose 1,6-bisphophate, is intriguing given that elevated expression is associated with raised BMI and obesity in genome wide association studies [38,39]. In iBAT, however, PFKP expression is induced by cold exposure and sympathetic activation with a β3-agonist and reduced at thermoneutrality [40]. This is in line with the downregulation of both thermogenic and metabolic genes and would suggest perturbed adipocyte function in PVAT. Furthermore, Growth Hormone Inducible Transmembrane Protein (GHITM), a mitochondrial protein involved in cristae organisation, cytochocrome C release and apoptosis was downregulated [41]. Alongside an upregulation of Ubiquitin Conjugating Enzyme E2 N (Ube2n) which regulates the TLR4 signalling pathway, and genes governing the inflammasome it points towards a pro-inflammatory, apoptotic environment in PVAT following only brief exposure to a HFD. Interestingly, Myotrophin (MTPN) and Capping Actin Protein Of Muscle Z-Line Subunit Alpha 1 (CAPZA1), both of which play a role in the growth of actin filaments, were upregulated in PVAT. Of these, MTPN drives the growth of cardiomyocytes and promotes cardiac hypertrophy, whilst reduced CAPZA1 improves post-ischemic cardiac function [42,43]. Whether these proteins in PVAT signal to the endothelium to regulate vascular remodelling is currently unknown.

The enrichment of lipid and cholesterol-related GO terms in iBAT are in accordance with a major role in lipoprotein metabolism [44,45]. Downregulation of proteins involved in reverse-transport of

cholesterol from fat to liver and the formation of high-density lipoproteins and chylomicrons (APOA1, 2 and 4) suggests changes in the uptake and processing of triglyceride-rich lipoproteins as fuel for iBAT [46]. Alternatively, and in the context of the rapid whole body weight gain, perturbation of PPAR signaling including reduced UCP1 and upregulation of white adipose adipokines i.e. adiponectin mRNA may indicate early stages of iBAT remodeling towards a white phenotype. In contrast, the enrichment of nuclear related GO terms in PVAT are indicative of dynamic changes in DNA replication, repair and gene transcription [47–49]. Whether the genes and proteins in these nuclear-related pathways act on the vascular wall to regulate vascular function following brief exposure to a HFD remains to be determined, as does the extent to which these adaptations can be reversed.

Impact analysis further highlights the divergent response in these two BAT depots with *fat digestion and absorption glucagon signaling* and *PPAR signalling* among those impacted in iBAT. Importantly, downregulation of UCP1 in the PPAR signalling pathway suggests impaired BAT function which may contribute to the rapid weight gain seen within 72h. Furthermore, downregulation of the long-chain fatty-acid CoA ligase 5 (ACSL5) in the PPAR pathway and the Mitochondrial Aspartate Aminotransferase 2 (GOT2), which facilitates cellular long chain fatty acid uptake and metabolite exchange between the cytosol and mitochondria, is significant as long-chain fatty acids activate UCP1 and are the preferred fuel of BAT for adaptive thermogenesis [5]. Any adaptations of this type could modulate NEFA handling and contribute in part to the decline in plasma NEFA with the HFD, although TG were unaffected. Conversely in PVAT, impacted pathways included retinol metabolism, cell adhesion molecules, ribosome and fluid shear stress and atherosclerosis. Retinoic acid regulates adipogenesis and cell migration, differentiation, apoptosis and vascular calcification in vascular smooth muscle cells [50]. A downregulation of Retinol Saturase (RETSAT) may also be indicative of the early stages of PVAT dysfunction. RETSAT knockout mice exhibit increased adiposity due to an upregulation of PPARγ and FABP4 and it is downregulated in obese humans where the infiltration of macrophages represses its function [51,52]. Altered cell adhesion and shear stress pathways in PVAT are intriguing due to their well-known role in driving atherogenesis [53,54]. For instance, the platelet and cell adhesion molecule PECAM1 is essential for vascular remodeling in mice with PECAM1 knockout mice, which are partially protected from atherosclerosis, exhibiting reduced aortic arch and sinus lesions [55,56]. How these proteins in PVAT regulate vascular function is currently unknown but we predict these may be the initial stages of PVAT dysfunction in response to a HFD and, as such, could be important in the initial stages of vascular dysfunction.

5. Conclusions

In conclusion, we show that two anatomically and developmentally distinct BAT depots exhibit a divergent response to short-term nutrient excess. We propose these alterations, which occur following rapid weight gain but prior to increased fat mass, are of importance in the development of subsequent adipocyte dysfunction in obesity.

Supplementary Materials: The following are available online at www.mdpi.com/xxx/s1, Figure S1: High fat diet (HFD) had no effect 24h energy expenditure (EE) as measured during either the light or dark phases, Figure S2: Validation of select genes from targeted array plate, Table S1: Details of probe assays used for qPCR, Table S2: Rat specific Forward and Reverse Oligonucleotide Primers Used for Real-Time PCR, Table S3: Depot fat mass following 72h HFD (grams).

Ethical approval: University of Nottingham Animal Welfare and Ethical Review Board, in accordance with the UK Animals (Scientific Procedures) Act (1986).

Availability of data and material: The datasets used and analysed during the current study are available from the corresponding author on reasonable request

Authors' contributions: P.A., H.B. and M.E.S. conceived the study and attained the funding; P.A. and M.E.S. developed and designed the experiments; P.A, J.E.L, A.K.M I.B. and D. J. B. performed the experiments; P.A., A.K.M. and D.J.B. analyzed the data; P.A. and M.E.S. wrote the paper which was revised critically by D.J.B., H.B., F.J.P.E, and J.E.L. for important intellectual content. All authors read and approved the final manuscript.

Funding: The British Heart Foundation [grant number FS/15/4/31184/].

Competing interests: The authors declare that they have no competing interests.

References

1. Sanchez-Gurmaches, J.; Guertin, D.A. Adipocyte lineages: Tracing back the origins of fat. *Biochim. Biophys. Acta* **2014**, *1842*, 340–351.
2. Chang, L.; Villacorta, L.;.Li, R.; Hamblin, M.; Xu, W.; Dou, C.; Zhang, J.; Wu, J.; Zeng, R.; Chen, Y.E. Loss of perivascular adipose tissue on peroxisome proliferator-activated receptor-gamma deletion in smooth muscle cells impairs intravascular thermoregulation and enhances atherosclerosis. *Circulation* **2012**, *126*, 1067–1078.
3. Blondin, D.P.; Tingelstad, H.C.; Noll, C.; Frisch, F.; Phoenix, S.; Guérin, B.; Turcotte, É.E.; Richard, D.; Haman, F.; Carpentier; A.C. Dietary fatty acid metabolism of brown adipose tissue in cold-acclimated men. *Nat. Commun.* **2017**, *8*, 14146.
4. Lee, P.; Bova, R.; Schofield, L.; Bryant, W.; Dieckmann, W.; Slattery, A.; Govendir, M.A.; Emmet. L.; Greenfield, J.R. Brown Adipose Tissue Exhibits a Glucose-Responsive Thermogenic Biorhythm in Humans. *Cell Metab.* **2016**, *23*, 602–609.
5. Cannon, B.; Nedergaard, J. Brown adipose tissue: Function and physiological significance. *Physiol. Rev.* **2004**, *84*, 277–359.
6. Scheele, C.; Nielsen, S. Metabolic regulation and the anti-obesity perspectives of human brown fat. *Redox. Biol.* **2017**, *12*, 770–775.
7. Nosalski, R.; Guzik, T.J. Perivascular adipose tissue inflammation in vascular disease. *Br. J. Pharm.* **2017**, *174*, 3496–3513.
8. Marlatt, K.L.; Ravussin, E. Brown Adipose Tissue: An Update on Recent Findings. *Curr. Obes. Rep.* **2017**, *6*, 389–396.
9. Waise, T.M.Z.; Toshinai, K.; Naznin, F.; NamKoong, C.; Md Moin, A.S.; Sakoda, H.; Nakazato, M. One-day high-fat diet induces inflammation in the nodose ganglion and hypothalamus of mice. *Biochem. Biophys. Res. Commun.* **2015**, *464*, 1157–1162.
10. Boghossian, S.; Lemmon, K.; Park, M.; York, D.A. High-fat diets induce a rapid loss of the insulin anorectic response in the amygdala. *Am. J. Physiol. Regul. Integr. Comp. Physiol.* **2009**, *297*, R1302–R1311.
11. Clegg, D.J.; Gotoh, K.; Kemp, C.; Wortman, M.D.; Benoit, S.C.; Brown, L.M.; D'Alessio, D.; Tso, P.; Seeley, R.J.; Woods, S.C. Consumption of a high-fat diet induces central insulin resistance independent of adiposity. *Physiol. Behav.* **2011**, *103*, 10–16.
12. Xiao, Y.; Wang, W.; Chen, L.; Chen, J.; Jiang, P.; Fu, X.; Nie, X.; Kwan, H.; Liu, Y.; Zhao, X. The effects of short-term high-fat feeding on exercise capacity: Multi-tissue transcriptome changes by RNA sequencing analysis. *Lipids Health Dis.* **2017**, *16*, 28.
13. Ji, Y.; Sun, S.; Xia, S.; Yang, L.; Li, X.; Qi, L. Short term high fat diet challenge promotes alternative macrophage polarization in adipose tissue via natural killer T cells and interleukin-4. *J. Biol. Chem.* **2012**, *287*, 24378–24386.
14. Lee, Y.S.; Li, P.; Huh, I.J.; Lu, M.; Kim, J.I.; Ham, M.; Talukdar, S.; Chen, A.; Lu, W.J. Inflammation is necessary for long-term but not short-term high-fat diet-induced insulin resistance. *Diabetes* **2011**, *60*, 2474–2483.
15. Wiedemann, M.S.; Wueest, S.; Item, F.; Schoenle, E.J.; Konrad, D. Adipose tissue inflammation contributes to short-term high-fat diet-induced hepatic insulin resistance. *Am. J. Physiol. Endocrinol. Metab.* **2013**, *305*, E388–E395.
16. Mullen, K.L.; Tishinsky, J.M.; Robinson, L.E.; Dyck, D.J. Skeletal muscle inflammation is not responsible for the rapid impairment in adiponectin response with high-fat feeding in rats. *Am. J. Physiol. Regul. Integr. Comp. Physiol.* **2010**, *299*, R500–R508.
17. Cuthbertson, D.J.; Steele, T.; Wilding, J.P.; Halford, J.C.; Harrold, J.A.; Hamer, M.; Karpe, F. What have human experimental overfeeding studies taught us about adipose tissue expansion and susceptibility to obesity and metabolic complications? *Int. J. Obes. (Lond.)* **2017**, *41*, 853–865.
18. Fitzgibbons, T.P.; Kogan, S.; Aouadi, M.; Hendricks, G.M.; Straubhaar, J.; Czech, M.P. Similarity of mouse perivascular and brown adipose tissues and their resistance to diet-induced inflammation. *Am. J. Physiol. Heart Circ. Physiol.* **2011**, *301*, H1425–H1437.

19. Gordon, C.J. The mouse thermoregulatory system: Its impact on translating biomedical data to humans. *Physiol. Behav.* **2017**, *179*, 55–66.
20. Tian, X.Y.; Ganeshan, K.; Hong, C.; Nguyen, K.D.; Qiu, Y.; Kim, J.; Tangirala, R.K.; Tontonoz, P.; Chawla, A. Thermoneutral Housing Accelerates Metabolic Inflammation to Potentiate Atherosclerosis but Not Insulin Resistance. *Cell Metab.* **2016**, *23*, 165–178.
21. Hawkins, P.; Golledge, H.D.R. The 9 to 5 Rodent—Time for Change? Scientific and animal welfare implications of circadian and light effects on laboratory mice and rats. *J. Neurosci. Methods* **2018**, *300*, 20–25.
22. Warner, A.; Jethwa, P.H.; Wyse, C.A.; l'Anson, H.; Brameld, J.M.; Ebling, F.J.P. Effects of photoperiod on daily locomotor activity, energy expenditure, and feeding behavior in a seasonal mammal. *Am. J. Physiol. Regul. Integr. Comp. Physiol.* **2010**, *298*, R1409–R1416.
23. Samms, R.J.; Lewis, J.E.; Lory, A.; Fowler, M.J.; Cooper, S.; Warner, A.; Emmerson, P.; Adams, A.C.; Luckett, J.C.; Perkins, A.C.; et al. Antibody-Mediated Inhibition of the FGFR1c Isoform Induces a Catabolic Lean State in Siberian Hamsters. *Curr. Biol.* **2015**, *25*, 2997–3003.
24. Frayn, K.N. Calculation of substrate oxidation rates in vivo from gaseous exchange. *J. Appl. Physiol. Respir. Environ. Exerc. Physiol.* **1983**, *55*, 628–634.
25. Gil-Ortega, M.; Somoza, B.; Huang, Y.; Gollasch, M.; Fernández-Alfonso, M.S. Regional differences in perivascular adipose tissue impacting vascular homeostasis. *Trends Endocrinol. Metab.* **2015**, *26*, 367–375.
26. Lambert, J.P.; Ivosev, G.; Couzens, A.L.; Larsen, B.; Taipale, M.; Lin, Z.Y.; Zhong, Q.; Lindquist, S.; Vidal, M.; Aebersold, R.; et al. Mapping differential interactomes by affinity purification coupled with data-independent mass spectrometry acquisition. *Nat. Methods* **2013**, *10*, 1239–1245.
27. Kanehisa, M. The KEGG database. *Novartis Found. Symp.* **2002**, *247*, 91–101; discussion 101–103, 119–128, 244–252.
28. Ashburner, M.; Ball C.A.; Blake, J.A.; Botstein, D.; Butler, H.; Cherry, J.M.; Davis, A.P.; Dolinski, K.; Dwight, S.S.; Eppig, J.T. Gene ontology: Tool for the unification of biology. The Gene Ontology Consortium. *Nat. Genet.* **2000**, *25*, 25–29.
29. Alexa, A.; Rahnenfuhrer, J.; Lengauer, T. Improved scoring of functional groups from gene expression data by decorrelating GO graph structure. *Bioinformatics* **2006**, *22*, 1600–1607.
30. Ussar, S.; Lee, K.Y.; Dankel, S.N.; Boucher, J.; Hearing, M.F.; Kleinridders, A.; Thomou, T.; Xue, R.; Macotela, Y.; Cypess, A.M.; et al. ASC-1, PAT2, and P2RX5 are cell surface markers for white, beige, and brown adipocytes. *Sci. Transl. Med.* **2014**, *6*, 247ra103.
31. Sakamuri, S.S.; Putcha, U.K.; Veettil, G.N.; Ayyalasomayajula, V. Transcriptome profiling of visceral adipose tissue in a novel obese rat model, WNIN/Ob & its comparison with other animal models. *Indian J. Med. Res.* **2016**, *144*, 409–423.
32. Bartelt, A.; Widenmaier, S.B.; Schlein, C.; Johann, K.; Goncalves, R.L.S.; Eguchi, K.; Fischer, A.W.; Parlakgül, G.; Snyder, N.A.; Nguyen, T.B.; et al. Brown adipose tissue thermogenic adaptation requires Nrf1-mediated proteasomal activity. *Nat. Med.* **2018**, *24*, 292–303.
33. Hanein, S.; Garcia, M.; Fares-Taie, L.; Serre, V.; De Keyzer, Y.; Delaveau, T.; Perrault, I.; Delphin, N.; Gerber, S.; Schmitt, A.; et al. TMEM126A is a mitochondrial located mRNA (MLR) protein of the mitochondrial inner membrane. *Biochim. Biophys. Acta* **2013**, *1830*, 3719–3733.
34. Hanein, S.; Perrault, I.; Roche, O.; Gerber, S.; Khadom, N.; Rio, M.; Boddaert, N.; Jean-Pierre, M.; Brahimi, N.; Serre, V.; et al. TMEM126A, encoding a mitochondrial protein, is mutated in autosomal-recessive nonsyndromic optic atrophy. *Am. J. Hum. Genet.* **2009**, *84*, 493–498.
35. Bae, J.S.; Choi, J.K.; Moon, J.H.; Kim, E.C.; Croft, M.; Lee, H.W. Novel transmembrane protein 126A (TMEM126A) couples with CD137L reverse signals in myeloid cells. *Cell Signal.* **2012**, *24*, 2227–2236.
36. Kim, E.C.; Moon, J.H.; Kang, S.W.; Kwon, B.; Lee, H.W. TMEM126A, a CD137 ligand binding protein, couples with the TLR4 signal transduction pathway in macrophages. *Mol. Immunol.* **2015**, *64*, 244–251.
37. Claussnitzer, M.; Dankel, S.N.; Kim, K.H.; Quon, G.; Meuleman, W.; Haugen, C.; Glunk, V.; Sousa, I.S.; Beaudry, J.L.; Puviindran, V.; et al. FTO Obesity Variant Circuitry and Adipocyte Browning in Humans. *N. Engl. J. Med.* **2015**, *373*, 895–907.
38. Scuteri, A.; Sanna, S.; Chen, W.M.; Uda, M.; Albai, G.; Strait, J.; Najjar, S.; Nagaraja, R.; Orrú, M.; Usala, G.; et al. Genome-wide association scan shows genetic variants in the FTO gene are associated with obesity-related traits. *PLoS Genet.* **2007**, *3*, e115.

39. Liu, Y.J.; Liu, X.G.; Wang, L.; Dina, C.; Yan, H.; Liu, J.F.; Levy, S.; Papasian, C.J.; Drees, B.M.; Hamilton, J.J.; et al. Genome-wide association scans identified CTNNBL1 as a novel gene for obesity. *Hum. Mol. Genet.* **2008**, *17*, 1803–1813.
40. Basse, A.L.; Isidor, M.S.; Winther, S.; Skjoldborg, N.B.; Murholm, M.; Andersen, E.S.; Pedersen, S.B.; Wolfrum, C.; Quistorff, B.; Hansen, J.B. Regulation of glycolysis in brown adipocytes by HIF-1alpha. *Sci. Rep.* **2017**, *7*, 4052.
41. Oka, T.; Sayano, T.; Tamai, S.; Yokota, S.; Kato, H.; Fujii, G.; Mihara, K. Identification of a novel protein MICS1 that is involved in maintenance of mitochondrial morphology and apoptotic release of cytochrome c. *Mol. Biol. Cell* **2008**, *19*, 2597–2608.
42. Yang, F.H.; Pyle, W.G. Reduced cardiac CapZ protein protects hearts against acute ischemia-reperfusion injury and enhances preconditioning. *J. Mol. Cell. Cardiol.* **2012**, *52*, 761–772.
43. Sarkar, S.; Leaman, D.W.; Gupta, S.; Sil, P.; Young, D.; Morehead, A.; Mukherjee, D.; Ratfliff, N.; Sun, Y.; Rayborn, M. Cardiac overexpression of myotrophin triggers myocardial hypertrophy and heart failure in transgenic mice. *J. Biol. Chem.* **2004**, *279*, 20422–20434.
44. Bartelt, A.; Bruns, O.T.; Reimer, R.; Hohenberg, H.; Ittrich H.; Peldschus, K.; Kaul, M.G.; Tromsdorf, U.I.; Weller, H.; Waurisch, C.; et al. Brown adipose tissue activity controls triglyceride clearance. *Nat. Med.* **2011**, *17*, 200–205.
45. Berbee, J.F.; Boon, M.R.; Khedoe, P.P.; Bartelt, A.; Schlein, C.; Worthmann, A.; Kooijman, S.; Hoeke, G.; Mol, I.M.; John, C.; et al. Brown fat activation reduces hypercholesterolaemia and protects from atherosclerosis development. *Nat. Commun.* **2015**, *6*, 6356.
46. Hoeke, G.; Kooijman, S.; Boon, M.R.; Rensen, P.C.; Berbee, J.F. Role of Brown Fat in Lipoprotein Metabolism and Atherosclerosis. *Circ. Res.* **2016**, *118*, 173–182.
47. Krude, T. Chromatin. Nucleosome assembly during DNA replication. *Curr. Biol.* **1995**, *5*, 1232–1234.
48. Venkatesh, S.; Workman, J.L. Histone exchange, chromatin structure and the regulation of transcription. *Nat. Rev. Mol. Cell Biol.* **2015**, *16*, 178–189.
49. Houseley, J.; Tollervey, D. The many pathways of RNA degradation. *Cell* **2009**, *136*, 763–776.
50. Rhee, E.J.; Nallamshetty, S.; Plutzky, J. Retinoid metabolism and its effects on the vasculature. *Biochim. Biophys. Acta* **2012**, *1821*, 230–240.
51. Schupp, M.; Lefterova, M.I.; Janke, J.; Leitner, K.; Cristancho, A.G.; Mullican, S.E.; Qatanani, M.; Szwergold, N.; Steger, D.J.; Curtin, J.C.; et al. Retinol saturase promotes adipogenesis and is downregulated in obesity. *Proc. Natl. Acad. Sci. USA* **2009**, *106*, 1105–1110.
52. Moise, A.R.; Lobo, G.P.; Erokwu, B.; Wilson, D.L.; Peck, D.; Alvarez, S.; Dominguez, M.; Alvarez, R.; Flask, C.A.; de Lera, A.R.; et al. Increased adiposity in the retinol saturase-knockout mouse. *FASEB J.* **2010**, *24*, 1261–1270.
53. Galkina, E.; Ley, K. Vascular adhesion molecules in atherosclerosis. *Arterioscler. Thromb. Vasc. Biol.* **2007**, *27*, 2292–2301.
54. Caro, C.G. Discovery of the role of wall shear in atherosclerosis. *Arterioscler. Thromb. Vasc. Biol.* **2009**, *29*, 158–161.
55. Stevens, H.Y.; Melchior, B.; Bell, K.S.; Yun, S.; Yeh, J.C.; Frangos, J.A. PECAM-1 is a critical mediator of atherosclerosis. *Dis. Models Mech.* **2008**, *1*, 175–181; discussion 179.
56. Chen, Z.; Tzima, E. PECAM-1 is necessary for flow-induced vascular remodeling. *Arterioscler. Thromb. Vasc. Biol.* **2009**, *29*, 1067–1073.

Chapter 3

Exercise Does Not Induce Browning at Thermoneutrality and Induces a Muscle-like Signature In Brown Adipose Tissue

---

Chapter 4

Cold but not B3-AR agonism drives adiposity in physiologically humanised animals

---

Chapter 5

General conclusions and future work

5.1 General conclusions

Overall, this work shows for the first time how adipose tissue responds to common dietary and thermogenic stimuli in the basal state (i.e. when UCP1 is not active) and is an important step in our understanding of rodent adipose tissue biology at thermoneutrality. Here, I will highlight the main findings from this body of work and the overall conclusions.

- At thermoneutrality, just 72h of high-fat diet is sufficient to induce diverse changes to the BAT proteome. These changes are depot-specific with perivascular BAT seemingly more susceptible to dysfunction.
- When animals are housed at thermoneutrality from weaning, with access to a high-fat diet UCP1 is not expressed in classic 'beige' inguinal white adipose tissue (IWAT) at 16 weeks of age.
- Further, exercise training does not induce 'browning' of this depot as is commonly shown. Instead, exercise training downregulates proteins involved in apoptosis, pre-mRNA synthesis and RNA metabolism in IWAT.
- In BAT, exercise training induces an oxidative, myogenic signature characterised by an upregulation of proteins involved in oxidative phosphorylation and skeletal muscle physiology.
- Under these conditions, modest reductions in ambient temperature drive weight gain and increase BAT and subcutaneous IWAT. This effect is not seen in animals treated with Mirabegron, suggesting a direct effect of reduced ambient temperature.

- This is associated with depot-specific changes to the adipose tissue proteome elucidating physiological processes which may be contributing to these effects.
- Thermoneutral housing is a potentially important tool for studying BAT in its' basal state (i.e. when UCP1 is inactive) as it is in the human population.

5.2 Future work

There are numerous potential avenues available to follow up on the work presented here. For instance, I have identified a number of novel proteins that are regulated by just 72h of a high-fat diet and their role in BAT metabolism is currently unclear. As discussed in Chapter 2, TMEM126a is an inner mitochondrial transmembrane and CD137 binding protein. As such, it would be interesting to know if TMEM126a regulates both UCP1 and 'browning' given the role of CD137 as a putative 'beige' marker. PON1 is a hepatic secreted protein that binds HDL. Further work could elucidate whether PON1 is a hepatokine that acts on BAT following uptake of HDL and whether it has meaningful effects on BAT metabolism.

As discussed in Chapter 3, future work should look to determine the physiological relevance of the induction of proteins associated with skeletal muscle physiology in BAT following exercise training. Myogenesis could be explored with lineage tracing experiments and through the quantification of cells expressing muscle specific markers. Further, quantification of protein synthesis would validate whether changes in proteins and pathways involved in amino acid synthesis relate to functional changes. With regards to white adipose tissue, future work should look to

determine why exercise training downregulates proteins involved in pre-mRNA synthesis and RNA metabolism and the impact of these changes on adipose tissue function. This also applied to the downregulation of apoptotic proteins and it would be essential to determine if these changes are also seen in human WAT following exercise training.

The mechanism governing the effect of mild cold-exposure in obese animals remains to be determined and, as discussed in chapter 4 future work is needed to elucidate whether this is indeed insulative in nature. In addition, it will be critical to discover the central pathways responsible for this and whether the results are due to chronic BAT inactivity or indeed due to a defect in activation of the sympathetic nervous system. Using gradual reductions in ambient temperature, and quantification of energy expenditure we could determine what temperature is needed to drive increased energy expenditure and weight loss in obese animals raised at thermoneutrality with the expectation that this may be more applicable to the obese, human population. Given Mirabegron is in use clinically it will be of importance to determine the significance of its effect on ribosomal proteins and how a downregulation of the ribosomal pathway, and potentially protein synthesis effects adipose tissue function. It will also be important to determine whether it effects this pathway in other tissues such as skeletal muscle and whether Mirabegron could have detrimental effects on skeletal muscle with ageing.

A caveat of this body of work is that there was no assessment of mitochondrial function. Future work should determine how these interventions, under these conditions, and how genetic manipulation of candidate proteins effect mitochondrial

respiration and other in-vitro parameters such as insulin stimulated glucose uptake and lipolysis.

References

1. Aldiss, P., et al., *Beyond obesity - thermogenic adipocytes and cardiometabolic health.* Horm Mol Biol Clin Investig, 2017. **31**(2).
2. Aldiss, P., et al., *'Browning' the cardiac and peri-vascular adipose tissues to modulate cardiovascular risk.* Int J Cardiol, 2017. **228**: p. 265-274.
3. Aldiss, P., et al., *Exercise-induced 'browning' of adipose tissues.* Metabolism, 2018. **81**: p. 63-70.
4. Symonds, M.E., et al., *Recent advances in our understanding of brown and beige adipose tissue: the good fat that keeps you healthy.* F1000Res, 2018. **7**.
5. Cinti, S., *The adipose organ at a glance.* Dis Model Mech, 2012. **5**(5): p. 588-94.
6. Sanchez-Gurmaches, J. and D.A. Guertin, *Adipocyte lineages: tracing back the origins of fat.* Biochim Biophys Acta, 2014. **1842**(3): p. 340-51.
7. de Jong, J.M., et al., *A stringent validation of mouse adipose tissue identity markers.* Am J Physiol Endocrinol Metab, 2015. **308**(12): p. E1085-105.
8. Grant, R.W. and V.D. Dixit, *Adipose tissue as an immunological organ.* Obesity (Silver Spring), 2015. **23**(3): p. 512-8.
9. Kershaw, E.E. and J.S. Flier, *Adipose tissue as an endocrine organ.* J Clin Endocrinol Metab, 2004. **89**(6): p. 2548-56.
10. Symonds, M.E., M. Pope, and H. Budge, *The Ontogeny of Brown Adipose Tissue.* Annu Rev Nutr, 2015. **35**: p. 295-320.
11. Heaton, J.M., *The distribution of brown adipose tissue in the human.* J Anat, 1972. **112**(Pt 1): p. 35-9.
12. Cypess, A.M., et al., *Anatomical localization, gene expression profiling and functional characterization of adult human neck brown fat.* Nat Med, 2013. **19**(5): p. 635-9.
13. Cypess, A.M., et al., *Identification and importance of brown adipose tissue in adult humans.* N Engl J Med, 2009. **360**(15): p. 1509-17.
14. Robinson, L., et al., *Body mass index as a determinant of brown adipose tissue function in healthy children.* J Pediatr, 2014. **164**(2): p. 318-22 e1.
15. Symonds, M.E., et al., *Thermal imaging to assess age-related changes of skin temperature within the supraclavicular region co-locating with brown adipose tissue in healthy children.* J Pediatr, 2012. **161**(5): p. 892-8.
16. Ouellet, V., et al., *Outdoor temperature, age, sex, body mass index, and diabetic status determine the prevalence, mass, and glucose-uptake activity of 18F-FDG-detected BAT in humans.* J Clin Endocrinol Metab, 2011. **96**(1): p. 192-9.
17. Yoneshiro, T., et al., *Age-related decrease in cold-activated brown adipose tissue and accumulation of body fat in healthy humans.* Obesity (Silver Spring), 2011. **19**(9): p. 1755-60.
18. Wu, J., et al., *Beige adipocytes are a distinct type of thermogenic fat cell in mouse and human.* Cell, 2012. **150**(2): p. 366-76.
19. De Matteis, R., et al., *Exercise as a new physiological stimulus for brown adipose tissue activity.* Nutr Metab Cardiovasc Dis, 2013. **23**(6): p. 582-90.
20. Sidossis, L.S., et al., *Browning of Subcutaneous White Adipose Tissue in Humans after Severe Adrenergic Stress.* Cell Metab, 2015. **22**(2): p. 219-27.
21. Shabalina, I.G., et al., *UCP1 in brite/beige adipose tissue mitochondria is functionally thermogenic.* Cell Rep, 2013. **5**(5): p. 1196-203.

22. Poekes, L., N. Lanthier, and I.A. Leclercq, *Brown adipose tissue: a potential target in the fight against obesity and the metabolic syndrome.* Clin Sci (Lond), 2015. **129**(11): p. 933-49.
23. Maloney, S.K., et al., *Translating animal model research: does it matter that our rodents are cold?* Physiology (Bethesda), 2014. **29**(6): p. 413-20.
24. Kalinovich, A.V., et al., *UCP1 in adipose tissues: two steps to full browning.* Biochimie, 2017. **134**: p. 127-137.
25. Cantley, J., *The control of insulin secretion by adipokines: current evidence for adipocyte-beta cell endocrine signalling in metabolic homeostasis.* Mamm Genome, 2014. **25**(9-10): p. 442-54.
26. Villarroya, F. and A. Vidal-Puig, *Beyond the sympathetic tone: the new brown fat activators.* Cell Metab, 2013. **17**(5): p. 638-43.
27. Cooney, G.J., I.D. Caterson, and E.A. Newsholme, *The effect of insulin and noradrenaline on the uptake of 2-[1-14C]deoxyglucose in vivo by brown adipose tissue and other glucose-utilising tissues of the mouse.* FEBS Lett, 1985. **188**(2): p. 257-61.
28. Zaid, H., et al., *Insulin action on glucose transporters through molecular switches, tracks and tethers.* Biochem J, 2008. **413**(2): p. 201-15.
29. Marette, A. and L.J. Bukowiecki, *Stimulation of glucose transport by insulin and norepinephrine in isolated rat brown adipocytes.* Am J Physiol, 1989. **257**(4 Pt 1): p. C714-21.
30. Dallner, O.S., et al., *Beta3-adrenergic receptors stimulate glucose uptake in brown adipocytes by two mechanisms independently of glucose transporter 4 translocation.* Endocrinology, 2006. **147**(12): p. 5730-9.
31. Olsen, J.M., et al., *Glucose uptake in brown fat cells is dependent on mTOR complex 2-promoted GLUT1 translocation.* J Cell Biol, 2014. **207**(3): p. 365-74.
32. Chernogubova, E., B. Cannon, and T. Bengtsson, *Norepinephrine increases glucose transport in brown adipocytes via beta3-adrenoceptors through a cAMP, PKA, and PI3-kinase-dependent pathway stimulating conventional and novel PKCs.* Endocrinology, 2004. **145**(1): p. 269-80.
33. Chondronikola, M., et al., *Brown adipose tissue improves whole-body glucose homeostasis and insulin sensitivity in humans.* Diabetes, 2014. **63**(12): p. 4089-99.
34. Hao, Q., et al., *Transcriptome profiling of brown adipose tissue during cold exposure reveals extensive regulation of glucose metabolism.* Am J Physiol Endocrinol Metab, 2015. **308**(5): p. E380-92.
35. Lee, P., et al., *Temperature-acclimated brown adipose tissue modulates insulin sensitivity in humans.* Diabetes, 2014. **63**(11): p. 3686-98.
36. Blondin, D.P., et al., *Contributions of white and brown adipose tissues and skeletal muscles to acute cold-induced metabolic responses in healthy men.* J Physiol, 2015. **593**(3): p. 701-14.
37. Hanssen, M.J., et al., *Short-term cold acclimation improves insulin sensitivity in patients with type 2 diabetes mellitus.* Nat Med, 2015. **21**(8): p. 863-5.
38. Lee, P., et al., *Brown Adipose Tissue Exhibits a Glucose-Responsive Thermogenic Biorhythm in Humans.* Cell Metab, 2016. **23**(4): p. 602-9.
39. Gunawardana, S.C. and D.W. Piston, *Insulin-independent reversal of type 1 diabetes in nonobese diabetic mice with brown adipose tissue transplant.* Am J Physiol Endocrinol Metab, 2015. **308**(12): p. E1043-55.
40. Stanford, K.I., et al., *Brown adipose tissue regulates glucose homeostasis and insulin sensitivity.* J Clin Invest, 2013. **123**(1): p. 215-23.
41. Yuan, X., et al., *Brown adipose tissue transplantation ameliorates polycystic ovary syndrome.* Proc Natl Acad Sci U S A, 2016. **113**(10): p. 2708-13.

42. Turban, S., et al., *Defining the contribution of AMP-activated protein kinase (AMPK) and protein kinase C (PKC) in regulation of glucose uptake by metformin in skeletal muscle cells.* J Biol Chem, 2012. **287**(24): p. 20088-99.
43. Zhou, G., et al., *Role of AMP-activated protein kinase in mechanism of metformin action.* J Clin Invest, 2001. **108**(8): p. 1167-74.
44. Hundal, R.S., et al., *Mechanism by which metformin reduces glucose production in type 2 diabetes.* Diabetes, 2000. **49**(12): p. 2063-9.
45. Beiroa, D., et al., *GLP-1 agonism stimulates brown adipose tissue thermogenesis and browning through hypothalamic AMPK.* Diabetes, 2014. **63**(10): p. 3346-58.
46. Tokubuchi, I., et al., *Beneficial effects of metformin on energy metabolism and visceral fat volume through a possible mechanism of fatty acid oxidation in human subjects and rats.* PLoS One, 2017. **12**(2): p. e0171293.
47. Keates, A.C. and C.J. Bailey, *Metformin does not increase energy expenditure of brown fat.* Biochem Pharmacol, 1993. **45**(4): p. 971-3.
48. Rouru, J., et al., *Metformin and brown adipose tissue thermogenetic activity in genetically obese Zucker rats.* Eur J Pharmacol, 1993. **246**(1): p. 67-71.
49. Savontaus, E., et al., *Differential regulation of uncoupling proteins by chronic treatments with beta 3-adrenergic agonist BRL 35135 and metformin in obese fa/fa Zucker rats.* Biochem Biophys Res Commun, 1998. **246**(3): p. 899-904.
50. Liang, X., et al., *Maternal high-fat diet during lactation impairs thermogenic function of brown adipose tissue in offspring mice.* Sci Rep, 2016. **6**: p. 34345.
51. Giralt, M., A. Gavalda-Navarro, and F. Villarroya, *Fibroblast growth factor-21, energy balance and obesity.* Mol Cell Endocrinol, 2015. **418 Pt 1**: p. 66-73.
52. Dutchak, P.A., et al., *Fibroblast growth factor-21 regulates PPARgamma activity and the antidiabetic actions of thiazolidinediones.* Cell, 2012. **148**(3): p. 556-67.
53. Moyers, J.S., et al., *Molecular determinants of FGF-21 activity-synergy and cross-talk with PPARgamma signaling.* J Cell Physiol, 2007. **210**(1): p. 1-6.
54. Douris, N., et al., *Central Fibroblast Growth Factor 21 Browns White Fat via Sympathetic Action in Male Mice.* Endocrinology, 2015. **156**(7): p. 2470-81.
55. Hondares, E., et al., *Thermogenic activation induces FGF21 expression and release in brown adipose tissue.* J Biol Chem, 2011. **286**(15): p. 12983-90.
56. Tan, B.K., et al., *Fibroblast growth factor 21 (FGF21) in human cerebrospinal fluid: relationship with plasma FGF21 and body adiposity.* Diabetes, 2011. **60**(11): p. 2758-62.
57. Fisher, F.M., et al., *Obesity is a fibroblast growth factor 21 (FGF21)-resistant state.* Diabetes, 2010. **59**(11): p. 2781-9.
58. Hale, C., et al., *Lack of overt FGF21 resistance in two mouse models of obesity and insulin resistance.* Endocrinology, 2012. **153**(1): p. 69-80.
59. Badman, M.K., et al., *Hepatic fibroblast growth factor 21 is regulated by PPARalpha and is a key mediator of hepatic lipid metabolism in ketotic states.* Cell Metab, 2007. **5**(6): p. 426-37.
60. Gaich, G., et al., *The effects of LY2405319, an FGF21 analog, in obese human subjects with type 2 diabetes.* Cell Metab, 2013. **18**(3): p. 333-40.
61. Kharitonenkov, A. and A.B. Shanafelt, *FGF21: a novel prospect for the treatment of metabolic diseases.* Curr Opin Investig Drugs, 2009. **10**(4): p. 359-64.
62. Xu, J., et al., *Fibroblast growth factor 21 reverses hepatic steatosis, increases energy expenditure, and improves insulin sensitivity in diet-induced obese mice.* Diabetes, 2009. **58**(1): p. 250-9.
63. Bernardo, B., et al., *FGF21 does not require interscapular brown adipose tissue and improves liver metabolic profile in animal models of obesity and insulin-resistance.* Sci Rep, 2015. **5**: p. 11382.

64. Coskun, T., et al., *Fibroblast growth factor 21 corrects obesity in mice.* Endocrinology, 2008. **149**(12): p. 6018-27.
65. Camporez, J.P., et al., *Cellular mechanisms by which FGF21 improves insulin sensitivity in male mice.* Endocrinology, 2013. **154**(9): p. 3099-109.
66. Hondares, E., et al., *Hepatic FGF21 expression is induced at birth via PPARalpha in response to milk intake and contributes to thermogenic activation of neonatal brown fat.* Cell Metab, 2010. **11**(3): p. 206-12.
67. Samms, R.J., et al., *Discrete Aspects of FGF21 In Vivo Pharmacology Do Not Require UCP1.* Cell Rep, 2015. **11**(7): p. 991-9.
68. Dong, J.Q., et al., *Pharmacokinetics and pharmacodynamics of PF-05231023, a novel long-acting FGF21 mimetic, in a first-in-human study.* Br J Clin Pharmacol, 2015. **80**(5): p. 1051-63.
69. Dockray, G.J., *Enteroendocrine cell signalling via the vagus nerve.* Curr Opin Pharmacol, 2013. **13**(6): p. 954-8.
70. Sisley, S., et al., *Neuronal GLP1R mediates liraglutide's anorectic but not glucose-lowering effect.* J Clin Invest, 2014. **124**(6): p. 2456-63.
71. Matthews, J.E., et al., *Pharmacodynamics, pharmacokinetics, safety, and tolerability of albiglutide, a long-acting glucagon-like peptide-1 mimetic, in patients with type 2 diabetes.* J Clin Endocrinol Metab, 2008. **93**(12): p. 4810-7.
72. Lockie, S.H., et al., *Direct control of brown adipose tissue thermogenesis by central nervous system glucagon-like peptide-1 receptor signaling.* Diabetes, 2012. **61**(11): p. 2753-62.
73. Kooijman, S., et al., *Central GLP-1 receptor signalling accelerates plasma clearance of triacylglycerol and glucose by activating brown adipose tissue in mice.* Diabetologia, 2015. **58**(11): p. 2637-46.
74. Heppner, K.M., et al., *Contribution of brown adipose tissue activity to the control of energy balance by GLP-1 receptor signalling in mice.* Diabetologia, 2015. **58**(9): p. 2124-32.
75. Tomas, E., et al., *GLP-1(32-36)amide Pentapeptide Increases Basal Energy Expenditure and Inhibits Weight Gain in Obese Mice.* Diabetes, 2015. **64**(7): p. 2409-19.
76. Wei, Q., et al., *Exendin-4 improves thermogenic capacity by regulating fat metabolism on brown adipose tissue in mice with diet-induced obesity.* Ann Clin Lab Sci, 2015. **45**(2): p. 158-65.
77. Xu, F., et al., *GLP-1 receptor agonist promotes brown remodelling in mouse white adipose tissue through SIRT1.* Diabetologia, 2016. **59**(5): p. 1059-69.
78. Dimitriadis, G., et al., *Insulin effects in muscle and adipose tissue.* Diabetes Res Clin Pract, 2011. **93 Suppl 1**: p. S52-9.
79. Bartelt, A., et al., *Brown adipose tissue activity controls triglyceride clearance.* Nat Med, 2011. **17**(2): p. 200-5.
80. Cannon, B. and J. Nedergaard, *Brown adipose tissue: function and physiological significance.* Physiol Rev, 2004. **84**(1): p. 277-359.
81. Mottillo, E.P., et al., *Coupling of lipolysis and de novo lipogenesis in brown, beige, and white adipose tissues during chronic beta3-adrenergic receptor activation.* J Lipid Res, 2014. **55**(11): p. 2276-86.
82. Laplante, M., et al., *Tissue-specific postprandial clearance is the major determinant of PPARgamma-induced triglyceride lowering in the rat.* Am J Physiol Regul Integr Comp Physiol, 2009. **296**(1): p. R57-66.
83. Dijk, W., et al., *ANGPTL4 mediates shuttling of lipid fuel to brown adipose tissue during sustained cold exposure.* Elife, 2015. **4**.

84. Berbee, J.F., et al., *Brown fat activation reduces hypercholesterolaemia and protects from atherosclerosis development.* Nat Commun, 2015. **6**: p. 6356.
85. Dong, M., et al., *Cold exposure promotes atherosclerotic plaque growth and instability via UCP1-dependent lipolysis.* Cell Metab, 2013. **18**(1): p. 118-29.
86. Zadelaar, S., et al., *Mouse models for atherosclerosis and pharmaceutical modifiers.* Arterioscler Thromb Vasc Biol, 2007. **27**(8): p. 1706-21.
87. von Scheidt, M., et al., *Applications and Limitations of Mouse Models for Understanding Human Atherosclerosis.* Cell Metab, 2017. **25**(2): p. 248-261.
88. Wang, Q., et al., *Brown adipose tissue activation is inversely related to central obesity and metabolic parameters in adult human.* PLoS One, 2015. **10**(4): p. e0123795.
89. Chechi, K., et al., *Brown fat like gene expression in the epicardial fat depot correlates with circulating HDL-cholesterol and triglycerides in patients with coronary artery disease.* Int J Cardiol, 2013. **167**(5): p. 2264-70.
90. Ouellet, V., et al., *Brown adipose tissue oxidative metabolism contributes to energy expenditure during acute cold exposure in humans.* J Clin Invest, 2012. **122**(2): p. 545-52.
91. Blondin, D.P., et al., *Selective Impairment of Glucose but Not Fatty Acid or Oxidative Metabolism in Brown Adipose Tissue of Subjects With Type 2 Diabetes.* Diabetes, 2015. **64**(7): p. 2388-97.
92. Chondronikola, M., et al., *Brown Adipose Tissue Activation Is Linked to Distinct Systemic Effects on Lipid Metabolism in Humans.* Cell Metab, 2016. **23**(6): p. 1200-6.
93. Johnson, F., et al., *Could increased time spent in a thermal comfort zone contribute to population increases in obesity?* Obes Rev, 2011. **12**(7): p. 543-51.
94. Betz, M.J. and S. Enerback, *Human Brown Adipose Tissue: What We Have Learned So Far.* Diabetes, 2015. **64**(7): p. 2352-60.
95. Hoeke, G., et al., *Role of Brown Fat in Lipoprotein Metabolism and Atherosclerosis.* Circ Res, 2016. **118**(1): p. 173-82.
96. Rothwell, N.J. and M.J. Stock, *Luxuskonsumption, diet-induced thermogenesis and brown fat: the case in favour.* Clin Sci (Lond), 1983. **64**(1): p. 19-23.
97. Fromme, T. and M. Klingenspor, *Uncoupling protein 1 expression and high-fat diets.* Am J Physiol Regul Integr Comp Physiol, 2011. **300**(1): p. R1-8.
98. Hanssen, M.J., et al., *Glucose uptake in human brown adipose tissue is impaired upon fasting-induced insulin resistance.* Diabetologia, 2015. **58**(3): p. 586-95.
99. Vosselman, M.J., et al., *Brown adipose tissue activity after a high-calorie meal in humans.* American Journal of Clinical Nutrition, 2013. **98**(1): p. 57-64.
100. Peterson, C.M., et al., *Brown adipose tissue does not seem to mediate metabolic adaptation to overfeeding in men.* Obesity (Silver Spring), 2017.
101. Blondin, D.P., et al., *Dietary fatty acid metabolism of brown adipose tissue in cold-acclimated men.* Nat Commun, 2017. **8**: p. 14146.
102. Iacobellis, G., *Local and systemic effects of the multifaceted epicardial adipose tissue depot.* Nat Rev Endocrinol, 2015. **11**(6): p. 363-71.
103. Gil-Ortega, M., et al., *Regional differences in perivascular adipose tissue impacting vascular homeostasis.* Trends Endocrinol Metab, 2015. **26**(7): p. 367-75.
104. Yamaguchi, Y., et al., *Adipogenesis and epicardial adipose tissue: a novel fate of the epicardium induced by mesenchymal transformation and PPARgamma activation.* Proc Natl Acad Sci U S A, 2015. **112**(7): p. 2070-5.
105. Sacks, H.S. and J.N. Fain, *Human epicardial adipose tissue: a review.* Am Heart J, 2007. **153**(6): p. 907-17.
106. Szasz, T. and R.C. Webb, *Perivascular adipose tissue: more than just structural support.* Clin Sci (Lond), 2012. **122**(1): p. 1-12.

107. Gao, Y.J., et al., *Modulation of vascular function by perivascular adipose tissue: the role of endothelium and hydrogen peroxide.* Br J Pharmacol, 2007. **151**(3): p. 323-31.
108. Lee, R.M., et al., *Endothelium-dependent relaxation factor released by perivascular adipose tissue.* J Hypertens, 2009. **27**(4): p. 782-90.
109. Marchington, J.M., C.A. Mattacks, and C.M. Pond, *Adipose tissue in the mammalian heart and pericardium: structure, foetal development and biochemical properties.* Comp Biochem Physiol B, 1989. **94**(2): p. 225-32.
110. Marchington, J.M. and C.M. Pond, *Site-specific properties of pericardial and epicardial adipose tissue: the effects of insulin and high-fat feeding on lipogenesis and the incorporation of fatty acids in vitro.* Int J Obes, 1990. **14**(12): p. 1013-22.
111. Sacks, H.S., et al., *Uncoupling protein-1 and related messenger ribonucleic acids in human epicardial and other adipose tissues: epicardial fat functioning as brown fat.* J Clin Endocrinol Metab, 2009. **94**(9): p. 3611-5.
112. Szasz, T., G.F. Bomfim, and R.C. Webb, *The influence of perivascular adipose tissue on vascular homeostasis.* Vasc Health Risk Manag, 2013. **9**: p. 105-16.
113. Ozen, G., et al., *Human perivascular adipose tissue dysfunction as a cause of vascular disease: Focus on vascular tone and wall remodeling.* Eur J Pharmacol, 2015. **766**: p. 16-24.
114. Ojha, S., et al., *Gene pathway development in human epicardial adipose tissue during early life.* JCI Insight, 2016. **1**(13): p. e87460.
115. Sacks, H.S., et al., *Adult epicardial fat exhibits beige features.* J Clin Endocrinol Metab, 2013. **98**(9): p. E1448-55.
116. Shimizu, I., et al., *Vascular rarefaction mediates whitening of brown fat in obesity.* J Clin Invest, 2014. **124**(5): p. 2099-112.
117. Shimizu, I. and K. Walsh, *The Whitening of Brown Fat and Its Implications for Weight Management in Obesity.* Curr Obes Rep, 2015. **4**(2): p. 224-9.
118. Roberts-Toler, C., B.T. O'Neill, and A.M. Cypess, *Diet-induced obesity causes insulin resistance in mouse brown adipose tissue.* Obesity (Silver Spring), 2015. **23**(9): p. 1765-70.
119. Chang, L., et al., *Loss of perivascular adipose tissue on peroxisome proliferator-activated receptor-gamma deletion in smooth muscle cells impairs intravascular thermoregulation and enhances atherosclerosis.* Circulation, 2012. **126**(9): p. 1067-78.
120. Buckley, M.L. and D.P. Ramji, *The influence of dysfunctional signaling and lipid homeostasis in mediating the inflammatory responses during atherosclerosis.* Biochim Biophys Acta, 2015. **1852**(7): p. 1498-510.
121. Carriere, A., et al., *Browning of white adipose cells by intermediate metabolites: an adaptive mechanism to alleviate redox pressure.* Diabetes, 2014. **63**(10): p. 3253-65.
122. Dozio, E., et al., *Increased reactive oxygen species production in epicardial adipose tissues from coronary artery disease patients is associated with brown-to-white adipocyte trans-differentiation.* Int J Cardiol, 2014. **174**(2): p. 413-4.
123. Friederich-Persson, M., et al., *Brown Adipose Tissue Regulates Small Artery Function Through NADPH Oxidase 4-Derived Hydrogen Peroxide and Redox-Sensitive Protein Kinase G-1alpha.* Arterioscler Thromb Vasc Biol, 2017. **37**(3): p. 455-465.

Appendices

Appendix 1

Supplementary data

1. Supplementary data for Chapter 2

Supplementary Table 1: Details of probe assays used for qPCR.

Gene	Assay ID
ADRB3 (Thermo)	Rn00565393_m1
ASC1 (Thermo)	qRnoCIP0039017
CITED1 (BioRad)	qRnoCIP0039088
DIO2 (Thermo)	Rn00581867_m1
FGF21 (BioRad)	qRnoCEP0024589
P2RX5 (BioRad)	qRnoCIP0024301
PGC1a (BioRad)	qRnoCIP0022855
SLC36a2 (BioRad)	qRnoCIP0039017
TBX1 (BioRad)	qRnoCIP0027898
TMEM26 (BioRad)	qRnoCEP0028673

Supplementary Table 2: Rat specific Forward and Reverse Oligonucleotide Primers Used for Real-Time PCR.

Gene	Forward primer	Reverse Primer
CIDEA	TCAGTGTCGTATGATATCCGCT	ACCTGGGCAGCATAGGATG
PRDM16	CGAGAAGTTCTGCGTGGATG	GGCACCTTCTTTCACATGCA
UCP1	GCCTAGCAGACATCATCACCT	GTTTCGGCAATCCTTCTGTC

Supplementary Table 3. Depot fat mass following 72h HFD (grams).

Depot	Chow	HFD
Paracardial AT	0.138±0.012g	0.138±0.023g
iBAT	0.627±0.096g	0.709±0.077g
Perirenal AT	7.48±1.67g	6.98±2.48g
Gonadal AT	6.31±0.83g	5.62±0.38g
Mesenteric AT	4.42±0.94g	5.60±0.71g
Inguinal AT	3.91±0.44g	4.51±0.7g
Total AT	22.87±3.31g	23.51±3.68g

Supplementary Figure 1: High fat diet (HFD) had no effect 24h energy expenditure (EE) as measured during either the light or dark phases. Data expressed as mean±SEM, n=6 per group.

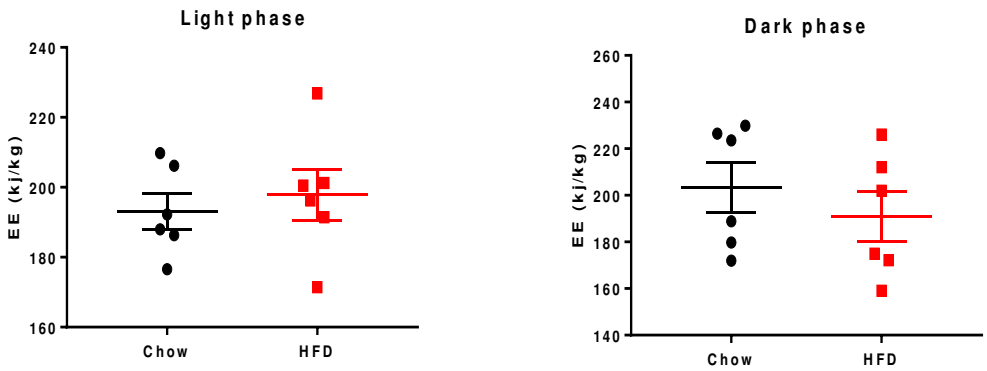

2. Supplementary data for Chapter 3

Supplementary Table 1: Serum parameters, liver weight and hepatic TG

	HFD	Ex
Glucose (mg/dl)	109.4 ± 7.25	103.8 ± 3.5
Insulin (ng/ml)	1 ± 0.45	0.85 ± 0.12
Homa-IR	6.8 ± 2.9	6 ± 1
Triglycerides (TG, mg/dl)	63 ± 41	60.6 ± 19
NEFA (mmol/L)	0.39 ± 0.04	0.34 ± 0.03
Liver weight (g)	18.1 ± 1.8	15.7 ± 0.95
Hepatic TG (mg/dl)	21 ± 4.3	16.5 ± 4.2

Supplementary Table 2: Differentially regulated proteins in BAT

symbol	entrez	logfc	adjpv
Picalm	89816	-1.78	0.000004
Scoc	364981	-1.85	0.000074
Trim72	365377	0.77	0.000139
Arf1	64310	-2.73	0.000150
Rbbp9	29459	-1.80	0.000168
Rps26	27139	-0.57	0.000217
Pgrmc2	361940	-1.29	0.000270
Atp5e	245958	1.30	0.000345
Ruvbl1	65137	-2.89	0.000414
Serpinb1a	291091	-0.68	0.000424
Rnmt	291534	2.86	0.000447
Nup35	295692	1.48	0.000704
Ggcx	81716	0.76	0.000880
Rpl21	79449	-3.79	0.000976
Farsa	288917	-2.24	0.001057
Pon1	84024	1.27	0.001358
Vars	25009	0.91	0.001382
Slc3a2	50567	1.68	0.001386
Acox1	50681	-1.05	0.001481
Rab7a	29448	-0.56	0.001598
Akr1b7	116463	1.15	0.001708
Ybx1	500538	-0.56	0.001734
Rpl27a	293418	-1.67	0.001752
Gdi1	25183	-0.57	0.001925
Lypla1	25514	0.78	0.001931
Ckb	24264	1.15	0.001942
Twf1	315265	-1.78	0.002050
Ilk	170922	-0.87	0.002684
F11r	116479	4.34	0.002740
Myl12a	501203	0.86	0.002753

Sec13	297522	2.87	0.003027
Smu1	117541	-2.69	0.003096
Aldh16a1	361571	2.47	0.003332
Arf4	79120	-0.84	0.003462
Mrfap1	282585	3.02	0.003490
Mat2a	171347	-1.05	0.003748
LOC100359498	100359498	-3.78	0.003871
Myl9	296313	1.38	0.004054
Vdac1	83529	0.69	0.004226
Atp6v1e1	297566	0.53	0.004351
Fabp3	79131	-0.95	0.004662
Csnk2a1	116549	-0.83	0.004812
Safb	64196	-1.90	0.005003
Tst	25274	-0.58	0.005274
Kirrel1	310695	2.09	0.005493
Gpd1	60666	0.55	0.005949
Psmb8	24968	-0.79	0.006059
Flot2	83764	2.59	0.006085
Ssbp1	54304	0.84	0.006147
Gnl1	309593	0.87	0.006282
Steap4	499991	-3.82	0.006402
Hnrnpl	80846	-2.97	0.006430
Prdx4	85274	-1.51	0.006529
Gnb2	81667	-2.07	0.007102
Cnbp	64530	2.51	0.007689
Adrm1	65138	-0.79	0.007875
Lipe	25330	-0.74	0.008475
Gnai1	25686	-3.93	0.009086
Got2	25721	0.89	0.009448
Oxct1	690163	1.08	0.009519
Mdh2	81829	0.77	0.010040
Pcyt2	89841	2.33	0.010292
Atp5d	245965	0.89	0.010468
Ccdc93	304743	-0.85	0.010497
Acy1	300981	-0.86	0.010542
Enpp3	54410	1.30	0.010658
Fhl1	25177	3.00	0.010919
Atp5b	171374	0.85	0.011316
Rpl29	29283	-2.55	0.011633
Ssr3	81784	2.93	0.011777
Jpt1	287828	2.32	0.011813
Atp5j	94271	0.61	0.012402
Mapre1	114764	3.45	0.012522
Rsl24d1	363099	0.79	0.012559
Hnrnpk	117282	-0.52	0.013031
Ak1	24183	1.51	0.013130
Prdx3	64371	0.95	0.013174
Caprin1	362173	-2.55	0.013285
Lrrc59	287633	-3.26	0.013322
Pnpo	64533	3.73	0.013417
Mfge8	25277	2.41	0.013605

Ikbip	314730	0.95	0.013649
Parva	57341	-1.48	0.013685
Canx	29144	-0.67	0.013691
Actr2	289820	-0.99	0.013761
RGD1564664	499839	-2.64	0.013794
Scgb2a1	25010	-1.17	0.014211
Impact	497198	-1.83	0.014980
Ptk2	25614	-1.62	0.015614
LOC103689947	103689947	-0.96	0.015631
Eepd1	315500	1.78	0.016096
Hmgn5b	681284	-2.24	0.016327
Snap23	64630	-0.97	0.016460
Ppif	282819	1.13	0.016485
Stmn1	29332	1.08	0.016813
Nedd4	25489	-1.15	0.017773
Rabep2	80754	2.46	0.018227
Rwdd1	259218	0.79	0.018511
Ostf1	259275	-2.88	0.019652
Cox5b	94194	0.94	0.020079
Acadsb	25618	-1.95	0.020232
Dld	298942	0.83	0.020561
Akt2	25233	-1.19	0.021849
Tomm22	300075	2.52	0.021870
Dnm2	25751	-1.34	0.022571
LOC100909840	100909840	0.57	0.026078
Ufc1	445268	-0.63	0.026505
Pecam1	29583	3.40	0.027233
Rab2a	65158	-0.55	0.028258
Fkbp9	297123	-2.09	0.028266
Ddx46	245957	2.43	0.028396
Tmed9	361207	1.91	0.029775
Retsat	246298	-1.78	0.030198
Nras	24605	-0.52	0.031192
Pdlim5	64353	0.87	0.031521
Aldh2	29539	-0.52	0.032339
Samm50	300111	2.52	0.032735
Pcyox1	246302	1.84	0.033267
Rps18	294282	-0.60	0.033608
Tsc22d1	498545	-2.60	0.034233
Gsta4	300850	-0.62	0.035195
Atp5o	192241	0.53	0.035395
Cps1	497840	-2.41	0.036115
Rps25	122799	-0.52	0.036500
Paics	140946	-1.21	0.037037
Ppp1r14b	259225	2.90	0.037840
Uqcrfs1	291103	0.52	0.037957
Aoc3	29473	-1.10	0.038141
Oat	64313	-2.43	0.039004
Scarb1	25073	2.61	0.039553
Sardh	114123	-0.75	0.039737
Gfm1	114017	1.64	0.041349

Tmc5	365360	5.71	0.042368
Asns	25612	-2.47	0.042482
Msh2	81709	0.68	0.042956
Rpl22	81768	4.13	0.043960
Add3	25230	3.15	0.045349
Elavl1	363854	-0.77	0.045888
Ddx39a	89827	-1.82	0.046585
Cdipt	192260	1.56	0.047053
Arcn1	300674	-0.87	0.047360
RGD1303003	294326	1.05	0.049330
Mb	59108	5.31	0.052570
Got1	24401	0.92	0.052958
Mapk1	116590	-3.62	0.053239
Cryab	25420	1.48	0.053648
Atp5a1	65262	0.53	0.053811
Sult1a1	83783	-1.26	0.054189
Sfswap	304431	1.71	0.055680
Timm9	171139	0.97	0.055722
Pfkl	25741	-1.09	0.056291
Mgst1	171341	-0.72	0.056293
Smarcad1	312398	-1.80	0.056638
Khdrbs1	117268	-1.85	0.056680
C1qb	29687	-2.19	0.057651
Pdcd6ip	501083	-3.60	0.059487
Ssrp1	81785	2.00	0.060232
Pafah1b1	83572	-1.99	0.060508
Ubr4	313658	-1.28	0.062780
Manf	315989	0.66	0.063485
Psmb5	29425	2.20	0.064190
Pdxk	83578	0.62	0.065427
Cdkl3	60396	-3.87	0.066289
LOC100364435	100364435	0.74	0.066647
Aebp1	305494	-2.30	0.067465
Nubp2	287125	-1.40	0.069635
Sar1b	287276	-0.63	0.071615
Casq1	686019	-4.64	0.073187
LOC100360117	100360117	-1.20	0.073724
Prdx5	113898	0.71	0.075140
Emd	25437	0.64	0.075803
Hsp90ab1	301252	-0.70	0.076030
LOC103689992	103689992	-2.04	0.076706
Napa	140673	-1.09	0.079278
Ctnnb1	84353	2.02	0.080415
Rpl4	64302	-1.17	0.081163
Sh3gl1	81922	-0.55	0.082156
Pcna	25737	1.76	0.082465
Hprt1	24465	-0.74	0.084325
Pir	363465	0.82	0.085585
Ugt1a6	113992	-1.81	0.085618
Pdia4	116598	-0.63	0.089608
Cttn	60465	1.51	0.089611

St13	81800	-0.72	0.089875
Cops4	360915	-1.96	0.089984
Aldh1l1	64392	-0.59	0.092890
Idh3a	114096	0.61	0.093937
Top2a	360243	-0.59	0.094134
Itga7	81008	-0.54	0.094593
Rpl35	296709	4.40	0.096043
Eif3d	362952	-1.44	0.096584
Hmgcs1	29637	-3.66	0.097233
Dctn1	29167	-1.90	0.098515
Atp5h	641434	0.52	0.099922
Gnai3	25643	-2.11	0.100267
Tkfc	361730	-4.30	0.100892
Bsg	25246	0.67	0.101244
Gstm2	24424	-0.91	0.101246
Ddx1	84474	0.88	0.102323
F13a1	60327	-1.92	0.102787
Txnrd1	58819	-1.75	0.104505
Hspb6	192245	5.06	0.104759
Pdcd4	64031	-1.97	0.106124
Hnrnpa3	362152	-0.95	0.107001
Vapb	60431	-1.71	0.107677
Wdr1	360950	-0.51	0.108763
Idh1	24479	-0.85	0.108862
Rdh16	299511	-3.14	0.109968
Cdk5	140908	1.63	0.110065
Ykt6	64351	0.60	0.110104
Cald1	25687	2.01	0.111411
Hspa13	29734	-2.13	0.113215
LOC684988	684988	-0.70	0.113256
Nes	25491	0.82	0.113860
Fcgrt	29558	-2.38	0.114757
Ncstn	289231	-2.73	0.115743
Eif4a2	303831	-0.92	0.122267
Rpl10a	81729	-1.92	0.122600
Zw10	363059	2.02	0.124740
Orm1	24614	1.14	0.127099
Nme1	191575	-2.79	0.128373
LOC100364457	100364457	3.51	0.131740
Ndel1	170845	2.18	0.131759
Rpl15	245981	-2.09	0.132344
Psmb9	24967	0.61	0.135388
Snd1	64635	1.85	0.136424
LOC108348260	108348260	3.39	0.138472
Hspd1	63868	1.00	0.138850
Park7	117287	0.57	0.139941
Timm8b	64372	0.88	0.141464
Myo1b	117057	2.10	0.141822
Pgk1	24644	0.67	0.141840
Pcyt1a	140544	-1.41	0.142742
Crip1	691657	2.15	0.143393

Wdr61	363064	1.74	0.143844
Bag6	94342	-3.54	0.144015
Cox7a2	29507	1.44	0.144661
Rad23b	298012	-2.45	0.146032
B2m	24223	-0.52	0.146645
Stoml2	298203	0.64	0.147220
C1qc	362634	-3.57	0.147757
Esyt1	29579	-0.65	0.147895
Letm1	305457	0.95	0.147977
Aacs	65984	3.31	0.148642
Cpne1	362249	-2.06	0.149046
Npas4	266734	-2.93	0.149382
Ace	24310	-1.49	0.149461
Rab6a	84379	0.66	0.152650
Gapdh	24383	0.84	0.152864
Ppp2r2a	117104	3.43	0.153227
Mesd	308796	1.38	0.155213
Arl6ip5	66028	5.19	0.156194
Pgam1	24642	0.83	0.157461
Vps26a	361846	-0.58	0.159039
Fahd2a	296131	0.57	0.159065
Clic4	83718	-1.92	0.159544
Hnrnpdl	305178	-0.74	0.160951
Actg2	25365	-0.89	0.161060
Rgn	25106	1.88	0.162047
Tollip	361677	-2.64	0.162653
Abhd5	316122	-0.71	0.164264
Dlst	299201	0.60	0.166679
Ist1	307833	-0.97	0.166705
Pdap1	64527	0.60	0.166984
Pck1	362282	-1.16	0.168424
Ifi30	290644	1.11	0.170114
Hsdl2	313200	0.67	0.170726
Hadh	113965	0.54	0.171038
Cox6c	54322	0.93	0.171268
Cpne9	297516	-1.95	0.172196
Pkm	25630	0.63	0.172311
Tmsb4x	81814	1.15	0.173148
Mpc2	100359982	1.78	0.175528
Phgdh	58835	-0.92	0.175599
Vps4a	246772	-1.33	0.175994
Pgam2	24959	3.45	0.176098
Cox5a	252934	1.01	0.176128
Sptan1	64159	-1.13	0.176749
Wdr77	310769	2.02	0.177932
Adprh	25371	-1.62	0.183279
Mlec	304543	-2.97	0.185597
Ecm1	116662	1.51	0.186983
Slc2a4	25139	-0.94	0.188195
P4ha1	64475	-1.73	0.188534
Trap1	287069	0.88	0.189767

Rnpep	81761	3.76	0.189955
Gusb	24434	1.64	0.190759
Ik	291659	1.88	0.191120
Eif3i	682390	0.81	0.193399
Rpl24	64307	0.98	0.195425
Acaa2	170465	0.70	0.195993
Actn1	81634	2.39	0.196673
Psmb7	85492	-3.46	0.198010
Fads2	83512	-3.03	0.198071
Eif3b	288516	2.49	0.198331
Dpysl3	25418	-1.70	0.198904
Dlat	81654	0.62	0.200109
Csad	60356	-1.42	0.204017
Prpf19	246216	-1.70	0.204243
Aldh9a1	64040	-0.52	0.206158
Tpm1	24851	1.21	0.206304
Tnni2	29389	4.09	0.207299
Lamtor1	308869	-2.14	0.207568
Xpnpep1	170751	-1.47	0.207898
LOC108350501	108350501	-2.43	0.210098
Ces1c	24346	-0.58	0.210303
Prep	83471	-1.55	0.210574
LOC100363502	100363502	0.97	0.210978
Cav2	363425	-1.87	0.212581
Rab14	94197	1.30	0.212835
Cox4i1	29445	0.82	0.213019
Mylpf	24584	3.42	0.213227
Dhfr	24312	-1.32	0.213228
Calm3	24244	-3.54	0.215148
Aldh3a2	65183	-0.91	0.215474
Myl6l	362816	0.62	0.217432
COX2	26198	0.53	0.218492
Sod1	24786	0.63	0.218695
Aldoa	24189	0.79	0.222836
LOC100359574	100359574	2.21	0.224398
Ddah2	294239	-0.88	0.226279
Ninj1	25338	2.01	0.226636
S100a10	81778	-1.20	0.227322
Ugdh	83472	2.11	0.227992
LOC100911186	100911186	0.62	0.228664
Tpi1	24849	0.69	0.229888
Cand1	117152	-2.49	0.230824
Timeless	83508	3.85	0.231260
Rps8	65136	1.29	0.232789
Cavin3	85332	-1.94	0.233017
Snrpn	81781	2.58	0.234247
Cd48	245962	0.85	0.234946
Eef1a1	171361	-0.57	0.234976
G6pd	24377	0.84	0.235912
Marcksl1	81520	2.83	0.236207
Sdhb	298596	0.83	0.239584

Pdlim3	114108	4.15	0.240689
Sars	266975	-3.39	0.242342
Myh4	360543	3.53	0.242512
Enpp1	85496	2.11	0.243007
Ccdc43	360637	-3.78	0.243166
Map4	367171	0.61	0.243767
Ccdc22	317381	-1.44	0.244454
Capn1	29153	-4.77	0.245231
Cygb	170520	-1.53	0.245820
Gnas	24896	-1.05	0.246029
Sec22b	310710	-2.77	0.246288
Dhx30	367172	0.89	0.246383
Aco1	50655	-0.70	0.246476
Tcp1	24818	3.51	0.246974
Lamb2	25473	-2.82	0.247789
Aldh1a1	24188	2.66	0.249144
Ca5b	302669	-1.41	0.249964

Supplementary Table 3: GO terms enriched in BAT

goId	goName	countDE	countAll	pv_elim
Biological Process				
GO:0003151	outflow tract morphogenesis	4	4	0.0053
GO:0006103	2-oxoglutarate metabolic process	6	8	0.0064
GO:0051304	chromosome separation	5	6	0.0067
GO:0007093	mitotic cell cycle checkpoint	6	9	0.0148
GO:0014075	response to amine	6	9	0.0148
GO:0014044	Schwann cell development	5	7	0.0182
GO:0018198	peptidyl-cysteine modification	5	7	0.0182
GO:2000273	positive regulation of receptor activity	5	7	0.0182
GO:0006091	generation of precursor metabolites and energy	31	82	0.0189
GO:0000132	establishment of mitotic spindle orientation	4	5	0.0209
GO:0006071	glycerol metabolic process	4	5	0.0209
GO:2000008	regulation of protein localization to cell surface	4	5	0.0209
GO:0006906	vesicle fusion	8	15	0.0272
GO:0006165	nucleoside diphosphate phosphorylation	12	26	0.0276
GO:0015986	ATP synthesis coupled proton transport	9	13	0.0279
GO:0055081	anion homeostasis	6	10	0.0287
GO:0071482	cellular response to light stimulus	6	10	0.0287
GO:0090317	negative regulation of intracellular protein transport	6	10	0.0287
GO:0006090	pyruvate metabolic process	13	29	0.0289

GO:0043087	regulation of GTPase activity	14	32	0.0297
GO:0030516	regulation of axon extension	9	18	0.0313
GO:1902600	hydrogen ion transmembrane transport	16	26	0.0335
GO:0007519	skeletal muscle tissue development	10	21	0.0343
GO:0030278	regulation of ossification	7	13	0.0365
GO:0034308	primary alcohol metabolic process	7	13	0.0365
GO:0048538	thymus development	5	8	0.0378
GO:0043603	cellular amide metabolic process	62	191	0.0443
GO:0046364	monosaccharide biosynthetic process	9	19	0.0457
GO:1990138	neuron projection extension	15	26	0.0466
GO:0055085	transmembrane transport	45	109	0.0469
GO:0051345	positive regulation of hydrolase activity	29	81	0.048
GO:0006081	cellular aldehyde metabolic process	10	22	0.0482
GO:0043010	camera-type eye development	10	22	0.0482
GO:0006739	NADP metabolic process	6	11	0.0491
GO:0009308	amine metabolic process	4	6	0.0494
GO:0032770	positive regulation of monooxygenase activity	4	6	0.0494
GO:0050771	negative regulation of axonogenesis	4	6	0.0494
GO:0090151	establishment of protein localization to mitochondrial membrane	4	6	0.0494
Molecular Function				
GO:0004129	cytochrome-c oxidase activity	6	7	0.002
GO:0004029	aldehyde dehydrogenase (NAD) activity	6	8	0.0061
GO:0035255	ionotropic glutamate receptor binding	5	6	0.0064
GO:0019905	syntaxin binding	6	9	0.0142
GO:0046933	proton-transporting ATP synthase activity, rotational mechanism	6	9	0.0142
GO:0070628	proteasome binding	3	3	0.0192
GO:0072341	modified amino acid binding	10	20	0.022
GO:0008026	ATP-dependent helicase activity	6	11	0.0471
GO:0030170	pyridoxal phosphate binding	6	11	0.0471
GO:0016769	transferase activity, transferring nitrogenous groups	4	6	0.0479
GO:0019888	protein phosphatase regulator activity	4	6	0.0479
GO:0042805	actinin binding	4	6	0.0479

GO:0005751	mitochondrial respiratory chain complex IV	6	8	0.0065
GO:0030017	sarcomere	20	47	0.0147
GO:0002080	acrosomal membrane	3	3	0.0199
GO:0000275	mitochondrial proton-transporting ATP synthase complex, catalytic core F(1)	4	5	0.0211
GO:0031201	SNARE complex	4	5	0.0211
GO:0005774	vacuolar membrane	17	40	0.0241
GO:0016459	myosin complex	7	13	0.0369
GO:0000922	spindle pole	8	16	0.0424

Supplementary Table 4: Impacted pathways in BAT

pName	pv
Alzheimer's disease	0.000999661
Adrenergic signaling in cardiomyocytes	0.001756899
Ascorbate and aldarate metabolism	0.00213192
Pertussis	0.004326391
Circadian entrainment	0.007909145
Alcoholism	0.008018337
Chagas disease (American trypanosomiasis)	0.010055862
Dopaminergic synapse	0.012724393
Biosynthesis of amino acids	0.014096695
Glycine, serine and threonine metabolism	0.01522383
Glycolysis / Gluconeogenesis	0.016627608
Arginine and proline metabolism	0.01706711
GABAergic synapse	0.017074995
Glycerophospholipid metabolism	0.018579947
Mismatch repair	0.020082392
Parkinson's disease	0.021279866
Sphingolipid signaling pathway	0.023392627
Carbon metabolism	0.023928025
Systemic lupus erythematosus	0.024367056
Oxidative phosphorylation	0.024454565
Leukocyte transendothelial migration	0.025964118
Gastric acid secretion	0.031732861
Staphylococcus aureus infection	0.032662385
Retrograde endocannabinoid signaling	0.040233625
RIG-I-like receptor signaling pathway	0.042793343
Metabolic pathways	0.044301877
Cholinergic synapse	0.045060684
Chemokine signaling pathway	0.046066085
Ras signaling pathway	0.048576277

Supplementary Table 5: Differentially regulated proteins in IWAT

symbol	entrez	logfc	adjpv
Lrrfip2	301035	-1.62	0.000008
RGD1311739	311428	0.89	0.000023
Psmb7	85492	2.73	0.000195
Ndufs6	29478	2.21	0.000496
Ezr	54319	-0.79	0.000500
Orm1	24614	1.12	0.001359
Bin1	117028	-3.22	0.001856
Stk3	65189	-1.52	0.001979
Gna11	81662	0.56	0.002852
Sult1a1	83783	0.87	0.003031
Sod3	25352	0.64	0.003225
Atg7	312647	-2.32	0.004631
Rpl38	689284	-1.10	0.006447
Pip4k2a	116723	-1.89	0.006578
Tusc5	360576	0.80	0.007389
Usp7	360471	-0.82	0.008410
Cd14	60350	0.94	0.008533
Pdcd10	494345	-0.80	0.009051
Timm8a1	84383	-1.10	0.010498
Egf	25313	3.51	0.010740
Rpl29	29283	-0.67	0.011947
Marcksl1	81520	-1.64	0.012738
Tor1aip1	246314	-1.69	0.014289
Vac14	307842	-0.69	0.014635
Por	29441	0.39	0.015849
Cd74	25599	-3.33	0.016453
Plek	364206	-1.18	0.018541
Tsc22d1	498545	2.48	0.020115
Abcd3	25270	-1.46	0.020545
Arhgap17	63994	-1.50	0.021408
Xpo1	85252	-0.81	0.022951
Dek	306817	-2.22	0.025033
Scarb1	25073	0.78	0.028908
Bckdhb	29711	-2.62	0.031066
Lgmn	63865	0.41	0.031760
Akr1c14	191574	0.70	0.032774
Rps25	122799	-0.58	0.034593
Prps1	29562	-0.53	0.036195
Rps26	27139	-0.55	0.036434
Kdelr2	304290	-0.69	0.038378
Gcs1	78947	0.32	0.046354
Lhpp	361663	-3.90	0.047177
Lss	81681	1.74	0.047278
Prdx6	94167	0.47	0.048182

Vcan	114122	2.79	0.050063
Nudcd2	287199	0.42	0.050985
Vamp3	29528	0.76	0.051092
Cox6a1	25282	-3.45	0.051458
Bcam	78958	1.64	0.051481
LOC100360087	100360087	-0.49	0.052279
Magoh	298385	-1.20	0.052385
Vcl	305679	0.67	0.053180
Ptprc	24699	-3.37	0.053283
Uqcrfs1	291103	-0.28	0.054115
Gpx3	64317	1.02	0.055570
Lrpprc	313867	-0.50	0.056488
Eepd1	315500	1.32	0.056613
Stxbp1	25558	2.27	0.057076
Rab8a	117103	-0.80	0.057651
Ilf2	310612	-0.86	0.057972
LOC100911615	100911615	0.72	0.058561
Trim28	116698	-1.00	0.060789
Hnrnpa1	29578	-0.70	0.060813
Ppid	361967	-1.92	0.061759
Necap2	298598	-2.01	0.064150
Grpel1	79563	-0.70	0.064308
Camk2d	24246	-1.11	0.065373
Gstm5	64352	0.80	0.068868
Tbca	366995	-0.63	0.069016
Alb	24186	0.44	0.069672
Src	83805	0.55	0.069673
Bcat2	64203	-1.14	0.071248
Vps29	288666	0.26	0.071307
Cnbp	64530	-0.93	0.071444
Otc	25611	1.20	0.073488
ND4	26201	-0.24	0.074632
Timm44	29635	-0.51	0.077253
Hba2	360504	1.08	0.078331
Gmfg	113940	-2.95	0.078606
Raver1	298705	2.25	0.079417
Ctsz	252929	-1.11	0.079684
Serbp1	246303	0.77	0.079726
Calm3	24244	0.26	0.082538
Ncald	553106	-1.36	0.084373
Gbp2	171164	-0.64	0.086240
Ppt1	29411	-0.47	0.086604
Eif4e	117045	-0.45	0.089913
Gnao1	50664	1.15	0.092194
Syncrip	363113	-0.36	0.092311
Alpl	25586	-2.22	0.093379

Rbmxrtl	307779	-0.90	0.096585
Hspb1	24471	1.11	0.096643
Cct5	294864	-0.43	0.097214
Arf5	79117	-0.22	0.098562
Andpro	25030	2.70	0.099775
Cndp2	291394	0.35	0.102047
Gmps	295088	0.65	0.102747
Limd2	360646	-3.93	0.103367
Rps28	691531	-0.68	0.103369
Dcn	29139	0.56	0.104287
C1qa	298566	0.65	0.105134
Lbr	89789	-2.13	0.105335
LOC619574	619574	-2.96	0.105834
Prpf19	246216	-1.37	0.106789
Cadm3	360882	1.55	0.107698
Pcolce	29569	-0.72	0.108282
Afdn	26955	0.37	0.109297
Cfd	54249	0.92	0.109855
Hsd17b11	289456	-0.72	0.111035
Stk24	361092	-0.61	0.111524
Iah1	298917	-0.54	0.111550
Srsf2	494445	-0.63	0.112424
Lypla2	83510	-0.70	0.113495
Rabggta	58983	-0.26	0.115613
Dynll1	58945	-0.63	0.116414
LOC103690821	103690821	-5.38	0.116555
Ddah2	294239	0.50	0.119324
Sptan1	64159	0.50	0.119658
Pycr3	300035	-2.47	0.120115
LOC100911248	100911248	-0.53	0.120469
Sdha	157074	-0.28	0.120567
Arpc5	360854	-0.96	0.120907
Pcbd1	29700	2.77	0.121663
Sccpdh	305021	0.56	0.121973
Gnb1	24400	0.46	0.122525
LOC684988	684988	-0.69	0.123734
Lum	81682	0.39	0.123888
S100a10	81778	1.13	0.124234
Aox3	493909	1.53	0.124551
Acadm	24158	-0.75	0.124567
Snap23	64630	0.42	0.124762
Myo1d	25485	1.92	0.125068
Anxa2	56611	0.91	0.126984
Sae1	308384	-1.38	0.127451
Tuba1c	300218	2.14	0.127541
Acsl4	113976	-2.66	0.127964

Rpl36	58927	-0.75	0.129174
Coro1b	29474	-0.91	0.129983
Ddx39b	114612	-0.76	0.130371
Serpina3n	24795	0.93	0.133059
Slc9a3r1	59114	-1.43	0.133111
Ufc1	445268	0.96	0.133723
Hagh	24439	0.56	0.133896
Set	307947	-2.75	0.134883
Abca2	79248	0.83	0.136241
Rpl10	81764	-0.63	0.137193
Epcam	171577	-2.83	0.139533
Nln	117041	-1.75	0.140227
Rps21	81775	-0.58	0.140256
Arpc5l	296710	-0.94	0.142448
Dpep1	94199	0.61	0.143621
Cdc42	64465	-0.40	0.143971
Hmgb1	25459	-2.74	0.145124
Prkcb	25023	-2.25	0.145733
Sirt2	361532	0.70	0.146533
Gsn	296654	0.84	0.149709
Arg1	29221	-3.18	0.150180
Arl8b	500282	-0.44	0.150719
Mybbp1a	60571	-2.43	0.152501
Oplah	116684	-1.84	0.152644
Bcat1	29592	0.70	0.154343
Dctn1	29167	2.23	0.155575
Ces1d	113902	0.77	0.155957
Mcts1	302500	1.12	0.156172
Dctn4	84428	-0.62	0.156189
Rps27l	681429	-1.15	0.156292
Pecr	113956	-1.79	0.157226
Tra2b	117259	-0.90	0.157773
Cpq	58952	0.63	0.158239
Vim	81818	0.71	0.158932
Coro1a	155151	-3.39	0.160831
Elavl1	363854	-0.65	0.161132
Psmc4	117262	-0.37	0.162250
Tubb4b	296554	0.47	0.162807
Plvap	56765	0.53	0.162951
Tpmt	690050	-0.80	0.164556
Gna13	303634	-0.51	0.165043
Ace	24310	0.92	0.165637
Coro7	192276	-2.98	0.165684
Aldh9a1	64040	0.45	0.167003
Nid2	302248	0.76	0.167451
Sumo2	690244	-0.74	0.167705

Ptbp3	83515	-2.44	0.169287
Mvp	64681	-0.73	0.173324
Pfn1	64303	-1.08	0.173499
Serpind1	79224	0.53	0.174777
Hnrnpf	64200	-1.02	0.176737
Apoc1	25292	3.77	0.177471
Cops2	261736	-3.04	0.177771
Cct3	295230	-0.51	0.179225
Aldh1a7	29651	4.10	0.179495
Pon1	84024	-1.45	0.179907
Atp5j	94271	-0.25	0.180618
Rpl4	64302	-0.78	0.180827
Hnrnpu	117280	-0.97	0.181579
Ufd1	84478	-0.21	0.182866
Scgb1d4	293731	2.70	0.184442
Ndufs2	289218	-0.42	0.185120
Calml3	307100	1.77	0.185649
Fabp3	79131	2.38	0.185749
Ppp3r1	29748	-0.99	0.185763
Acox3	83522	0.75	0.187330
Cox4i1	29445	-0.36	0.187695
Anp32a	25379	-1.35	0.187706
Plbd1	297694	-1.59	0.190050
Kpnb1	24917	-0.30	0.191047
Cndp1	307212	2.81	0.192754
Rpl35	296709	-0.75	0.194182
Arl3	64664	-0.35	0.194833
Psmb10	291983	-1.33	0.195615
Tppp3	291966	0.55	0.196539
Ugt1a6	113992	0.90	0.197351
Hnrnpl	80846	-0.59	0.197806
Atp6v0c	170667	-0.42	0.197838
Arpc1b	54227	-1.25	0.197860
Cavin2	316384	1.21	0.198691
Gdi1	25183	0.33	0.199526
Uqcrh	366448	0.29	0.201902
Ybx1	500538	-0.83	0.202578
Itgb1	24511	0.59	0.203687
Anxa8	306283	0.82	0.203910
Tgfb1i1	84574	0.53	0.205149
Nsfl1c	83809	-0.39	0.205591
Slc2a4	25139	0.97	0.206215
Psmb9	24967	-0.95	0.206320
Fubp1	654496	-1.23	0.206714
Cap1	64185	-0.94	0.207328
Gimap4	286938	-1.53	0.208766

Cavin3	85332	1.06	0.210014
Rps15a	117053	-0.88	0.210580
Ecm1	116662	0.96	0.213777
Cd44	25406	3.24	0.216345
Tuba4a	316531	-0.63	0.217005
Khsrp	171137	-0.83	0.217712
Krt2	406228	0.20	0.221107
Irgm	303090	2.07	0.224959
LOC501110	501110	-0.31	0.225656
Rpl22	81768	-0.43	0.226122
C4a	24233	0.77	0.227035
Rgn	25106	1.62	0.227052
Cpped1	302890	0.33	0.227974
Prg2	58826	-1.79	0.227978
Pecam1	29583	0.59	0.230352
Hsd17b4	79244	0.69	0.230746
Mccc1	294972	-0.21	0.230971
Ca5b	302669	1.19	0.231316
Sncg	64347	1.19	0.232565
Tufm	293481	-0.49	0.233099
Nap1l1	89825	-0.41	0.233641
Plp2	302562	0.77	0.235671
Gphn	64845	3.39	0.236104
Cst3	25307	0.27	0.236295
Hacl1	85255	-0.97	0.236649
Slc25a5	25176	-0.36	0.236974
Trap1	287069	-0.30	0.237825
Hnrnpm	116655	-0.96	0.237910
Myo1c	65261	0.56	0.238350
Enpp3	54410	0.17	0.238398
Gyg1	81675	0.45	0.238519
Erp29	117030	-0.28	0.239909
Mpc2	100359982	-0.50	0.239949
Dnaja1	65028	-1.08	0.240466
Pir	363465	0.47	0.241062
Qsox1	84491	1.93	0.242226
Psme2	29614	-0.97	0.243823
Aimp2	288480	-0.60	0.243916
F13a1	60327	0.45	0.244852
Uggt1	171129	-0.53	0.245593
Car1	310218	1.39	0.246783
Psma1	29668	-0.46	0.247564
Rpl27a	293418	-0.71	0.248685
Rgs18	289076	0.38	0.249498

Supplementary Table 6: GO terms enriched in WAT

goId	goName	countDE	countAll	pv_elim
Biological Process				
GO:0000381	regulation of alternative mRNA splicing, via spliceosome	6	12	0.0029
GO:0032781	positive regulation of ATPase activity	6	12	0.0029
GO:0032760	positive regulation of tumor necrosis factor production	5	10	0.0066
GO:0042742	defense response to bacterium	6	14	0.0073
GO:0043065	positive regulation of apoptotic process	18	73	0.0074
GO:0000122	negative regulation of transcription from RNA polymerase II promoter	11	37	0.0083
GO:0000077	DNA damage checkpoint	3	4	0.0093
GO:0001960	negative regulation of cytokine-mediated signaling pathway	3	4	0.0093
GO:0002828	regulation of type 2 immune response	3	4	0.0093
GO:0010799	regulation of peptidyl-threonine phosphorylation	3	4	0.0093
GO:0034142	toll-like receptor 4 signaling pathway	3	4	0.0093
GO:0035767	endothelial cell chemotaxis	3	4	0.0093
GO:0044319	wound healing, spreading of cells	3	4	0.0093
GO:0051126	negative regulation of actin nucleation	3	4	0.0093
GO:1990774	tumor necrosis factor secretion	3	4	0.0093
GO:2000648	positive regulation of stem cell proliferation	3	4	0.0093
GO:0033273	response to vitamin	10	25	0.0126
GO:0051384	response to glucocorticoid	12	45	0.0148
GO:0043388	positive regulation of DNA binding	4	8	0.0156
GO:0046717	acid secretion	4	8	0.0156
GO:0032374	regulation of cholesterol transport	5	12	0.0165
GO:0000245	spliceosomal complex assembly	3	5	0.0209
GO:0008209	androgen metabolic process	3	5	0.0209
GO:0032369	negative regulation of lipid transport	3	5	0.0209
GO:0033280	response to vitamin D	3	5	0.0209
GO:0045581	negative regulation of T cell differentiation	3	5	0.0209
GO:0051785	positive regulation of nuclear division	3	5	0.0209
GO:2000279	negative regulation of DNA	3	5	0.0209

	biosynthetic process			
GO:2001020	regulation of response to DNA damage stimulus	6	17	0.021
GO:0007346	regulation of mitotic cell cycle	10	37	0.0232
GO:0034314	Arp2/3 complex-mediated actin nucleation	5	13	0.0239
GO:0061515	myeloid cell development	4	9	0.0251
GO:0051252	regulation of RNA metabolic process	44	195	0.0258
GO:0032845	negative regulation of homeostatic process	8	28	0.0298
GO:0045893	positive regulation of transcription, DNA-templated	17	78	0.031
GO:0001935	endothelial cell proliferation	5	14	0.0331
GO:0015718	monocarboxylic acid transport	5	14	0.0331
GO:0051053	negative regulation of DNA metabolic process	6	11	0.0363
GO:0015758	glucose transport	6	19	0.0364
GO:0010506	regulation of autophagy	7	24	0.0371
GO:0055081	anion homeostasis	4	10	0.0374
GO:0030330	DNA damage response, signal transduction by p53 class mediator	3	6	0.0375
GO:0048026	positive regulation of mRNA splicing, via spliceosome	3	6	0.0375
GO:0048255	mRNA stabilization	3	6	0.0375
GO:0008284	positive regulation of cell proliferation	20	86	0.0429
GO:0030334	regulation of cell migration	18	87	0.0433
GO:0014909	smooth muscle cell migration	5	15	0.0442
GO:0034341	response to interferon-gamma	5	15	0.0442
GO:0071222	cellular response to lipopolysaccharide	6	20	0.0462
GO:0071384	cellular response to corticosteroid stimulus	6	20	0.0462
Molecular Function				
GO:0070573	metallodipeptidase activity	3	3	0.0026
GO:0019955	cytokine binding	4	6	0.0043
GO:0051015	actin filament binding	12	40	0.0058
GO:0060590	ATPase regulator activity	4	7	0.009
GO:0005080	protein kinase C binding	6	15	0.0112
GO:0003727	single-stranded RNA binding	6	16	0.0159
GO:0004180	carboxypeptidase activity	4	9	0.0258

GO:0036002	pre-mRNA binding	4	9	0.0258
GO:0003697	single-stranded DNA binding	5	14	0.0341
GO:0003725	double-stranded RNA binding	6	19	0.0376
GO:0001530	lipopolysaccharide binding	3	6	0.0383
GO:0008201	heparin binding	5	15	0.0455
GO:0003682	chromatin binding	7	25	0.0475
Cellular Component				
GO:0071013	catalytic step 2 spliceosome	7	16	0.0032
GO:0031528	microvillus membrane	4	6	0.0041
GO:0005811	lipid droplet	8	24	0.0113
GO:0005681	spliceosomal complex	10	22	0.0346
GO:0030315	T-tubule	4	10	0.037
GO:0005885	Arp2/3 protein complex	3	6	0.0372
GO:0016604	nuclear body	11	46	0.0412
GO:0000776	kinetochore	5	15	0.0437

Supplementary Table 7: Pathways impacted in IWAT

pName	pv
Spliceosome	0.000141924
Melanoma	0.016101272
Valine, leucine and isoleucine biosynthesis	0.019168336
ABC transporters	0.019168336
Phospholipase D signaling pathway	0.021481217
Pancreatic cancer	0.024046645
Cytokine-cytokine receptor interaction	0.024280456
HIF-1 signaling pathway	0.027970102
FoxO signaling pathway	0.030910267
PI3K-Akt signaling pathway	0.031324199
Fc gamma R-mediated phagocytosis	0.032654499
Drug metabolism - other enzymes	0.038234041
Non-small cell lung cancer	0.04040074
Gap junction	0.047624149

Table 8. List of nodes in protein-protein interaction network in BAT with exercise training

Id	Label	Degree	Betweenness
ENSRNOP00000013462	Rpl4	403	174197.3
ENSRNOP00000019247	Rpl27a	368	142415.7
ENSRNOP00000002194	Rpl24	367	25541.66
ENSRNOP00000000603	Rpl10a	290	103764.5
ENSRNOP00000014849	Rpl29	278	11315.43
ENSRNOP00000040081	Gfm1	138	11143.29
ENSRNOP00000026710	Gnai3	110	111426.7
ENSRNOP00000028887	Pcna	94	116410.5
ENSRNOP00000002533	Mapk1	91	290801.3
ENSRNOP00000025303	Akt2	61	200959.2
ENSRNOP00000025980	Hnrnpk	47	385423.2
ENSRNOP00000020647	Tpi1	36	47910.3
ENSRNOP00000001911	Gnb2	34	21856.2
ENSRNOP00000057188	Eif3b	30	15939.55
ENSRNOP00000019531	Tcp1	29	39505.48
ENSRNOP00000024609	Uqcrfs1	27	11648.4
ENSRNOP00000002732	Atp5o	25	14455.11
ENSRNOP00000002484	Eif4a2	25	9881.91
ENSRNOP00000059076	Dctn1	24	33858.5
ENSRNOP00000025525	Cox5a	23	5885.71
ENSRNOP00000003965	Atp5b	22	12328.27
ENSRNOP00000022487	Cox5b	21	6761.27
ENSRNOP00000032361	Eif3d	19	5751.89
ENSRNOP00000007298	Dlst	18	19106.12
ENSRNOP00000067815	Atp5e	18	4932.53
ENSRNOP00000002044	Napa	17	19368
ENSRNOP00000001958	Mdh2	16	63676.24
ENSRNOP00000008980	Dld	15	48405.47
ENSRNOP00000025906	Ilk	14	25291.5
ENSRNOP00000007558	Csnk2a1	14	19795.87
ENSRNOP00000002116	Atp5j	14	3417.8
ENSRNOP00000024033	Cox4i1	14	2422.6
ENSRNOP00000011052	Cdk5	13	106253.7
ENSRNOP00000060140	Acaa2	12	21722.5
ENSRNOP00000015102	Idh3a	11	26421.81
ENSRNOP00000046690	Vps4a	11	19340.5
ENSRNOP00000050322	Actg2	11	12135
ENSRNOP00000016432	Rab7a	11	10926.5
ENSRNOP00000019021	Cps1	10	29996.3
ENSRNOP00000043366	Timeless	10	9716.5
ENSRNOP00000023256	Slc2a4	9	77101.2
ENSRNOP00000020322	Idh1	9	30158.91
ENSRNOP00000006141	F11r	9	9716

ENSRNOP00000016520	Samm50	9	9716
ENSRNOP00000066894	Khdrbs1	9	8497.22
ENSRNOP00000025880	Dpysl3	8	157067.4
ENSRNOP00000015956	Got2	8	113550.5
ENSRNOP00000023554	Hmgcs1	8	6685
ENSRNOP00000017230	RGD1565317	8	5039.53
ENSRNOP00000040548	RGD1563570	8	3738.91
ENSRNOP00000051318	LOC100359563	8	2390.52
ENSRNOP00000023447	Acly	7	34806.19
ENSRNOP00000005574	Ndel1	7	32587.47
ENSRNOP00000027073	Uba52	7	31171
ENSRNOP00000021514	Uqcrc2	7	13424.48
ENSRNOP00000044696	Uqcrc1	7	13424.48
ENSRNOP00000010593	Sdhb	7	8258.96
ENSRNOP00000001625	Pfkl	7	7293
ENSRNOP00000012114	Pdcd6ip	7	6080.5
ENSRNOP00000010383	LOC100911372	7	3603.5
ENSRNOP00000026576	Rps16	7	3603.5
ENSRNOP00000026528	Rps5	7	3542
ENSRNOP00000061250	Rps11	7	3491.37
ENSRNOP00000009988	RGD1560831	7	896.66
ENSRNOP00000023935	Rps3	7	896.66
ENSRNOP00000046737	Rps15al4	7	896.66
ENSRNOP00000017239	Wdr61	6	6080
ENSRNOP00000063201	RGD1561102	6	1680.08
ENSRNOP00000056750	LOC100364509	6	850.16
ENSRNOP00000001518	Rplp0	6	0.34
ENSRNOP00000005471	Rpl23	6	0.34
ENSRNOP00000005511		6	0.34
ENSRNOP00000005588	Rpl26	6	0.34
ENSRNOP00000009431	Rpl7	6	0.34
ENSRNOP00000011314	Rps20	6	0.34
ENSRNOP00000021725	Rpl12	6	0.34
ENSRNOP00000022348	Rps23	6	0.34
ENSRNOP00000024678	Rps15a	6	0.34
ENSRNOP00000025217	Rpl17	6	0.34
ENSRNOP00000030437	RGD1563956	6	0.34
ENSRNOP00000032635	LOC100360449	6	0.34
ENSRNOP00000034364	Rpl17	6	0.34
ENSRNOP00000034767	RGD1359290	6	0.34
ENSRNOP00000036391	Rpl23a	6	0.34
ENSRNOP00000036514	Rpl5	6	0.34
ENSRNOP00000037110	Rpl11	6	0.34
ENSRNOP00000039111		6	0.34
ENSRNOP00000039774	RGD1560017	6	0.34
ENSRNOP00000046553	Rpl8	6	0.34

ENSRNOP00000066050	LOC100364116	6	0.34
ENSRNOP00000065886	LOC100362684	6	0.34
ENSRNOP00000064822	RGD1565048	6	0.34
ENSRNOP00000047328	RGD1561333	6	0.34
ENSRNOP00000066260	LOC103692519	6	0.34
ENSRNOP00000042242	Rps15al4	6	0.34
ENSRNOP00000045335		6	0.34
ENSRNOP00000066866	LOC103690796	6	0.34
ENSRNOP00000066750	LOC100909911	6	0.34
ENSRNOP00000042929	LOC688981	6	0.34
ENSRNOP00000067080	LOC100360117	6	0.34
ENSRNOP00000067881	RGD1564378	6	0.34
ENSRNOP00000049710		6	0.34
ENSRNOP00000067887	LOC100910721	6	0.34
ENSRNOP00000066077	LOC100359951	6	0.34
ENSRNOP00000064197	Rpl12	6	0.34
ENSRNOP00000040966	Rpl10l	6	0.34
ENSRNOP00000065065	LOC100910721	6	0.34
ENSRNOP00000049652	LOC689899	6	0.34
ENSRNOP00000041817	LOC100360449	6	0.34
ENSRNOP00000043004	RGD1564606	6	0.34
ENSRNOP00000067446	LOC100909911	6	0.34
ENSRNOP00000065901		6	0.34
ENSRNOP00000040232		6	0.34
ENSRNOP00000064959	LOC103692519	6	0.34
ENSRNOP00000045458	Rpl26-ps1	6	0.34
ENSRNOP00000050700	LOC690335	6	0.34
ENSRNOP00000057758	Rpl26-ps2	6	0.34
ENSRNOP00000060662	Rpl3	6	0.34
ENSRNOP00000064566	LOC100910370	6	0.34
ENSRNOP00000050533	RGD1563705	6	0.34
ENSRNOP00000047749	LOC680441	6	0.34
ENSRNOP00000064524	RGD1563124	6	0.34
ENSRNOP00000046487	RGD1562755	6	0.34
ENSRNOP00000053082	Rpl5l1	6	0.34
ENSRNOP00000051016	LOC100364191	6	0.34
ENSRNOP00000049286	Rps15al2	6	0.34
ENSRNOP00000044111	RGD1565170	6	0.34
ENSRNOP00000065423		6	0.34
ENSRNOP00000041462	LOC102555453	6	0.34
ENSRNOP00000050047		6	0.34
ENSRNOP00000047840	Tp53	5	98266.48
ENSRNOP00000022892	Atp5a1	5	18899.62
ENSRNOP00000049879	Taf3	5	18899.62
ENSRNOP00000008477	Vdac1	5	14868.26
ENSRNOP00000063666	Hspd1	5	3410.54

ENSRNOP00000025446	Echs1	5	3040
ENSRNOP00000020670	Atp5d	5	2925.58
ENSRNOP00000022897	Rps27	5	1355.98
ENSRNOP00000048624	RGD1565415	5	0.34
ENSRNOP00000055298		5	0.34
ENSRNOP00000063004		5	0.34
ENSRNOP00000045344	RGD1559972	5	0.34
ENSRNOP00000044949	RGD1560633	5	0.34
ENSRNOP00000048422	RGD1562402	5	0.34
ENSRNOP00000004583		5	0.24
ENSRNOP00000005089	Mrps7	5	0.24
ENSRNOP00000019508	Rps2	5	0.24
ENSRNOP00000019660	Rpl3l	5	0.24
ENSRNOP00000021803	Rpl7l1	5	0.24
ENSRNOP00000036343	LOC688473	5	0.24
ENSRNOP00000039003		5	0.24
ENSRNOP00000057658	Rps2-ps6	5	0.24
ENSRNOP00000046157	RGD1564469	5	0.24
ENSRNOP00000045798	LOC367195	5	0.24
ENSRNOP00000056260	Rps14	5	0.24
ENSRNOP00000044837		5	0.24
ENSRNOP00000066548		5	0.24
ENSRNOP00000058859		5	0.24
ENSRNOP00000066792	LOC100364509	5	0.24
ENSRNOP00000047760		5	0.24
ENSRNOP00000044563	LOC680646	5	0.24
ENSRNOP00000055288	RGD1562399	5	0.24
ENSRNOP00000001265	Rpl21	5	0
ENSRNOP00000002177		5	0
ENSRNOP00000004213		5	0
ENSRNOP00000004303	RGD1559951	5	0
ENSRNOP00000005872	Rps27a	5	0
ENSRNOP00000006359	Rpl19	5	0
ENSRNOP00000006754	Rpl7a	5	0
ENSRNOP00000009046	Rpl34	5	0
ENSRNOP00000010759	Rpl15	5	0
ENSRNOP00000011244	LOC688684	5	0
ENSRNOP00000012255	LOC690096	5	0
ENSRNOP00000014493	Rpl32	5	0
ENSRNOP00000014905	LOC100360057	5	0
ENSRNOP00000015408	RGD1565894	5	0
ENSRNOP00000015756	Rpl22l1	5	0
ENSRNOP00000015893		5	0
ENSRNOP00000016329	Rps3a	5	0
ENSRNOP00000018820	Rplp1	5	0
ENSRNOP00000019162	Rpl35	5	0

ENSRNOP00000059662	LOC103693375	5	0
ENSRNOP00000049014	Rpl36al	5	0
ENSRNOP00000051203		5	0
ENSRNOP00000046409		5	0
ENSRNOP00000061874		5	0
ENSRNOP00000057262	LOC690384	5	0
ENSRNOP00000054703	Rpl34-ps1	5	0
ENSRNOP00000034657	Fau	5	0
ENSRNOP00000037396	LOC100359986	5	0
ENSRNOP00000055726	Rpl28	5	0
ENSRNOP00000042031	LOC100360647	5	0
ENSRNOP00000044605	LOC100361060	5	0
ENSRNOP00000039287	LOC102550668	5	0
ENSRNOP00000042920	Rpl22l2	5	0
ENSRNOP00000048019	RGD1563145	5	0
ENSRNOP00000025421	Rpl18a	5	0
ENSRNOP00000055334	RGD1565767	5	0
ENSRNOP00000041435		5	0
ENSRNOP00000066592		5	0
ENSRNOP00000039099	Rpl35al1	5	0
ENSRNOP00000051482	Rpl31l3	5	0
ENSRNOP00000041263		5	0
ENSRNOP00000041209	Rpl35al1	5	0
ENSRNOP00000051427	RGD1563958	5	0
ENSRNOP00000054497	LOC100912027	5	0
ENSRNOP00000058614	RGD1564095	5	0
ENSRNOP00000051332		5	0
ENSRNOP00000064082	LOC100360491	5	0
ENSRNOP00000047010		5	0
ENSRNOP00000045739		5	0
ENSRNOP00000067354	LOC100361079	5	0
ENSRNOP00000039179		5	0
ENSRNOP00000050175		5	0
ENSRNOP00000051188	Rpl35a	5	0
ENSRNOP00000060476	LOC680579	5	0
ENSRNOP00000042127	RGD1566373	5	0
ENSRNOP00000049635	LOC102550734	5	0
ENSRNOP00000063355	LOC100361259	5	0
ENSRNOP00000046515		5	0
ENSRNOP00000053991		5	0
ENSRNOP00000046070		5	0
ENSRNOP00000044275	LOC100910017	5	0
ENSRNOP00000038214	LOC100911575	5	0
ENSRNOP00000047513	Rpl37a	5	0
ENSRNOP00000048003	LOC100912182	5	0
ENSRNOP00000054398	Rpl30	5	0

ENSRNOP00000041966	Rpl21	5	0
ENSRNOP00000033369		5	0
ENSRNOP00000060629	RGD1561870	5	0
ENSRNOP00000040611	Rpl35a	5	0
ENSRNOP00000054699	RGD1560069	5	0
ENSRNOP00000048252	RGD1564617	5	0
ENSRNOP00000041774	RGD1564730	5	0
ENSRNOP00000065371	RGD1564617	5	0
ENSRNOP00000064270	RGD1561137	5	0
ENSRNOP00000049416	RGD1563835	5	0
ENSRNOP00000046600	LOC306079	5	0
ENSRNOP00000067572	Rps6	5	0
ENSRNOP00000046301	RGD1564839	5	0
ENSRNOP00000040955	LOC100361079	5	0
ENSRNOP00000048495		5	0
ENSRNOP00000054048	LOC100912182	5	0
ENSRNOP00000048999	Rpl31l4	5	0
ENSRNOP00000064745		5	0
ENSRNOP00000020635	LOC100359922	5	0
ENSRNOP00000065066	LOC100365839	5	0
ENSRNOP00000047511		5	0
ENSRNOP00000053986	RGD1565183	5	0
ENSRNOP00000046281	LOC686074	5	0
ENSRNOP00000051114		5	0
ENSRNOP00000049709		5	0
ENSRNOP00000041625	LOC100362751	5	0
ENSRNOP00000042633		5	0
ENSRNOP00000050328	RGD1562055	5	0
ENSRNOP00000043092	RGD1561317	5	0
ENSRNOP00000038065	Rpl6	5	0
ENSRNOP00000051743		5	0
ENSRNOP00000047759		5	0
ENSRNOP00000051312	Rpl21	5	0
ENSRNOP00000041191		5	0
ENSRNOP00000040073	LOC103691563	5	0
ENSRNOP00000051134		5	0
ENSRNOP00000049054	Rpl35a	5	0
ENSRNOP00000055671		5	0
ENSRNOP00000022184	Rps12	5	0
ENSRNOP00000059772	RGD1565566	5	0
ENSRNOP00000049666		5	0
ENSRNOP00000028481	Fau	5	0
ENSRNOP00000053160		5	0
ENSRNOP00000042277		5	0
ENSRNOP00000046578		5	0
ENSRNOP00000058934	Rpl36	5	0

ENSRNOP00000041199		5	0
ENSRNOP00000046953	LOC102554602	5	0
ENSRNOP00000042068		5	0
ENSRNOP00000048808	Rpl21	5	0
ENSRNOP00000028555	Rpl18	5	0
ENSRNOP00000065877	LOC102548369	5	0
ENSRNOP00000054740	LOC498555	5	0
ENSRNOP00000041530		5	0
ENSRNOP00000042454		5	0
ENSRNOP00000049831		5	0
ENSRNOP00000031078	Rpl31	5	0
ENSRNOP00000067596	Rpl30l1	5	0
ENSRNOP00000053863	LOC100911575	5	0
ENSRNOP00000066420	LOC100361143	5	0
ENSRNOP00000051135	Rpl6-ps1	5	0
ENSRNOP00000066016	LOC100912027	5	0
ENSRNOP00000067411		5	0
ENSRNOP00000046669		5	0
ENSRNOP00000055393		5	0
ENSRNOP00000041638	Rpl32	5	0
ENSRNOP00000042567		5	0
ENSRNOP00000045849	RGD1561195	5	0
ENSRNOP00000039786		5	0
ENSRNOP00000045195	LOC100360439	5	0
ENSRNOP00000061747	Rpl14	5	0
ENSRNOP00000027976	Rpl13a	5	0
ENSRNOP00000021161		5	0
ENSRNOP00000028060	Rpl27	5	0
ENSRNOP00000048311	RGD1563157	5	0
ENSRNOP00000042560		5	0
ENSRNOP00000052049	Eftud2	4	352858
ENSRNOP00000000733	Fyn	4	165535.3
ENSRNOP00000027999	Acadsb	4	25159
ENSRNOP00000019059	Idh2	4	14033.68
ENSRNOP00000044732	Prkaca	4	13570.3
ENSRNOP00000009681	Idh3B	4	10942.57
ENSRNOP00000027911	Lipe	4	2449.78
ENSRNOP00000060568	Rps28	4	1452.04
ENSRNOP00000018227	Pgam2	4	1178
ENSRNOP00000035156	Rps15	4	327.19
ENSRNOP00000062631	Rps15-ps2	4	327.19
ENSRNOP00000008337	Aco1	4	16.83
ENSRNOP00000015278	LOC680700	4	0.24
ENSRNOP00000036943		4	0.24
ENSRNOP00000039797	LOC103690888	4	0.24
ENSRNOP00000047911	RGD1563352	4	0.24

ENSRNOP00000052873	LOC100911847	4	0.24
ENSRNOP00000004278	Rps4x	4	0
ENSRNOP00000004836	Atp5h	4	0
ENSRNOP00000005815	Mrpl13	4	0
ENSRNOP00000006662	RGD1566369	4	0
ENSRNOP00000007683		4	0
ENSRNOP00000011333	Rps7	4	0
ENSRNOP00000013868	LOC100361180	4	0
ENSRNOP00000017067	Cyc1	4	0
ENSRNOP00000017280	Mrpl3	4	0
ENSRNOP00000020451	Mrps5	4	0
ENSRNOP00000021920	LOC100911417	4	0
ENSRNOP00000023456	Imp3	4	0
ENSRNOP00000024326	Mrto4	4	0
ENSRNOP00000024380	Mrpl2	4	0
ENSRNOP00000027029	Mrps12	4	0
ENSRNOP00000027091	mrpl11	4	0
ENSRNOP00000028517	Mrpl16	4	0
ENSRNOP00000029336	Mrpl22	4	0
ENSRNOP00000034042	mrpl24	4	0
ENSRNOP00000040969	Atp5l	4	0
ENSRNOP00000048498	LOC500350	4	0
ENSRNOP00000065147	Atp5f1	4	0
ENSRNOP00000067503	LOC691427	4	0
ENSRNOP00000045007	Mrpl17	4	0
ENSRNOP00000043988	Rps4x	4	0
ENSRNOP00000033162	LOC500594	4	0
ENSRNOP00000036690	Rps13	4	0
ENSRNOP00000046067	Mrps10	4	0
ENSRNOP00000033144	Rps25	4	0
ENSRNOP00000067129	Rps27l	4	0
ENSRNOP00000051848	Mrpl12	4	0
ENSRNOP00000021625	Npsr1	4	0
ENSRNOP00000065173		4	0
ENSRNOP00000066863	RGD1560821	4	0
ENSRNOP00000049546	Rps4y2	4	0
ENSRNOP00000025224	Rpsa	4	0
ENSRNOP00000066808	LOC100910336	4	0
ENSRNOP00000067470	LOC683961	4	0
ENSRNOP00000065487	LOC100363452	4	0
ENSRNOP00000042941	LOC500148	4	0
ENSRNOP00000042092	Rsl1d1	4	0
ENSRNOP00000041853	LOC297756	4	0
ENSRNOP00000066362	LOC100362987	4	0
ENSRNOP00000049713	LOC103693375	4	0
ENSRNOP00000045098	LOC103690821	4	0

ENSRNOP00000050353	LOC682793	4	0
ENSRNOP00000055790	LOC103692831	4	0
ENSRNOP00000042286	LOC680512	4	0
ENSRNOP00000041329	LOC103694404	4	0
ENSRNOP00000044553	LOC103694404	4	0
ENSRNOP00000027226	LOC100360573	4	0
ENSRNOP00000049665	LOC103692785	4	0
ENSRNOP00000047281	Rps27a-ps6	4	0
ENSRNOP00000063142		4	0
ENSRNOP00000061370		4	0
ENSRNOP00000044116	RGD1561310	4	0
ENSRNOP00000050202	Rpl38	4	0
ENSRNOP00000066511		4	0
ENSRNOP00000056331	Rpl37-ps1	4	0
ENSRNOP00000045213	RGD1561636	4	0
ENSRNOP00000048664	Rps27a	4	0
ENSRNOP00000042288	LOC685963	4	0
ENSRNOP00000065827		4	0
ENSRNOP00000049028	LOC680353	4	0
ENSRNOP00000025888	Rps17	4	0
ENSRNOP00000039155	Rpl37	4	0
ENSRNOP00000048903	LOC100363469	4	0
ENSRNOP00000064320	Rps17	4	0
ENSRNOP00000054474	LOC100360654	4	0
ENSRNOP00000042022	LOC685963	4	0
ENSRNOP00000023368	Rpl38	4	0
ENSRNOP00000067793		4	0
ENSRNOP00000045912		4	0
ENSRNOP00000041920	RGD1559955	4	0
ENSRNOP00000041458	RGD1562381	4	0
ENSRNOP00000031121	LOC100362366	4	0
ENSRNOP00000062764		4	0
ENSRNOP00000059382	Rps24	4	0
ENSRNOP00000049205	Rpl37	4	0
ENSRNOP00000045390	RGD1562265	4	0
ENSRNOP00000064461		4	0
ENSRNOP00000040295	Rpl39l	4	0
ENSRNOP00000048620	RGD1561453	4	0
ENSRNOP00000058757		4	0
ENSRNOP00000027086	Cnbd2	4	0
ENSRNOP00000044063	LOC686066	4	0
ENSRNOP00000065074	Uqcrq	4	0
ENSRNOP00000046414	Mt-co2	4	0
ENSRNOP00000048723	Cox6b1	4	0
ENSRNOP00000026908	Cox6a2	4	0
ENSRNOP00000030997	Cox6b1	4	0

ENSRNOP00000049222	Cox7c	4	0
ENSRNOP00000012739	Src	3	217843
ENSRNOP00000030030	Cad	3	114054.3
ENSRNOP00000003867	Gsk3b	3	77508.73
ENSRNOP00000007621	Ppp2ca	3	41511.36
ENSRNOP00000040878	Gapdh	3	26447.65
ENSRNOP00000001292	Aacs	3	23538.18
ENSRNOP00000022862	Ppp2r5d	3	20403.85
ENSRNOP00000013249	Bckdhb	3	17389.33
ENSRNOP00000043928	Pxn	3	13288
ENSRNOP00000026920	Hsp90ab1	3	6046.07
ENSRNOP00000062228	Prkacb	3	1206.5
ENSRNOP00000038369	Akt1	3	737
ENSRNOP00000034921	Cs	3	29.22
ENSRNOP00000010573	Acat1	3	6
ENSRNOP00000005786	LOC100911110	3	1.22
ENSRNOP00000063484	Eif3a	3	1.22
ENSRNOP00000000072	Atp5i	3	0
ENSRNOP00000000617	Mapk14	3	0
ENSRNOP00000000700		3	0
ENSRNOP00000001545	Cox6a1	3	0
ENSRNOP00000002834	Mrpl1	3	0
ENSRNOP00000004114	LOC690271	3	0
ENSRNOP00000007194		3	0
ENSRNOP00000009325	Mapk11	3	0
ENSRNOP00000009815	Atp5g1	3	0
ENSRNOP00000010418	Cox4i2	3	0
ENSRNOP00000011619	Mrpl15	3	0
ENSRNOP00000013548	Mrps2	3	0
ENSRNOP00000014058	LOC100363502	3	0
ENSRNOP00000014407	Cox6c	3	0
ENSRNOP00000017602	LOC100359763	3	0
ENSRNOP00000017738		3	0
ENSRNOP00000020675	Atp5g2	3	0
ENSRNOP00000025007	Mrps11	3	0
ENSRNOP00000026373	Gnao1	3	0
ENSRNOP00000029426	Atp5j2	3	0
ENSRNOP00000036682	LOC100359687	3	0
ENSRNOP00000049769	Mt-atp6	3	0
ENSRNOP00000055032	Atp5g3	3	0
ENSRNOP00000042935	Rps21-ps1	3	0
ENSRNOP00000049519	Efl1	3	0
ENSRNOP00000021899	Mrps9	3	0
ENSRNOP00000045893	Mrpl4	3	0
ENSRNOP00000056140		3	0
ENSRNOP00000043087	Gfm2	3	0

ENSRNOP00000041821	Eef2	3	0
ENSRNOP00000064782		3	0
ENSRNOP00000044874	RGD1559877	3	0
ENSRNOP00000042164	LOC100359671	3	0
ENSRNOP00000065999	LOC100911337	3	0
ENSRNOP00000065281	LOC100911337	3	0
ENSRNOP00000048847		3	0
ENSRNOP00000061442	LOC100362339	3	0
ENSRNOP00000045516	Wdr31	3	0
ENSRNOP00000042902	LOC100360843	3	0
ENSRNOP00000063451	RGD1559724	3	0
ENSRNOP00000048979	Rps27a-ps5	3	0
ENSRNOP00000030289		3	0
ENSRNOP00000041612		3	0
ENSRNOP00000061911		3	0
ENSRNOP00000044806	RGD1565117	3	0
ENSRNOP00000027780	Rps27a-ps12	3	0
ENSRNOP00000064853	LOC100911371	3	0
ENSRNOP00000040306	RGD1563613	3	0
ENSRNOP00000047999		3	0
ENSRNOP00000056689		3	0
ENSRNOP00000039845	Rps19l1	3	0
ENSRNOP00000047391	LOC100912210	3	0
ENSRNOP00000065157		3	0
ENSRNOP00000051317		3	0
ENSRNOP00000048658	LOC102554992	3	0
ENSRNOP00000041744	RGD1564138	3	0
ENSRNOP00000048116	LOC100361854	3	0
ENSRNOP00000044301	LOC688899	3	0
ENSRNOP00000043543	LOC103690015	3	0
ENSRNOP00000031049	RGD1563300	3	0
ENSRNOP00000027246	Rps19	3	0
ENSRNOP00000064904		3	0
ENSRNOP00000067306		3	0
ENSRNOP00000048289		3	0
ENSRNOP00000027054	Ogdhl	3	0
ENSRNOP00000054026	Ogdh	3	0
ENSRNOP00000050941	RGD1564325	3	0
ENSRNOP00000033706	Uqcrb	3	0
ENSRNOP00000048883	Uqcrb	3	0
ENSRNOP00000039048	Mt-co1	3	0
ENSRNOP00000039818	RGD1562758	2	24087.5
ENSRNOP00000026224	Stx4	2	20434
ENSRNOP00000043542	Bcl2l1	2	15861.62
ENSRNOP00000000628	Cdkn1a	2	12658.67
ENSRNOP00000050173	Cdkn1b	2	12658.67

ENSRNOP00000060736	Acacb	2	12194.92
ENSRNOP00000049438	Acaca	2	12194.92
ENSRNOP00000000157	Pik3r3	2	11603.06
ENSRNOP00000025687	Pik3r1	2	11603.06
ENSRNOP00000038073	Hadha	2	11390.5
ENSRNOP00000066388	LOC100911186	2	11390.5
ENSRNOP00000025281	Tomm40	2	10890
ENSRNOP00000003768	Bcl2	2	9947.43
ENSRNOP00000013831	Raf1	2	9947.43
ENSRNOP00000016221	Tsc2	2	9947.43
ENSRNOP00000016885	Eif4ebp1	2	9947.43
ENSRNOP00000018326	Creb1	2	9947.43
ENSRNOP00000061683	Pdpk1	2	9947.43
ENSRNOP00000020267	Dbt	2	8922.67
ENSRNOP00000003696	Pafah1b1	2	8899.91
ENSRNOP00000008120	Dctn2	2	8899.91
ENSRNOP00000054753	Disc1	2	8899.91
ENSRNOP00000029515	Gpi	2	8484
ENSRNOP00000020663	Ppp2cb	2	7796.79
ENSRNOP00000023741	Ctr9	2	7278
ENSRNOP00000022779	Actr1b	2	6040
ENSRNOP00000026792	Actr1a	2	6040
ENSRNOP00000011226	Chek1	2	5440.5
ENSRNOP00000022231	Mcm2	2	5440.5
ENSRNOP00000013720	Chmp4c	2	3636
ENSRNOP00000045686	Chmp4bl1	2	3636
ENSRNOP00000026470	Jund	2	3537.56
ENSRNOP00000011732	Jun	2	3537.56
ENSRNOP00000007100	Ywhae	2	3297.28
ENSRNOP00000004797	Tuba4a	2	2639.59
ENSRNOP00000013863	Tubb4b	2	2639.59
ENSRNOP00000065633	Tubb4a	2	2639.59
ENSRNOP00000009556	LOC103692716	2	1931.55
ENSRNOP00000001415	Elavl1	2	1218
ENSRNOP00000052160	Hnrnpa1	2	1208.67
ENSRNOP00000027057	Xrcc1	2	965.17
ENSRNOP00000028328	Bax	2	165.64
ENSRNOP00000022309	Got1	2	53.48
ENSRNOP00000018177	Pgk2	2	9.95
ENSRNOP00000065201		2	9.95
ENSRNOP00000024106	Eno1	2	9.95
ENSRNOP00000014637	Hadhb	2	6
ENSRNOP00000000621	Mapk13	2	0
ENSRNOP00000005389	Adcy3	2	0
ENSRNOP00000006789	Adcy8	2	0
ENSRNOP00000008011	Gngt2	2	0

ENSRNOP00000011429	Mdh1	2	0
ENSRNOP00000012274	Dpysl5	2	0
ENSRNOP00000012996	Dpysl2	2	0
ENSRNOP00000013375	Eif2s1	2	0
ENSRNOP00000013695	Eif5	2	0
ENSRNOP00000014219	Gngt1	2	0
ENSRNOP00000014817	Eif3l	2	0
ENSRNOP00000014871	Gnb4	2	0
ENSRNOP00000017017	Pmpcb	2	0
ENSRNOP00000017409	Eif3m	2	0
ENSRNOP00000017718	LOC100912445	2	0
ENSRNOP00000018336	Sdha	2	0
ENSRNOP00000020700	Adcy7	2	0
ENSRNOP00000021017	Eif3f	2	0
ENSRNOP00000021480	Gnb3	2	0
ENSRNOP00000021671	Parva	2	0
ENSRNOP00000022437	Eif3j	2	0
ENSRNOP00000025782	Eif3c	2	0
ENSRNOP00000027986	Eif3g	2	0
ENSRNOP00000029790	Eif3el1	2	0
ENSRNOP00000030371	Rps18	2	0
ENSRNOP00000040056	RGD1561919	2	0
ENSRNOP00000043254	Eif4h	2	0
ENSRNOP00000049629	Eif4g1	2	0
ENSRNOP00000038994	Adcy2	2	0
ENSRNOP00000046455	Mapk12	2	0
ENSRNOP00000066965	LOC100912034	2	0
ENSRNOP00000022550	Gnai2	2	0
ENSRNOP00000046488	Adcy5	2	0
ENSRNOP00000016417	Prkcb	2	0
ENSRNOP00000065598	Gng4	2	0
ENSRNOP00000004699	Prkca	2	0
ENSRNOP00000027719	Adcy4	2	0
ENSRNOP00000065327		2	0
ENSRNOP00000047355		2	0
ENSRNOP00000049626		2	0
ENSRNOP00000039429		2	0
ENSRNOP00000047767		2	0
ENSRNOP00000063940		2	0
ENSRNOP00000045954		2	0
ENSRNOP00000063128	Rpl7a	2	0
ENSRNOP00000049619		2	0
ENSRNOP00000046036		2	0
ENSRNOP00000046427		2	0
ENSRNOP00000042800		2	0
ENSRNOP00000045940		2	0

ENSRNOP00000048713		2	0
ENSRNOP00000036381	Nras	2	0
ENSRNOP00000044340	Gnb1	2	0
ENSRNOP00000065820		2	0
ENSRNOP00000008736	Atp6v0c	2	0
ENSRNOP00000026704	Atp6v0b	2	0
ENSRNOP00000048392	RGD1559629	2	0
ENSRNOP00000060229	Sucla2	2	0
ENSRNOP00000059952	Dhtkd1	2	0
ENSRNOP00000032890	Dlat	2	0
ENSRNOP00000010545	Pdhb	2	0
ENSRNOP00000067239		2	0
ENSRNOP00000064678	LOC100912024	2	0
ENSRNOP00000047371	Rps18l1	2	0
ENSRNOP00000040282	RGD1565912	2	0
ENSRNOP00000046090	LOC100362298	2	0
ENSRNOP00000063671	Crmp1	2	0
ENSRNOP00000035591	Cox6b2	2	0
ENSRNOP00000051326	Mt-cox3	2	0
ENSRNOP00000061674	Pik3cd	2	0
ENSRNOP00000035786	LOC100910021	2	0
ENSRNOP00000061066	Eif3k	2	0
ENSRNOP00000067288		2	0
ENSRNOP00000000078	Ppp2r5a	1	0
ENSRNOP00000000102	LOC103691556	1	0
ENSRNOP00000000174	Chm	1	0
ENSRNOP00000000249	Grm6	1	0
ENSRNOP00000000327	Foxo3	1	0
ENSRNOP00000000553	Pfdn6	1	0
ENSRNOP00000000576	Bak1	1	0
ENSRNOP00000000627	Srsf3	1	0
ENSRNOP00000000783	Cdk1	1	0
ENSRNOP00000000904	Chmp2b	1	0
ENSRNOP00000000907	Htr1f	1	0
ENSRNOP00000001054	Gja1	1	0
ENSRNOP00000001123	Csnk2b	1	0
ENSRNOP00000001154	Rbmx	1	0
ENSRNOP00000001227	Cct6a	1	0
ENSRNOP00000001417	Rac1	1	0
ENSRNOP00000001444	Rfc3	1	0
ENSRNOP00000001498	Rfc5	1	0
ENSRNOP00000001539	Srsf9	1	0
ENSRNOP00000001556	Acads	1	0
ENSRNOP00000001605	Pwp2	1	0
ENSRNOP00000001654	Gna12	1	0
ENSRNOP00000001685	Clip1	1	0

ENSRNOP00000001779	Gnaz	1	0
ENSRNOP00000001825	Mcm7	1	0
ENSRNOP00000001989	Rfc2	1	0
ENSRNOP00000002053	Snrpa	1	0
ENSRNOP00000002064	RGD1559534	1	0
ENSRNOP00000002072	Pdk1	1	0
ENSRNOP00000002134	Mtx2	1	0
ENSRNOP00000002169	Cct8	1	0
ENSRNOP00000002174	Atf2	1	0
ENSRNOP00000002247	Ets2	1	0
ENSRNOP00000002299	Chaf1b	1	0
ENSRNOP00000002323	Dvl3	1	0
ENSRNOP00000002410	Ehhadh	1	0
ENSRNOP00000002487	Rfc4	1	0
ENSRNOP00000002510	Mcm4	1	0
ENSRNOP00000002907	Aasdh	1	0
ENSRNOP00000003092	Casr	1	0
ENSRNOP00000003188	RGD1566265	1	0
ENSRNOP00000003460	Mrps14	1	0
ENSRNOP00000003715	Vps4b	1	0
ENSRNOP00000003735	Sstr2	1	0
ENSRNOP00000003840	Phlpp1	1	0
ENSRNOP00000003907	Rfc1	1	0
ENSRNOP00000003954	Ccnb3	1	0
ENSRNOP00000004228	Sdhc	1	0
ENSRNOP00000004229	Rpa1	1	0
ENSRNOP00000004232	Parp1	1	0
ENSRNOP00000004406	Cxcr3	1	0
ENSRNOP00000004495	Cdc73	1	0
ENSRNOP00000004499	Mcm9	1	0
ENSRNOP00000004570	Gcdh	1	0
ENSRNOP00000004602	Adora1	1	0
ENSRNOP00000004947	Mrpl27	1	0
ENSRNOP00000004969	Mcm6	1	0
ENSRNOP00000005039	Rilp	1	0
ENSRNOP00000005076	Rgs9	1	0
ENSRNOP00000005143	Cxcr4	1	0
ENSRNOP00000005226	Rps6kb1	1	0
ENSRNOP00000005337	Rptor	1	0
ENSRNOP00000005346	Pfdn2	1	0
ENSRNOP00000005347	Grb2	1	0
ENSRNOP00000005379	Chmp6	1	0
ENSRNOP00000005535	LOC100911625	1	0
ENSRNOP00000005576	Dtl	1	0
ENSRNOP00000005577	Rps29	1	0
ENSRNOP00000005601	LOC100911625	1	0

ENSRNOP00000005612	Eno3	1	0
ENSRNOP00000005641	Pdk2	1	0
ENSRNOP00000005835	Pole2	1	0
ENSRNOP00000005953	Bdkrb1	1	0
ENSRNOP00000006004	Dpys	1	0
ENSRNOP00000006389	Plcb1	1	0
ENSRNOP00000006470	Gen1	1	0
ENSRNOP00000006527	Strn	1	0
ENSRNOP00000006741	Sh3kbp1	1	0
ENSRNOP00000006852	Hus1	1	0
ENSRNOP00000006900	Snrpb2	1	0
ENSRNOP00000006953	Dync2li1	1	0
ENSRNOP00000007117	S1pr4	1	0
ENSRNOP00000007572	Grm3	1	0
ENSRNOP00000007583	Srsf5	1	0
ENSRNOP00000007595	Ppp2r5c	1	0
ENSRNOP00000007624	Suclg1	1	0
ENSRNOP00000007649	Traf3ip3	1	0
ENSRNOP00000007698	Gadd45a	1	0
ENSRNOP00000007738	Pde4b	1	0
ENSRNOP00000007828	Dlg5	1	0
ENSRNOP00000008269	Ccr9	1	0
ENSRNOP00000008294	Cxcr6	1	0
ENSRNOP00000008300	Pde11a	1	0
ENSRNOP00000008355	Sf3a1	1	0
ENSRNOP00000008427	Srsf6	1	0
ENSRNOP00000008772	Ccr1	1	0
ENSRNOP00000008783	Ccr1l1	1	0
ENSRNOP00000008809	Ccr3	1	0
ENSRNOP00000008959	Spo11	1	0
ENSRNOP00000009124	Cry1	1	0
ENSRNOP00000009207	Mrps16	1	0
ENSRNOP00000009317	Htr5a	1	0
ENSRNOP00000009612	Sstr3	1	0
ENSRNOP00000009840	Trib3	1	0
ENSRNOP00000009944	Cct6b	1	0
ENSRNOP00000009985	Cyp51	1	0
ENSRNOP00000010032	Npbwr1	1	0
ENSRNOP00000010142	Cry2	1	0
ENSRNOP00000010197	Rab11b	1	0
ENSRNOP00000010253	Chmp3	1	0
ENSRNOP00000010255	Oprk1	1	0
ENSRNOP00000010850	Cnr1	1	0
ENSRNOP00000010935	Usp1	1	0
ENSRNOP00000011123	Rpa3	1	0
ENSRNOP00000011155	Vps39	1	0

ENSRNOP00000011784	Eci1	1	0
ENSRNOP00000011883	Mtnr1b	1	0
ENSRNOP00000011907	Chmp5	1	0
ENSRNOP00000011963	Gnb5	1	0
ENSRNOP00000012279	Dynll2	1	0
ENSRNOP00000012322	Adra2c	1	0
ENSRNOP00000012342	Cnr2	1	0
ENSRNOP00000012379	Aplnr	1	0
ENSRNOP00000012400	Fermt2	1	0
ENSRNOP00000012432	Hck	1	0
ENSRNOP00000012492	Orc1	1	0
ENSRNOP00000012597	Cdk6	1	0
ENSRNOP00000012600	Tbc1d4	1	0
ENSRNOP00000012847	Cct4	1	0
ENSRNOP00000012936	Lck	1	0
ENSRNOP00000013058	Nos3	1	0
ENSRNOP00000013070	Rad52	1	0
ENSRNOP00000013176	Apex1	1	0
ENSRNOP00000013184	Dync1i1	1	0
ENSRNOP00000013301	Srsf4	1	0
ENSRNOP00000013510	Leo1	1	0
ENSRNOP00000013618	Htr1a	1	0
ENSRNOP00000013705	Ccr4	1	0
ENSRNOP00000013919	H2afz	1	0
ENSRNOP00000014020	Tlr4	1	0
ENSRNOP00000014034	Ptger3	1	0
ENSRNOP00000014084	Oprd1	1	0
ENSRNOP00000014167	Mtor	1	0
ENSRNOP00000014611	Smptb	1	0
ENSRNOP00000014658	Hadh	1	0
ENSRNOP00000014701	Fabp4	1	0
ENSRNOP00000014747	Ednrb	1	0
ENSRNOP00000014785	Itgb1	1	0
ENSRNOP00000014841	Fpr1	1	0
ENSRNOP00000015019	Ppp2r1a	1	0
ENSRNOP00000015152	Hnrnpa2b1	1	0
ENSRNOP00000015179	Vcl	1	0
ENSRNOP00000015440	Echdc1	1	0
ENSRNOP00000015498	Pde3b	1	0
ENSRNOP00000015518	Hnrnph2	1	0
ENSRNOP00000015875	Ybx1	1	0
ENSRNOP00000015886	Cct5	1	0
ENSRNOP00000015971	Hnrnpr	1	0
ENSRNOP00000016032	Fes	1	0
ENSRNOP00000016047	Htr1d	1	0
ENSRNOP00000016189	Poli	1	0

ENSRNOP00000016220	Mapre1	1	0
ENSRNOP00000016580	Cxcr5	1	0
ENSRNOP00000016742	LOC103694902	1	0
ENSRNOP00000016751	Uqcrh	1	0
ENSRNOP00000016904	Tsc1	1	0
ENSRNOP00000016946	Plk4	1	0
ENSRNOP00000017081	Mcm3	1	0
ENSRNOP00000017109	Lpxn	1	0
ENSRNOP00000017353	Ehd2	1	0
ENSRNOP00000017411	Htr1b	1	0
ENSRNOP00000017421	Magoh	1	0
ENSRNOP00000017549	Rpa2	1	0
ENSRNOP00000017607	Grm2	1	0
ENSRNOP00000017794	Pfdn5	1	0
ENSRNOP00000017900	Ireb2	1	0
ENSRNOP00000017972	Casp9	1	0
ENSRNOP00000018147	Pola1	1	0
ENSRNOP00000018190	Rala	1	0
ENSRNOP00000018244	Foxo1	1	0
ENSRNOP00000018251	Gadd45g	1	0
ENSRNOP00000018278	Kif26a	1	0
ENSRNOP00000018449	Msh3	1	0
ENSRNOP00000018556	Pde7b	1	0
ENSRNOP00000018584	Adra2b	1	0
ENSRNOP00000018600	P2ry12	1	0
ENSRNOP00000018646	Snrpd1	1	0
ENSRNOP00000018923	Cdt1	1	0
ENSRNOP00000018934	Acat2l1	1	0
ENSRNOP00000018952	Npy1r	1	0
ENSRNOP00000018967	Nmur2	1	0
ENSRNOP00000018976	Npy5r	1	0
ENSRNOP00000019109	Cxcr2	1	0
ENSRNOP00000019126	Sf3b1	1	0
ENSRNOP00000019288	Pold2	1	0
ENSRNOP00000019473	S1pr3	1	0
ENSRNOP00000019529	Hnrnpf	1	0
ENSRNOP00000019561	Dctn3	1	0
ENSRNOP00000019579	Irs1	1	0
ENSRNOP00000019767	Fahd1	1	0
ENSRNOP00000019799	Lig1	1	0
ENSRNOP00000019810	Dhx38	1	0
ENSRNOP00000020544	Etfa	1	0
ENSRNOP00000020656	Lpar3	1	0
ENSRNOP00000021073	Tpm4	1	0
ENSRNOP00000021221	Snrpd2	1	0
ENSRNOP00000021289	Sorbs1	1	0

ENSRNOP00000021392	U2af2	1	0
ENSRNOP00000021475	Chmp1a	1	0
ENSRNOP00000021538	Msh2	1	0
ENSRNOP00000021657	Pccb	1	0
ENSRNOP00000021745	Phlpp2	1	0
ENSRNOP00000021923	Msh6	1	0
ENSRNOP00000022179	Pik3cb	1	0
ENSRNOP00000022190	Map3k8	1	0
ENSRNOP00000022256	Ns5atp9	1	0
ENSRNOP00000022400	Galr1	1	0
ENSRNOP00000022401	Tln1	1	0
ENSRNOP00000022744	Hrh4	1	0
ENSRNOP00000022963	Pgm2l1	1	0
ENSRNOP00000023137	Poll	1	0
ENSRNOP00000023586	Chrm4	1	0
ENSRNOP00000023786	Eif2s2	1	0
ENSRNOP00000023854	Sf3b3	1	0
ENSRNOP00000024137	Drd4	1	0
ENSRNOP00000024375	Mutyh	1	0
ENSRNOP00000024406	Ube2i	1	0
ENSRNOP00000024493	Tpm1	1	0
ENSRNOP00000024529	Rbm5	1	0
ENSRNOP00000024557	Rad1	1	0
ENSRNOP00000024875	Pold3	1	0
ENSRNOP00000024932	Per3	1	0
ENSRNOP00000025024	Nmur1	1	0
ENSRNOP00000025203	Tufm	1	0
ENSRNOP00000025451	Sstr5	1	0
ENSRNOP00000025507	Pold4	1	0
ENSRNOP00000025564	Mchr1	1	0
ENSRNOP00000025615	Eif1b	1	0
ENSRNOP00000026049	Polh	1	0
ENSRNOP00000026122	Hmgcs2	1	0
ENSRNOP00000026139	Chtf18	1	0
ENSRNOP00000026457	Pde4c	1	0
ENSRNOP00000026558	Ackr3	1	0
ENSRNOP00000026586	Pde2a	1	0
ENSRNOP00000026696	Hspa9	1	0
ENSRNOP00000026797	Pold1	1	0
ENSRNOP00000026871	Gadd45b	1	0
ENSRNOP00000027370	Tubg1	1	0
ENSRNOP00000027445	Myl9	1	0
ENSRNOP00000027507	Per2	1	0
ENSRNOP00000027842	Fen1	1	0
ENSRNOP00000028141	Cdc25a	1	0
ENSRNOP00000028411	Ccnd1	1	0

ENSRNOP00000029646	Dync1li2	1	0
ENSRNOP00000038229	Chmp2a	1	0
ENSRNOP00000041459	Eif1	1	0
ENSRNOP00000041515		1	0
ENSRNOP00000043252	Dync2h1	1	0
ENSRNOP00000043608	Hsd17b10	1	0
ENSRNOP00000044473	Tpm2	1	0
ENSRNOP00000045992	Myl12b	1	0
ENSRNOP00000046345	Eif1a	1	0
ENSRNOP00000047300	Rasa1	1	0
ENSRNOP00000049419	Eif4a1	1	0
ENSRNOP00000053093	Yes1	1	0
ENSRNOP00000058234	Clasp1	1	0
ENSRNOP00000063624	Prmt1	1	0
ENSRNOP00000053643	Chek2	1	0
ENSRNOP00000035212	Pfkfb1	1	0
ENSRNOP00000024863	Taldo1	1	0
ENSRNOP00000023252	Pfkp	1	0
ENSRNOP00000005729	Pfkfb2	1	0
ENSRNOP00000061383	Pfkfb4	1	0
ENSRNOP00000062965	Pfkfb3	1	0
ENSRNOP00000026237	Gnat2	1	0
ENSRNOP00000030270	Gng13	1	0
ENSRNOP00000067190	Gng12	1	0
ENSRNOP00000023791	Gnat1	1	0
ENSRNOP00000007032	Gnat3	1	0
ENSRNOP00000026539	Gng3	1	0
ENSRNOP00000020707	Gng10	1	0
ENSRNOP00000026893	Gng7	1	0
ENSRNOP00000022441	Gng8	1	0
ENSRNOP00000006162	Cacna1b	1	0
ENSRNOP00000051938	Gna13	1	0
ENSRNOP00000051845	Gcgr	1	0
ENSRNOP00000013244	Me1	1	0
ENSRNOP00000023329	Me3	1	0
ENSRNOP00000041737	Me2	1	0
ENSRNOP00000024471	Ndufab1	1	0
ENSRNOP00000027700	Pklr	1	0
ENSRNOP00000015331	Pkm	1	0
ENSRNOP00000004917	Fh	1	0
ENSRNOP00000035601	Aldh5a1	1	0
ENSRNOP00000026316	Pc	1	0
ENSRNOP00000021318	Stx7	1	0
ENSRNOP00000025327	Sec22b	1	0
ENSRNOP00000020693	Ykt6	1	0
ENSRNOP00000028535	Stx3	1	0

ENSRNOP00000005204	Stx8	1	0
ENSRNOP00000054114	Vamp2	1	0
ENSRNOP00000007641	Stx17	1	0
ENSRNOP00000017301	Vamp8	1	0
ENSRNOP00000014810	Bet1	1	0
ENSRNOP00000011065	Vamp7	1	0
ENSRNOP00000058953	Vti1a	1	0
ENSRNOP00000040699	Stx1a	1	0
ENSRNOP00000048364	Vamp3	1	0
ENSRNOP00000017227	Stx12	1	0
ENSRNOP00000007998	Snap25	1	0
ENSRNOP00000025664	Stx5	1	0
ENSRNOP00000039276	LOC100359503	1	0
ENSRNOP00000044197		1	0
ENSRNOP00000067492	LOC100912571	1	0
ENSRNOP00000020155	Pdcd4	1	0
ENSRNOP00000013719	Eif4e3	1	0
ENSRNOP00000062967	Eif4g2	1	0
ENSRNOP00000059390	Eif4g3	1	0
ENSRNOP00000064962	Pea15	1	0
ENSRNOP00000016328	Dusp4	1	0
ENSRNOP00000006401	Ptprr	1	0
ENSRNOP00000019465	Stat4	1	0
ENSRNOP00000014604	Braf	1	0
ENSRNOP00000009151	Dusp16	1	0
ENSRNOP00000026207	Arrb2	1	0
ENSRNOP00000026760	Stat3	1	0
ENSRNOP00000011130	Lyn	1	0
ENSRNOP00000037346	Smad3	1	0
ENSRNOP00000005400	Dusp10	1	0
ENSRNOP00000018021	Iqgap1	1	0
ENSRNOP00000059867	Ptpn6	1	0
ENSRNOP00000046497	Dusp8	1	0
ENSRNOP00000007833	Ptpn7	1	0
ENSRNOP00000013342	Spry2	1	0
ENSRNOP00000044350	Mitf	1	0
ENSRNOP00000027809	Rras	1	0
ENSRNOP00000008938	Rps6ka3	1	0
ENSRNOP00000019737	Clta	1	0
ENSRNOP00000036595	Creb5	1	0
ENSRNOP00000039672	Mknk2	1	0
ENSRNOP00000026354	Stat5b	1	0
ENSRNOP00000048329	Smad2	1	0
ENSRNOP00000043407	Hmg1l1	1	0
ENSRNOP00000013522	Elk1	1	0
ENSRNOP00000013933	Map2k1	1	0

ENSRNOP00000062321	Camk2g	1	0
ENSRNOP00000060054	Rps6ka1	1	0
ENSRNOP00000041940	Camk2a	1	0
ENSRNOP00000018549	Dusp2	1	0
ENSRNOP00000017809	Rps6ka2	1	0
ENSRNOP00000010712	Fos	1	0
ENSRNOP00000047030	Hsf1	1	0
ENSRNOP00000016026	Camk2d	1	0
ENSRNOP00000016704	Smad5	1	0
ENSRNOP00000022363	Hras	1	0
ENSRNOP00000027684	Erf	1	0
ENSRNOP00000046069	Arrb1	1	0
ENSRNOP00000003512	Rps6ka6	1	0
ENSRNOP00000014770	Dusp7	1	0
ENSRNOP00000052065	Dusp3	1	0
ENSRNOP00000018860	Ptpn5	1	0
ENSRNOP00000025079	Smad1	1	0
ENSRNOP00000018889	Dusp5	1	0
ENSRNOP00000054682		1	0
ENSRNOP00000026662	Stat5a	1	0
ENSRNOP00000061535	Mknk1	1	0
ENSRNOP00000059567	Elk4	1	0
ENSRNOP00000022303	Mbp	1	0
ENSRNOP00000021310	Ap2s1	1	0
ENSRNOP00000006188	Myc	1	0
ENSRNOP00000032969	Dusp6	1	0
ENSRNOP00000005383	Dusp1	1	0
ENSRNOP00000041486		1	0
ENSRNOP00000027272	Map2k2	1	0
ENSRNOP00000007472	Frs2	1	0
ENSRNOP00000003630	Pla2g4a	1	0
ENSRNOP00000043144	Esr2	1	0
ENSRNOP00000012616	Ndufb9	1	0
ENSRNOP00000018644	Ndc80	1	0
ENSRNOP00000042114	Bub1	1	0
ENSRNOP00000048964	Pard3	1	0
ENSRNOP00000028440	Cgn	1	0
ENSRNOP00000012924	Prkci	1	0
ENSRNOP00000024404	Itgal	1	0
ENSRNOP00000021285	Prkcz	1	0
ENSRNOP00000029044	Mllt4	1	0
ENSRNOP00000051321	Mpdz	1	0
ENSRNOP00000014988	Tjp1	1	0
ENSRNOP00000030279	Pdha1	1	0
ENSRNOP00000015217	Ndufs4	1	0
ENSRNOP00000027995	Bckdha	1	0

ENSRNOP00000060990	Suclg2	1	0
ENSRNOP00000035059	Sec63	1	0
ENSRNOP00000026439	Dvl1	1	0
ENSRNOP00000051745	Nap1l4	1	0
ENSRNOP00000009894	Nfkbia	1	0
ENSRNOP00000012022	Ssrp1	1	0
ENSRNOP00000024348	Dvl2	1	0
ENSRNOP00000015913	Slc25a5	1	0
ENSRNOP00000009552	Pdhx	1	0
ENSRNOP00000016965	Ndufv2	1	0
ENSRNOP00000015851	Ndufs1	1	0
ENSRNOP00000055942	Sdhd	1	0
ENSRNOP00000012617	Abl1	1	0
ENSRNOP00000011604	Nefh	1	0
ENSRNOP00000054180	Cdk5r2	1	0
ENSRNOP00000044534	LOC100909750	1	0
ENSRNOP00000059045	Dlg4	1	0
ENSRNOP00000062473	Cdk5r1	1	0
ENSRNOP00000034614	Ppp1r1b	1	0
ENSRNOP00000019735	Pdcd6	1	0
ENSRNOP00000022133	Cep55	1	0
ENSRNOP00000018194	Tsg101	1	0
ENSRNOP00000066181	Naca	1	0
ENSRNOP00000018455	Sec61a1	1	0
ENSRNOP00000036212	Sec61a2	1	0
ENSRNOP00000017851	Ldhc	1	0
ENSRNOP00000017965	Ldhb	1	0
ENSRNOP00000017468	Ldha	1	0
ENSRNOP00000059463	Mfn2	1	0
ENSRNOP00000024952	Gdi2	1	0
ENSRNOP00000024966	Mon1a	1	0
ENSRNOP00000052539	Mfn2	1	0
ENSRNOP00000018961	Ntrk1	1	0
ENSRNOP00000061267	Mtx1	1	0
ENSRNOP00000027088	Tomm20	1	0
ENSRNOP00000051091	Immt	1	0
ENSRNOP00000060340	Tomm7	1	0
ENSRNOP00000019323	Tomm22	1	0
ENSRNOP00000018001	Chchd3	1	0
ENSRNOP00000058722	Ttc37	1	0
ENSRNOP00000026778	Paf1	1	0
ENSRNOP00000040635	Impdh2	1	0
ENSRNOP00000029334	Dpysl4	1	0
ENSRNOP00000031981	Stk24	1	0
ENSRNOP00000062778	Stk3	1	0
ENSRNOP00000025824	Cct3	1	0

ENSRNOP00000023452	Tubb3	1	0
ENSRNOP00000024947	Tubb6	1	0
ENSRNOP00000024487	Stk25	1	0
ENSRNOP00000023611	Tubb2a	1	0
ENSRNOP00000049998	Tuba3b	1	0
ENSRNOP00000020932	LOC100909441	1	0
ENSRNOP00000044296	Actb	1	0
ENSRNOP00000021030	Cct7	1	0
ENSRNOP00000023582	Tubb2b	1	0
ENSRNOP00000029234	Cct2	1	0
ENSRNOP00000021976	Strn4	1	0
ENSRNOP00000066907	LOC103690168	1	0
ENSRNOP00000029144	Aco2	1	0
ENSRNOP00000044007		1	0
ENSRNOP00000028518	Gapdhs	1	0
ENSRNOP00000065406		1	0
ENSRNOP00000043492		1	0
ENSRNOP00000055701		1	0
ENSRNOP00000062809		1	0
ENSRNOP00000061570		1	0
ENSRNOP00000054584		1	0
ENSRNOP00000043166		1	0
ENSRNOP00000044449		1	0
ENSRNOP00000064899		1	0
ENSRNOP00000063070	Eno4	1	0
ENSRNOP00000053537		1	0
ENSRNOP00000022610	Pnmal2	1	0
ENSRNOP00000041672		1	0
ENSRNOP00000033769		1	0
ENSRNOP00000035891		1	0
ENSRNOP00000050213	Gapdh-ps2	1	0
ENSRNOP00000064549		1	0
ENSRNOP00000040641		1	0
ENSRNOP00000042858		1	0
ENSRNOP00000044014		1	0
ENSRNOP00000064663		1	0
ENSRNOP00000039874	LOC291543	1	0
ENSRNOP00000063376	LOC688739	1	0
ENSRNOP00000067292		1	0
ENSRNOP00000041521	Cycs	1	0
ENSRNOP00000022747	Uqcr11	1	0
ENSRNOP00000065234	Rab10	1	0
ENSRNOP00000025649	Rab14	1	0
ENSRNOP00000063646	Oxct1	1	0
ENSRNOP00000050691	Acaa1b	1	0
ENSRNOP00000031191	Fdps	1	0

ENSRNOP00000059561	Acat2	1	0
ENSRNOP00000047954	Mt-cyb	1	0
ENSRNOP00000063449	Mdm2	1	0
ENSRNOP00000067118	Foxg1	1	0
ENSRNOP00000037374	Tcl1a	1	0
ENSRNOP00000051338	Map3k5	1	0
ENSRNOP00000032902	Hspb1	1	0
ENSRNOP00000027677	Gsk3a	1	0
ENSRNOP00000029993	Rps6kb2	1	0
ENSRNOP00000042383	Foxo4	1	0
ENSRNOP00000030885	Ywhaz	1	0
ENSRNOP00000061371	Inppl1	1	0
ENSRNOP00000059428	Ppp2r1b	1	0
ENSRNOP00000025851	Ikbkb	1	0
ENSRNOP00000030782	Rictor	1	0
ENSRNOP00000028260	Them4	1	0
ENSRNOP00000028143	Pten	1	0
ENSRNOP00000027478	Akt1s1	1	0
ENSRNOP00000034134	Chuk	1	0
ENSRNOP00000026210	Pik3r2	1	0
ENSRNOP00000057770	Lims2	1	0
ENSRNOP00000062647	Lims1	1	0
ENSRNOP00000027295	Ilkap	1	0
ENSRNOP00000054688	Akt3	1	0
ENSRNOP00000051863	Tgfb1i1	1	0
ENSRNOP00000039298	Snrpb	1	0
ENSRNOP00000033029	Fus	1	0
ENSRNOP00000026202	Sf3a2	1	0
ENSRNOP00000046783	Hnrnpu	1	0
ENSRNOP00000048698	Ybx1-ps3	1	0
ENSRNOP00000043202	Srsf11	1	0
ENSRNOP00000057257	Hnrnpc	1	0
ENSRNOP00000035155	Srsf7	1	0
ENSRNOP00000065463	Lsm2	1	0
ENSRNOP00000064264	Vav1	1	0
ENSRNOP00000028176	Snrnp70	1	0
ENSRNOP00000028074	Cpsf7	1	0
ENSRNOP00000061368	Dhx9	1	0
ENSRNOP00000055962	Hnrnph1	1	0
ENSRNOP00000064933	Srsf1	1	0
ENSRNOP00000032108	Hnrnpm	1	0
ENSRNOP00000046491	Hnrnpd	1	0
ENSRNOP00000026297	Nudt21	1	0
ENSRNOP00000042416	Snrpep2	1	0
ENSRNOP00000027425	Hnrnpl	1	0
ENSRNOP00000064990	Bdkrb2	1	0

ENSRNOP00000042428	Fpr3	1	0
ENSRNOP00000058977	Lpar2	1	0
ENSRNOP00000067147	Npy2r	1	0
ENSRNOP00000051290	Oprm1	1	0
ENSRNOP00000064709	Agtr2	1	0
ENSRNOP00000032501	Rxfp3	1	0
ENSRNOP00000067355	Sstr1	1	0
ENSRNOP00000057815	Pde4a	1	0
ENSRNOP00000034328	Mtnr1a	1	0
ENSRNOP00000028034	S1pr2	1	0
ENSRNOP00000032046	Gpr17	1	0
ENSRNOP00000060834	Pde10a	1	0
ENSRNOP00000047532	P2ry13	1	0
ENSRNOP00000043652	Lpar1	1	0
ENSRNOP00000028720	Plcb3	1	0
ENSRNOP00000052627	S1pr1	1	0
ENSRNOP00000028380	S1pr5	1	0
ENSRNOP00000045972	Plcb4	1	0
ENSRNOP00000043759	Drd2	1	0
ENSRNOP00000060812	Grm4	1	0
ENSRNOP00000060777	Pde7a	1	0
ENSRNOP00000047053	Oprl1	1	0
ENSRNOP00000066242	Adra2a	1	0
ENSRNOP00000066690	Gnb5	1	0
ENSRNOP00000064558	C5ar1	1	0
ENSRNOP00000066231	Sstr4	1	0
ENSRNOP00000061809	Plin1	1	0
ENSRNOP00000028997	Ube2u	1	0
ENSRNOP00000061228	LOC100911727	1	0
ENSRNOP00000051355	Dntt	1	0
ENSRNOP00000039931	Ccna1	1	0
ENSRNOP00000053270	Rad51	1	0
ENSRNOP00000063994	Chaf1a	1	0
ENSRNOP00000063831	Dnmt1	1	0
ENSRNOP00000033080	Sprtn	1	0
ENSRNOP00000032177	Cdc6	1	0
ENSRNOP00000054053	Rev3l	1	0
ENSRNOP00000060925	Apex2	1	0
ENSRNOP00000062102	Ube2v2	1	0
ENSRNOP00000062763	Kmt5a	1	0
ENSRNOP00000053707	Ung	1	0
ENSRNOP00000034638	Poln	1	0
ENSRNOP00000056107	Ercc5	1	0
ENSRNOP00000053576	LOC100362927	1	0
ENSRNOP00000065285	RGD1561853	1	0
ENSRNOP00000061834	Mlh1	1	0

ENSRNOP00000067214	Zfpl1	1	0
ENSRNOP00000036568	Rbbp4	1	0
ENSRNOP00000053086	Tyms	1	0
ENSRNOP00000058920	Pole	1	0
ENSRNOP00000062524	Mcm5	1	0
ENSRNOP00000058174	Ube2a	1	0
ENSRNOP00000064704	Ccnd3	1	0
ENSRNOP00000059094	Cdc7	1	0
ENSRNOP00000059807	Rev1	1	0
ENSRNOP00000032191	Cdk2	1	0
ENSRNOP00000055596	Wrn	1	0
ENSRNOP00000063400	Rad18	1	0
ENSRNOP00000028898	Mcm8	1	0
ENSRNOP00000034754	Cdk4	1	0
ENSRNOP00000040703	Rps29	1	0
ENSRNOP00000043270	Rps29	1	0
ENSRNOP00000044909	Rps29	1	0
ENSRNOP00000059833	Tipin	1	0
ENSRNOP00000053083	Tipinl1	1	0
ENSRNOP00000066206	Cdc45	1	0
ENSRNOP00000053964	Per1	1	0
ENSRNOP00000061074	Vta1	1	0
ENSRNOP00000063822	Calm2	1	0
ENSRNOP00000060919	Dync1i2	1	0
ENSRNOP00000066312	Dync1h1	1	0
ENSRNOP00000059841	Dnah1	1	0
ENSRNOP00000061342	Dynll1	1	0

Table 9. GO enrichment of BAT protein-protein interaction network

Pathway	Total	Expected	Hits	P.Value	FDR
Biological Process					
Chromatin assembly or disassembly	248	9.1	77	4.48E-51	3.02E-48
Nucleosome assembly	42	1.54	14	1.35E-10	4.55E-08
Developmental growth	31	1.14	12	3.84E-10	8.65E-08
Transcription, DNA_dependent	21	0.771	9	2.21E-08	3.73E-06
Sensory perception of taste	5	0.183	5	6.51E-08	8.02E-06
Regulation of transcription, DNA_dependent	434	15.9	40	7.13E-08	8.02E-06
Hemostasis	80	2.94	14	1.07E-06	0.000103
Keratinocyte differentiation	345	12.7	32	1.33E-06	0.000112
Cellular localization	12	0.44	6	1.81E-06	0.00013
Negative regulation of DNA metabolic process	25	0.917	8	1.92E-06	0.00013
Secretion by cell	20	0.734	7	4.37E-06	0.000268

N_acetylglucosamine metabolic process	14	0.514	6	5.52E-06	0.00031
Glucosamine metabolic process	70	2.57	12	7.90E-06	0.00041
Cytokine biosynthetic process	151	5.54	18	1.03E-05	0.000499
Regulation of cyclin_dependent protein kinase activity	17	0.624	6	2.07E-05	0.000931
DNA damage response, signal transduction by p53 class mediator	11	0.404	5	2.50E-05	0.00106
Heterophilic cell_cell adhesion	199	7.3	20	4.29E-05	0.0017
Anatomical structure formation involved in morphogenesis	38	1.39	8	5.72E-05	0.00214
DNA_dependent transcription, initiation	99	3.63	13	6.39E-05	0.00227
Negative regulation of MAP kinase activity	102	3.74	13	8.75E-05	0.00295
Protein complex disassembly	4	0.147	3	0.000191	0.00614
Xenobiotic metabolic process	191	7.01	18	0.000232	0.00712
Multicellular organismal development	17	0.624	5	0.000279	0.00819
Establishment of organelle localization	29	1.06	6	0.000546	0.0154
Tyrosine phosphorylation of STAT protein	41	1.5	7	0.000651	0.0176
Regulation of transcription from RNA polymerase II promoter	86	3.16	10	0.00117	0.0303
Regulation of actin filament length	35	1.28	6	0.00155	0.0387
Muscle organ development	36	1.32	6	0.0018	0.0412
Interleukin_1 secretion	36	1.32	6	0.0018	0.0412
DNA damage checkpoint	62	2.28	8	0.00183	0.0412
Molecular Function					
RNA binding	270	10.2	88	1.89E-59	6.26E-57
Steroid dehydrogenase activity	334	12.7	45	7.97E-14	1.32E-11
RNA helicase activity	49	1.86	17	1.08E-12	1.19E-10
Transferase activity, transferring acyl groups	253	9.59	35	2.52E-11	2.09E-09
Neuropeptide hormone activity	1270	48.3	92	4.53E-10	3.00E-08
DNA_directed DNA polymerase activity	26	0.986	11	9.51E-10	5.24E-08
Transcription cofactor activity	356	13.5	36	7.27E-08	3.44E-06
Cation_transporting ATPase activity	64	2.43	13	6.31E-07	2.61E-05
Antioxidant activity	72	2.73	13	2.58E-06	9.50E-05
Exopeptidase activity	103	3.91	15	7.25E-06	0.00024
DNA helicase activity	15	0.569	6	1.07E-05	0.000323
Nuclease activity	225	8.53	23	1.47E-05	0.000406
Lipase activity	69	2.62	11	5.14E-05	0.00131
Ion binding	21	0.796	6	9.59E-05	0.00227
Translation initiation factor activity	162	6.14	17	0.000138	0.00306
G_protein coupled receptor binding	53	2.01	9	0.00015	0.0031
Nucleotide binding	273	10.4	23	0.000289	0.00541
Damaged DNA binding	46	1.74	8	0.000294	0.00541

Carbon_carbon lyase activity	17	0.645	5	0.000325	0.00566
Endonuclease activity	279	10.6	23	0.000394	0.00652
Transcription corepressor activity	101	3.83	12	0.000425	0.0067
Hydrolase activity, hydrolyzing O_glycosyl compounds	92	3.49	11	0.000694	0.0102
Nucleobase_containing compound transmembrane transporter activity	291	11	23	0.00071	0.0102
Kinase activity	212	8.04	18	0.00118	0.0163
Protein binding, bridging	62	2.35	8	0.00225	0.0298
Organic anion transmembrane transporter activity	65	2.46	8	0.00304	0.0387
Ubiquitin binding	17	0.645	4	0.00328	0.0402
Hydrolase activity, acting on acid anhydrides	512	19.4	32	0.00376	0.0438
Low_density lipoprotein particle binding	9	0.341	3	0.00383	0.0438
Regulation of DNA_dependent transcription, elongation	41	1.55	6	0.00419	0.0462
Cellular component					
Nucleolus	1280	38.6	113	1.77E-26	3.11E-24
Microtubule organizing center	109	3.3	29	9.09E-20	8.00E-18
Mitochondrial envelope	235	7.11	40	3.74E-19	2.20E-17
Centrosome	1180	35.7	92	1.32E-17	5.83E-16
Vesicle membrane	1670	50.5	102	1.65E-12	5.81E-11
Nucleus	3830	116	179	3.00E-11	8.79E-10
Nucleoplasm	1450	44	89	6.19E-11	1.56E-09
Spindle	13	0.394	8	7.48E-10	1.65E-08
Integral to organelle membrane	411	12.4	37	3.23E-09	6.32E-08
Chromosome	4070	123	179	5.85E-09	1.03E-07
Nuclear lumen	71	2.15	14	2.21E-08	3.54E-07
Cell_cell junction	307	9.29	29	6.05E-08	8.61E-07
Endomembrane system	14	0.424	7	6.36E-08	8.61E-07
Golgi stack	376	11.4	32	1.43E-07	1.80E-06
Eukaryotic translation initiation factor 3 complex	191	5.78	20	1.43E-06	1.67E-05
Clathrin_coated vesicle	85	2.57	13	1.54E-06	1.69E-05
Pore complex	40	1.21	9	2.34E-06	2.42E-05
Vesicle coat	292	8.84	25	3.05E-06	2.98E-05
Cell surface	128	3.87	13	0.000135	0.00123
Mitochondrial respiratory chain	112	3.39	12	0.000146	0.00123
Membrane coat	222	6.72	18	0.000147	0.00123
Mitochondrial matrix	18	0.545	5	0.000154	0.00123
Transport vesicle	96	2.91	10	0.000646	0.00494
Cell leading edge	260	7.87	18	0.000982	0.00698
Extracellular matrix	68	2.06	8	0.000998	0.00698
Apical junction complex	467	14.1	27	0.00103	0.00698
Golgi_associated vesicle	90	2.72	9	0.00159	0.0104
U12_type spliceosomal complex	612	18.5	32	0.00192	0.0121

Mitochondrion	89	2.69	8	0.00551	0.0334
Mitochondrial inner membrane	39	1.18	5	0.00613	0.036
Kinetochore	73	2.21	7	0.00649	0.0369
Anchored to membrane	112	3.39	9	0.00693	0.0381
Endosome	96	2.91	8	0.00862	0.0456
Cortical cytoskeleton	137	4.15	10	0.00881	0.0456
Sarcomere	43	1.3	5	0.00929	0.0467

Table 10. List of nodes in protein-protein interaction network in WAT with exercise training

Id	Label	Degree	Betweenness
ENSRNOP00000013462	Rpl4	403	77156.57
ENSRNOP00000019247	Rpl27a	368	48351.63
ENSRNOP00000014849	Rpl29	278	19304.72
ENSRNOP00000060568	Rps28	249	20954.5
ENSRNOP00000026462	Psmb10	60	42504.83
ENSRNOP00000017421	Magoh	45	29814
ENSRNOP00000026279	Psme2	33	17171.42
ENSRNOP00000059076	Dctn1	24	10456.5
ENSRNOP00000020748	Rab8a	14	18059.5
ENSRNOP00000032902	Hspb1	12	32101.83
ENSRNOP00000023256	Slc2a4	9	22219.5
ENSRNOP00000027073	Uba52	6	39925.52
ENSRNOP00000041134	Usp7	6	2935
ENSRNOP00000059012	Srsf2	5	2350
ENSRNOP00000004867	Sumo2	4	1764
ENSRNOP00000000603	Rpl10a	4	10.4
ENSRNOP00000001265	Rpl21	4	10.4
ENSRNOP00000002194	Rpl24	4	10.4
ENSRNOP00000004303	RGD1559951	4	10.4
ENSRNOP00000005471	Rpl23	4	10.4
ENSRNOP00000005872	Rps27a	4	10.4
ENSRNOP00000006359	Rpl19	4	10.4
ENSRNOP00000006754	Rpl7a	4	10.4
ENSRNOP00000007683		4	10.4
ENSRNOP00000009988	RGD1560831	4	10.4
ENSRNOP00000010383	LOC100911372	4	10.4
ENSRNOP00000010759	Rpl15	4	10.4
ENSRNOP00000011314	Rps20	4	10.4
ENSRNOP00000011333	Rps7	4	10.4
ENSRNOP00000013868	LOC100361180	4	10.4
ENSRNOP00000015893		4	10.4
ENSRNOP00000016329	Rps3a	4	10.4
ENSRNOP00000017230	RGD1565317	4	10.4

ENSRNOP00000018820	Rplp1	4	10.4
ENSRNOP00000020635	LOC100359922	4	10.4
ENSRNOP00000021161		4	10.4
ENSRNOP00000022184	Rps12	4	10.4
ENSRNOP00000022348	Rps23	4	10.4
ENSRNOP00000023368	Rpl38	4	10.4
ENSRNOP00000023935	Rps3	4	10.4
ENSRNOP00000024678	Rps15a	4	10.4
ENSRNOP00000025217	Rpl17	4	10.4
ENSRNOP00000025888	Rps17	4	10.4
ENSRNOP00000026576	Rps16	4	10.4
ENSRNOP00000027086	Cnbd2	4	10.4
ENSRNOP00000027226	LOC100360573	4	10.4
ENSRNOP00000028060	Rpl27	4	10.4
ENSRNOP00000028481	LOC100360647	4	10.4
ENSRNOP00000028555	Rpl18	4	10.4
ENSRNOP00000031121	LOC100362366	4	10.4
ENSRNOP00000032635	LOC100360449	4	10.4
ENSRNOP00000033369		4	10.4
ENSRNOP00000034364	Rpl17	4	10.4
ENSRNOP00000034657	LOC687780	4	10.4
ENSRNOP00000034767	RGD1359290	4	10.4
ENSRNOP00000036391	Rpl23a	4	10.4
ENSRNOP00000036514	Rpl5	4	10.4
ENSRNOP00000037110	Rpl11	4	10.4
ENSRNOP00000038065	Rpl6	4	10.4
ENSRNOP00000039111		4	10.4
ENSRNOP00000039179		4	10.4
ENSRNOP00000039287	LOC102550668	4	10.4
ENSRNOP00000039774	RGD1560017	4	10.4
ENSRNOP00000039786		4	10.4
ENSRNOP00000040548	RGD1563570	4	10.4
ENSRNOP00000040955	LOC103691423	4	10.4
ENSRNOP00000040966	Rpl10l	4	10.4
ENSRNOP00000041191		4	10.4
ENSRNOP00000041199		4	10.4
ENSRNOP00000041263		4	10.4
ENSRNOP00000041435		4	10.4
ENSRNOP00000041458	RGD1562381	4	10.4
ENSRNOP00000041530		4	10.4
ENSRNOP00000041774	RGD1564730	4	10.4
ENSRNOP00000041817	Rpl9	4	10.4
ENSRNOP00000041920	RGD1559955	4	10.4
ENSRNOP00000041966	Rpl21	4	10.4
ENSRNOP00000042022	LOC690468	4	10.4
ENSRNOP00000042031	LOC100360647	4	10.4

ENSRNOP00000042242	LOC100909878	4	10.4
ENSRNOP00000042277		4	10.4
ENSRNOP00000042286	LOC680512	4	10.4
ENSRNOP00000042288	LOC682793	4	10.4
ENSRNOP00000042454		4	10.4
ENSRNOP00000042560		4	10.4
ENSRNOP00000042567		4	10.4
ENSRNOP00000042941	LOC500148	4	10.4
ENSRNOP00000044063	LOC686066	4	10.4
ENSRNOP00000044605	LOC100361060	4	10.4
ENSRNOP00000045195	LOC100360439	4	10.4
ENSRNOP00000045213	RGD1561636	4	10.4
ENSRNOP00000045335		4	10.4
ENSRNOP00000045390	RGD1562265	4	10.4
ENSRNOP00000045739		4	10.4
ENSRNOP00000045912		4	10.4
ENSRNOP00000046070		4	10.4
ENSRNOP00000046409		4	10.4
ENSRNOP00000046578		4	10.4
ENSRNOP00000046600	LOC306079	4	10.4
ENSRNOP00000046669		4	10.4
ENSRNOP00000046737	LOC691716	4	10.4
ENSRNOP00000047281	Rps27a-ps6	4	10.4
ENSRNOP00000047511		4	10.4
ENSRNOP00000047513	Rpl37a	4	10.4
ENSRNOP00000048019	RGD1563145	4	10.4
ENSRNOP00000048495		4	10.4
ENSRNOP00000048620	RGD1561453	4	10.4
ENSRNOP00000048664	Rps27a	4	10.4
ENSRNOP00000048808	Rpl21	4	10.4
ENSRNOP00000048903	LOC100363469	4	10.4
ENSRNOP00000049028	LOC680353	4	10.4
ENSRNOP00000049286	Rps15al2	4	10.4
ENSRNOP00000049416	RGD1563835	4	10.4
ENSRNOP00000049709		4	10.4
ENSRNOP00000049710		4	10.4
ENSRNOP00000049831		4	10.4
ENSRNOP00000050047		4	10.4
ENSRNOP00000050202	LOC682793	4	10.4
ENSRNOP00000050353	LOC682793	4	10.4
ENSRNOP00000050533	RGD1563705	4	10.4
ENSRNOP00000050941	Rps24	4	10.4
ENSRNOP00000051016	LOC100364191	4	10.4
ENSRNOP00000051135	Rpl6-ps1	4	10.4
ENSRNOP00000051203		4	10.4
ENSRNOP00000051312	Rpl21	4	10.4

ENSRNOP00000051318	LOC100359563	4	10.4
ENSRNOP00000051332		4	10.4
ENSRNOP00000051743		4	10.4
ENSRNOP00000053082	Rpl5l1	4	10.4
ENSRNOP00000053160		4	10.4
ENSRNOP00000053991		4	10.4
ENSRNOP00000054497	LOC100912027	4	10.4
ENSRNOP00000054699	RGD1560069	4	10.4
ENSRNOP00000055334	RGD1565767	4	10.4
ENSRNOP00000055393		4	10.4
ENSRNOP00000055671		4	10.4
ENSRNOP00000058757		4	10.4
ENSRNOP00000058934	Rpl36	4	10.4
ENSRNOP00000059382	Rps24	4	10.4
ENSRNOP00000060476	LOC680579	4	10.4
ENSRNOP00000065066	LOC100365839	4	10.4
ENSRNOP00000066016	LOC100912027	4	10.4
ENSRNOP00000064959	LOC103692519	4	10.4
ENSRNOP00000065901		4	10.4
ENSRNOP00000067446	LOC100909911	4	10.4
ENSRNOP00000061370		4	10.4
ENSRNOP00000067411		4	10.4
ENSRNOP00000067793		4	10.4
ENSRNOP00000066511		4	10.4
ENSRNOP00000064524	RGD1563124	4	10.4
ENSRNOP00000066077	LOC100362684	4	10.4
ENSRNOP00000065886	LOC100359951	4	10.4
ENSRNOP00000063201	RGD1561102	4	10.4
ENSRNOP00000065423		4	10.4
ENSRNOP00000064082	LOC100360491	4	10.4
ENSRNOP00000060629	RGD1561870	4	10.4
ENSRNOP00000064320	LOC100365810	4	10.4
ENSRNOP00000066866	LOC103690796	4	10.4
ENSRNOP00000062764		4	10.4
ENSRNOP00000064745		4	10.4
ENSRNOP00000061747	Rpl14	4	10.4
ENSRNOP00000064822	RGD1565048	4	10.4
ENSRNOP00000064270	RGD1561137	4	10.4
ENSRNOP00000066050	LOC100364116	4	10.4
ENSRNOP00000063355	LOC100361259	4	10.4
ENSRNOP00000067572	Rps6	4	10.4
ENSRNOP00000066863	RGD1560821	4	10.4
ENSRNOP00000064461		4	10.4
ENSRNOP00000065877	LOC102548369	4	10.4
ENSRNOP00000067354	LOC100361079	4	10.4
ENSRNOP00000066750	LOC100909911	4	10.4

ENSRNOP00000065827		4	10.4
ENSRNOP00000066260	LOC103692519	4	10.4
ENSRNOP00000066592		4	10.4
ENSRNOP00000063142		4	10.4
ENSRNOP00000052049	Eftud2	3	28944
ENSRNOP00000013997	Psmc5	3	15870
ENSRNOP00000025819	Psmc4	3	15870
ENSRNOP00000047840	Tp53	3	4668
ENSRNOP00000004278	Rps4x	3	8.54
ENSRNOP00000004583		3	8.54
ENSRNOP00000006662	RGD1566369	3	8.54
ENSRNOP00000007194		3	8.54
ENSRNOP00000017602	LOC100359763	3	8.54
ENSRNOP00000017738		3	8.54
ENSRNOP00000019508	Rps2	3	8.54
ENSRNOP00000022897	Rps27	3	8.54
ENSRNOP00000026528	Rps5	3	8.54
ENSRNOP00000027246	LOC100910336	3	8.54
ENSRNOP00000033144	Rps25	3	8.54
ENSRNOP00000033162	LOC500594	3	8.54
ENSRNOP00000036343	LOC688473	3	8.54
ENSRNOP00000036690	LOC684988	3	8.54
ENSRNOP00000036943		3	8.54
ENSRNOP00000039003		3	8.54
ENSRNOP00000039845	Rps19l1	3	8.54
ENSRNOP00000040306	RGD1563613	3	8.54
ENSRNOP00000041853	LOC297756	3	8.54
ENSRNOP00000042092	Rsl1d1	3	8.54
ENSRNOP00000042902	LOC100360843	3	8.54
ENSRNOP00000043543	LOC103690015	3	8.54
ENSRNOP00000043988	Rps4x-ps9	3	8.54
ENSRNOP00000044301	LOC688899	3	8.54
ENSRNOP00000044563	LOC680646	3	8.54
ENSRNOP00000045516	Wdr31	3	8.54
ENSRNOP00000047391	RGD1564597	3	8.54
ENSRNOP00000047760		3	8.54
ENSRNOP00000049546	Rps4y2	3	8.54
ENSRNOP00000052873	LOC100911847	3	8.54
ENSRNOP00000055288	RGD1562399	3	8.54
ENSRNOP00000056260	LOC100911847	3	8.54
ENSRNOP00000056750	LOC100364509	3	8.54
ENSRNOP00000057658	Rps2-ps6	3	8.54
ENSRNOP00000065281	LOC685085	3	8.54
ENSRNOP00000066792	LOC100364509	3	8.54
ENSRNOP00000065999	LOC100911337	3	8.54
ENSRNOP00000061442	LOC100362339	3	8.54

ENSRNOP00000067129	Rps27l	3	8.54
ENSRNOP00000064853	LOC100911337	3	8.54
ENSRNOP00000066362	LOC100362987	3	8.54
ENSRNOP00000067470	LOC683961	3	8.54
ENSRNOP00000066548		3	8.54
ENSRNOP00000065487	LOC100363452	3	8.54
ENSRNOP00000065173		3	8.54
ENSRNOP00000063451	RGD1559724	3	8.54
ENSRNOP00000066808	LOC100910336	3	8.54
ENSRNOP00000025224	Rpsa	3	6.31
ENSRNOP00000044806	RGD1565117	3	6.31
ENSRNOP00000048116	LOC100361854	3	6.31
ENSRNOP00000027780	Rps27a-ps12	3	5.96
ENSRNOP00000035156	Rps15	3	5.96
ENSRNOP00000048979	Rps27a-ps5	3	5.96
ENSRNOP00000062631	Rps15-ps2	3	5.96
ENSRNOP00000001518	Rplp0	3	0
ENSRNOP00000002177		3	0
ENSRNOP00000004213		3	0
ENSRNOP00000005511		3	0
ENSRNOP00000005588	Rpl26	3	0
ENSRNOP00000009046	Rpl34	3	0
ENSRNOP00000009431	Rpl7	3	0
ENSRNOP00000011244	LOC688684	3	0
ENSRNOP00000012255	LOC690096	3	0
ENSRNOP00000014493	Rpl32	3	0
ENSRNOP00000014905	LOC100360057	3	0
ENSRNOP00000015408	RGD1565894	3	0
ENSRNOP00000015756	Rpl22l1	3	0
ENSRNOP00000019162	Rpl35	3	0
ENSRNOP00000044553	LOC103694169	3	0
ENSRNOP00000038214	LOC100911575	3	0
ENSRNOP00000048252	LOC100911426	3	0
ENSRNOP00000059662	LOC103690821	3	0
ENSRNOP00000045098	LOC103694169	3	0
ENSRNOP00000061874		3	0
ENSRNOP00000039155	Rpl37	3	0
ENSRNOP00000043092	RGD1561317	3	0
ENSRNOP00000054740	LOC100362751	3	0
ENSRNOP00000050175		3	0
ENSRNOP00000067881	RGD1564378	3	0
ENSRNOP00000067080	LOC100360117	3	0
ENSRNOP00000044275	LOC100910017	3	0
ENSRNOP00000055790	LOC103692785	3	0
ENSRNOP00000050700	LOC690335	3	0
ENSRNOP00000041638	Rpl32	3	0

ENSRNOP00000054398	LOC100362027	3	0
ENSRNOP00000048999	Rpl31l4	3	0
ENSRNOP00000049665	LOC103690821	3	0
ENSRNOP00000049713	LOC103693375	3	0
ENSRNOP00000051188	Rpl35al1	3	0
ENSRNOP00000065371	LOC100911426	3	0
ENSRNOP00000058614	RGD1564095	3	0
ENSRNOP00000042633		3	0
ENSRNOP00000059772	RGD1565566	3	0
ENSRNOP00000041209	Rpl35a	3	0
ENSRNOP00000043004	RGD1564606	3	0
ENSRNOP00000039099	Rpl35a	3	0
ENSRNOP00000053986	RGD1565183	3	0
ENSRNOP00000037396	LOC100359986	3	0
ENSRNOP00000046553	LOC100360117	3	0
ENSRNOP00000046515		3	0
ENSRNOP00000064197	RGD1564883	3	0
ENSRNOP00000047749	LOC680441	3	0
ENSRNOP00000031078	Rpl31	3	0
ENSRNOP00000049652	LOC689899	3	0
ENSRNOP00000065065	Rpl26-ps3	3	0
ENSRNOP00000021725	Rpl12	3	0
ENSRNOP00000041329	LOC103693375	3	0
ENSRNOP00000064566	LOC100910370	3	0
ENSRNOP00000067887	LOC100910721	3	0
ENSRNOP00000025421	Rpl18a	3	0
ENSRNOP00000057262	LOC690384	3	0
ENSRNOP00000046301	RGD1564839	3	0
ENSRNOP00000054048	Rpl36al	3	0
ENSRNOP00000048311	RGD1563157	3	0
ENSRNOP00000042127	RGD1566373	3	0
ENSRNOP00000051134		3	0
ENSRNOP00000041462	LOC102555453	3	0
ENSRNOP00000053863	Rplp2	3	0
ENSRNOP00000049014	LOC100912182	3	0
ENSRNOP00000055726	Rpl28	3	0
ENSRNOP00000057758	Rpl26-ps2	3	0
ENSRNOP00000044116	RGD1561310	3	0
ENSRNOP00000048003	LOC100912182	3	0
ENSRNOP00000054703	Rpl34-ps1	3	0
ENSRNOP00000044111	RGD1565170	3	0
ENSRNOP00000040232		3	0
ENSRNOP00000049054	Rpl35al1	3	0
ENSRNOP00000045849	RGD1561195	3	0
ENSRNOP00000042068		3	0
ENSRNOP00000040295	Rpl39l	3	0

ENSRNOP00000045458	Rpl26-ps1	3	0
ENSRNOP00000040611	Rpl35al1	3	0
ENSRNOP00000047759		3	0
ENSRNOP00000030437	RGD1563956	3	0
ENSRNOP00000047328	RGD1561333	3	0
ENSRNOP00000050328	RGD1562055	3	0
ENSRNOP00000047010		3	0
ENSRNOP00000042920	Rpl22l2	3	0
ENSRNOP00000049205	LOC100360841	3	0
ENSRNOP00000046953	LOC102554602	3	0
ENSRNOP00000049635	LOC102550734	3	0
ENSRNOP00000027976	Rpl13a	3	0
ENSRNOP00000056331	Rpl37-ps1	3	0
ENSRNOP00000042929	LOC688981	3	0
ENSRNOP00000046487	RGD1562755	3	0
ENSRNOP00000046281	LOC686074	3	0
ENSRNOP00000060662	Rpl3	3	0
ENSRNOP00000051427	RGD1563958	3	0
ENSRNOP00000051482	Rpl31l3	3	0
ENSRNOP00000066420	LOC100361143	3	0
ENSRNOP00000067596	Rpl30l1	3	0
ENSRNOP00000049666		3	0
ENSRNOP00000040073	LOC103691563	3	0
ENSRNOP00000041625	LOC100362751	3	0
ENSRNOP00000051114		3	0
ENSRNOP00000054474	LOC100360654	3	0
ENSRNOP00000025649	Rab14	2	18381
ENSRNOP00000025303	Akt2	2	11234
ENSRNOP00000038369	Akt1	2	11234
ENSRNOP00000018455	Sec61a1	2	7772.48
ENSRNOP00000036212	Sec61a2	2	7772.48
ENSRNOP00000064933	Srsf1	2	2925
ENSRNOP00000063941	Ranbp2	2	2344
ENSRNOP00000004797	Tuba4a	2	1792.33
ENSRNOP00000013863	Tubb4b	2	1792.33
ENSRNOP00000026792	Actr1a	2	1792.33
ENSRNOP00000027370	Tubg1	2	1792.33
ENSRNOP00000065633	Tubb4a	2	1792.33
ENSRNOP00000066312	Dync1h1	2	1792.33
ENSRNOP00000001415	Elavl1	2	589
ENSRNOP00000030371	Rps18	2	4.44
ENSRNOP00000039429		2	4.44
ENSRNOP00000040056	RGD1561919	2	4.44
ENSRNOP00000040282	RGD1565912	2	4.44
ENSRNOP00000042800		2	4.44
ENSRNOP00000042935	Rps21-ps1	2	4.44

ENSRNOP00000045940		2	4.44
ENSRNOP00000045954		2	4.44
ENSRNOP00000046036		2	4.44
ENSRNOP00000046090	LOC100362298	2	4.44
ENSRNOP00000046427		2	4.44
ENSRNOP00000047355		2	4.44
ENSRNOP00000047371	Rps18l1	2	4.44
ENSRNOP00000047767		2	4.44
ENSRNOP00000047911	RGD1563352	2	4.44
ENSRNOP00000048713		2	4.44
ENSRNOP00000049619		2	4.44
ENSRNOP00000049626		2	4.44
ENSRNOP00000056140		2	4.44
ENSRNOP00000065327		2	4.44
ENSRNOP00000063940		2	4.44
ENSRNOP00000067239		2	4.44
ENSRNOP00000064678	LOC100912024	2	4.44
ENSRNOP00000061250	Rps11	2	4.44
ENSRNOP00000063128	Rpl7a	2	4.44
ENSRNOP00000000528	Psmb8	2	0
ENSRNOP00000000532	Psmb9	2	0
ENSRNOP00000000628	Cdkn1a	2	0
ENSRNOP00000002037	Psmb1	2	0
ENSRNOP00000002358	Psmd2	2	0
ENSRNOP00000002834	Mrpl1	2	0
ENSRNOP00000004114	LOC690271	2	0
ENSRNOP00000005089	Mrps7	2	0
ENSRNOP00000005815	Mrpl13	2	0
ENSRNOP00000009249	Psmd6	2	0
ENSRNOP00000009649	Psmc6	2	0
ENSRNOP00000009666	Psma6	2	0
ENSRNOP00000010753	Psma3	2	0
ENSRNOP00000015278	LOC680700	2	0
ENSRNOP00000015618	Psmb2	2	0
ENSRNOP00000015747		2	0
ENSRNOP00000015757	Psmc3	2	0
ENSRNOP00000015946	Psma1	2	0
ENSRNOP00000016450	Psmc2	2	0
ENSRNOP00000016876	Psmb7	2	0
ENSRNOP00000017280	Mrpl3	2	0
ENSRNOP00000018005	Psmb5	2	0
ENSRNOP00000018173	Psma4	2	0
ENSRNOP00000019104	Psmd7	2	0
ENSRNOP00000019781	Smurf2	2	0
ENSRNOP00000024306	Psmd1	2	0
ENSRNOP00000025887	Psme1	2	0

ENSRNOP00000046157	RGD1564469	2	0
ENSRNOP00000027029	Mrps12	2	0
ENSRNOP00000031049	RGD1563300	2	0
ENSRNOP00000041612		2	0
ENSRNOP00000021899	Mrps9	2	0
ENSRNOP00000024326	Mrto4	2	0
ENSRNOP00000051848	Mrpl12	2	0
ENSRNOP00000044874	RGD1559877	2	0
ENSRNOP00000064904		2	0
ENSRNOP00000030289		2	0
ENSRNOP00000044949	RGD1560633	2	0
ENSRNOP00000065157		2	0
ENSRNOP00000064782		2	0
ENSRNOP00000023456	Imp3	2	0
ENSRNOP00000020451	Mrps5	2	0
ENSRNOP00000041821	Eef2	2	0
ENSRNOP00000055298		2	0
ENSRNOP00000036682	Mrpl1	2	0
ENSRNOP00000039797	LOC103690888	2	0
ENSRNOP00000048422	RGD1562402	2	0
ENSRNOP00000045798	LOC367195	2	0
ENSRNOP00000044837		2	0
ENSRNOP00000043087	Gfm2	2	0
ENSRNOP00000049519	Efl1	2	0
ENSRNOP00000019660	Rpl3l	2	0
ENSRNOP00000048289		2	0
ENSRNOP00000034042	mrpl24	2	0
ENSRNOP00000027091	mrpl11	2	0
ENSRNOP00000045344	RGD1559972	2	0
ENSRNOP00000028517	Mrpl16	2	0
ENSRNOP00000048847		2	0
ENSRNOP00000041744	RGD1564138	2	0
ENSRNOP00000048624	RGD1565415	2	0
ENSRNOP00000021625	Npsr1	2	0
ENSRNOP00000042164	LOC100359671	2	0
ENSRNOP00000058859		2	0
ENSRNOP00000045007	Mrpl17	2	0
ENSRNOP00000048658	LOC102554992	2	0
ENSRNOP00000047999		2	0
ENSRNOP00000046067	Mrps10	2	0
ENSRNOP00000056689		2	0
ENSRNOP00000025007	Mrps11	2	0
ENSRNOP00000040081	Gfm1	2	0
ENSRNOP00000061911		2	0
ENSRNOP00000063004		2	0
ENSRNOP00000024380	Mrpl2	2	0

ENSRNOP00000021803	Rpl7l1	2	0
ENSRNOP00000029336	Mrpl22	2	0
ENSRNOP00000067306		2	0
ENSRNOP00000051317		2	0
ENSRNOP00000031927	Smurf1	2	0
ENSRNOP00000050173	Cdkn1b	2	0
ENSRNOP00000026928	Psma5	2	0
ENSRNOP00000042447	Psma8	2	0
ENSRNOP00000028484	Psmb4	2	0
ENSRNOP00000026507	Psmb6	2	0
ENSRNOP00000028589	Psmd4	2	0
ENSRNOP00000062146	Psmd11	2	0
ENSRNOP00000000529	Tap1	1	0
ENSRNOP00000000559	Daxx	1	0
ENSRNOP00000000612	Srpk1	1	0
ENSRNOP00000000627	Srsf3	1	0
ENSRNOP00000000750	Ube2d1	1	0
ENSRNOP00000000783	Cdk1	1	0
ENSRNOP00000001115	Ddx39b	1	0
ENSRNOP00000001154	Rbmx	1	0
ENSRNOP00000001402	Snrnp35	1	0
ENSRNOP00000001539	Srsf9	1	0
ENSRNOP00000001685	Clip1	1	0
ENSRNOP00000001817	Mapkapk5	1	0
ENSRNOP00000001954	Ywhag	1	0
ENSRNOP00000003060	Hspbap1	1	0
ENSRNOP00000003696	Pafah1b1	1	0
ENSRNOP00000004283	Psmd12	1	0
ENSRNOP00000004947	Mrpl27	1	0
ENSRNOP00000005016	Prpf8	1	0
ENSRNOP00000005267	Ocrl	1	0
ENSRNOP00000005329	Psmc1	1	0
ENSRNOP00000005577	Rps29	1	0
ENSRNOP00000005832	Klhl12	1	0
ENSRNOP00000006148	Traf6	1	0
ENSRNOP00000006953	Dync2li1	1	0
ENSRNOP00000007100	Ywhae	1	0
ENSRNOP00000007258	Rab3ip	1	0
ENSRNOP00000007583	Srsf5	1	0
ENSRNOP00000007620	Cul1	1	0
ENSRNOP00000007676	Skp1	1	0
ENSRNOP00000007963	Cdc27	1	0
ENSRNOP00000008120	Dctn2	1	0
ENSRNOP00000008355	Sf3a1	1	0
ENSRNOP00000008427	Srsf6	1	0
ENSRNOP00000008492	Aurkb	1	0

ENSRNOP00000011619	Mrpl15	1	0
ENSRNOP00000011653	Ube2e1	1	0
ENSRNOP00000012279	Dynll2	1	0
ENSRNOP00000012984	Mdm4	1	0
ENSRNOP00000013184	Dync1i1	1	0
ENSRNOP00000013204	Casc3	1	0
ENSRNOP00000013301	Srsf4	1	0
ENSRNOP00000015152	Hnrnpa2b1	1	0
ENSRNOP00000015518	Hnrnph2	1	0
ENSRNOP00000015813	Tnks	1	0
ENSRNOP00000016220	Mapre1	1	0
ENSRNOP00000016946	Plk4	1	0
ENSRNOP00000017353	Ehd2	1	0
ENSRNOP00000017718	LOC100912445	1	0
ENSRNOP00000018278	Kif26a	1	0
ENSRNOP00000019561	Dctn3	1	0
ENSRNOP00000019642	Psmd13	1	0
ENSRNOP00000020065	Mapkapk3	1	0
ENSRNOP00000020323	Ube2c	1	0
ENSRNOP00000021528	Cul3	1	0
ENSRNOP00000022779	Actr1b	1	0
ENSRNOP00000023342	Ide	1	0
ENSRNOP00000025433	Psmd5	1	0
ENSRNOP00000028176	Snrnp70	1	0
ENSRNOP00000029646	Dync1li2	1	0
ENSRNOP00000029790	Eif3el1	1	0
ENSRNOP00000032361	Eif3d	1	0
ENSRNOP00000038586	Klhdc10	1	0
ENSRNOP00000040703	Rps29	1	0
ENSRNOP00000043252	Dync2h1	1	0
ENSRNOP00000043254	Eif4h	1	0
ENSRNOP00000043270	Rps29	1	0
ENSRNOP00000044909	Rps29	1	0
ENSRNOP00000054753	Disc1	1	0
ENSRNOP00000057188	Eif3b	1	0
ENSRNOP00000058234	Clasp1	1	0
ENSRNOP00000053643	Chek2	1	0
ENSRNOP00000050029	Rangap1	1	0
ENSRNOP00000024406	Ube2i	1	0
ENSRNOP00000020402	Sae1	1	0
ENSRNOP00000013548	Mrps2	1	0
ENSRNOP00000066181	Naca	1	0
ENSRNOP00000035155	Srsf7	1	0
ENSRNOP00000039298	Snrpb	1	0
ENSRNOP00000019529	Hnrnpf	1	0
ENSRNOP00000057257	LOC100911576	1	0

ENSRNOP00000052955	Srrm1	1	0
ENSRNOP00000026033	Nxf1	1	0
ENSRNOP00000051838	Alyref	1	0
ENSRNOP00000042416	Snrpep2	1	0
ENSRNOP00000065463	Lsm2	1	0
ENSRNOP00000048598	Snrnp200	1	0
ENSRNOP00000061368	Dhx9	1	0
ENSRNOP00000060194	Upf3a	1	0
ENSRNOP00000052160	Hnrnpa1	1	0
ENSRNOP00000021221	Snrpd2	1	0
ENSRNOP00000066302	Eif4a3	1	0
ENSRNOP00000019126	Sf3b1	1	0
ENSRNOP00000055962	Hnrnph1	1	0
ENSRNOP00000018646	Snrpd1	1	0
ENSRNOP00000023854	Sf3b3	1	0
ENSRNOP00000046491	Hnrnpd	1	0
ENSRNOP00000028807	Rbm8a	1	0
ENSRNOP00000025980	Hnrnpk	1	0
ENSRNOP00000027425	Hnrnpl	1	0
ENSRNOP00000058923	Cdc40	1	0
ENSRNOP00000032108	Hnrnpm	1	0
ENSRNOP00000019810	Dhx38	1	0
ENSRNOP00000029696	Upf3b	1	0
ENSRNOP00000038996	LOC688526	1	0
ENSRNOP00000061492	Polr2a	1	0
ENSRNOP00000024529	Rbm5	1	0
ENSRNOP00000045893	Mrpl4	1	0
ENSRNOP00000021837	Ckap5	1	0
ENSRNOP00000045795	Optn	1	0
ENSRNOP00000033018	Tbc1d1	1	0
ENSRNOP00000065234	Rab10	1	0
ENSRNOP00000040878	Gapdh	1	0
ENSRNOP00000026224	Stx4	1	0
ENSRNOP00000039818	RGD1562758	1	0
ENSRNOP00000054528	Psmd9	1	0
ENSRNOP00000032191	Cdk2	1	0
ENSRNOP00000065348	Psmb11	1	0
ENSRNOP00000037928	Psmd3	1	0
ENSRNOP00000066229		1	0
ENSRNOP00000051977	Aurka	1	0
ENSRNOP00000066950	Psma2	1	0
ENSRNOP00000055036	RGD1564425	1	0
ENSRNOP00000032953	RGD1562029	1	0
ENSRNOP00000051863	Tgfb1i1	1	0
ENSRNOP00000057786	Mapkapk2	1	0
ENSRNOP00000063449	Mdm2	1	0

ENSRNOP00000063831	Dnmt1	1	0
ENSRNOP00000067005	U2af1	1	0
ENSRNOP00000060919	Dync1i2	1	0
ENSRNOP00000059841	Dnah1	1	0
ENSRNOP00000061342	Dynll1	1	0
ENSRNOP00000061642	Rps10	1	0

Table 11. GO enrichment of WAT protein-protein interaction network

Pathway	Total	Expected	Hits	P.Value	FDR
Biological Process					
Chromatin assembly or disassembly	248	2.85	74	5.83E-91	3.93E-88
Sensory perception of taste	5	0.0575	5	1.87E-10	6.31E-08
Ras protein signal transduction	63	0.725	10	2.21E-09	4.97E-07
Positive regulation of DNA metabolic process	90	1.04	11	5.94E-09	1.00E-06
Regulation of organelle organization	51	0.587	6	2.44E-05	0.00329
Chromatin remodeling	38	0.437	5	6.91E-05	0.00778
Molecular Function					
RNA binding	270	3.65	87	1.53E-104	5.06E-102
Transcription cofactor activity	356	4.81	33	7.17E-19	1.19E-16
Nucleotide binding	273	3.69	23	1.82E-12	2.01E-10
Transcription corepressor activity	101	1.36	14	6.98E-11	5.78E-09
RNA helicase activity	49	0.662	5	0.000499	0.033
Cellular Component					
Microtubule organizing center	109	1.03	26	1.02E-29	1.80E-27
Proteasome complex	44	0.416	13	1.12E-16	9.81E-15
Endomembrane system	14	0.132	7	1.89E-11	1.11E-09
Clathrin_coated vesicle	85	0.803	10	7.09E-09	3.12E-07
Vesicle membrane	1670	15.8	39	5.26E-08	1.85E-06
Mitochondrial matrix	18	0.17	5	5.46E-07	1.60E-05
Nucleus	3830	36.2	63	7.37E-07	1.85E-05
Golgi stack	376	3.55	15	2.74E-06	6.04E-05
Transcription factor TFIID complex	62	0.586	6	2.55E-05	0.000499
U12_type spliceosomal complex	612	5.78	17	6.63E-05	0.00117
Apical plasma membrane	122	1.15	7	0.000158	0.00252
Nucleoplasm	1450	13.7	26	0.00107	0.0157

Synapse	23	0.217	3	0.00127	0.0173
Adherens junction	91	0.86	5	0.00171	0.0214
Nucleolus	1280	12.1	23	0.00192	0.0226
Kinesin complex	29	0.274	3	0.00252	0.0278

3. Supplementary data for Chapter 4

Table 1. Differentially regulated proteins in BAT with SHT and YM-178

GeneID	Gene name	logfc	adjpv
SHT			
80754	Rabep2	3.69	6.35E-05
114122	Vcan	2.74	0.000269
292073	Galns	-2.75	0.00027
64012	Rad50	1.50	0.000288
171139	Timm9	-1.94	0.00037
295088	Gmps	0.67	0.000396
81716	Ggcx	1.44	0.000639
25622	Ptpn11	-2.47	0.000975
289590	Ociad1	-1.41	0.000988
29384	H2afy	-1.15	0.001077
302669	Ca5b	1.18	0.001237
499991	Steap4	-3.88	0.00228
315265	Twf1	-1.54	0.00248
25283	Gclc	2.57	0.002571
84474	Ddx1	2.23	0.00326
94342	Bag6	-1.26	0.0036
89827	Ddx39a	1.26	0.00397
64679	Tgm4	0.95	0.00616
64517	Thop1	1.25	0.006186
29743	Slc25a1	1.10	0.006388
64630	Snap23	-0.57	0.006562
79449	Rpl21	-2.43	0.007106
57341	Parva	-1.36	0.009375
305178	Hnrnpdl	-0.75	0.00987
85274	Prdx4	-3.77	0.010514
259275	Ostf1	0.84	0.010579
29688	Minpp1	-2.07	0.013155
445268	Ufc1	-2.04	0.014068
24959	Pgam2	1.80	0.014105
361613	Ppme1	2.03	0.014231
307039	Rab18	-0.80	0.015098
304024	Cpox	2.64	0.017902
100909840	LOC100909840	-0.60	0.017981
81781	Snrpn	-0.51	0.018985
690131	Hist2h2aa2	-0.61	0.019641
497198	Impact	-1.80	0.020479
307905	Usp10	-3.13	0.020618
499839	RGD1564664	-2.70	0.021669
25010	Scgb2a1	-3.44	0.022101
308650	Hnrnph2	2.88	0.022881

310695	Kirrel1	2.62	0.025104
363013	Tmem123	2.59	0.026566
170751	Xpnpep1	3.29	0.02881
100360180	Pgd	0.53	0.028867
25420	Cryab	0.90	0.029983
311422	Itpa	0.78	0.032824
29676	Psmb3	-1.65	0.033466
29734	Hspa13	0.88	0.034403
25537	Rock2	2.20	0.036381
305497	Cobl	2.18	0.03795
290640	Map1s	-3.42	0.042638
29637	Hmgcs1	4.22	0.042914
308384	Sae1	-2.63	0.043105
300757	Hexa	1.15	0.046193
83764	Flot2	1.95	0.048583
103689947	LOC103689947	-0.50	0.055615
25425	Ctsh	0.58	0.055862
140868	Fabp5	0.63	0.057439
50681	Acox1	-1.28	0.058114
295692	Nup35	0.61	0.063838
314648	Ncln	-4.13	0.063902
64157	Ddah1	1.36	0.066755
81666	Gnaq	-1.16	0.068826
192360	Eml2	0.81	0.07351
303518	Smarce1	4.10	0.073866
307503	Etf1	-1.94	0.074281
192235	Hyou1	1.79	0.074523
287828	Jpt1	0.79	0.074615
297566	Atp6v1e1	0.62	0.074767
84357	Sh3kbp1	1.45	0.075562
117104	Ppp2r2a	0.71	0.075654
192249	Ehd3	1.65	0.075682
58815	Glrx3	-3.87	0.077933
117028	Bin1	-0.89	0.082843
59303	Tmem33	1.06	0.085507
29425	Psmb5	2.58	0.08587
24157	Acaa1a	-0.72	0.089194
306283	Anxa8	-0.66	0.089575
362015	Ampd2	1.19	0.090078
691657	Crip1	1.32	0.094208
294673	Hexb	-2.92	0.102142
79210	Fstl1	1.71	0.102491
680522	Hist1h1b	1.38	0.103409
683788	Fscn1	0.53	0.106285
64032	Ctgf	-0.50	0.106913
100361558	LOC100361558	1.24	0.107837

114766	Phb2	-1.11	0.108469
29254	Mgll	0.74	0.112464
287042	Nubp1	1.49	0.114342
64203	Bcat2	-1.08	0.114377
102550391	LOC102550391	-0.71	0.114543
361532	Sirt2	1.80	0.115482
361635	LOC361635	-1.12	0.120085
157074	Sdha	0.55	0.122822
64347	Sncg	0.94	0.132378
361884	Mccc2	-0.58	0.13291
298609	Efhd2	1.97	0.132936
89841	Pcyt2	2.41	0.133672
25277	Mfge8	1.81	0.133882
27139	Rps26	-0.91	0.134129
83781	Lgals3	0.70	0.13543
299027	Eif2s3	0.53	0.136792
361092	Stk24	1.58	0.138388
360820	Pxn	2.40	0.138502
29153	Capn1	1.18	0.140233
287125	Nubp2	-1.48	0.142311
89825	Nap1l1	-2.20	0.144302
85492	Psmb7	2.27	0.147263
63938	Hibadh	-0.71	0.152486
60373	Nop58	2.02	0.153349
64538	Ilkap	-1.24	0.153505
301252	Hsp90ab1	-0.69	0.154211
25177	Fhl1	1.57	0.154475
252928	Timm13	-1.25	0.154815
54321	Cnn3	2.50	0.155197
362634	C1qc	-1.45	0.155978
300981	Acy1	-0.60	0.15657
117041	Nln	-2.71	0.161382
24655	Plcd1	1.36	0.16585
25344	Phb	-0.91	0.166831
300968	Uba5	2.00	0.167161
25380	Anxa1	0.91	0.170097
315707	Csk	-3.52	0.170238
282827	Aip	0.99	0.171773
114123	Sardh	0.82	0.172193
114113	Pafah1b3	-3.72	0.173067
108348260	LOC108348260	-1.77	0.17431
301618	Ppp1r7	2.07	0.176101
81661	Gmfb	-3.15	0.179404
361927	Fxr1	1.22	0.182166
315664	Kdelc2	-3.19	0.182306
297893	Hdac1	1.93	0.185012

117130	Grifin	-1.17	0.187328
60466	Stx7	1.26	0.191458
313770	Mxra8	1.83	0.191508
29318	Ddt	-0.85	0.191745
291081	Tubb2b	0.53	0.195288
314644	Dohh	-2.00	0.196706
24437	H1f0	5.60	0.197351
24787	Sod2	-0.79	0.197772
29332	Stmn1	-3.43	0.198118
60384	Copb2	-1.96	0.198454
501232	Cesl1	1.17	0.198671
29681	C1qbp	-0.75	0.199398
362282	Pck1	-0.86	0.199468
298370	Txndc12	-0.69	0.199832
298441	Nasp	-1.22	0.200112
24377	G6pd	0.71	0.201778
317259	Nono	-0.71	0.202927
58835	Phgdh	0.60	0.203119
297699	Strap	3.00	0.204399
83572	Pafah1b1	-0.64	0.204626
25581	Psmc2	-2.54	0.205136
64201	Slc25a11	-4.80	0.207437
25643	Gnai3	2.86	0.207957
286896	Sgpl1	1.24	0.209271
246298	Retsat	0.60	0.209863
691947	Eif3j	1.23	0.211981
171155	Hadhb	-0.80	0.212642
64665	Flot1	1.11	0.216866
79248	Abca2	0.82	0.218028
293719	Ubxn1	1.55	0.220695
65204	Cnn1	5.54	0.223415
24265	Ckm	2.78	0.223581
287876	Actg1	0.54	0.229322
117103	Rab8a	2.01	0.229323
299201	Dlst	-0.60	0.230346
140934	Elp1	0.69	0.23234
313047	Yars	1.50	0.233809
171133	Gcsh	-1.65	0.23408
140931	Hnrnph1	-1.11	0.235857
290401	Esd	1.41	0.238483
66028	Arl6ip5	3.95	0.238743
310635	Arhgef2	-2.38	0.239455
25697	Ctsl	1.23	0.23982
YM-178			
116689	Ptpn6	-3.56	0.000154
25650	Atp1b1	-1.40	0.000303

59108	Mb	2.71	0.000548
306262	Btd	2.72	0.000735
501167	Gmppa	1.58	0.000934
64528	Golga2	0.98	0.001723
287633	Lrrc59	-0.62	0.002902
81726	Mvd	-3.82	0.004012
363425	Cav2	-2.41	0.004547
114559	Arhgef7	-1.54	0.005187
25737	Pcna	1.41	0.005462
171516	Akr1c3	-3.61	0.006199
311328	Rmdn3	-2.54	0.006373
312398	Smarcad1	-2.97	0.006491
29583	Pecam1	3.43	0.006613
25491	Nes	-1.35	0.008957
25106	Rgn	1.79	0.009092
117099	Bdh1	-1.76	0.009659
100364457	LOC100364457	0.98	0.010813
681429	Rps27l	1.68	0.011212
24439	Hagh	4.52	0.01207
365377	Trim72	-2.27	0.012326
266605	Dcps	0.74	0.012836
113922	Selenof	-1.84	0.013927
81922	Sh3gl1	-0.70	0.015702
116463	Akr1b7	-4.12	0.016705
309593	Gnl1	1.21	0.017056
360543	Myh4	3.19	0.021934
294853	Krt18	-4.53	0.022348
291434	Rpl17	0.57	0.024257
266759	Hspa4	1.93	0.025477
29671	Psma4	2.04	0.027228
100910732	LOC100910732	-4.65	0.02735
29437	Acta1	2.41	0.031493
295703	Serping1	1.24	0.033653
25618	Acadsb	-2.31	0.034211
81651	Cspg4	1.02	0.034735
124461	Pacsin2	-1.11	0.036395
260321	Fkbp4	-1.82	0.039467
364064	Pycr2	1.40	0.040704
681913	Gstz1	1.68	0.041137
170845	Ndel1	-5.37	0.041759
116547	S100a8	-1.40	0.045185
366734	Bag5	-3.35	0.04572
296570	Edf1	-2.35	0.046418
81520	Marcksl1	-0.88	0.046841
140544	Pcyt1a	-2.97	0.047611
501203	Myl12a	0.52	0.049269

83712	Rbbp7	-2.70	0.051168
25371	Adprh	-1.34	0.052742
498545	Tsc22d1	-2.36	0.056873
108348287	LOC108348287	1.58	0.05858
29435	Ssr4	2.47	0.061261
25484	Myo1e	-2.31	0.062683
287191	Rars	3.19	0.067376
81815	Tpp2	-2.81	0.069101
84379	Rab6a	0.51	0.070121
59114	Slc9a3r1	1.19	0.078356
140673	Napa	1.34	0.07892
313647	Hp1bp3	6.26	0.079022
298098	Pole3	0.74	0.079152
362154	Zc3h15	-1.20	0.08213
25338	Ninj1	-2.78	0.082898
25621	Cd81	-0.60	0.084793
81761	Rnpep	1.43	0.086835
361207	Tmed9	2.00	0.089368
114861	Scpep1	0.83	0.089463
65028	Dnaja1	-1.01	0.089869
59107	Ltbp1	-2.60	0.092309
292023	Aars	-0.73	0.092548
29285	Rps15	-2.97	0.096805
29283	Rpl29	0.70	0.097067
24946	F9	1.73	0.098183
191576	Tecr	-2.74	0.098231
296320	Ctnnbl1	-1.42	0.10886
289456	Hsd17b11	0.92	0.110043
686019	Casq1	2.72	0.110524
100359982	Mpc2	-5.03	0.113167
29158	Fbln5	2.97	0.114676
314730	Ikbip	-1.76	0.116982
246325	Kcnh8	0.84	0.117573
58945	Dynll1	5.47	0.118062
408248	Psma3l	-0.90	0.119604
361730	Tkfc	-2.20	0.12089
259246	LOC259246	-0.81	0.124788
360629	Nt5c3b	-1.17	0.126636
684527	Crtc1	2.24	0.127565
171063	Gtf3c1	-1.91	0.130115
94266	Rps27	0.77	0.136434
288022	Ccdc50	-2.18	0.143163
192269	Sub1	2.53	0.143954
362173	Caprin1	-3.02	0.144588
299923	Ndrg1	-1.10	0.148883
114023	Copb1	1.04	0.155732

116482	Sacm1l	2.79	0.155855
25291	Anxa3	-0.51	0.159588
117268	Khdrbs1	-3.10	0.165319
619580	Ctps2	-0.62	0.166527
94174	Tinagl1	-3.84	0.166646
298566	C1qa	1.55	0.171369
25475	Lgals5	2.84	0.171861
313200	Hsdl2	0.77	0.17566
25073	Scarb1	1.21	0.176283
296851	Pon2	-0.64	0.179464
113956	Pecr	2.01	0.181245
308796	Mesd	-1.28	0.183137
289144	Cacybp	-0.55	0.183169
171105	Lnpep	-1.78	0.183999
94197	Rab14	2.32	0.188069
64367	Ppib	-0.58	0.191775
25125	Stat3	-2.20	0.19204
245955	Lgals3bp	-1.76	0.194232
301442	Sumo1	-0.98	0.194283
171562	Ero1a	0.75	0.196251
81827	Psmc5	-2.94	0.199308
25614	Ptk2	1.49	0.201321
290500	Ggact	2.29	0.204519
93646	Sec31a	1.75	0.211889
54318	Eif2s1	-2.50	0.216204
296554	Tubb4b	-0.53	0.216562
266760	Nalcn	-3.14	0.217229
81763	Rpl5	2.72	0.222544
84401	Puf60	-2.17	0.224326
29389	Tnni2	2.61	0.224664
117152	Cand1	0.74	0.224995
140922	Txnl1	-0.68	0.231544
24614	Orm1	0.85	0.233416
117272	Prpsap2	1.91	0.233601
338401	Crip2	1.21	0.237137
64196	Safb	0.53	0.238084
116666	Lman1	-0.57	0.242846
64667	Sgta	-0.88	0.242935
81776	Rps24	1.18	0.24314
84471	Snx1	-2.20	0.243648
64198	Pmpcb	-1.07	0.246348
171145	Eif2b3	2.20	0.248176
81653	Dbn1	-1.67	0.248852

Table 2. GO terms enriched in BAT with SHT and YM-178

gold	goName	countDE	countAll	pv_elim
SHT				
Biological Process				
GO:0000122	negative regulation of transcription from RNA polymerase II promoter	14	40	0.008
GO:0003006	developmental process involved in reproduction	20	68	0.0146
GO:0071786	endoplasmic reticulum tubular network organization	3	4	0.0209
GO:0019098	reproductive behavior	3	4	0.0209
GO:0006544	glycine metabolic process	3	4	0.0209
GO:0016226	iron-sulfur cluster assembly	3	4	0.0209
GO:0090068	positive regulation of cell cycle process	7	17	0.0231
GO:0046323	glucose import	6	14	0.0285
GO:0001932	regulation of protein phosphorylation	32	129	0.0316
GO:0098969	neurotransmitter receptor transport to postsynaptic membrane	2	2	0.0333
GO:1903044	protein localization to membrane raft	2	2	0.0333
GO:0032962	positive regulation of inositol trisphosphate biosynthetic process	2	2	0.0333
GO:0032986	protein-DNA complex disassembly	2	2	0.0333
GO:0050884	neuromuscular process controlling posture	2	2	0.0333
GO:0051482	positive regulation of cytosolic calcium ion concentration involved in phospholipase C-activating G-protein coupled signaling pathway	2	2	0.0333
GO:1902667	regulation of axon guidance	2	2	0.0333
GO:0031498	chromatin disassembly	2	2	0.0333
GO:0019322	pentose biosynthetic process	2	2	0.0333
GO:0060766	negative regulation of androgen receptor signaling pathway	2	2	0.0333
GO:0060338	regulation of type I interferon-mediated signaling pathway	2	2	0.0333
GO:1990592	protein K69-linked ufmylation	2	2	0.0333
GO:0003085	negative regulation of systemic arterial blood pressure	2	2	0.0333
GO:2000757	negative regulation of peptidyl-lysine acetylation	2	2	0.0333
GO:1900138	negative regulation of phospholipase A2 activity	2	2	0.0333
GO:0045039	protein import into mitochondrial inner membrane	2	2	0.0333
GO:0006689	ganglioside catabolic process	2	2	0.0333
GO:2000322	regulation of glucocorticoid receptor	2	2	0.0333

	signaling pathway			
GO:0071169	establishment of protein localization to chromatin	2	2	0.0333
GO:0061582	intestinal epithelial cell migration	2	2	0.0333
GO:0009051	pentose-phosphate shunt, oxidative branch	2	2	0.0333
GO:0070193	synaptonemal complex organization	2	2	0.0333
GO:0070192	chromosome organization involved in meiotic cell cycle	2	2	0.0333
GO:0008277	regulation of G-protein coupled receptor protein signaling pathway	5	11	0.0349
GO:0006334	nucleosome assembly	6	15	0.0405
GO:0046578	regulation of Ras protein signal transduction	6	15	0.0405
GO:0010501	RNA secondary structure unwinding	4	8	0.0413
GO:0007626	locomotory behavior	7	19	0.043
GO:0043901	negative regulation of multi-organism process	7	19	0.043
GO:0072321	chaperone-mediated protein transport	3	5	0.0452
GO:0071468	cellular response to acidic pH	3	5	0.0452
GO:0051785	positive regulation of nuclear division	3	5	0.0452
GO:0045599	negative regulation of fat cell differentiation	3	5	0.0452
GO:0031647	regulation of protein stability	15	53	0.0455
GO:1901653	cellular response to peptide	16	58	0.0492
Molecular Function				
GO:0000980	RNA polymerase II distal enhancer sequence-specific DNA binding	4	5	0.0046
GO:0030984	kininogen binding	3	3	0.006
GO:0031492	nucleosomal DNA binding	4	6	0.0119
GO:0001846	opsonin binding	3	4	0.0207
GO:0005212	structural constituent of eye lens	3	4	0.0207
GO:0016634	oxidoreductase activity, acting on the CH-CH group of donors, oxygen as acceptor	3	4	0.0207
GO:0016831	carboxy-lyase activity	5	10	0.022
GO:0016746	transferase activity, transferring acyl groups	9	25	0.0259
GO:0004616	phosphogluconate dehydrogenase (decarboxylating) activity	2	2	0.0331
GO:0008484	sulfuric ester hydrolase activity	2	2	0.0331
GO:0004563	beta-N-acetylhexosaminidase activity	2	2	0.0331
GO:0017136	NAD-dependent histone deacetylase activity	2	2	0.0331
GO:0102148	N-acetyl-beta-D-galactosaminidase activity	2	2	0.0331
GO:0008026	ATP-dependent helicase activity	5	11	0.0344

GO:0005546	phosphatidylinositol-4,5-bisphosphate binding	4	8	0.0409
GO:0004527	exonuclease activity	3	5	0.0449
GO:0030246	carbohydrate binding	12	40	0.0457
Cellular Component				
GO:0042582	azurophil granule	4	4	0.0011
GO:0000790	nuclear chromatin	12	27	0.0014
GO:0031616	spindle pole centrosome	3	4	0.0209
GO:0000786	nucleosome	5	10	0.0223
GO:0042719	mitochondrial intermembrane space protein transporter complex	2	2	0.0333
GO:0001740	Barr body	2	2	0.0333
GO:0072687	meiotic spindle	2	2	0.0333
GO:0034751	aryl hydrocarbon receptor complex	2	2	0.0333
GO:0043196	varicosity	2	2	0.0333
GO:0001931	uropod	3	5	0.0453
YM-178				
Biological Process				
GO:0003009	skeletal muscle contraction	5	7	0.0015
GO:0051897	positive regulation of protein kinase B signaling	6	11	0.0034
GO:0010677	negative regulation of cellular carbohydrate metabolic process	3	3	0.0039
GO:1901896	positive regulation of calcium-transporting ATPase activity	3	3	0.0039
GO:0032781	positive regulation of ATPase activity	9	15	0.0055
GO:0050873	brown fat cell differentiation	3	4	0.0138
GO:0006937	regulation of muscle contraction	8	22	0.0147
GO:0071560	cellular response to transforming growth factor beta stimulus	8	22	0.0147
GO:0060048	cardiac muscle contraction	6	15	0.0209
GO:0048193	Golgi vesicle transport	12	42	0.024
GO:1903630	regulation of aminoacyl-tRNA ligase activity	2	2	0.0249
GO:0070836	caveola assembly	2	2	0.0249
GO:1901017	negative regulation of potassium ion transmembrane transporter activity	2	2	0.0249
GO:0009226	nucleotide-sugar biosynthetic process	2	2	0.0249
GO:0071481	cellular response to X-ray	2	2	0.0249
GO:0031571	mitotic G1 DNA damage checkpoint	2	2	0.0249
GO:1904398	positive regulation of neuromuscular junction development	2	2	0.0249
GO:0035414	negative regulation of catenin import into nucleus	2	2	0.0249
GO:0030643	cellular phosphate ion homeostasis	2	2	0.0249
GO:0071378	cellular response to growth	3	5	0.0305

	hormone stimulus			
GO:2000059	negative regulation of protein ubiquitination involved in ubiquitin-dependent protein catabolic process	3	5	0.0305
GO:0035774	positive regulation of insulin secretion involved in cellular response to glucose stimulus	3	5	0.0305
GO:0046627	negative regulation of insulin receptor signaling pathway	3	5	0.0305
GO:0032780	negative regulation of ATPase activity	3	5	0.0305
GO:0034260	negative regulation of GTPase activity	3	5	0.0305
GO:0043392	negative regulation of DNA binding	3	5	0.0305
GO:0008286	insulin receptor signaling pathway	7	14	0.0384
GO:0030518	intracellular steroid hormone receptor signaling pathway	6	17	0.0392
GO:0045913	positive regulation of carbohydrate metabolic process	4	9	0.0399
GO:0000086	G2/M transition of mitotic cell cycle	4	9	0.0399
GO:0097421	liver regeneration	5	13	0.0411
GO:0050772	positive regulation of axonogenesis	5	13	0.0411
GO:0007030	Golgi organization	7	22	0.046
Molecular Function				
GO:0035259	glucocorticoid receptor binding	3	4	0.013
GO:0001671	ATPase activator activity	3	4	0.013
GO:0008134	transcription factor binding	15	55	0.016
GO:0050431	transforming growth factor beta binding	2	2	0.024
GO:0031730	CCR5 chemokine receptor binding	2	2	0.024
GO:0031014	troponin T binding	2	2	0.024
GO:0005044	scavenger receptor activity	3	5	0.029
GO:0019905	syntaxin binding	4	9	0.037
GO:0016779	nucleotidyltransferase activity	4	9	0.037
GO:0004888	transmembrane signaling receptor activity	4	9	0.037
Cellular Component				
GO:0005887	integral component of plasma membrane	12	32	0.002
GO:0030134	COPII-coated ER to Golgi transport vesicle	5	9	0.0067
GO:0005861	troponin complex	2	2	0.0245
GO:0001741	XY body	2	2	0.0245
GO:0043596	nuclear replication fork	3	5	0.0299
GO:0044295	axonal growth cone	3	5	0.0299
GO:0016459	myosin complex	5	13	0.0399

Table 3. Differentially regulated proteins in WAT with SHT and YM-178

GeneID	Gene name	logfc	adjpv
SHT			
117028	Bin1	-2.79	8.97E-06
304290	Kdelr2	-2.68	4.47E-05
24667	Ppm1b	-2.65	0.000108
84114	Agps	-1.35	0.000125
84401	Puf60	-2.94	0.000753
300983	Abhd14b	0.94	0.000791
29218	Rcn2	-2.40	0.000854
290028	Osgep	-0.94	0.002064
24230	Tspo	-2.34	0.00248
171452	Rab3il1	-2.15	0.00629
84355	Atox1	-0.89	0.007345
311428	RGD1311739	1.07	0.007461
25246	Bsg	0.84	0.007876
25027	Slc16a1	1.02	0.008061
361999	Anp32e	-3.03	0.00862
24788	Sord	0.81	0.01132
301384	Hibch	1.64	0.013339
83576	Sort1	0.96	0.014054
29666	Psmb6	0.72	0.017559
690131	Hist2h2aa2	0.92	0.024289
29428	Celf2	-1.64	0.024896
84428	Dctn4	1.81	0.031509
54321	Cnn3	-1.91	0.032921
29528	Vamp3	0.68	0.034143
313200	Hsdl2	0.66	0.034361
25287	Acadl	0.67	0.03642
83472	Ugdh	0.61	0.041704
689284	Rpl38	-3.68	0.042184
24383	Gapdh	-0.72	0.046605
287633	Lrrc59	1.23	0.050259
25604	Pcmt1	-0.69	0.053192
681059	Vps25	-1.20	0.054081
79223	Gk	1.62	0.058056
691947	Eif3j	-0.97	0.062525
302500	Mcts1	1.98	0.065517
64517	Thop1	-1.02	0.066596
84472	Ilf3	-3.91	0.067026
65033	Stx12	0.65	0.06742
79131	Fabp3	2.67	0.067767
24172	Adh1	3.28	0.075818
114612	Ddx39b	-3.63	0.076071
369017	Krt5	2.80	0.076106

362809	Ptges3	-0.62	0.079947
54231	Car2	1.69	0.081896
171164	Gbp2	-0.65	0.08245
171155	Hadhb	0.65	0.087263
25104	Pc	0.63	0.087972
294673	Hexb	2.37	0.088946
65152	Pfkm	-2.15	0.091004
24918	Stat5a	1.42	0.094928
362115	Fam129b	0.99	0.106174
25725	Prkar1a	-1.02	0.106696
64362	Des	-0.74	0.108631
29651	Aldh1a7	3.17	0.111891
59108	Mb	-2.51	0.114158
25698	Ass1	3.41	0.115407
114123	Sardh	3.01	0.117946
65151	Rida	1.40	0.118124
84357	Sh3kbp1	-2.26	0.118967
24248	Cat	0.94	0.119545
295284	Rbm8a	-2.91	0.121692
83527	Dbnl	-2.21	0.122676
83805	Src	1.55	0.123643
363854	Elavl1	-0.67	0.125734
29271	Cfl1	-1.02	0.126378
307842	Vac14	-1.03	0.128208
294568	Wasf1	-2.01	0.128265
64526	Ech1	0.62	0.128887
113965	Hadh	0.89	0.131054
64679	Tgm4	-1.15	0.131104
683313	LOC683313	0.77	0.13306
63864	Hsd17b10	0.86	0.138671
299194	Ptgr2	1.16	0.138818
24307	Cyp4b1	-3.32	0.143961
297893	Hdac1	-1.83	0.151039
79248	Abca2	1.01	0.151314
300218	Tuba1c	-3.89	0.152971
81521	Msn	-0.84	0.160485
24666	Ppm1a	1.18	0.162655
102550391	LOC102550391	1.19	0.165852
64533	Pnpo	-4.31	0.166568
84478	Ufd1	0.87	0.172453
500419	Rmdn1	0.96	0.180088
24360	Fabp1	3.63	0.180799
100125372	Ces1f	-1.25	0.182806
24284	Csn1s1	2.46	0.186806
299923	Ndrg1	0.63	0.187013
24159	Acly	1.25	0.19101

681429	Rps27l	-0.63	0.193334
84509	Ran	-0.74	0.194937
246298	Retsat	0.97	0.195298
117130	Grifin	-2.17	0.195614
29474	Coro1b	-0.63	0.196282
500040	Tes	2.33	0.198406
116689	Ptpn6	-1.10	0.202346
25499	Nrdc	1.35	0.202642
678759	Ndufa10	-2.34	0.203597
683788	Fscn1	-0.70	0.20588
29459	Rbbp9	-1.22	0.207521
25106	Rgn	2.76	0.208098
64158	Tuba1a	5.02	0.218196
497811	Xdh	0.79	0.221165
25371	Adprh	-2.29	0.224889
306332	Ap1m1	0.71	0.227335
117282	Hnrnpk	-0.75	0.229928
296710	Arpc5l	-0.95	0.232611
29443	Ahcy	-0.90	0.23316
113940	Gmfg	-1.53	0.234475
24957	Glul	1.73	0.235712
60356	Csad	1.10	0.236915
24223	B2m	-0.64	0.238063
363425	Cav2	0.88	0.238385
50671	Fasn	1.48	0.239956
64040	Aldh9a1	0.62	0.241028
56781	Myl1	-3.64	0.241232
89827	Ddx39a	-0.78	0.244658
YM-178			
83730	Vamp8	-3.75	6.93E-05
29521	Scamp1	1.51	0.000111
25116	Hsd11b1	0.92	0.000382
117045	Eif4e	-0.69	0.000942
25342	Oxtr	1.79	0.001104
298566	C1qa	0.85	0.001124
445268	Ufc1	-0.65	0.001133
78947	Gcs1	0.61	0.00204
266734	Npas4	0.87	0.004234
246303	Serbp1	0.78	0.004516
25139	Slc2a4	1.36	0.005653
619574	LOC619574	-1.74	0.006446
64317	Gpx3	1.00	0.006558
84474	Ddx1	-0.73	0.007131
24471	Hspb1	1.26	0.007327
170673	Palm	2.47	0.007749
313035	Dnajc8	-2.09	0.008094

64045	Glrx	-3.30	0.008229
122799	Rps25	-1.04	0.009005
252928	Timm13	-0.62	0.009087
25611	Otc	0.72	0.009208
54319	Ezr	-2.37	0.009756
171114	Ndrg2	0.99	0.011103
64306	Rpl27	-0.99	0.013106
170520	Cygb	0.73	0.01364
85333	Slc25a4	0.74	0.014342
303606	Ccdc47	1.69	0.015281
81520	Marcksl1	-2.76	0.016098
116547	S100a8	2.76	0.018187
497009	Naaa	-3.00	0.018457
494345	Pdcd10	-0.80	0.020933
361663	Lhpp	-1.87	0.022049
25339	Npr3	1.07	0.022951
24233	C4a	0.96	0.023674
64152	Chp1	1.02	0.025969
300757	Hexa	-0.66	0.026564
361051	Phf11	-1.84	0.026791
260321	Fkbp4	-0.91	0.028603
292148	Eif3a	-0.71	0.030009
64028	Tsnax	-3.94	0.031875
100134871	LOC100134871	2.33	0.032522
117259	Tra2b	-1.82	0.032726
24648	Serpina1	0.98	0.033119
100911615	LOC100911615	1.62	0.03415
292925	Tsg101	-1.88	0.035767
300035	Pycr3	-0.66	0.036528
360882	Cadm3	1.85	0.036758
308650	Hnrnph2	-1.01	0.038168
58927	Rpl36	-0.84	0.039681
29635	Timm44	-2.58	0.041016
25282	Cox6a1	-1.73	0.041823
81504	Grb2	-1.13	0.043459
29360	Selenop	0.91	0.044436
29286	Rps17	-0.67	0.046061
24674	Ppp3ca	-1.18	0.04939
25524	Psap	-0.99	0.050226
64352	Gstm5	1.30	0.050372
116698	Trim28	-1.28	0.050847
24614	Orm1	1.57	0.051012
171133	Gcsh	3.37	0.051166
305679	Vcl	0.78	0.051276
25030	Andpro	2.99	0.051519
288001	Kng1	0.86	0.05194

64665	Flot1	0.79	0.053329
78958	Bcam	1.37	0.053481
681544	LOC681544	0.77	0.053624
24439	Hagh	1.13	0.056742
367562	Gaa	1.10	0.057099
58827	Mest	-0.74	0.057415
362401	Tmem43	0.61	0.060953
191574	Akr1c14	0.70	0.062102
294239	Ddah2	0.66	0.063782
24825	Tf	0.96	0.066528
65261	Myo1c	0.67	0.067612
58917	Hpx	0.65	0.068548
85332	Cavin3	0.87	0.069924
690050	Tpmt	-2.40	0.069953
60581	Acaca	-3.44	0.071
252929	Ctsz	-1.05	0.072146
363113	Syncrip	-0.63	0.072433
296709	Rpl35	-0.99	0.072466
300075	Tomm22	-0.76	0.07444
100359922	LOC100359922	-0.80	0.074441
29236	Rpsa	-0.68	0.074828
25420	Cryab	5.29	0.074881
83712	Rbbp7	-0.76	0.075646
25473	Lamb2	0.88	0.075929
29558	Fcgrt	0.80	0.076078
56780	Acpp	-1.89	0.078124
81775	Rps21	-1.16	0.078693
29669	Psma2	-0.61	0.078717
24440	Hbb	2.07	0.078843
360504	Hba2	0.96	0.079007
83783	Sult1a1	0.62	0.07972
117041	Nln	3.09	0.080074
25742	S100b	1.24	0.080926
300677	Atp5l	0.67	0.081587
246233	Macrod1	2.41	0.082923
64507	Fmod	2.19	0.083367
116549	Csnk2a1	-0.85	0.083542
499782	Rpl12	-0.67	0.085869
29283	Rpl29	-0.65	0.086577
108348260	LOC108348260	-0.73	0.092616
81766	Rpl18	-0.67	0.096475
29288	Rps3a	-0.79	0.097091
500538	Ybx1	-0.62	0.097152
360646	Limd2	-4.82	0.098828
360471	Usp7	-1.03	0.103854
364838	Reep5	1.15	0.105331

57341	Parva	0.76	0.106336
171137	Khsrp	-1.01	0.10724
315218	Lmf2	0.95	0.108704
25035	Cyb5r3	1.02	0.110565
116662	Ecm1	1.41	0.111825
171577	Epcam	-1.15	0.112584
307779	Rbmxrtl	-0.96	0.115081
307947	Set	-2.08	0.117698
60571	Mybbp1a	-1.40	0.11861
64031	Pdcd4	-1.13	0.119102
65984	Aacs	-3.23	0.120908
362855	Rtcb	-0.61	0.121081
56611	Anxa2	0.97	0.122294
296596	Rpl7a	-0.70	0.12345
114113	Pafah1b3	-1.02	0.12414
369016	Myadm	0.73	0.124691
28298	Rpl32	-1.06	0.125753
450225	Krt10	1.17	0.127176
59114	Slc9a3r1	-1.09	0.12891
25757	Cpt1a	3.07	0.12931
317381	Ccdc22	5.59	0.129886
85255	Hacl1	-2.44	0.130084
302562	Plp2	0.71	0.131025
362631	Rpl11	-0.75	0.132254
691531	Rps28	-0.87	0.133683
79224	Serpind1	0.66	0.134675
192276	Coro7	-1.16	0.136285
81681	Lss	1.38	0.141036
55939	Apom	0.63	0.141553
81729	Rpl10a	-0.98	0.142368
360626	Krt19	-2.95	0.142817
291434	Rpl17	-0.66	0.143666
305343	Pds5a	-3.37	0.145504
25419	Crp	0.87	0.147213
290651	Isyna1	-1.36	0.148286
360854	Arpc5	-0.76	0.151956
80846	Hnrnpl	-1.05	0.153574
300079	Rpl3	-0.81	0.153618
50664	Gnao1	0.91	0.153753
29491	Itsn1	-3.57	0.153827
113936	Cpb2	0.93	0.154271
100360522	LOC100360522	-1.22	0.155548
79256	Hnrnpd	-1.69	0.15639
360576	Tusc5	1.02	0.158706
308384	Sae1	-1.99	0.159931
296654	Gsn	0.87	0.160988

361673	Ifitm3	-1.59	0.165339
29389	Tnni2	-4.01	0.165619
29671	Psma4	-0.73	0.166824
65204	Cnn1	2.94	0.168593
301252	Hsp90ab1	-0.75	0.170109
24786	Sod1	-0.92	0.170236
81008	Itga7	1.13	0.170372
117557	Tpm3	-0.84	0.173177
497794	Mug1	0.61	0.174553
58952	Cpq	0.62	0.175249
114499	Hdgf	-0.82	0.178124
65137	Ruvbl1	-1.53	0.178135
25010	Scgb2a1	4.76	0.179267
117042	Rpl6	-0.79	0.180849
287191	Rars	-0.82	0.181074
25686	Gnai1	0.63	0.183971
294853	Krt18	-2.59	0.185246
286938	Gimap4	-1.75	0.186195
29648	Nudc	-0.86	0.186791
85496	Enpp1	-1.97	0.18985
83502	Cdh1	-1.92	0.19445
25330	Lipe	1.13	0.195171
83510	Lypla2	-0.91	0.195635
29473	Aoc3	0.70	0.195941
117280	Hnrnpu	-1.07	0.196818
116655	Hnrnpm	-1.12	0.200116
25126	Stat5b	-0.87	0.200585
24366	Fgb	0.86	0.200904
108350501	LOC108350501	-1.35	0.202062
64205	Rplp0	-0.79	0.205181
79116	Apex1	-3.25	0.206758
25368	Adk	-0.72	0.210856
290641	Rpl18a	-0.77	0.211728
170724	Anp32b	-1.02	0.212806
297699	Strap	-0.70	0.213497
100362830	LOC100362830	-0.77	0.218146
24968	Psmb8	-0.84	0.219647
252922	Pzp	0.96	0.223427
291983	Psmb10	-1.07	0.22378
116685	Lmnb1	-1.10	0.224812
361512	Ehd2	1.19	0.227089
25269	Pvalb	2.17	0.227186
108348062	LOC108348062	-2.51	0.228587
29563	Crabp2	-3.47	0.238336
64347	Sncg	1.49	0.23862
25292	Apoc1	2.25	0.239531

309187	Atl3	0.84	0.240149
290644	Ifi30	-0.70	0.240249
24346	Ces1c	0.91	0.243417
103690821	LOC103690821	-0.66	0.245662
293692	Ehd1	1.02	0.247676

Table 4. GO terms enriched in WAT with SHT and YM-178

gold	goName	countDE	countAll	pv_elim
SHT				
Biological Process				
GO:0030330	DNA damage response, signal transduction by p53 class mediator	5	6	0.0022
GO:0048711	positive regulation of astrocyte differentiation	3	3	0.0023
GO:0071498	cellular response to fluid shear stress	3	3	0.0023
GO:0032780	negative regulation of ATPase activity	3	3	0.0023
GO:0051607	defense response to virus	5	9	0.003
GO:0001822	kidney development	11	35	0.0036
GO:0050731	positive regulation of peptidyl-tyrosine phosphorylation	7	17	0.0037
GO:0002244	hematopoietic progenitor cell differentiation	3	4	0.0081
GO:0045577	regulation of B cell differentiation	3	4	0.0081
GO:0042130	negative regulation of T cell proliferation	3	4	0.0081
GO:0000077	DNA damage checkpoint	3	4	0.0081
GO:0002763	positive regulation of myeloid leukocyte differentiation	3	4	0.0081
GO:0071803	positive regulation of podosome assembly	3	4	0.0081
GO:0016477	cell migration	26	127	0.0104
GO:0034314	Arp2/3 complex-mediated actin nucleation	8	13	0.0124
GO:0010592	positive regulation of lamellipodium assembly	4	8	0.0133
GO:0120033	negative regulation of plasma membrane bounded cell projection assembly	4	8	0.0133
GO:0051289	protein homotetramerization	8	26	0.0147
GO:1902743	regulation of lamellipodium organization	8	13	0.0164
GO:2000279	negative regulation of DNA biosynthetic process	4	5	0.017
GO:0000245	spliceosomal complex assembly	4	5	0.017

GO:2000573	positive regulation of DNA biosynthetic process	6	17	0.017
GO:1902570	protein localization to nucleolus	2	2	0.0173
GO:0032480	negative regulation of type I interferon production	2	2	0.0173
GO:0071362	cellular response to ether	2	2	0.0173
GO:0034616	response to laminar fluid shear stress	2	2	0.0173
GO:0006499	N-terminal protein myristoylation	2	2	0.0173
GO:0097484	dendrite extension	2	2	0.0173
GO:0035855	megakaryocyte development	2	2	0.0173
GO:0099601	regulation of neurotransmitter receptor activity	2	2	0.0173
GO:0035970	peptidyl-threonine dephosphorylation	2	2	0.0173
GO:2000394	positive regulation of lamellipodium morphogenesis	2	2	0.0173
GO:0010870	positive regulation of receptor biosynthetic process	2	2	0.0173
GO:0031954	positive regulation of protein autophosphorylation	2	2	0.0173
GO:0060740	prostate gland epithelium morphogenesis	2	2	0.0173
GO:2000601	positive regulation of Arp2/3 complex-mediated actin nucleation	2	2	0.0173
GO:1902463	protein localization to cell leading edge	2	2	0.0173
GO:2000107	negative regulation of leukocyte apoptotic process	3	5	0.0184
GO:0048011	neurotrophin TRK receptor signaling pathway	3	5	0.0184
GO:0042475	odontogenesis of dentin-containing tooth	3	5	0.0184
GO:0051701	interaction with host	8	27	0.0187
GO:0030203	glycosaminoglycan metabolic process	4	9	0.0215
GO:0050792	regulation of viral process	8	28	0.0232
GO:0051091	positive regulation of DNA binding transcription factor activity	7	23	0.0236
Molecular Function				
GO:0051287	NAD binding	11	31	0.0013
GO:0008144	drug binding	9	29	0.0101
GO:0005001	transmembrane receptor protein tyrosine phosphatase activity	2	2	0.0178
GO:0005521	lamin binding	3	5	0.0191
GO:0042393	histone binding	5	13	0.021
GO:0033613	activating transcription factor binding	3	6	0.0345

GO:0003857	3-hydroxyacyl-CoA dehydrogenase activity	3	6	0.0345
GO:0045296	cadherin binding	22	113	0.0365
GO:0004028	3-chloroallyl aldehyde dehydrogenase activity	2	3	0.0486
GO:0071933	Arp2/3 complex binding	2	3	0.0486
GO:0004854	xanthine dehydrogenase activity	2	3	0.0486
GO:0003785	actin monomer binding	2	3	0.0486
GO:0046912	transferase activity, transferring acyl groups, acyl groups converted into alkyl on transfer	2	3	0.0486
GO:0005324	long-chain fatty acid transporter activity	2	3	0.0486
GO:0005540	hyaluronic acid binding	2	3	0.0486
Cellular Component				
GO:0005884	actin filament	9	24	0.0021
GO:0032993	protein-DNA complex	5	11	0.0088
GO:0002102	podosome	7	14	0.013
GO:0016607	nuclear speck	8	26	0.0146
GO:0031209	SCAR complex	2	2	0.0172
GO:0042611	MHC protein complex	2	2	0.0172
GO:0005687	U4 snRNP	2	2	0.0172
GO:0005856	cytoskeleton	49	238	0.0284
GO:0030054	cell junction	41	216	0.0291
GO:0005681	spliceosomal complex	9	22	0.0311
GO:0031258	lamellipodium membrane	3	6	0.033
GO:0071437	invadopodium	3	6	0.033
GO:0005912	adherens junction	29	162	0.0408
GO:0000407	pre-autophagosomal structure	2	3	0.0471
GO:0002080	acrosomal membrane	2	3	0.0471
YM-178				
Biological Process				
GO:0006953	acute-phase response	7	12	0.0035
GO:0000381	regulation of alternative mRNA splicing, via spliceosome	7	12	0.0035
GO:0034113	heterotypic cell-cell adhesion	8	12	0.0061
GO:0070528	protein kinase C signaling	4	5	0.0063
GO:0015671	oxygen transport	4	5	0.0063
GO:1901741	positive regulation of myoblast fusion	3	3	0.0077
GO:0070934	CRD-mediated mRNA stabilization	3	3	0.0077
GO:0007566	embryo implantation	6	12	0.0179
GO:0040007	growth	29	103	0.0209
GO:0071345	cellular response to cytokine stimulus	25	86	0.0211
GO:0009059	macromolecule biosynthetic process	84	332	0.0239
GO:0070293	renal absorption	3	4	0.0261

GO:0071392	cellular response to estradiol stimulus	3	4	0.0261
GO:0042993	positive regulation of transcription factor import into nucleus	3	4	0.0261
GO:0048821	erythrocyte development	3	4	0.0261
GO:0046597	negative regulation of viral entry into host cell	3	4	0.0261
GO:0044319	wound healing, spreading of cells	3	4	0.0261
GO:0043516	regulation of DNA damage response, signal transduction by p53 class mediator	3	4	0.0261
GO:0031953	negative regulation of protein autophosphorylation	3	4	0.0261
GO:2000648	positive regulation of stem cell proliferation	3	4	0.0261
GO:1900087	positive regulation of G1/S transition of mitotic cell cycle	3	4	0.0261
GO:0042273	ribosomal large subunit biogenesis	8	15	0.027
GO:0030032	lamellipodium assembly	6	13	0.0278
GO:0006281	DNA repair	10	22	0.0281
GO:0032103	positive regulation of response to external stimulus	11	31	0.0287
GO:0051241	negative regulation of multicellular organismal process	33	123	0.0288
GO:0042255	ribosome assembly	8	20	0.0291
GO:0042307	positive regulation of protein import into nucleus	7	11	0.0307
GO:0070670	response to interleukin-4	5	10	0.0308
GO:0072659	protein localization to plasma membrane	15	47	0.0309
GO:0071407	cellular response to organic cyclic compound	33	103	0.0311
GO:0034114	regulation of heterotypic cell-cell adhesion	4	7	0.0317
GO:0042755	eating behavior	4	7	0.0317
GO:2001235	positive regulation of apoptotic signaling pathway	9	24	0.0325
GO:0019915	lipid storage	7	17	0.0346
GO:0051090	regulation of DNA binding transcription factor activity	10	28	0.0348
GO:0090316	positive regulation of intracellular protein transport	15	32	0.0354
GO:0045861	negative regulation of proteolysis	21	67	0.0377
GO:0060088	auditory receptor cell stereocilium organization	2	2	0.039
GO:0032415	regulation of sodium:proton antiporter activity	2	2	0.039
GO:0061158	3'-UTR-mediated mRNA	2	2	0.039

	destabilization			
GO:2001014	regulation of skeletal muscle cell differentiation	2	2	0.039
GO:0050884	neuromuscular process controlling posture	2	2	0.039
GO:2001026	regulation of endothelial cell chemotaxis	2	2	0.039
GO:0019731	antibacterial humoral response	2	2	0.039
GO:0071386	cellular response to corticosterone stimulus	2	2	0.039
GO:0006388	tRNA splicing, via endonucleolytic cleavage and ligation	2	2	0.039
GO:2000047	regulation of cell-cell adhesion mediated by cadherin	2	2	0.039
GO:0006407	rRNA export from nucleus	2	2	0.039
GO:2001137	positive regulation of endocytic recycling	2	2	0.039
GO:0019886	antigen processing and presentation of exogenous peptide antigen via MHC class II	2	2	0.039
GO:0060355	positive regulation of cell adhesion molecule production	2	2	0.039
GO:0002523	leukocyte migration involved in inflammatory response	2	2	0.039
GO:0031643	positive regulation of myelination	2	2	0.039
GO:0072697	protein localization to cell cortex	2	2	0.039
GO:0010642	negative regulation of platelet-derived growth factor receptor signaling pathway	2	2	0.039
GO:0080111	DNA demethylation	2	2	0.039
GO:0052405	negative regulation by host of symbiont molecular function	2	2	0.039
GO:1905063	regulation of vascular smooth muscle cell differentiation	2	2	0.039
GO:0030643	cellular phosphate ion homeostasis	2	2	0.039
GO:0010757	negative regulation of plasminogen activation	2	2	0.039
GO:0071763	nuclear membrane organization	2	2	0.039
GO:0060669	embryonic placenta morphogenesis	2	2	0.039
GO:0035176	social behavior	2	2	0.039
GO:0018065	protein-cofactor linkage	2	2	0.039
GO:0015886	heme transport	2	2	0.039
GO:0050427	3'-phosphoadenosine 5'-phosphosulfate metabolic process	2	2	0.039
GO:0002925	positive regulation of humoral immune response mediated by circulating immunoglobulin	2	2	0.039

GO:0010998	regulation of translational initiation by eIF2 alpha phosphorylation	2	2	0.039
GO:0007156	homophilic cell adhesion via plasma membrane adhesion molecules	2	2	0.039
GO:0000387	spliceosomal snRNP assembly	2	2	0.039
GO:0007194	negative regulation of adenylate cyclase activity	2	2	0.039
GO:1904401	cellular response to Thyroid stimulating hormone	2	2	0.039
GO:0005984	disaccharide metabolic process	2	2	0.039
GO:0000447	endonucleolytic cleavage in ITS1 to separate SSU-rRNA from 5.8S rRNA and LSU-rRNA from tricistronic rRNA transcript (SSU-rRNA, 5.8S rRNA, LSU-rRNA)	2	2	0.039
GO:0000461	endonucleolytic cleavage to generate mature 3'-end of SSU-rRNA from (SSU-rRNA, 5.8S rRNA, LSU-rRNA)	2	2	0.039
GO:0000463	maturation of LSU-rRNA from tricistronic rRNA transcript (SSU-rRNA, 5.8S rRNA, LSU-rRNA)	2	2	0.039
GO:0038089	positive regulation of cell migration by vascular endothelial growth factor signaling pathway	2	2	0.039
GO:1903533	regulation of protein targeting	6	14	0.0408
GO:0000165	MAPK cascade	22	78	0.0414
GO:0022409	positive regulation of cell-cell adhesion	9	25	0.0423
GO:0006396	RNA processing	31	75	0.0432
GO:0045596	negative regulation of cell differentiation	19	66	0.0463
GO:0032092	positive regulation of protein binding	7	18	0.0474
GO:0051053	negative regulation of DNA metabolic process	5	11	0.0475
GO:0007188	adenylate cyclase-modulating G-protein coupled receptor signaling pathway	5	11	0.0475
GO:0034381	plasma lipoprotein particle clearance	5	11	0.0475
GO:0008154	actin polymerization or depolymerization	17	42	0.0483
Molecular Function				
GO:0003735	structural constituent of ribosome	24	62	0.00037
GO:0005344	oxygen carrier activity	4	5	0.00657
GO:0003730	mRNA 3'-UTR binding	8	18	0.01548

GO:0003682	chromatin binding	10	25	0.01623
GO:0140097	catalytic activity, acting on DNA	5	9	0.01908
GO:0042162	telomeric DNA binding	3	4	0.02688
GO:0045294	alpha-catenin binding	3	4	0.02688
GO:0004527	exonuclease activity	3	4	0.02688
GO:0003723	RNA binding	73	281	0.02734
GO:0019825	oxygen binding	4	7	0.03278
GO:0031720	haptoglobin binding	2	2	0.03976
GO:0001091	RNA polymerase II basal transcription factor binding	2	2	0.03976
GO:0001105	RNA polymerase II transcription coactivator activity	2	2	0.03976
GO:0015926	glucosidase activity	2	2	0.03976
GO:0005055	laminin receptor activity	2	2	0.03976
GO:0005089	Rho guanyl-nucleotide exchange factor activity	2	2	0.03976
GO:0045159	myosin II binding	2	2	0.03976
GO:0043395	heparan sulfate proteoglycan binding	2	2	0.03976
GO:0046790	virion binding	2	2	0.03976
GO:0004888	transmembrane signaling receptor activity	7	13	0.04822
GO:0070851	growth factor receptor binding	5	11	0.04938
Cellular Component				
GO:0022625	cytosolic large ribosomal subunit	15	30	0.00018
GO:0016323	basolateral plasma membrane	14	32	0.00164
GO:0005833	hemoglobin complex	3	3	0.00782
GO:0005903	brush border	10	23	0.00812
GO:0030864	cortical actin cytoskeleton	9	20	0.00918
GO:0016327	apicolateral plasma membrane	3	4	0.02666
GO:0044451	nucleoplasm part	18	58	0.0269
GO:0005637	nuclear inner membrane	5	10	0.03167
GO:0035770	ribonucleoprotein granule	11	32	0.03804
GO:0097225	sperm midpiece	2	2	0.03953
GO:0032426	stereocilium tip	2	2	0.03953
GO:0061827	sperm head	2	2	0.03953
GO:0070937	CRD-mediated mRNA stability complex	2	2	0.03953
GO:0072669	tRNA-splicing ligase complex	2	2	0.03953
GO:0071204	histone pre-mRNA 3'end processing complex	2	2	0.03953
GO:0034451	centriolar satellite	2	2	0.03953
GO:0030686	90S preribosome	2	2	0.03953

Table 5. List of nodes in protein-protein interaction network in BAT with SHT and YM-178

STRINGID	Label	Degree	Betweenness
SHT			
ENSRNOP00000026710	Gnai3	110	23372.17
ENSRNOP00000019174	Gnaq	75	15635.06
ENSRNOP00000041842	Ptpn11	72	26537.66
ENSRNOP00000026358	Csk	24	3470.94
ENSRNOP00000051859	Actg1	21	5630
ENSRNOP00000031981	Stk24	20	5220.5
ENSRNOP00000025687	Pik3r1	3	7843.19
ENSRNOP00000015019	Ppp2r1a	3	5959
ENSRNOP00000012739	Src	3	4609.39
ENSRNOP00000043928	Pxn	3	580
ENSRNOP00000042428	Fpr3	3	452.98
ENSRNOP00000023649	Ppme1	3	426.5
ENSRNOP00000066672	Rhoa	2	5691
ENSRNOP00000000157	Pik3r3	2	4161.26
ENSRNOP00000036381	Nras	2	4161.26
ENSRNOP00000021671	Parva	2	291
ENSRNOP00000000617	Mapk14	2	253.49
ENSRNOP00000003092	Casr	2	253.49
ENSRNOP00000005953	Bdkrb1	2	253.49
ENSRNOP00000006389	Plcb1	2	253.49
ENSRNOP00000014747	Ednrb	2	253.49
ENSRNOP00000018967	Nmur2	2	253.49
ENSRNOP00000020656	Lpar3	2	253.49
ENSRNOP00000025024	Nmur1	2	253.49
ENSRNOP00000025564	Mchr1	2	253.49
ENSRNOP00000066690	Gnb5	2	253.49
ENSRNOP00000028720	Plcb3	2	253.49
ENSRNOP00000064990	Bdkrb2	2	253.49
ENSRNOP00000032046	Gpr17	2	253.49
ENSRNOP00000058977	Lpar2	2	253.49
ENSRNOP00000064709	Agtr2	2	253.49
ENSRNOP00000044340	Gnb1	2	253.49
ENSRNOP00000043652	Lpar1	2	253.49
ENSRNOP00000045972	Plcb4	2	253.49
ENSRNOP00000014841	Fpr1	2	93.17
ENSRNOP00000007621	Ppp2ca	2	19
ENSRNOP00000023664	Anxa1	2	3.16
ENSRNOP00000004403	Cd247	2	0
ENSRNOP00000005347	Grb2	2	0
ENSRNOP00000006087	Egfr	2	0
ENSRNOP00000012936	Lck	2	0
ENSRNOP00000017109	Lpxn	2	0

ENSRNOP00000021915	Cd4	2	0
ENSRNOP00000024390	Gab1	2	0
ENSRNOP00000039940	Bcar1	2	0
ENSRNOP00000059867	Ptpn6	2	0
ENSRNOP00000047591	Cd3e	2	0
ENSRNOP00000000249	Grm6	1	0
ENSRNOP00000000451	Gprc6a	1	0
ENSRNOP00000000621	Mapk13	1	0
ENSRNOP00000000675	Npffr1	1	0
ENSRNOP00000000733	Fyn	1	0
ENSRNOP00000000907	Htr1f	1	0
ENSRNOP00000001911	Gnb2	1	0
ENSRNOP00000002169	Cct8	1	0
ENSRNOP00000002533	Mapk1	1	0
ENSRNOP00000002755	Gnrhr	1	0
ENSRNOP00000003050	Kit	1	0
ENSRNOP00000003735	Sstr2	1	0
ENSRNOP00000003940	Socs3	1	0
ENSRNOP00000004147	Myh3	1	0
ENSRNOP00000004153	Npffr2	1	0
ENSRNOP00000004236	Myh2	1	0
ENSRNOP00000004295	Myh1	1	0
ENSRNOP00000004406	Cxcr3	1	0
ENSRNOP00000004602	Adora1	1	0
ENSRNOP00000005055	Gpr65	1	0
ENSRNOP00000005076	Rgs9	1	0
ENSRNOP00000005143	Cxcr4	1	0
ENSRNOP00000005156	Rgs2	1	0
ENSRNOP00000005324	Rgs18	1	0
ENSRNOP00000005370	Pfn1	1	0
ENSRNOP00000005389	Adcy3	1	0
ENSRNOP00000005470	Ptger1	1	0
ENSRNOP00000005559	Grpr	1	0
ENSRNOP00000005829	Avpr1a	1	0
ENSRNOP00000006407	Crk	1	0
ENSRNOP00000006408	Sirpa	1	0
ENSRNOP00000006425	Sos2	1	0
ENSRNOP00000006527	Strn	1	0
ENSRNOP00000006783	Trhr	1	0
ENSRNOP00000006789	Adcy8	1	0
ENSRNOP00000006796	Erbb3	1	0
ENSRNOP00000007117	S1pr4	1	0
ENSRNOP00000007472	Frs2	1	0
ENSRNOP00000007572	Grm3	1	0
ENSRNOP00000007649	Traf3ip3	1	0
ENSRNOP00000007724	Oxtr	1	0

ENSRNOP00000007738	Pde4b	1	0
ENSRNOP00000008011	Gngt2	1	0
ENSRNOP00000008269	Ccr9	1	0
ENSRNOP00000008294	Cxcr6	1	0
ENSRNOP00000008300	Pde11a	1	0
ENSRNOP00000008387	Chrm5	1	0
ENSRNOP00000008471	Kitlg	1	0
ENSRNOP00000008772	Ccr1	1	0
ENSRNOP00000008783	Ccr1l1	1	0
ENSRNOP00000008809	Ccr3	1	0
ENSRNOP00000008947	RGD1560028	1	0
ENSRNOP00000009317	Htr5a	1	0
ENSRNOP00000009325	Mapk11	1	0
ENSRNOP00000009359	Sos1	1	0
ENSRNOP00000009511	Rap1b	1	0
ENSRNOP00000009612	Sstr3	1	0
ENSRNOP00000009775	Hrh1	1	0
ENSRNOP00000009893	Vav2	1	0
ENSRNOP00000010032	Npbwr1	1	0
ENSRNOP00000010255	Oprk1	1	0
ENSRNOP00000010596	Stk26	1	0
ENSRNOP00000010850	Cnr1	1	0
ENSRNOP00000011130	Lyn	1	0
ENSRNOP00000011219	Ptk2	1	0
ENSRNOP00000011883	Mtnr1b	1	0
ENSRNOP00000011937	Arpc4	1	0
ENSRNOP00000011963	Gnb5	1	0
ENSRNOP00000012322	Adra2c	1	0
ENSRNOP00000012342	Cnr2	1	0
ENSRNOP00000012379	Aplnr	1	0
ENSRNOP00000012432	Hck	1	0
ENSRNOP00000012588	Kras	1	0
ENSRNOP00000012736	Adra1a	1	0
ENSRNOP00000012847	Cct4	1	0
ENSRNOP00000012913	Prokr1	1	0
ENSRNOP00000013342	Spry2	1	0
ENSRNOP00000013408	Htr2a	1	0
ENSRNOP00000013618	Htr1a	1	0
ENSRNOP00000013705	Ccr4	1	0
ENSRNOP00000013779	Fgr	1	0
ENSRNOP00000014034	Ptger3	1	0
ENSRNOP00000014084	Oprd1	1	0
ENSRNOP00000014175	Agtr1b	1	0
ENSRNOP00000014219	Gngt1	1	0
ENSRNOP00000014309	Ptpn1	1	0
ENSRNOP00000014871	Gnb4	1	0

ENSRNOP00000015687	Grk5	1	0
ENSRNOP00000015824	Hcrtr2	1	0
ENSRNOP00000015886	Cct5	1	0
ENSRNOP00000016047	Htr1d	1	0
ENSRNOP00000016162	Cab39l	1	0
ENSRNOP00000016215	Nmbr	1	0
ENSRNOP00000016286	Ifngr1	1	0
ENSRNOP00000016395	Kiss1r	1	0
ENSRNOP00000016580	Cxcr5	1	0
ENSRNOP00000016784	Trio	1	0
ENSRNOP00000017411	Htr1b	1	0
ENSRNOP00000017607	Grm2	1	0
ENSRNOP00000018021	Iqgap1	1	0
ENSRNOP00000018492	Tnfrsf14	1	0
ENSRNOP00000018556	Pde7b	1	0
ENSRNOP00000018584	Adra2b	1	0
ENSRNOP00000018600	P2ry12	1	0
ENSRNOP00000018674	Hcrtr1	1	0
ENSRNOP00000018877	Il6st	1	0
ENSRNOP00000018952	Npy1r	1	0
ENSRNOP00000018976	Npy5r	1	0
ENSRNOP00000019109	Cxcr2	1	0
ENSRNOP00000019267	Igf1r	1	0
ENSRNOP00000019283	Erbb4	1	0
ENSRNOP00000019404	Frs3	1	0
ENSRNOP00000019465	Stat1	1	0
ENSRNOP00000019473	S1pr3	1	0
ENSRNOP00000019531	Tcp1	1	0
ENSRNOP00000019579	Irs1	1	0
ENSRNOP00000019680	Cttnbp2nl	1	0
ENSRNOP00000020663	Ppp2cb	1	0
ENSRNOP00000020700	Adcy7	1	0
ENSRNOP00000021030	Cct7	1	0
ENSRNOP00000021223	Arhgap35	1	0
ENSRNOP00000021390	Cd3g	1	0
ENSRNOP00000021480	Gnb3	1	0
ENSRNOP00000021489	Cd3d	1	0
ENSRNOP00000021976	Strn4	1	0
ENSRNOP00000022363	Hras	1	0
ENSRNOP00000022400	Galr1	1	0
ENSRNOP00000022401	Tln1	1	0
ENSRNOP00000022744	Hrh4	1	0
ENSRNOP00000023301	Myh6	1	0
ENSRNOP00000023586	Chrm4	1	0
ENSRNOP00000024137	Drd4	1	0
ENSRNOP00000024186	Myh7	1	0

ENSRNOP00000024270	Sike1	1	0
ENSRNOP00000024272	Apbb1ip	1	0
ENSRNOP00000024487	Stk25	1	0
ENSRNOP00000025036	Strip1	1	0
ENSRNOP00000025312	Jak3	1	0
ENSRNOP00000025451	Sstr5	1	0
ENSRNOP00000025824	Cct3	1	0
ENSRNOP00000025859	Myh7b	1	0
ENSRNOP00000026210	Pik3r2	1	0
ENSRNOP00000026373	Gnao1	1	0
ENSRNOP00000026457	Pde4c	1	0
ENSRNOP00000026558	Ackr3	1	0
ENSRNOP00000026586	Pde2a	1	0
ENSRNOP00000026601	Mk1	1	0
ENSRNOP00000026662	Stat5a	1	0
ENSRNOP00000026760	Stat3	1	0
ENSRNOP00000027073	Uba52	1	0
ENSRNOP00000027132	Myh14	1	0
ENSRNOP00000027813	Vav3	1	0
ENSRNOP00000029234	Cct2	1	0
ENSRNOP00000029992	Cd274	1	0
ENSRNOP00000030928	Cdc42	1	0
ENSRNOP00000031611	Ifnar1	1	0
ENSRNOP00000031615	Ptk2b	1	0
ENSRNOP00000035136	RGD1562847	1	0
ENSRNOP00000035440	Myh9	1	0
ENSRNOP00000035786	LOC100910021	1	0
ENSRNOP00000036086	Tek	1	0
ENSRNOP00000036862	Irs2	1	0
ENSRNOP00000040591	Erbb2	1	0
ENSRNOP00000046362	Myh4	1	0
ENSRNOP00000034687	Agtr1a	1	0
ENSRNOP00000022059	Grm5	1	0
ENSRNOP00000027932	Tbxa2r	1	0
ENSRNOP00000023829	Htr2b	1	0
ENSRNOP00000022451	Rgs19	1	0
ENSRNOP00000051809	Uts2r	1	0
ENSRNOP00000019319	Grm1	1	0
ENSRNOP00000025847	Adrbk1	1	0
ENSRNOP00000060345	Htr2c	1	0
ENSRNOP00000063137	Cckar	1	0
ENSRNOP00000035997	Ntsr1	1	0
ENSRNOP00000028877	Adra1d	1	0
ENSRNOP00000024785	Chrm1	1	0
ENSRNOP00000067435	Chrm3	1	0
ENSRNOP00000053557	Ffar3	1	0

ENSRNOP00000028532	Ffar2	1	0
ENSRNOP00000039072	Kalrn	1	0
ENSRNOP00000038418	Ghsr	1	0
ENSRNOP00000021625	Npsr1	1	0
ENSRNOP00000024077	Cckbr	1	0
ENSRNOP00000027647	Ltb4r	1	0
ENSRNOP00000065624	F2r	1	0
ENSRNOP00000054967	Ednra	1	0
ENSRNOP00000065253	Ptgfr	1	0
ENSRNOP00000051845	Gcgr	1	0
ENSRNOP00000028533	Ffar1	1	0
ENSRNOP00000027619	Ltb4r2	1	0
ENSRNOP00000028889	Prokr2	1	0
ENSRNOP00000025906	Ilk	1	0
ENSRNOP00000061683	Pdpk1	1	0
ENSRNOP00000040409	Rap1a	1	0
ENSRNOP00000028038	Shc1	1	0
ENSRNOP00000063859	Ptprc	1	0
ENSRNOP00000038369	Akt1	1	0
ENSRNOP00000044732	Prkaca	1	0
ENSRNOP00000067147	Npy2r	1	0
ENSRNOP00000062228	Prkacb	1	0
ENSRNOP00000038994	Adcy2	1	0
ENSRNOP00000051290	Oprm1	1	0
ENSRNOP00000032501	Rxfp3	1	0
ENSRNOP00000067355	Sstr1	1	0
ENSRNOP00000046455	Mapk12	1	0
ENSRNOP00000057815	Pde4a	1	0
ENSRNOP00000034328	Mtnr1a	1	0
ENSRNOP00000028034	S1pr2	1	0
ENSRNOP00000066965	Gng11	1	0
ENSRNOP00000060834	Pde10a	1	0
ENSRNOP00000047532	P2ry13	1	0
ENSRNOP00000052627	S1pr1	1	0
ENSRNOP00000028380	S1pr5	1	0
ENSRNOP00000043759	Drd2	1	0
ENSRNOP00000065598	Gng4	1	0
ENSRNOP00000060812	Grm4	1	0
ENSRNOP00000027719	Adcy4	1	0
ENSRNOP00000060777	Pde7a	1	0
ENSRNOP00000046488	Adcy5	1	0
ENSRNOP00000047053	Oprl1	1	0
ENSRNOP00000066242	Adra2a	1	0
ENSRNOP00000064558	C5ar1	1	0
ENSRNOP00000066231	Sstr4	1	0
ENSRNOP00000060405	Slmap	1	0

ENSRNOP00000039568	Fgfr1op2	1	0
ENSRNOP00000050172	Btla	1	0
ENSRNOP00000044119	Ghr	1	0
ENSRNOP00000050380	Unc5c	1	0
ENSRNOP00000061674	Pik3cd	1	0
ENSRNOP00000046028	Stat2	1	0
ENSRNOP00000050879	Lcp2	1	0
ENSRNOP00000064264	Vav1	1	0
ENSRNOP00000061649	Jak1	1	0
ENSRNOP00000053093	Yes1	1	0
ENSRNOP00000063226	Cbl	1	0
ENSRNOP00000060534	Pdgfrb	1	0
ENSRNOP00000046647	Lepr	1	0
ENSRNOP00000048018	Tyk2	1	0
ENSRNOP00000045635	Ntrk2	1	0
ENSRNOP00000067174	Cfl2	1	0
ENSRNOP00000062744	Myh10	1	0
ENSRNOP00000062782	LOC100909840	1	0
ENSRNOP00000061832	RSA-14-44	1	0
ENSRNOP00000059624	Cfl1	1	0
ENSRNOP00000064666	Pfn4	1	0
YM-178			
ENSRNOP00000036514	Rpl5	406	63301.96
ENSRNOP00000034364	Rpl17	395	99393.96
ENSRNOP00000014849	Rpl29	278	29069.68
ENSRNOP00000059382	Rps24	257	31132.49
ENSRNOP00000028887	Pcna	94	71958.83
ENSRNOP00000026760	Stat3	66	63760
ENSRNOP00000018173	Psma4	62	138403.3
ENSRNOP00000013375	Eif2s1	22	13566.7
ENSRNOP00000023628	Hspa4	21	22507
ENSRNOP00000010061	Dnaja1	17	8613
ENSRNOP00000004351	Slc9a3r1	12	7898
ENSRNOP00000066894	Khdrbs1	9	2891
ENSRNOP00000040162	LOC100910732	6	3605
ENSRNOP00000027073	Uba52	5	79067.26
ENSRNOP00000017230	RGD1565317	5	4987.4
ENSRNOP00000063201	RGD1561102	5	4987.4
ENSRNOP00000010720	Cand1	5	2166.5
ENSRNOP00000022897	Rps27	4	4065.79
ENSRNOP00000001265	Rpl21	4	0.2
ENSRNOP00000002177		4	0.2
ENSRNOP00000002194	Rpl24	4	0.2
ENSRNOP00000004213		4	0.2
ENSRNOP00000004303	RGD1559951	4	0.2
ENSRNOP00000005511		4	0.2

ENSRNOP00000005588	Rpl26	4	0.2
ENSRNOP00000006359	Rpl19	4	0.2
ENSRNOP00000006754	Rpl7a	4	0.2
ENSRNOP00000007683		4	0.2
ENSRNOP00000009046	Rpl34	4	0.2
ENSRNOP00000009431	Rpl7	4	0.2
ENSRNOP00000010383	LOC100911372	4	0.2
ENSRNOP00000010759	Rpl15	4	0.2
ENSRNOP00000011244	LOC688684	4	0.2
ENSRNOP00000011314	Rps20	4	0.2
ENSRNOP00000011333	Rps7	4	0.2
ENSRNOP00000013462	Rpl4	4	0.2
ENSRNOP00000013868	LOC100361180	4	0.2
ENSRNOP00000014493	Rpl32	4	0.2
ENSRNOP00000015408	RGD1565894	4	0.2
ENSRNOP00000016329	Rps3a	4	0.2
ENSRNOP00000019162	Rpl35	4	0.2
ENSRNOP00000019247	Rpl27a	4	0.2
ENSRNOP00000022184	Rps12	4	0.2
ENSRNOP00000022348	Rps23	4	0.2
ENSRNOP00000023935	Rps3	4	0.2
ENSRNOP00000025224	Rpsa	4	0.2
ENSRNOP00000025421	Rpl18a	4	0.2
ENSRNOP00000025888	Rps17	4	0.2
ENSRNOP00000026576	Rps16	4	0.2
ENSRNOP00000027086	Cnbd2	4	0.2
ENSRNOP00000027226	LOC100360573	4	0.2
ENSRNOP00000027976	Rpl13a	4	0.2
ENSRNOP00000028060	Rpl27	4	0.2
ENSRNOP00000028481	LOC100360647	4	0.2
ENSRNOP00000028555	Rpl18	4	0.2
ENSRNOP00000031078	Rpl31	4	0.2
ENSRNOP00000031121	LOC100362366	4	0.2
ENSRNOP00000032635	LOC100360449	4	0.2
ENSRNOP00000033369		4	0.2
ENSRNOP00000034657	LOC687780	4	0.2
ENSRNOP00000036391	Rpl23a	4	0.2
ENSRNOP00000037110	Rpl11	4	0.2
ENSRNOP00000037396	LOC100359986	4	0.2
ENSRNOP00000038065	Rpl6	4	0.2
ENSRNOP00000038214	LOC100911575	4	0.2
ENSRNOP00000039099	Rpl35al1	4	0.2
ENSRNOP00000039111		4	0.2
ENSRNOP00000040073	LOC103691563	4	0.2
ENSRNOP00000040548	RGD1563570	4	0.2
ENSRNOP00000040611	Rpl35a	4	0.2

ENSRNOP00000040955	LOC103691423	4	0.2
ENSRNOP00000041209	Rpl35al1	4	0.2
ENSRNOP00000041263		4	0.2
ENSRNOP00000041458	RGD1562381	4	0.2
ENSRNOP00000041625	LOC100362751	4	0.2
ENSRNOP00000041638	Rpl32	4	0.2
ENSRNOP00000041774	RGD1564730	4	0.2
ENSRNOP00000041817	Rpl9	4	0.2
ENSRNOP00000041920	RGD1559955	4	0.2
ENSRNOP00000041966	Rpl21	4	0.2
ENSRNOP00000042031	LOC100360647	4	0.2
ENSRNOP00000042068		4	0.2
ENSRNOP00000042127	RGD1566373	4	0.2
ENSRNOP00000042454		4	0.2
ENSRNOP00000042633		4	0.2
ENSRNOP00000042929	LOC688981	4	0.2
ENSRNOP00000042941	LOC500148	4	0.2
ENSRNOP00000043004	RGD1564606	4	0.2
ENSRNOP00000043092	RGD1561317	4	0.2
ENSRNOP00000044275	LOC100910017	4	0.2
ENSRNOP00000044605	LOC100361060	4	0.2
ENSRNOP00000044806	RGD1565117	4	0.2
ENSRNOP00000044949	RGD1560633	4	0.2
ENSRNOP00000045195	LOC100360439	4	0.2
ENSRNOP00000045335		4	0.2
ENSRNOP00000045344	RGD1559972	4	0.2
ENSRNOP00000045390	RGD1562265	4	0.2
ENSRNOP00000045458	Rpl26-ps1	4	0.2
ENSRNOP00000045849	RGD1561195	4	0.2
ENSRNOP00000045912		4	0.2
ENSRNOP00000046281	LOC686074	4	0.2
ENSRNOP00000046301	RGD1564839	4	0.2
ENSRNOP00000046515		4	0.2
ENSRNOP00000046600	LOC306079	4	0.2
ENSRNOP00000046953	LOC102554602	4	0.2
ENSRNOP00000047010		4	0.2
ENSRNOP00000047513	Rpl37a	4	0.2
ENSRNOP00000047759		4	0.2
ENSRNOP00000048003	Rpl36a-ps2	4	0.2
ENSRNOP00000048116	LOC100361854	4	0.2
ENSRNOP00000048252	LOC100911426	4	0.2
ENSRNOP00000048311	RGD1563157	4	0.2
ENSRNOP00000048422	RGD1562402	4	0.2
ENSRNOP00000048620	RGD1561453	4	0.2
ENSRNOP00000048624	RGD1565415	4	0.2
ENSRNOP00000048808	Rpl21	4	0.2

ENSRNOP00000048999	Rpl31l4	4	0.2
ENSRNOP00000049014	LOC100912182	4	0.2
ENSRNOP00000049054	Rpl35a	4	0.2
ENSRNOP00000049416	RGD1563835	4	0.2
ENSRNOP00000049635	LOC102550734	4	0.2
ENSRNOP00000049652	LOC689899	4	0.2
ENSRNOP00000049666		4	0.2
ENSRNOP00000049710		4	0.2
ENSRNOP00000050047		4	0.2
ENSRNOP00000050175		4	0.2
ENSRNOP00000050328	RGD1562055	4	0.2
ENSRNOP00000050533	RGD1563705	4	0.2
ENSRNOP00000051114		4	0.2
ENSRNOP00000051134		4	0.2
ENSRNOP00000051135	Rpl6-ps1	4	0.2
ENSRNOP00000051188	LOC103690996	4	0.2
ENSRNOP00000051312	Rpl21	4	0.2
ENSRNOP00000051318	LOC100359563	4	0.2
ENSRNOP00000051332		4	0.2
ENSRNOP00000051427	RGD1563958	4	0.2
ENSRNOP00000051482	Rpl31l3	4	0.2
ENSRNOP00000053863	Rplp2	4	0.2
ENSRNOP00000054048	Rpl36a	4	0.2
ENSRNOP00000054398	LOC100362027	4	0.2
ENSRNOP00000054497	LOC100912027	4	0.2
ENSRNOP00000054699	RGD1560069	4	0.2
ENSRNOP00000054703	Rpl34-ps1	4	0.2
ENSRNOP00000054740	LOC100362751	4	0.2
ENSRNOP00000055298		4	0.2
ENSRNOP00000055334	RGD1565767	4	0.2
ENSRNOP00000057262	LOC690384	4	0.2
ENSRNOP00000057758	Rpl26-ps2	4	0.2
ENSRNOP00000058614	RGD1564095	4	0.2
ENSRNOP00000058757		4	0.2
ENSRNOP00000058934	Rpl36	4	0.2
ENSRNOP00000064320	LOC100365810	4	0.2
ENSRNOP00000059662	LOC103690821	4	0.2
ENSRNOP00000066511		4	0.2
ENSRNOP00000062764		4	0.2
ENSRNOP00000067793		4	0.2
ENSRNOP00000066420	LOC100361143	4	0.2
ENSRNOP00000065877	LOC102548369	4	0.2
ENSRNOP00000065065	Rpl26-ps3	4	0.2
ENSRNOP00000065827		4	0.2
ENSRNOP00000066863	RGD1560821	4	0.2
ENSRNOP00000066260	LOC103692519	4	0.2

ENSRNOP00000066050	LOC100364116	4	0.2
ENSRNOP00000066016	LOC100912027	4	0.2
ENSRNOP00000066866	LOC103690796	4	0.2
ENSRNOP00000063004		4	0.2
ENSRNOP00000065371	LOC100911426	4	0.2
ENSRNOP00000067887	LOC100910721	4	0.2
ENSRNOP00000066077	LOC100362684	4	0.2
ENSRNOP00000060476	LOC680579	4	0.2
ENSRNOP00000059772	RGD1565566	4	0.2
ENSRNOP00000066750	LOC100909911	4	0.2
ENSRNOP00000061747	Rpl14	4	0.2
ENSRNOP00000065066	LOC100365839	4	0.2
ENSRNOP00000064822	RGD1565048	4	0.2
ENSRNOP00000064461		4	0.2
ENSRNOP00000061370		4	0.2
ENSRNOP00000065886	LOC100359951	4	0.2
ENSRNOP00000064959	LOC103692519	4	0.2
ENSRNOP00000067596	Rpl30l1	4	0.2
ENSRNOP00000067354	LOC100361079	4	0.2
ENSRNOP00000065423		4	0.2
ENSRNOP00000064270	RGD1561137	4	0.2
ENSRNOP00000067446	LOC100909911	4	0.2
ENSRNOP00000060629	RGD1561870	4	0.2
ENSRNOP00000064524	RGD1563124	4	0.2
ENSRNOP00000067572	Rps6	4	0.2
ENSRNOP00000061874		4	0.2
ENSRNOP00000000628	Cdkn1a	3	41275.25
ENSRNOP00000050173	Cdkn1b	3	41275.25
ENSRNOP00000047840	Tp53	3	24745.17
ENSRNOP00000004278	Rps4x	3	0.2
ENSRNOP00000006662	RGD1566369	3	0.2
ENSRNOP00000007194		3	0.2
ENSRNOP00000017602	LOC100359763	3	0.2
ENSRNOP00000017738		3	0.2
ENSRNOP00000019508	Rps2	3	0.2
ENSRNOP00000026528	Rps5	3	0.2
ENSRNOP00000027246	LOC100910336	3	0.2
ENSRNOP00000030289		3	0.2
ENSRNOP00000030371	Rps18	3	0.2
ENSRNOP00000031049	RGD1563300	3	0.2
ENSRNOP00000033144	Rps25	3	0.2
ENSRNOP00000033162	LOC500594	3	0.2
ENSRNOP00000035156	Rps15	3	0.2
ENSRNOP00000036690	LOC684988	3	0.2
ENSRNOP00000039276	LOC100359503	3	0.2
ENSRNOP00000039845	Rps19l1	3	0.2

ENSRNOP00000040056	RGD1561919	3	0.2
ENSRNOP00000040282	RGD1565912	3	0.2
ENSRNOP00000040306	RGD1563613	3	0.2
ENSRNOP00000041612		3	0.2
ENSRNOP00000041744	RGD1564138	3	0.2
ENSRNOP00000041853	LOC297756	3	0.2
ENSRNOP00000042164	LOC100359671	3	0.2
ENSRNOP00000042902	LOC100360843	3	0.2
ENSRNOP00000042935	Rps21-ps1	3	0.2
ENSRNOP00000043543	LOC103690015	3	0.2
ENSRNOP00000043988	Rps4x-ps9	3	0.2
ENSRNOP00000044197		3	0.2
ENSRNOP00000044301	LOC688899	3	0.2
ENSRNOP00000044874	RGD1559877	3	0.2
ENSRNOP00000045516	Wdr31	3	0.2
ENSRNOP00000046090	LOC100362298	3	0.2
ENSRNOP00000047371	Rps18l1	3	0.2
ENSRNOP00000047391	RGD1564597	3	0.2
ENSRNOP00000047999		3	0.2
ENSRNOP00000048289		3	0.2
ENSRNOP00000048658	LOC102554992	3	0.2
ENSRNOP00000048847		3	0.2
ENSRNOP00000051317		3	0.2
ENSRNOP00000053082	Rpl5l1	3	0.2
ENSRNOP00000056689		3	0.2
ENSRNOP00000056750	LOC100364509	3	0.2
ENSRNOP00000057658	Rps2-ps6	3	0.2
ENSRNOP00000062631	Rps15-ps2	3	0.2
ENSRNOP00000061250	Rps11	3	0.2
ENSRNOP00000063451	RGD1559724	3	0.2
ENSRNOP00000067306		3	0.2
ENSRNOP00000061911		3	0.2
ENSRNOP00000060568	Rps28	3	0.2
ENSRNOP00000065999	LOC100911337	3	0.2
ENSRNOP00000061442	LOC100362339	3	0.2
ENSRNOP00000064782		3	0.2
ENSRNOP00000065281	LOC100911337	3	0.2
ENSRNOP00000064678	LOC100912024	3	0.2
ENSRNOP00000064904		3	0.2
ENSRNOP00000066362	LOC100362987	3	0.2
ENSRNOP00000066808	LOC100910336	3	0.2
ENSRNOP00000067129	Rps27l	3	0.2
ENSRNOP00000067470	LOC683961	3	0.2
ENSRNOP00000065157		3	0.2
ENSRNOP00000066792	LOC100364509	3	0.2
ENSRNOP00000064853	LOC100911337	3	0.2

ENSRNOP00000067239		3	0.2
ENSRNOP00000065487	LOC100363452	3	0.2
ENSRNOP00000000603	Rpl10a	3	0
ENSRNOP00000001518	Rplp0	3	0
ENSRNOP00000005471	Rpl23	3	0
ENSRNOP00000005872	Rps27a	3	0
ENSRNOP00000009988	RGD1560831	3	0
ENSRNOP00000012255	LOC690096	3	0
ENSRNOP00000014905	LOC100360057	3	0
ENSRNOP00000015893		3	0
ENSRNOP00000018820	Rplp1	3	0
ENSRNOP00000020635	LOC100359922	3	0
ENSRNOP00000021161		3	0
ENSRNOP00000021725	Rpl12	3	0
ENSRNOP00000023368	Rpl38	3	0
ENSRNOP00000024678	Rps15a	3	0
ENSRNOP00000030437	RGD1563956	3	0
ENSRNOP00000047281	Rps27a-ps6	3	0
ENSRNOP00000048664	Rps27a	3	0
ENSRNOP00000049665	LOC103693375	3	0
ENSRNOP00000067080	Rpl8	3	0
ENSRNOP00000051203		3	0
ENSRNOP00000050202	LOC690468	3	0
ENSRNOP00000046669		3	0
ENSRNOP00000048495		3	0
ENSRNOP00000053991		3	0
ENSRNOP00000041329	LOC103693375	3	0
ENSRNOP00000049713	LOC103694404	3	0
ENSRNOP00000041462	Rpl12	3	0
ENSRNOP00000067411		3	0
ENSRNOP00000045098	LOC103694404	3	0
ENSRNOP00000039786		3	0
ENSRNOP00000055790	LOC103690821	3	0
ENSRNOP00000044553	Rpl39	3	0
ENSRNOP00000050353	Rpl38-ps2	3	0
ENSRNOP00000045739		3	0
ENSRNOP00000049286	Rps15al2	3	0
ENSRNOP00000046553	LOC100910370	3	0
ENSRNOP00000050700	LOC690335	3	0
ENSRNOP00000064566	Rpl8	3	0
ENSRNOP00000064197	Rpl12	3	0
ENSRNOP00000055671		3	0
ENSRNOP00000051743		3	0
ENSRNOP00000039179		3	0
ENSRNOP00000042022	LOC682793	3	0
ENSRNOP00000053160		3	0

ENSRNOP00000042288	LOC682793	3	0
ENSRNOP00000046578		3	0
ENSRNOP00000063355	LOC100361259	3	0
ENSRNOP00000045213	RGD1561636	3	0
ENSRNOP00000042277		3	0
ENSRNOP00000067881	RGD1564378	3	0
ENSRNOP00000064082	LOC100360491	3	0
ENSRNOP00000041199		3	0
ENSRNOP00000066592		3	0
ENSRNOP00000042242	Rps15al4	3	0
ENSRNOP00000065901		3	0
ENSRNOP00000046737	LOC100909878	3	0
ENSRNOP00000047511		3	0
ENSRNOP00000041435		3	0
ENSRNOP00000063142		3	0
ENSRNOP00000042560		3	0
ENSRNOP00000041530		3	0
ENSRNOP00000055393		3	0
ENSRNOP00000053986	RGD1565183	3	0
ENSRNOP00000044111	RGD1565170	3	0
ENSRNOP00000047749	LOC680441	3	0
ENSRNOP00000051016	LOC100364191	3	0
ENSRNOP00000046409		3	0
ENSRNOP00000049028	LOC680353	3	0
ENSRNOP00000040232		3	0
ENSRNOP00000047328	RGD1561333	3	0
ENSRNOP00000042286	LOC680512	3	0
ENSRNOP00000046070		3	0
ENSRNOP00000039287	LOC102550668	3	0
ENSRNOP00000040295	Rpl39l	3	0
ENSRNOP00000064745		3	0
ENSRNOP00000046487	RGD1562755	3	0
ENSRNOP00000060662	Rpl3	3	0
ENSRNOP00000041191		3	0
ENSRNOP00000048019	RGD1563145	3	0
ENSRNOP00000040966	Rpl10l	3	0
ENSRNOP00000042567		3	0
ENSRNOP00000049831		3	0
ENSRNOP00000044063	LOC686066	3	0
ENSRNOP00000055726	Rpl28	3	0
ENSRNOP00000049709		3	0
ENSRNOP00000018455	Sec61a1	2	22014.52
ENSRNOP00000036212	Sec61a2	2	22014.52
ENSRNOP00000000783	Cdk1	2	14350.58
ENSRNOP00000032191	Cdk2	2	14350.58
ENSRNOP00000060534	Pdgfrb	2	8544

ENSRNOP00000001417	Rac1	2	4308
ENSRNOP00000028411	Ccnd1	2	1942.17
ENSRNOP00000004881	Uchl5	2	1444
ENSRNOP00000007620	Cul1	2	1438
ENSRNOP00000021528	Cul3	2	1438
ENSRNOP00000025510	Txnl1	2	723
ENSRNOP00000000733	Fyn	2	715
ENSRNOP00000012432	Hck	2	715
ENSRNOP00000012739	Src	2	715
ENSRNOP00000012936	Lck	2	715
ENSRNOP00000053093	Yes1	2	715
ENSRNOP00000002834	Mrpl1	2	0
ENSRNOP00000004114	LOC690271	2	0
ENSRNOP00000004583		2	0
ENSRNOP00000005089	Mrps7	2	0
ENSRNOP00000005815	Mrpl13	2	0
ENSRNOP00000009556	LOC103692716	2	0
ENSRNOP00000011619	Mrpl15	2	0
ENSRNOP00000013548	Mrps2	2	0
ENSRNOP00000015278	LOC680700	2	0
ENSRNOP00000015756	Rpl22l1	2	0
ENSRNOP00000017280	Mrpl3	2	0
ENSRNOP00000019660	Rpl3l	2	0
ENSRNOP00000020451	Mrps5	2	0
ENSRNOP00000021625	Npsr1	2	0
ENSRNOP00000021803	Rpl7l1	2	0
ENSRNOP00000021899	Mrps9	2	0
ENSRNOP00000023456	Imp3	2	0
ENSRNOP00000024326	Mrto4	2	0
ENSRNOP00000024380	Mrpl2	2	0
ENSRNOP00000025007	Mrps11	2	0
ENSRNOP00000025217	Rpl17	2	0
ENSRNOP00000027029	Mrps12	2	0
ENSRNOP00000027091	mrpl11	2	0
ENSRNOP00000027780	Rps27a-ps12	2	0
ENSRNOP00000028517	Mrpl16	2	0
ENSRNOP00000034042	mrpl24	2	0
ENSRNOP00000034767	RGD1359290	2	0
ENSRNOP00000036343	LOC688473	2	0
ENSRNOP00000034846	Hsp90b1	2	0
ENSRNOP00000026920	Hsp90ab1	2	0
ENSRNOP00000061858	Grpel2	2	0
ENSRNOP00000042920	Rpl22l2	2	0
ENSRNOP00000049205	Rpl37	2	0
ENSRNOP00000048903	LOC100363469	2	0
ENSRNOP00000054474	LOC100360654	2	0

ENSRNOP00000039155	LOC100360841	2	0
ENSRNOP00000039774	RGD1560017	2	0
ENSRNOP00000048979	Rps27a-ps5	2	0
ENSRNOP00000050941	RGD1564325	2	0
ENSRNOP00000044116	RGD1561310	2	0
ENSRNOP00000056331	LOC100360654	2	0
ENSRNOP00000042092	Rsl1d1	2	0
ENSRNOP00000044837		2	0
ENSRNOP00000065173		2	0
ENSRNOP00000066548		2	0
ENSRNOP00000045940		2	0
ENSRNOP00000039797	LOC103690888	2	0
ENSRNOP00000043087	Gfm2	2	0
ENSRNOP00000039429		2	0
ENSRNOP00000049546	Rps4y2	2	0
ENSRNOP00000036943		2	0
ENSRNOP00000047760		2	0
ENSRNOP00000045798	LOC367195	2	0
ENSRNOP00000036682	Mrpl1	2	0
ENSRNOP00000056260	Rps14	2	0
ENSRNOP00000041821	Eef2	2	0
ENSRNOP00000058859		2	0
ENSRNOP00000052049	Eftud2	2	0
ENSRNOP00000056140		2	0
ENSRNOP00000039003		2	0
ENSRNOP00000044563	LOC680646	2	0
ENSRNOP00000040081	Gfm1	2	0
ENSRNOP00000051848	Mrpl12	2	0
ENSRNOP00000045007	Mrpl17	2	0
ENSRNOP00000049519	Efl1	2	0
ENSRNOP00000047767		2	0
ENSRNOP00000048713		2	0
ENSRNOP00000055288	RGD1562399	2	0
ENSRNOP00000063128	Rpl7a	2	0
ENSRNOP00000045954		2	0
ENSRNOP00000046157	RGD1564469	2	0
ENSRNOP00000042800		2	0
ENSRNOP00000046036		2	0
ENSRNOP00000045893	Mrpl4	2	0
ENSRNOP00000046427		2	0
ENSRNOP00000049619		2	0
ENSRNOP00000046067	Mrps10	2	0
ENSRNOP00000049626		2	0
ENSRNOP00000063940		2	0
ENSRNOP00000047911	RGD1563352	2	0
ENSRNOP00000047355		2	0

ENSRNOP00000065327		2	0
ENSRNOP00000052873	LOC100911847	2	0
ENSRNOP00000061642	Rps10	2	0
ENSRNOP00000000142	Dnajb5	1	0
ENSRNOP00000000206	Ep300	1	0
ENSRNOP00000000528	Psmb8	1	0
ENSRNOP00000000529	Tap1	1	0
ENSRNOP00000000532	Psmb9	1	0
ENSRNOP00000000750	Ube2d1	1	0
ENSRNOP00000001201	Hsph1	1	0
ENSRNOP00000001373	Eif2b1	1	0
ENSRNOP00000001392	Eif2ak1	1	0
ENSRNOP00000001444	Rfc3	1	0
ENSRNOP00000001498	Rfc5	1	0
ENSRNOP00000001825	Mcm7	1	0
ENSRNOP00000001989	Rfc2	1	0
ENSRNOP00000002037	Psmb1	1	0
ENSRNOP00000002299	Chaf1b	1	0
ENSRNOP00000002321	Eif2b5	1	0
ENSRNOP00000002358	Psmd2	1	0
ENSRNOP00000002484	Eif4a2	1	0
ENSRNOP00000002487	Rfc4	1	0
ENSRNOP00000002510	Mcm4	1	0
ENSRNOP00000002533	Mapk1	1	0
ENSRNOP00000003050	Kit	1	0
ENSRNOP00000003458	Socs1	1	0
ENSRNOP00000003768	Bcl2	1	0
ENSRNOP00000003907	Rfc1	1	0
ENSRNOP00000003940	Socs3	1	0
ENSRNOP00000003954	Ccnb3	1	0
ENSRNOP00000004229	Rpa1	1	0
ENSRNOP00000004232	Parp1	1	0
ENSRNOP00000004283	Psmd12	1	0
ENSRNOP00000004499	Mcm9	1	0
ENSRNOP00000004969	Mcm6	1	0
ENSRNOP00000005329	Psmc1	1	0
ENSRNOP00000005347	Grb2	1	0
ENSRNOP00000005363	Dnajb9	1	0
ENSRNOP00000005576	Dtl	1	0
ENSRNOP00000005577	Rps29	1	0
ENSRNOP00000005832	Klhl12	1	0
ENSRNOP00000005835	Pole2	1	0
ENSRNOP00000006087	Egfr	1	0
ENSRNOP00000006188	Myc	1	0
ENSRNOP00000006470	Gen1	1	0
ENSRNOP00000006591	Npm1	1	0

ENSRNOP00000006796	Erbb3	1	0
ENSRNOP00000006852	Hus1	1	0
ENSRNOP00000007079	Crebbp	1	0
ENSRNOP00000007676	Skp1	1	0
ENSRNOP00000007698	Gadd45a	1	0
ENSRNOP00000007763	Eif2b4	1	0
ENSRNOP00000007828	Dlg5	1	0
ENSRNOP00000007963	Cdc27	1	0
ENSRNOP00000008451	Eif2ak3	1	0
ENSRNOP00000008504	Hspa2	1	0
ENSRNOP00000008730	Eif2b2	1	0
ENSRNOP00000008930	Grpel1	1	0
ENSRNOP00000009129	Ar	1	0
ENSRNOP00000009222	Eif2ak4	1	0
ENSRNOP00000009249	Psmd6	1	0
ENSRNOP00000009649	Psmc6	1	0
ENSRNOP00000009666	Psma6	1	0
ENSRNOP00000009994	Rac2	1	0
ENSRNOP00000010151	Il23r	1	0
ENSRNOP00000010712	Fos	1	0
ENSRNOP00000010753	Psma3	1	0
ENSRNOP00000010935	Usp1	1	0
ENSRNOP00000010968	Irf1	1	0
ENSRNOP00000011123	Rpa3	1	0
ENSRNOP00000011130	Lyn	1	0
ENSRNOP00000011219	Ptk2	1	0
ENSRNOP00000011226	Chek1	1	0
ENSRNOP00000011455	Bag1	1	0
ENSRNOP00000011565	Mrps15	1	0
ENSRNOP00000011653	Ube2e1	1	0
ENSRNOP00000011732	Jun	1	0
ENSRNOP00000011948		1	0
ENSRNOP00000012492	Orc1	1	0
ENSRNOP00000012597	Cdk6	1	0
ENSRNOP00000013070	Rad52	1	0
ENSRNOP00000013176	Apex1	1	0
ENSRNOP00000013919	H2afz	1	0
ENSRNOP00000013997	Psmc5	1	0
ENSRNOP00000014167	Mtor	1	0
ENSRNOP00000015120	Socs4	1	0
ENSRNOP00000015618	Psmb2	1	0
ENSRNOP00000015641	Foxp3	1	0
ENSRNOP00000015747		1	0
ENSRNOP00000015757	Psmc3	1	0
ENSRNOP00000015813	Tnks	1	0
ENSRNOP00000015946	Psma1	1	0

ENSRNOP00000016189	Poli	1	0
ENSRNOP00000016204	RGD1559708	1	0
ENSRNOP00000016450	Psmc2	1	0
ENSRNOP00000016664	Il17a	1	0
ENSRNOP00000016742	LOC103694902	1	0
ENSRNOP00000016876	Psmb7	1	0
ENSRNOP00000016942	Syk	1	0
ENSRNOP00000017053	Dnaja4	1	0
ENSRNOP00000017081	Mcm3	1	0
ENSRNOP00000017381	Dnajb4	1	0
ENSRNOP00000017549	Rpa2	1	0
ENSRNOP00000018005	Psmb5	1	0
ENSRNOP00000018147	Pola1	1	0
ENSRNOP00000018251	Gadd45g	1	0
ENSRNOP00000018449	Msh3	1	0
ENSRNOP00000018877	Il6st	1	0
ENSRNOP00000018923	Cdt1	1	0
ENSRNOP00000019267	Igf1r	1	0
ENSRNOP00000019283	Erbb4	1	0
ENSRNOP00000019288	Pold2	1	0
ENSRNOP00000019465	Stat1	1	0
ENSRNOP00000019574	Txndc17	1	0
ENSRNOP00000019767	Fahd1	1	0
ENSRNOP00000019799	Lig1	1	0
ENSRNOP00000020330	Nck1	1	0
ENSRNOP00000020346	Socs5	1	0
ENSRNOP00000021538	Msh2	1	0
ENSRNOP00000021923	Msh6	1	0
ENSRNOP00000022138	Nsa2	1	0
ENSRNOP00000022231	Mcm2	1	0
ENSRNOP00000022256	Ns5atp9	1	0
ENSRNOP00000022573	Dnaja2	1	0
ENSRNOP00000022963	Pgm2l1	1	0
ENSRNOP00000023029	Nck2	1	0
ENSRNOP00000023036	Zap70	1	0
ENSRNOP00000023137	Poll	1	0
ENSRNOP00000023886	Pias2	1	0
ENSRNOP00000024375	Mutyh	1	0
ENSRNOP00000024406	Ube2i	1	0
ENSRNOP00000024557	Rad1	1	0
ENSRNOP00000024831	Smad7	1	0
ENSRNOP00000024875	Pold3	1	0
ENSRNOP00000025312	Jak3	1	0
ENSRNOP00000025507	Pold4	1	0
ENSRNOP00000025902	Prkcq	1	0
ENSRNOP00000025977	Il12rb1	1	0

ENSRNOP00000026049	Polh	1	0
ENSRNOP00000026139	Chtf18	1	0
ENSRNOP00000026354	Stat5b	1	0
ENSRNOP00000026364	Irf9	1	0
ENSRNOP00000026637	Vegfa	1	0
ENSRNOP00000026662	Stat5a	1	0
ENSRNOP00000026797	Pold1	1	0
ENSRNOP00000026871	Gadd45b	1	0
ENSRNOP00000027057	Xrcc1	1	0
ENSRNOP00000027305	Eef1g	1	0
ENSRNOP00000027842	Fen1	1	0
ENSRNOP00000028141	Cdc25a	1	0
ENSRNOP00000029336	Mrpl22	1	0
ENSRNOP00000030928	Cdc42	1	0
ENSRNOP00000032662	LOC100910528	1	0
ENSRNOP00000040086	LOC502176	1	0
ENSRNOP00000040703	Rps29	1	0
ENSRNOP00000041788	RGD1561871	1	0
ENSRNOP00000041943	LOC100361240	1	0
ENSRNOP00000043270	Rps29	1	0
ENSRNOP00000043693	Rps10l1	1	0
ENSRNOP00000044909	Rps29	1	0
ENSRNOP00000046992	RGD1564698	1	0
ENSRNOP00000047300	Rasa1	1	0
ENSRNOP00000052160	Hnrnpa1	1	0
ENSRNOP00000063624	Prmt1	1	0
ENSRNOP00000028143	Pten	1	0
ENSRNOP00000031764	Slc34a1	1	0
ENSRNOP00000010690	Nf2	1	0
ENSRNOP00000042886	Trpc4	1	0
ENSRNOP00000009400	Trpc5	1	0
ENSRNOP00000004391	Slc4a4	1	0
ENSRNOP00000046593	Ezr	1	0
ENSRNOP00000021270	Slc9a2	1	0
ENSRNOP00000008759	Slc4a7	1	0
ENSRNOP00000020711	Slc9a3	1	0
ENSRNOP00000028435	Pth1r	1	0
ENSRNOP00000065828	Hspa8	1	0
ENSRNOP00000050605	Hspa1b	1	0
ENSRNOP00000020854	Hspa14	1	0
ENSRNOP00000042159	Hspa8	1	0
ENSRNOP00000025064	Hspa5	1	0
ENSRNOP00000015474	Hspa4l	1	0
ENSRNOP00000063974	Hspa1l	1	0
ENSRNOP00000067749	Hspa1b	1	0
ENSRNOP00000067224		1	0

ENSRNOP00000058593	LOC680121	1	0
ENSRNOP00000010956	Cul5	1	0
ENSRNOP00000060639	Cul4b	1	0
ENSRNOP00000026653	Cul4a	1	0
ENSRNOP00000024841	Eif2b3	1	0
ENSRNOP00000049629	Eif4g1	1	0
ENSRNOP00000022437	Eif3j	1	0
ENSRNOP00000067694	Eif2ak2	1	0
ENSRNOP00000057188	Eif3b	1	0
ENSRNOP00000013695	Eif5	1	0
ENSRNOP00000023786	Eif2s2	1	0
ENSRNOP00000025782	Eif3c	1	0
ENSRNOP00000063484	Eif3a	1	0
ENSRNOP00000067288		1	0
ENSRNOP00000049419	Eif4a1	1	0
ENSRNOP00000066950	Psma2	1	0
ENSRNOP00000025819	Psmc4	1	0
ENSRNOP00000065857	LOC100911238	1	0
ENSRNOP00000019642	Psmd13	1	0
ENSRNOP00000026928	Psma5	1	0
ENSRNOP00000055036	RGD1564425	1	0
ENSRNOP00000066229		1	0
ENSRNOP00000026462	Psmb10	1	0
ENSRNOP00000019104	Psmd7	1	0
ENSRNOP00000025887	Psme1	1	0
ENSRNOP00000026507	Psmb6	1	0
ENSRNOP00000026279	Psme2	1	0
ENSRNOP00000028484	Psmb4	1	0
ENSRNOP00000031927	Smurf1	1	0
ENSRNOP00000046491	Hnrnpd	1	0
ENSRNOP00000028589	Psmd4	1	0
ENSRNOP00000054528	Psmd9	1	0
ENSRNOP00000037928	Psmd3	1	0
ENSRNOP00000020323	Ube2c	1	0
ENSRNOP00000042447	Psma8	1	0
ENSRNOP00000032953	RGD1562029	1	0
ENSRNOP00000066877	LOC100911238	1	0
ENSRNOP00000024306	Psmd1	1	0
ENSRNOP00000027937	Psmd8	1	0
ENSRNOP00000019781	Smurf2	1	0
ENSRNOP00000025433	Psmd5	1	0
ENSRNOP00000062146	Psmd11	1	0
ENSRNOP00000026467	Dnajb2	1	0
ENSRNOP00000027616	Bag3	1	0
ENSRNOP00000026921	Stub1	1	0
ENSRNOP00000024256	Dnajb13	1	0

ENSRNOP00000026665	Clpb	1	0
ENSRNOP00000032313	Dnajb1	1	0
ENSRNOP00000028743	Stip1	1	0
ENSRNOP00000047030	Hsf1	1	0
ENSRNOP00000047793	Ret	1	0
ENSRNOP00000034983	Stat6	1	0
ENSRNOP00000027441	Pias4	1	0
ENSRNOP00000043542	Bcl2l1	1	0
ENSRNOP00000041734	Cish	1	0
ENSRNOP00000046647	Leprot	1	0
ENSRNOP00000066672	Rhoa	1	0
ENSRNOP00000028814	Pias3	1	0
ENSRNOP00000040591	Erbb2	1	0
ENSRNOP00000061649	Jak1	1	0
ENSRNOP00000065216	Pou5f1	1	0
ENSRNOP00000044119	Ghr	1	0
ENSRNOP00000059152	Pias1	1	0
ENSRNOP00000048018	Tyk2	1	0
ENSRNOP00000044552	Rela	1	0
ENSRNOP00000038369	Akt1	1	0
ENSRNOP00000041842	Ptpn11	1	0
ENSRNOP00000066184	Lep	1	0
ENSRNOP00000028997	Ube2u	1	0
ENSRNOP00000061228	LOC100911727	1	0
ENSRNOP00000051355	Dntt	1	0
ENSRNOP00000039931	Ccna1	1	0
ENSRNOP00000053270	Rad51	1	0
ENSRNOP00000063994	Chaf1a	1	0
ENSRNOP00000063831	Dnmt1	1	0
ENSRNOP00000033080	Sprtn	1	0
ENSRNOP00000032177	Cdc6	1	0
ENSRNOP00000054053	Rev3l	1	0
ENSRNOP00000060925	Apex2	1	0
ENSRNOP00000062102	Ube2v2	1	0
ENSRNOP00000062763	Kmt5a	1	0
ENSRNOP00000053707	Ung	1	0
ENSRNOP00000034638	Poln	1	0
ENSRNOP00000056107	Ercc5	1	0
ENSRNOP00000053576	LOC100362927	1	0
ENSRNOP00000065285	RGD1561853	1	0
ENSRNOP00000061834	Mlh1	1	0
ENSRNOP00000067214	Zfpl1	1	0
ENSRNOP00000036568	Rbbp4	1	0
ENSRNOP00000053086	Tyms	1	0
ENSRNOP00000058920	Pole	1	0
ENSRNOP00000062524	Mcm5	1	0

ENSRNOP00000058174	Ube2a	1	0
ENSRNOP00000064704	Ccnd3	1	0
ENSRNOP00000059094	Cdc7	1	0
ENSRNOP00000059807	Rev1	1	0
ENSRNOP00000055596	Wrn	1	0
ENSRNOP00000063400	Rad18	1	0
ENSRNOP00000028898	Mcm8	1	0
ENSRNOP00000034754	Cdk4	1	0
ENSRNOP00000045761	RGD1560186	1	0
ENSRNOP00000067146	Mrpl36	1	0
ENSRNOP00000067869	RGD1560073	1	0

Table 6. GO enrichment of BAT protein-protein interaction network

Pathway	Total	Expected	Hits	P.Value	FDR
SHT					
Biological Process					
Anatomical structure formation involved in morphogenesis	38	0.504	13	9.79E-16	6.61E-13
Developmental growth	31	0.412	12	2.23E-15	7.51E-13
Regulation of DNA binding	90	1.19	14	1.12E-11	2.12E-09
ER_nucleus signaling pathway	74	0.982	13	1.26E-11	2.12E-09
Cytokine biosynthetic process	151	2	15	1.36E-09	1.84E-07
Defense response	71	0.943	11	2.05E-09	2.31E-07
Stress_activated protein kinase signaling cascade	41	0.544	9	2.48E-09	2.39E-07
Striated muscle contraction	461	6.12	24	8.67E-09	7.31E-07
Monocarboxylic acid transport	160	2.12	14	2.56E-08	1.92E-06
DNA damage checkpoint	62	0.823	9	1.13E-07	7.64E-06
Vitamin metabolic process	215	2.85	15	1.64E-07	1.01E-05
Activation of JUN kinase activity	386	5.12	20	1.84E-07	1.03E-05
Inflammatory response	29	0.385	6	1.84E-06	9.53E-05
Response to DNA damage stimulus	17	0.226	5	2.10E-06	0.000101
Microtubule_based process	93	1.23	9	3.78E-06	0.00017
Catabolic process	153	2.03	11	5.87E-06	0.000248
Negative regulation of MAP kinase activity	102	1.35	9	8.14E-06	0.000323
Homeostasis of number of cells	160	2.12	11	9.01E-06	0.000323
Post_translational protein modification	4	0.0531	3	9.09E-06	0.000323
Regulation of peptidyl_tyrosine phosphorylation	39	0.518	6	1.13E-05	0.000381
RNA 3'_end processing	40	0.531	6	1.32E-05	0.000423
Adenylate cyclase_activating G_protein coupled receptor signaling pathway	26	0.345	5	2.03E-05	0.000623
Nuclear export	16	0.212	4	4.80E-05	0.00141
Negative regulation of cell migration	389	5.16	16	5.90E-05	0.00166
Regulation of small GTPase mediated signal transduction	36	0.478	5	0.000105	0.00273
Humoral immune response	1970	26.1	45	0.000105	0.00273
Carboxylic acid metabolic process	333	4.42	14	0.000138	0.00346
Phototransduction	61	0.81	6	0.000151	0.00365
Negative regulation of programmed cell death	23	0.305	4	0.000217	0.00506

Regulation of RNA metabolic process	11	0.146	3	0.00035	0.00788
Actin filament polymerization	168	2.23	9	0.000399	0.00869
Small GTPase mediated signal transduction	104	1.38	7	0.00046	0.0097
Adenylate cyclase_modulating G_protein coupled receptor signaling pathway	76	1.01	6	0.000506	0.0103
Meiosis I	214	2.84	10	0.000565	0.0112
Carbohydrate biosynthetic process	13	0.173	3	0.000595	0.0112
Detection of stimulus	13	0.173	3	0.000595	0.0112
Regulation of transcription, DNA_dependent	434	5.76	15	0.000655	0.012
Neuron projection development	81	1.08	6	0.000711	0.0126
Microtubule polymerization or depolymerization	34	0.451	4	0.00102	0.0176
Muscle organ development	36	0.478	4	0.00127	0.0213
Generation of neurons	17	0.226	3	0.00136	0.0224
Oligosaccharide metabolic process	5	0.0664	2	0.00171	0.0262
Response to hormone stimulus	5	0.0664	2	0.00171	0.0262
Signal transduction in response to DNA damage	5	0.0664	2	0.00171	0.0262
DNA_dependent transcription, initiation	99	1.31	6	0.00202	0.0303
Keratinocyte differentiation	345	4.58	12	0.00216	0.0317
Proteoglycan biosynthetic process	21	0.279	3	0.00256	0.0368
Regulation of cellular protein metabolic process	184	2.44	8	0.00315	0.0442
Molecular Function					
Exonuclease activity	63	0.708	11	8.87E-11	2.93E-08
Steroid dehydrogenase activity	334	3.76	20	8.62E-10	1.43E-07
Lipase activity	69	0.776	10	4.41E-09	4.87E-07
Regulation of DNA_dependent transcription, elongation	41	0.461	8	1.44E-08	1.19E-06
Neuropeptide hormone activity	1270	14.3	37	3.10E-08	2.06E-06
Deoxyribonuclease activity	23	0.259	6	1.55E-07	8.57E-06
Carbon_carbon lyase activity	17	0.191	5	9.24E-07	4.37E-05
Copper ion binding	9	0.101	4	1.84E-06	7.62E-05
Transmembrane receptor protein tyrosine kinase activity	13	0.146	4	1.01E-05	0.000371
Kinase activity	212	2.38	11	2.62E-05	0.000792
Sodium channel activity	78	0.877	7	2.63E-05	0.000792
Cation_transporting ATPase activity	64	0.72	6	7.91E-05	0.00218

Nucleobase_containing compound transmembrane transporter activity	291	3.27	12	0.000105	0.00268
MRNA binding	191	2.15	9	0.000299	0.00684
G_protein coupled receptor binding	53	0.596	5	0.00031	0.00684
Antigen binding	13	0.146	3	0.000366	0.00757
Hydrolase activity, acting on acid anhydrides	512	5.76	15	0.00062	0.0121
Organic anion transmembrane transporter activity	65	0.731	5	0.000801	0.0147
GTPase binding	17	0.191	3	0.000842	0.0147
Nuclease activity	225	2.53	9	0.000979	0.0162
Small conjugating protein ligase activity	104	1.17	6	0.00111	0.0175
Delayed rectifier potassium channel activity	5	0.0562	2	0.00123	0.0185
Enzyme inhibitor activity	81	0.911	5	0.00215	0.031
Hydrolase activity, acting on glycosyl bonds	25	0.281	3	0.00267	0.0368
Protein serine/threonine phosphatase activity	168	1.89	7	0.00286	0.0378
Phosphatase regulator activity	431	4.85	12	0.00335	0.0426
Cellular Component					
Intermediate filament	688	7.23	32	8.67E-13	1.53E-10
Nuclear lumen	71	0.746	12	8.96E-12	7.89E-10
Spindle microtubule	3420	36	74	2.14E-11	1.26E-09
Cell_cell junction	307	3.23	19	5.50E-10	2.42E-08
Vesicle coat	292	3.07	16	7.54E-08	2.65E-06
Macromolecular complex	177	1.86	11	2.66E-06	7.80E-05
Vesicle membrane	1670	17.5	36	1.86E-05	0.000467
External side of plasma membrane	146	1.53	9	2.36E-05	0.000512
Membrane	34	0.357	5	2.62E-05	0.000512
Centrosome	1180	12.4	28	3.72E-05	0.000654
Cytoplasmic vesicle	104	1.09	7	0.000112	0.00176
Membrane coat	222	2.33	10	0.00012	0.00176
Actin cytoskeleton	145	1.52	8	0.000147	0.00194
Lysosome	186	1.95	9	0.000154	0.00194
Chromosome	4070	42.8	64	0.000166	0.00195
Voltage_gated potassium channel complex	451	4.74	14	0.000293	0.00322
Cell leading edge	260	2.73	10	0.000428	0.00443
Pore complex	40	0.42	4	8.00E-04	0.00782
Acetylcholine_gated channel complex	150	1.58	7	0.00104	0.00964
Apical junction complex	467	4.91	13	0.00132	0.0116
Synaptic vesicle	171	1.8	7	0.00221	0.0185

Cytosol	177	1.86	7	0.00268	0.0214
Cortical cytoskeleton	137	1.44	6	0.00325	0.0249
Transport vesicle	96	1.01	5	0.00341	0.025
Eukaryotic translation initiation factor 3 complex	191	2.01	7	0.00408	0.0287
YM-178					
Biological Process					
Chromatin assembly or disassembly	248	4.55	77	1.92E-76	1.29E-73
Regulation of DNA binding	90	1.65	14	8.52E-10	2.87E-07
Sensory perception of taste	5	0.0917	5	1.99E-09	4.47E-07
Glucosamine metabolic process	70	1.28	12	4.49E-09	7.57E-07
Generation of neurons	17	0.312	7	1.06E-08	1.43E-06
Cellular localization	12	0.22	6	3.00E-08	3.38E-06
Nucleosome assembly	42	0.771	9	5.27E-08	5.08E-06
N_acetylglucosamine metabolic process	14	0.257	6	9.46E-08	7.98E-06
Cytokine biosynthetic process	151	2.77	13	4.02E-06	0.000302
Defense response	71	1.3	9	5.55E-06	0.000375
Establishment of organelle localization	29	0.532	6	1.19E-05	0.00073
Generation of precursor metabolites and energy	129	2.37	11	2.46E-05	0.00139
Activation of JUN kinase activity	386	7.08	20	2.83E-05	0.00147
Cellular aromatic compound metabolic process	22	0.404	5	4.06E-05	0.0019
Skeletal muscle tissue development	52	0.954	7	4.22E-05	0.0019
DNA_dependent transcription, initiation	99	1.82	9	8.28E-05	0.00349
Negative regulation of cell migration	389	7.14	19	9.94E-05	0.00395
Positive regulation of I_kappaB kinase/NF_kappaB cascade	42	0.771	6	0.000108	0.00404
Xenobiotic metabolic process	191	3.5	12	0.000208	0.0074
Amine metabolic process	116	2.13	9	0.000279	0.00941
Regulation of organelle organization	51	0.936	6	0.000322	0.0104
Sphingolipid metabolic process	34	0.624	5	0.000358	0.011
Transcription, DNA_dependent	21	0.385	4	0.000516	0.0152
Hemostasis	80	1.47	7	0.000649	0.0179
Response to external stimulus	10	0.183	3	0.000665	0.0179
Cell development	89	1.63	7	0.00123	0.0318
Keratinocyte differentiation	345	6.33	15	0.00175	0.0438
Inflammatory response	29	0.532	4	0.00183	0.044
Organ morphogenesis	49	0.899	5	0.00196	0.0457
Catabolic process	153	2.81	9	0.00203	0.0458

Molecular Function					
RNA binding	270	5.46	89	8.55E-88	2.83E-85
Transcription cofactor activity	356	7.2	29	1.40E-10	2.32E-08
Lipase activity	69	1.4	12	1.12E-08	1.24E-06
Neuropeptide hormone activity	1270	25.7	55	2.90E-08	2.40E-06
RNA helicase activity	49	0.991	10	3.89E-08	2.57E-06
DNA helicase activity	15	0.303	6	2.76E-07	1.52E-05
Exonuclease activity	63	1.27	10	4.72E-07	2.23E-05
Cation_transporting ATPase activity	64	1.29	10	5.49E-07	2.27E-05
Ion binding	21	0.425	6	2.70E-06	9.93E-05
Damaged DNA binding	46	0.93	8	3.34E-06	0.00011
Deoxyribonuclease activity	23	0.465	6	4.85E-06	0.000146
Growth factor binding	65	1.31	9	5.79E-06	0.00016
Transferase activity, transferring acyl groups	253	5.12	17	1.48E-05	0.000377
Nucleobase_containing compound transmembrane transporter activity	291	5.89	17	8.70E-05	0.00206
Regulation of DNA_dependent transcription, elongation	41	0.829	6	0.000159	0.00352
Transcription corepressor activity	101	2.04	9	0.000201	0.00417
Exopeptidase activity	103	2.08	9	0.000234	0.00444
Protein binding, bridging	62	1.25	7	0.000241	0.00444
Ubiquitin binding	17	0.344	4	0.000315	0.00549
Metal ion transmembrane transporter activity	19	0.384	4	0.000498	0.00824
Cellular Component					
Microtubule organizing center	109	1.61	30	3.95E-30	6.95E-28
Proteasome complex	44	0.651	16	8.98E-19	7.91E-17
Nucleus	3830	56.6	112	1.11E-15	6.50E-14
Endomembrane system	14	0.207	7	4.46E-10	1.96E-08
Nucleoplasm	1450	21.5	48	7.85E-08	2.59E-06
Nucleolus	1280	18.9	44	8.84E-08	2.59E-06
Chromosome	4070	60.3	95	3.28E-07	8.23E-06
Vesicle membrane	1670	24.7	50	7.58E-07	1.67E-05
Centrosome	1180	17.5	39	1.61E-06	3.15E-05
Mitochondrial matrix	18	0.267	5	4.98E-06	8.77E-05
Microtubule cytoskeleton	227	3.36	14	7.38E-06	0.000118
U12_type spliceosomal complex	612	9.06	24	1.35E-05	0.000198
Actin cytoskeleton	145	2.15	9	0.000309	0.00419
Spindle	13	0.192	3	0.000821	0.0103
Clathrin_coated vesicle	85	1.26	6	0.00163	0.0191
Basolateral plasma membrane	61	0.903	5	0.00206	0.0227
Integral to organelle	411	6.09	14	0.00331	0.0343

membrane					
Protein serine/threonine phosphatase complex	22	0.326	3	0.00401	0.0384
Apical junction complex	467	6.91	15	0.00414	0.0384
Cytoplasmic vesicle	104	1.54	6	0.00448	0.0394

Table 7. List of nodes in protein-protein interaction network in WAT with SHT and YM-178

Id	Label	Degree	Betweenness
SHT			
ENSRNOP00000025980	Hnrnpk	47	6588.5
ENSRNOP00000026662	Stat5a	45	8433.5
ENSRNOP00000012854	Hdac1	42	5781
ENSRNOP00000028807	Rbm8a	30	1708
ENSRNOP00000039333	Hist2h2aa2	7	306
ENSRNOP00000007079	Crebbp	3	2793
ENSRNOP00000008841	Fabp1	3	301
ENSRNOP00000000733	Fyn	2	2697
ENSRNOP00000012739	Src	2	2697
ENSRNOP00000000206	Ep300	2	2346
ENSRNOP00000047840	Tp53	2	300
ENSRNOP00000063195	Magohb	2	300
ENSRNOP00000001415	Elavl1	2	151
ENSRNOP00000040666	Ddx39a	2	151
ENSRNOP00000022630	Hist1h2ba	2	87
ENSRNOP00000042464	Hist2h2be	2	87
ENSRNOP00000065543	LOC684444	2	87
ENSRNOP00000067000	Hist3h2bb	2	87
ENSRNOP00000060972	Hist3h2ba	2	87
ENSRNOP00000000627	Srsf3	2	68.57
ENSRNOP00000001154	Rbmx	2	68.57
ENSRNOP00000001539	Srsf9	2	68.57
ENSRNOP00000007583	Srsf5	2	68.57
ENSRNOP00000008427	Srsf6	2	68.57
ENSRNOP00000013301	Srsf4	2	68.57
ENSRNOP00000015152	Hnrnpa2b1	2	68.57
ENSRNOP00000017421	Magoh	2	68.57
ENSRNOP00000018646	Snrpd1	2	68.57
ENSRNOP00000019810	Dhx38	2	68.57
ENSRNOP00000021221	Snrpd2	2	68.57
ENSRNOP00000039298	Snrpb	2	68.57
ENSRNOP00000057257	Hnrnpc	2	68.57
ENSRNOP00000035155	Srsf7	2	68.57
ENSRNOP00000065463	Lsm2	2	68.57
ENSRNOP00000061368	Dhx9	2	68.57
ENSRNOP00000064933	Srsf1	2	68.57
ENSRNOP00000032108	Hnrnpm	2	68.57
ENSRNOP00000046491	Hnrnpd	2	68.57
ENSRNOP00000042416	Snrpep2	2	68.57
ENSRNOP00000052160	Hnrnpa1	2	68.57
ENSRNOP00000001334	Ncor2	1	0
ENSRNOP00000002053	Snrpa	1	0

ENSRNOP00000002313	Runx1	1	0
ENSRNOP00000002522	Bcl6	1	0
ENSRNOP00000002533	Mapk1	1	0
ENSRNOP00000002552	Crkl	1	0
ENSRNOP00000003050	Kit	1	0
ENSRNOP00000003458	Socs1	1	0
ENSRNOP00000003768	Bcl2	1	0
ENSRNOP00000003940	Socs3	1	0
ENSRNOP00000005743	Yy1	1	0
ENSRNOP00000006087	Egfr	1	0
ENSRNOP00000006886	Prdm4	1	0
ENSRNOP00000006900	Snrpb2	1	0
ENSRNOP00000007351	Snrpf	1	0
ENSRNOP00000008149	Ezh2	1	0
ENSRNOP00000008355	Sf3a1	1	0
ENSRNOP00000009155	Sarnp	1	0
ENSRNOP00000010277	Rbpj	1	0
ENSRNOP00000011130	Lyn	1	0
ENSRNOP00000011948		1	0
ENSRNOP00000012432	Hck	1	0
ENSRNOP00000012617	LOC100909750	1	0
ENSRNOP00000012936	Lck	1	0
ENSRNOP00000013204	Casc3	1	0
ENSRNOP00000014611	Smptb	1	0
ENSRNOP00000015120	Socs4	1	0
ENSRNOP00000015518	Hnrnph2	1	0
ENSRNOP00000015875	Ybx1	1	0
ENSRNOP00000015971	Hnrnpr	1	0
ENSRNOP00000017369	Epor	1	0
ENSRNOP00000019126	Sf3b1	1	0
ENSRNOP00000019283	Erbb4	1	0
ENSRNOP00000019465	Stat1	1	0
ENSRNOP00000019529	Hnrnpf	1	0
ENSRNOP00000020346	Socs5	1	0
ENSRNOP00000021392	U2af2	1	0
ENSRNOP00000023854	Sf3b3	1	0
ENSRNOP00000023886	Pias2	1	0
ENSRNOP00000024529	Rbm5	1	0
ENSRNOP00000025312	Jak3	1	0
ENSRNOP00000026033	Nxf1	1	0
ENSRNOP00000026354	Stat5b	1	0
ENSRNOP00000053643	Chek2	1	0
ENSRNOP00000038651	Ppara	1	0
ENSRNOP00000011978	Hnf4a	1	0
ENSRNOP00000021752	Rb1	1	0
ENSRNOP00000031717	H2afy2	1	0

ENSRNOP00000063017	Rbl1	1	0
ENSRNOP00000052823	Chd4	1	0
ENSRNOP00000063831	Dnmt1	1	0
ENSRNOP00000027141	Mta2	1	0
ENSRNOP00000023404	Ctbp2	1	0
ENSRNOP00000013694	Lef1	1	0
ENSRNOP00000065485	Rbpj	1	0
ENSRNOP00000013166	Smarca4	1	0
ENSRNOP00000058599	Kat2b	1	0
ENSRNOP00000019127	Rbpjl	1	0
ENSRNOP00000017361	Rbl2	1	0
ENSRNOP00000053890	Chd3	1	0
ENSRNOP00000055692	Tle1	1	0
ENSRNOP00000012892	Rxra	1	0
ENSRNOP00000060549	Trim17	1	0
ENSRNOP00000044552	Rela	1	0
ENSRNOP00000049143	H2afy	1	0
ENSRNOP00000062945	Ctbp1	1	0
ENSRNOP00000062148	Rbbp7	1	0
ENSRNOP00000021145	E2f4	1	0
ENSRNOP00000064384	Sin3b	1	0
ENSRNOP00000055480	Sin3a	1	0
ENSRNOP00000013919	H2afz	1	0
ENSRNOP00000024732	Chd5	1	0
ENSRNOP00000051141	Mta1	1	0
ENSRNOP00000017652	Sap30	1	0
ENSRNOP00000033029	Fus	1	0
ENSRNOP00000026202	Sf3a2	1	0
ENSRNOP00000046783	Hnrnpu	1	0
ENSRNOP00000048698	Ybx1-ps3	1	0
ENSRNOP00000043202	Srsf11	1	0
ENSRNOP00000064264	Vav1	1	0
ENSRNOP00000028176	Snrnp70	1	0
ENSRNOP00000028074	Cpsf7	1	0
ENSRNOP00000055962	Hnrnph1	1	0
ENSRNOP00000052049	Eftud2	1	0
ENSRNOP00000026297	Nudt21	1	0
ENSRNOP00000027425	Hnrnpl	1	0
ENSRNOP00000028814	Pias3	1	0
ENSRNOP00000053093	Yes1	1	0
ENSRNOP00000046647	Lepr	1	0
ENSRNOP00000034983	Stat6	1	0
ENSRNOP00000061649	Jak1	1	0
ENSRNOP00000066383	Il2ra	1	0
ENSRNOP00000066184	Lep	1	0
ENSRNOP00000027441	Pias4	1	0

ENSRNOP00000044534	Abl1	1	0
ENSRNOP00000054982	Socs6	1	0
ENSRNOP00000038369	Akt1	1	0
ENSRNOP00000043542	Bcl2l1	1	0
ENSRNOP00000026760	Stat3	1	0
ENSRNOP00000041842	Ptpn11	1	0
ENSRNOP00000044119	Ghr	1	0
ENSRNOP00000048018	Tyk2	1	0
ENSRNOP00000041734	Cish	1	0
ENSRNOP00000059152	Pias1	1	0
ENSRNOP00000060534	Pdgfrb	1	0
ENSRNOP00000050241	Il2rg	1	0
ENSRNOP00000029085	Rae1	1	0
ENSRNOP00000066302	Eif4a3	1	0
ENSRNOP00000029696	Upf3b	1	0
ENSRNOP00000051838	Alyref	1	0
ENSRNOP00000038996	LOC688526	1	0
ENSRNOP00000067813	LOC102551184	1	0
ENSRNOP00000066653	Hist1h4a	1	0
YM-178			
ENSRNOP00000034364	Rpl17	395	53728.91
ENSRNOP00000028555	Rpl18	379	28422.12
ENSRNOP00000038065	Rpl6	363	25262.43
ENSRNOP00000020635	LOC100359922	359	25553.57
ENSRNOP00000016329	Rps3a	355	28645.52
ENSRNOP00000025224	Rpsa	336	34879.79
ENSRNOP00000000603	Rpl10a	290	27340.56
ENSRNOP00000014849	Rpl29	278	16685.97
ENSRNOP00000060568	Rps28	249	17769.17
ENSRNOP00000005347	Grb2	120	141611
ENSRNOP00000046491	Hnrnpd	73	46142.01
ENSRNOP00000018173	Psma4	62	42143.53
ENSRNOP00000026462	Psmb10	60	26354.83
ENSRNOP00000066950	Psma2	42	4227.73
ENSRNOP00000026354	Stat5b	35	16992.5
ENSRNOP00000063484	Eif3a	34	16231.53
ENSRNOP00000015518	Hnrnph2	33	7337.93
ENSRNOP00000017301	Vamp8	20	14952.5
ENSRNOP00000007558	Csnk2a1	14	10543
ENSRNOP00000061516	Arpc5	14	10543
ENSRNOP00000027073	Uba52	12	135970.9
ENSRNOP00000032902	Hspb1	12	28578.74
ENSRNOP00000004351	Slc9a3r1	12	8932
ENSRNOP00000009988	RGD1560831	10	1325.54
ENSRNOP00000017230	RGD1565317	10	1325.54
ENSRNOP00000023935	Rps3	10	1325.54

ENSRNOP00000040548	RGD1563570	10	1325.54
ENSRNOP00000046737	LOC691716	10	1325.54
ENSRNOP00000051318	LOC100359563	10	1325.54
ENSRNOP00000023256	Slc2a4	9	26209.54
ENSRNOP00000033144	Rps25	9	1198.37
ENSRNOP00000061250	Rps11	9	1198.37
ENSRNOP00000001265	Rpl21	9	0.03
ENSRNOP00000002194	Rpl24	9	0.03
ENSRNOP00000004303	RGD1559951	9	0.03
ENSRNOP00000005471	Rpl23	9	0.03
ENSRNOP00000006359	Rpl19	9	0.03
ENSRNOP00000006754	Rpl7a	9	0.03
ENSRNOP00000010383	LOC100911372	9	0.03
ENSRNOP00000010759	Rpl15	9	0.03
ENSRNOP00000011314	Rps20	9	0.03
ENSRNOP00000011333	Rps7	9	0.03
ENSRNOP00000015893		9	0.03
ENSRNOP00000018820	Rplp1	9	0.03
ENSRNOP00000021161		9	0.03
ENSRNOP00000022184	Rps12	9	0.03
ENSRNOP00000022348	Rps23	9	0.03
ENSRNOP00000024678	Rps15a	9	0.03
ENSRNOP00000026576	Rps16	9	0.03
ENSRNOP00000028060	Rpl27	9	0.03
ENSRNOP00000028481	LOC100360647	9	0.03
ENSRNOP00000032635	LOC100360449	9	0.03
ENSRNOP00000033369		9	0.03
ENSRNOP00000034657	LOC687780	9	0.03
ENSRNOP00000036391	Rpl23a	9	0.03
ENSRNOP00000036514	Rpl5	9	0.03
ENSRNOP00000037110	Rpl11	9	0.03
ENSRNOP00000039111		9	0.03
ENSRNOP00000039179		9	0.03
ENSRNOP00000039287	LOC102550668	9	0.03
ENSRNOP00000039786		9	0.03
ENSRNOP00000040966	Rpl10l	9	0.03
ENSRNOP00000041191		9	0.03
ENSRNOP00000041199		9	0.03
ENSRNOP00000041263		9	0.03
ENSRNOP00000041435		9	0.03
ENSRNOP00000041530		9	0.03
ENSRNOP00000041817	Rpl9	9	0.03
ENSRNOP00000041966	Rpl21	9	0.03
ENSRNOP00000042031	LOC100360647	9	0.03
ENSRNOP00000042242	LOC100909878	9	0.03
ENSRNOP00000042277		9	0.03

ENSRNOP00000042454		9	0.03
ENSRNOP00000042560		9	0.03
ENSRNOP00000042567		9	0.03
ENSRNOP00000042941	LOC500148	9	0.03
ENSRNOP00000045335		9	0.03
ENSRNOP00000045739		9	0.03
ENSRNOP00000046070		9	0.03
ENSRNOP00000046409		9	0.03
ENSRNOP00000046578		9	0.03
ENSRNOP00000046600	LOC306079	9	0.03
ENSRNOP00000046669		9	0.03
ENSRNOP00000047511		9	0.03
ENSRNOP00000047513	Rpl37a	9	0.03
ENSRNOP00000048495		9	0.03
ENSRNOP00000048808	Rpl21	9	0.03
ENSRNOP00000049286	Rps15al2	9	0.03
ENSRNOP00000049416	RGD1563835	9	0.03
ENSRNOP00000049709		9	0.03
ENSRNOP00000049710		9	0.03
ENSRNOP00000049831		9	0.03
ENSRNOP00000050047		9	0.03
ENSRNOP00000050533	RGD1563705	9	0.03
ENSRNOP00000051016	LOC100364191	9	0.03
ENSRNOP00000051203		9	0.03
ENSRNOP00000051312	Rpl21	9	0.03
ENSRNOP00000051332		9	0.03
ENSRNOP00000051743		9	0.03
ENSRNOP00000053082	Rpl5l1	9	0.03
ENSRNOP00000053160		9	0.03
ENSRNOP00000053991		9	0.03
ENSRNOP00000054497	LOC100912027	9	0.03
ENSRNOP00000054699	RGD1560069	9	0.03
ENSRNOP00000055334	RGD1565767	9	0.03
ENSRNOP00000055393		9	0.03
ENSRNOP00000055671		9	0.03
ENSRNOP00000060476	LOC680579	9	0.03
ENSRNOP00000066050	LOC100364116	9	0.03
ENSRNOP00000065886	LOC100362684	9	0.03
ENSRNOP00000064822	RGD1565048	9	0.03
ENSRNOP00000066260	LOC103692519	9	0.03
ENSRNOP00000066866	LOC103690796	9	0.03
ENSRNOP00000066750	LOC100909911	9	0.03
ENSRNOP00000066592		9	0.03
ENSRNOP00000066077	LOC100359951	9	0.03
ENSRNOP00000060629	RGD1561870	9	0.03
ENSRNOP00000064270	RGD1561137	9	0.03

ENSRNOP00000067446	LOC100909911	9	0.03
ENSRNOP00000065901		9	0.03
ENSRNOP00000067572	Rps6	9	0.03
ENSRNOP00000064959	LOC103692519	9	0.03
ENSRNOP00000064745		9	0.03
ENSRNOP00000066863	RGD1560821	9	0.03
ENSRNOP00000064524	RGD1563124	9	0.03
ENSRNOP00000065877	LOC102548369	9	0.03
ENSRNOP00000066016	LOC100912027	9	0.03
ENSRNOP00000067411		9	0.03
ENSRNOP00000065423		9	0.03
ENSRNOP00000061747	Rpl14	9	0.03
ENSRNOP00000056750	LOC100364509	8	1045.89
ENSRNOP00000063201	RGD1561102	8	1037.61
ENSRNOP00000007683		8	0.03
ENSRNOP00000013868	LOC100361180	8	0.03
ENSRNOP00000025217	Rpl17	8	0.03
ENSRNOP00000025888	Rps17	8	0.03
ENSRNOP00000027086	Cnbd2	8	0.03
ENSRNOP00000027226	LOC100360573	8	0.03
ENSRNOP00000031121	LOC100362366	8	0.03
ENSRNOP00000034767	RGD1359290	8	0.03
ENSRNOP00000039774	RGD1560017	8	0.03
ENSRNOP00000040955	LOC103691423	8	0.03
ENSRNOP00000041458	RGD1562381	8	0.03
ENSRNOP00000041774	RGD1564730	8	0.03
ENSRNOP00000041920	RGD1559955	8	0.03
ENSRNOP00000044605	LOC100361060	8	0.03
ENSRNOP00000045195	LOC100360439	8	0.03
ENSRNOP00000045912		8	0.03
ENSRNOP00000048019	RGD1563145	8	0.03
ENSRNOP00000051135	Rpl6-ps1	8	0.03
ENSRNOP00000058757		8	0.03
ENSRNOP00000058934	Rpl36	8	0.03
ENSRNOP00000064082	LOC100360491	8	0.03
ENSRNOP00000067354	LOC100361079	8	0.03
ENSRNOP00000063355	LOC100361259	8	0.03
ENSRNOP00000065066	LOC100365839	8	0.03
ENSRNOP00000064320	LOC100365810	8	0.03
ENSRNOP00000066511		8	0.03
ENSRNOP00000067793		8	0.03
ENSRNOP00000065827		8	0.03
ENSRNOP00000064461		8	0.03
ENSRNOP00000001518	Rplp0	8	0
ENSRNOP00000002177		8	0
ENSRNOP00000004213		8	0

ENSRNOP00000004278	Rps4x	8	0
ENSRNOP00000004583		8	0
ENSRNOP00000005511		8	0
ENSRNOP00000006662	RGD1566369	8	0
ENSRNOP00000009431	Rpl7	8	0
ENSRNOP00000011244	LOC688684	8	0
ENSRNOP00000013462	Rpl4	8	0
ENSRNOP00000014493	Rpl32	8	0
ENSRNOP00000015408	RGD1565894	8	0
ENSRNOP00000019162	Rpl35	8	0
ENSRNOP00000019508	Rps2	8	0
ENSRNOP00000022897	Rps27	8	0
ENSRNOP00000025421	Rpl18a	8	0
ENSRNOP00000026528	Rps5	8	0
ENSRNOP00000027976	Rpl13a	8	0
ENSRNOP00000031078	Rpl31	8	0
ENSRNOP00000033162	LOC500594	8	0
ENSRNOP00000036343	LOC688473	8	0
ENSRNOP00000036690	LOC684988	8	0
ENSRNOP00000037396	LOC100359986	8	0
ENSRNOP00000039003		8	0
ENSRNOP00000041853	LOC297756	8	0
ENSRNOP00000042092	Rsl1d1	8	0
ENSRNOP00000042935	Rps21-ps1	8	0
ENSRNOP00000043988	Rps4x-ps9	8	0
ENSRNOP00000044563	LOC680646	8	0
ENSRNOP00000047760		8	0
ENSRNOP00000047911	RGD1563352	8	0
ENSRNOP00000049546	Rps4y2	8	0
ENSRNOP00000055288	RGD1562399	8	0
ENSRNOP00000056140		8	0
ENSRNOP00000056260	LOC100911847	8	0
ENSRNOP00000057658	Rps2-ps6	8	0
ENSRNOP00000046553	Rpl8	8	0
ENSRNOP00000047328	RGD1561333	8	0
ENSRNOP00000061874		8	0
ENSRNOP00000057262	LOC690384	8	0
ENSRNOP00000051482	Rpl31l3	8	0
ENSRNOP00000051427	RGD1563958	8	0
ENSRNOP00000067080	LOC100360117	8	0
ENSRNOP00000067881	RGD1564378	8	0
ENSRNOP00000058614	RGD1564095	8	0
ENSRNOP00000050175		8	0
ENSRNOP00000049635	LOC102550734	8	0
ENSRNOP00000046515		8	0
ENSRNOP00000044275	LOC100910017	8	0

ENSRNOP00000038214	LOC100911575	8	0
ENSRNOP00000049652	LOC689899	8	0
ENSRNOP00000054398	Rpl30	8	0
ENSRNOP00000043004	RGD1564606	8	0
ENSRNOP00000067129	Rps27l	8	0
ENSRNOP00000046301	RGD1564839	8	0
ENSRNOP00000040232		8	0
ENSRNOP00000048999	Rpl31l4	8	0
ENSRNOP00000065173		8	0
ENSRNOP00000046281	LOC686074	8	0
ENSRNOP00000041625	LOC100362751	8	0
ENSRNOP00000042633		8	0
ENSRNOP00000066548		8	0
ENSRNOP00000050328	RGD1562055	8	0
ENSRNOP00000043092	RGD1561317	8	0
ENSRNOP00000040073	LOC103691563	8	0
ENSRNOP00000051134		8	0
ENSRNOP00000050700	LOC690335	8	0
ENSRNOP00000059772	RGD1565566	8	0
ENSRNOP00000049666		8	0
ENSRNOP00000060662	Rpl3	8	0
ENSRNOP00000064566	LOC100910370	8	0
ENSRNOP00000046953	LOC102554602	8	0
ENSRNOP00000047749	LOC680441	8	0
ENSRNOP00000046487	RGD1562755	8	0
ENSRNOP00000054740	LOC498555	8	0
ENSRNOP00000067596	Rpl30l1	8	0
ENSRNOP00000053863	LOC100911575	8	0
ENSRNOP00000066420	LOC100361143	8	0
ENSRNOP00000067470	LOC683961	8	0
ENSRNOP00000044111	RGD1565170	8	0
ENSRNOP00000065487	LOC100363452	8	0
ENSRNOP00000041638	Rpl32	8	0
ENSRNOP00000045849	RGD1561195	8	0
ENSRNOP00000048311	RGD1563157	8	0
ENSRNOP00000066362	LOC100362987	8	0
ENSRNOP00000051714	Ehd1	7	4481
ENSRNOP00000005872	Rps27a	7	0.03
ENSRNOP00000044806	RGD1565117	7	0.03
ENSRNOP00000045390	RGD1562265	7	0.03
ENSRNOP00000048116	LOC100361854	7	0.03
ENSRNOP00000048620	RGD1561453	7	0.03
ENSRNOP00000062764		7	0.03
ENSRNOP00000061370		7	0.03
ENSRNOP00000063142		7	0.03
ENSRNOP00000005588	Rpl26	7	0

ENSRNOP00000012255	LOC690096	7	0
ENSRNOP00000017602	LOC100359763	7	0
ENSRNOP00000019247	Rpl27a	7	0
ENSRNOP00000019660	Rpl3l	7	0
ENSRNOP00000021625	Npsr1	7	0
ENSRNOP00000021725	Rpl12	7	0
ENSRNOP00000021803	Rpl7l1	7	0
ENSRNOP00000030437	RGD1563956	7	0
ENSRNOP00000036943		7	0
ENSRNOP00000039429		7	0
ENSRNOP00000040306	RGD1563613	7	0
ENSRNOP00000042800		7	0
ENSRNOP00000045516	Wdr31	7	0
ENSRNOP00000045940		7	0
ENSRNOP00000045954		7	0
ENSRNOP00000046036		7	0
ENSRNOP00000046427		7	0
ENSRNOP00000047355		7	0
ENSRNOP00000047391	RGD1564597	7	0
ENSRNOP00000047767		7	0
ENSRNOP00000048713		7	0
ENSRNOP00000049619		7	0
ENSRNOP00000049626		7	0
ENSRNOP00000052873	LOC100911847	7	0
ENSRNOP00000048624	RGD1565415	7	0
ENSRNOP00000049014	Rpl36al	7	0
ENSRNOP00000055726	Rpl28	7	0
ENSRNOP00000042929	LOC688981	7	0
ENSRNOP00000046157	RGD1564469	7	0
ENSRNOP00000055298		7	0
ENSRNOP00000063004		7	0
ENSRNOP00000067887	LOC100910721	7	0
ENSRNOP00000064197	Rpl12	7	0
ENSRNOP00000042127	RGD1566373	7	0
ENSRNOP00000045798	LOC367195	7	0
ENSRNOP00000065065	LOC100910721	7	0
ENSRNOP00000048003	LOC100912182	7	0
ENSRNOP00000048252	RGD1564617	7	0
ENSRNOP00000065371	RGD1564617	7	0
ENSRNOP00000045344	RGD1559972	7	0
ENSRNOP00000054048	LOC100912182	7	0
ENSRNOP00000044949	RGD1560633	7	0
ENSRNOP00000044837		7	0
ENSRNOP00000053986	RGD1565183	7	0
ENSRNOP00000045458	Rpl26-ps1	7	0
ENSRNOP00000057758	Rpl26-ps2	7	0

ENSRNOP00000066808	LOC100910336	7	0
ENSRNOP00000058859		7	0
ENSRNOP00000048422	RGD1562402	7	0
ENSRNOP00000066792	LOC100364509	7	0
ENSRNOP00000041462	LOC102555453	7	0
ENSRNOP00000065281	LOC100911337	7	0
ENSRNOP00000065327		7	0
ENSRNOP00000064853	LOC100911337	7	0
ENSRNOP00000063940		7	0
ENSRNOP00000065999	LOC100911337	7	0
ENSRNOP00000063128	Rpl7a	7	0
ENSRNOP00000041134	Usp7	6	4075
ENSRNOP00000023368	Rpl38	6	0.03
ENSRNOP00000035156	Rps15	6	0.03
ENSRNOP00000042022	LOC690468	6	0.03
ENSRNOP00000042286	LOC680512	6	0.03
ENSRNOP00000042288	LOC682793	6	0.03
ENSRNOP00000044063	LOC686066	6	0.03
ENSRNOP00000045213	RGD1561636	6	0.03
ENSRNOP00000047281	Rps27a-ps6	6	0.03
ENSRNOP00000048664	Rps27a	6	0.03
ENSRNOP00000048903	LOC100363469	6	0.03
ENSRNOP00000049028	LOC680353	6	0.03
ENSRNOP00000050202	LOC682793	6	0.03
ENSRNOP00000050353	LOC682793	6	0.03
ENSRNOP00000059382	Rps24	6	0.03
ENSRNOP00000062631	Rps15-ps2	6	0.03
ENSRNOP00000007194		6	0
ENSRNOP00000009046	Rpl34	6	0
ENSRNOP00000017738		6	0
ENSRNOP00000027246	LOC100910336	6	0
ENSRNOP00000030289		6	0
ENSRNOP00000031049	RGD1563300	6	0
ENSRNOP00000039845	Rps19l1	6	0
ENSRNOP00000042902	LOC100360843	6	0
ENSRNOP00000043543	LOC103690015	6	0
ENSRNOP00000044301	LOC688899	6	0
ENSRNOP00000059662	LOC103693375	6	0
ENSRNOP00000054703	Rpl34-ps1	6	0
ENSRNOP00000039099	Rpl35al1	6	0
ENSRNOP00000041209	Rpl35al1	6	0
ENSRNOP00000047010		6	0
ENSRNOP00000051188	Rpl35a	6	0
ENSRNOP00000040611	Rpl35a	6	0
ENSRNOP00000051114		6	0
ENSRNOP00000047759		6	0

ENSRNOP00000049054	Rpl35a	6	0
ENSRNOP00000042068		6	0
ENSRNOP00000041821	Eef2	6	0
ENSRNOP00000061911		6	0
ENSRNOP00000051317		6	0
ENSRNOP00000041744	RGD1564138	6	0
ENSRNOP00000044197		6	0
ENSRNOP00000064782		6	0
ENSRNOP00000039276	LOC100359503	6	0
ENSRNOP00000065157		6	0
ENSRNOP00000044874	RGD1559877	6	0
ENSRNOP00000064904		6	0
ENSRNOP00000042164	LOC100359671	6	0
ENSRNOP00000061442	LOC100362339	6	0
ENSRNOP00000048658	LOC102554992	6	0
ENSRNOP00000048847		6	0
ENSRNOP00000067306		6	0
ENSRNOP00000063451	RGD1559724	6	0
ENSRNOP00000041612		6	0
ENSRNOP00000047999		6	0
ENSRNOP00000056689		6	0
ENSRNOP00000048289		6	0
ENSRNOP00000052049	Eftud2	5	28724.4
ENSRNOP00000013997	Psmc5	5	10321.19
ENSRNOP00000025819	Psmc4	5	10321.19
ENSRNOP00000005089	Mrps7	5	0
ENSRNOP00000014905	LOC100360057	5	0
ENSRNOP00000015278	LOC680700	5	0
ENSRNOP00000030371	Rps18	5	0
ENSRNOP00000040056	RGD1561919	5	0
ENSRNOP00000040282	RGD1565912	5	0
ENSRNOP00000046090	LOC100362298	5	0
ENSRNOP00000047371	Rps18l1	5	0
ENSRNOP00000049665	LOC103693375	5	0
ENSRNOP00000041329	LOC103693375	5	0
ENSRNOP00000049713	LOC103694404	5	0
ENSRNOP00000045098	LOC103694404	5	0
ENSRNOP00000055790	LOC103690821	5	0
ENSRNOP00000044553	Rpl39	5	0
ENSRNOP00000049205	Rpl37	5	0
ENSRNOP00000054474	LOC100360654	5	0
ENSRNOP00000039155	LOC100360841	5	0
ENSRNOP00000044116	RGD1561310	5	0
ENSRNOP00000040295	Rpl39l	5	0
ENSRNOP00000056331	LOC100360654	5	0
ENSRNOP00000039797	LOC103690888	5	0

ENSRNOP00000064678	LOC100912024	5	0
ENSRNOP00000067239		5	0
ENSRNOP00000047840	Tp53	4	17636
ENSRNOP00000009649	Psmc6	4	84.2
ENSRNOP00000015757	Psmc3	4	84.2
ENSRNOP00000016450	Psmc2	4	84.2
ENSRNOP00000028484	Psmb4	4	84.2
ENSRNOP00000042447	Psma8	4	84.2
ENSRNOP00000027780	Rps27a-ps12	4	0.03
ENSRNOP00000048979	Rps27a-ps5	4	0.03
ENSRNOP00000050941	Rps24	4	0.03
ENSRNOP00000005577	Rps29	4	0
ENSRNOP00000005815	Mrpl13	4	0
ENSRNOP00000015756	Rpl22l1	4	0
ENSRNOP00000017280	Mrpl3	4	0
ENSRNOP00000021899	Mrps9	4	0
ENSRNOP00000023456	Imp3	4	0
ENSRNOP00000024380	Mrpl2	4	0
ENSRNOP00000040703	Rps29	4	0
ENSRNOP00000043270	Rps29	4	0
ENSRNOP00000044909	Rps29	4	0
ENSRNOP00000042920	Rpl22l2	4	0
ENSRNOP00000045893	Mrpl4	4	0
ENSRNOP00000038369	Akt1	3	31710.75
ENSRNOP00000050173	Cdkn1b	3	11343.91
ENSRNOP00000018455	Sec61a1	3	3873.73
ENSRNOP00000036212	Sec61a2	3	3873.73
ENSRNOP00000054528	Psmd9	3	26.42
ENSRNOP00000000528	Psmb8	3	0
ENSRNOP00000000532	Psmb9	3	0
ENSRNOP00000002037	Psmb1	3	0
ENSRNOP00000002358	Psmd2	3	0
ENSRNOP00000004114	LOC690271	3	0
ENSRNOP00000004283	Psmd12	3	0
ENSRNOP00000005329	Psmc1	3	0
ENSRNOP00000009249	Psmd6	3	0
ENSRNOP00000009666	Psma6	3	0
ENSRNOP00000010753	Psma3	3	0
ENSRNOP00000013548	Mrps2	3	0
ENSRNOP00000015618	Psmb2	3	0
ENSRNOP00000015747		3	0
ENSRNOP00000015946	Psma1	3	0
ENSRNOP00000016876	Psmb7	3	0
ENSRNOP00000018005	Psmb5	3	0
ENSRNOP00000019104	Psmd7	3	0
ENSRNOP00000019642	Psmd13	3	0

ENSRNOP00000020451	Mrps5	3	0
ENSRNOP00000024306	Psmd1	3	0
ENSRNOP00000024326	Mrto4	3	0
ENSRNOP00000025007	Mrps11	3	0
ENSRNOP00000026507	Psmb6	3	0
ENSRNOP00000026928	Psma5	3	0
ENSRNOP00000027029	Mrps12	3	0
ENSRNOP00000028517	Mrpl16	3	0
ENSRNOP00000028589	Psmd4	3	0
ENSRNOP00000037928	Psmd3	3	0
ENSRNOP00000055036	RGD1564425	3	0
ENSRNOP00000062146	Psmd11	3	0
ENSRNOP00000066229		3	0
ENSRNOP00000046067	Mrps10	3	0
ENSRNOP00000029336	Mrpl22	3	0
ENSRNOP00000061642	Rps10	3	0
ENSRNOP00000026224	Stx4	2	15434
ENSRNOP00000066881	Was	2	11256
ENSRNOP00000060534	Pdgfrb	2	9672
ENSRNOP00000017353	Ehd2	2	5144.5
ENSRNOP00000049629	Eif4g1	2	3636.7
ENSRNOP00000025303	Akt2	2	2511.84
ENSRNOP00000043928	Pxn	2	1632
ENSRNOP00000051906	Cd19	2	1632
ENSRNOP00000000733	Fyn	2	1230.43
ENSRNOP00000003050	Kit	2	1230.43
ENSRNOP00000003458	Socs1	2	1230.43
ENSRNOP00000006087	Egfr	2	1230.43
ENSRNOP00000011130	Lyn	2	1230.43
ENSRNOP00000012617	LOC100909750	2	1230.43
ENSRNOP00000012739	Src	2	1230.43
ENSRNOP00000012936	Lck	2	1230.43
ENSRNOP00000019283	Erbb4	2	1230.43
ENSRNOP00000025312	Jak3	2	1230.43
ENSRNOP00000048018	Tyk2	2	1230.43
ENSRNOP00000044534	LOC100909750	2	1230.43
ENSRNOP00000053093	Yes1	2	1230.43
ENSRNOP00000061649	Jak1	2	1230.43
ENSRNOP00000001743	S100b	2	817
ENSRNOP00000020265	Ifitm3	2	817
ENSRNOP00000021671	Parva	2	817
ENSRNOP00000002550	Snap29	2	126.5
ENSRNOP00000029790	Eif3el1	2	111.86
ENSRNOP00000032361	Eif3d	2	111.86
ENSRNOP00000043254	Eif4h	2	111.86
ENSRNOP00000057188	Eif3b	2	111.86

ENSRNOP00000000529	Tap1	2	0
ENSRNOP00000000627	Srsf3	2	0
ENSRNOP00000000628	Cdkn1a	2	0
ENSRNOP00000000750	Ube2d1	2	0
ENSRNOP00000000783	Cdk1	2	0
ENSRNOP00000001154	Rbmx	2	0
ENSRNOP00000001539	Srsf9	2	0
ENSRNOP00000002053	Snrpa	2	0
ENSRNOP00000002834	Mrpl1	2	0
ENSRNOP00000004881	Uchl5	2	0
ENSRNOP00000005016	Prpf8	2	0
ENSRNOP00000005832	Klhl12	2	0
ENSRNOP00000006900	Snrpb2	2	0
ENSRNOP00000007583	Srsf5	2	0
ENSRNOP00000007620	Cul1	2	0
ENSRNOP00000007676	Skp1	2	0
ENSRNOP00000007963	Cdc27	2	0
ENSRNOP00000008427	Srsf6	2	0
ENSRNOP00000010373	Sf3a3	2	0
ENSRNOP00000011619	Mrpl15	2	0
ENSRNOP00000011653	Ube2e1	2	0
ENSRNOP00000013301	Srsf4	2	0
ENSRNOP00000015152	Hnrnpa2b1	2	0
ENSRNOP00000015813	Tnks	2	0
ENSRNOP00000015971	Hnrnpr	2	0
ENSRNOP00000017421	Magoh	2	0
ENSRNOP00000019529	Hnrnpf	2	0
ENSRNOP00000019781	Smurf2	2	0
ENSRNOP00000019810	Dhx38	2	0
ENSRNOP00000020323	Ube2c	2	0
ENSRNOP00000021392	U2af2	2	0
ENSRNOP00000021528	Cul3	2	0
ENSRNOP00000024529	Rbm5	2	0
ENSRNOP00000025433	Psmd5	2	0
ENSRNOP00000025887	Psme1	2	0
ENSRNOP00000025980	Hnrnpk	2	0
ENSRNOP00000026279	Psme2	2	0
ENSRNOP00000027091	mrpl11	2	0
ENSRNOP00000027425	Hnrnpl	2	0
ENSRNOP00000027937	Psmd8	2	0
ENSRNOP00000028100	Hnrnpul1	2	0
ENSRNOP00000028176	Snrnp70	2	0
ENSRNOP00000028758	Sf3b4	2	0
ENSRNOP00000032108	Hnrnpm	2	0
ENSRNOP00000034042	mrpl24	2	0
ENSRNOP00000035155	Srsf7	2	0

ENSRNOP00000038713	Ncbp1	2	0
ENSRNOP00000065348	Psmb11	2	0
ENSRNOP00000065857	Pomp	2	0
ENSRNOP00000066877	Pomp	2	0
ENSRNOP00000045007	Mrpl17	2	0
ENSRNOP00000040081	Gfm1	2	0
ENSRNOP00000049519	Efl1	2	0
ENSRNOP00000051848	Mrpl12	2	0
ENSRNOP00000043087	Gfm2	2	0
ENSRNOP00000061368	Dhx9	2	0
ENSRNOP00000061492	Polr2a	2	0
ENSRNOP00000064933	Srsf1	2	0
ENSRNOP00000057257	Hnrnpc	2	0
ENSRNOP00000052160	Hnrnpa1	2	0
ENSRNOP00000041943	LOC100361240	2	0
ENSRNOP00000046992	RGD1564698	2	0
ENSRNOP00000043693	Rps10l1	2	0
ENSRNOP00000032191	Cdk2	2	0
ENSRNOP00000031927	Smurf1	2	0
ENSRNOP00000032953	RGD1562029	2	0
ENSRNOP00000036682	Mrpl1	2	0
ENSRNOP00000000206	Ep300	1	0
ENSRNOP00000000559	Daxx	1	0
ENSRNOP00000001123	Csnk2b	1	0
ENSRNOP00000001248	Flt1	1	0
ENSRNOP00000001315	Arpc1b	1	0
ENSRNOP00000001319	Arpc1a	1	0
ENSRNOP00000001417	Rac1	1	0
ENSRNOP00000001766	Bcr	1	0
ENSRNOP00000001817	Mapkapk5	1	0
ENSRNOP00000002044	Napa	1	0
ENSRNOP00000002323	Dvl3	1	0
ENSRNOP00000002411	Tnk2	1	0
ENSRNOP00000002484	Eif4a2	1	0
ENSRNOP00000002533	Mapk1	1	0
ENSRNOP00000002552	Crkl	1	0
ENSRNOP00000002719	Cblb	1	0
ENSRNOP00000003026	Klhl8	1	0
ENSRNOP00000003060	Hspbap1	1	0
ENSRNOP00000003077	Pdgfra	1	0
ENSRNOP00000003125	Tec	1	0
ENSRNOP00000003460	Mrps14	1	0
ENSRNOP00000003519	Flt4	1	0
ENSRNOP00000003940	Socs3	1	0
ENSRNOP00000004236	Myh2	1	0
ENSRNOP00000004520	Actr3	1	0

ENSRNOP00000005204	Stx8	1	0
ENSRNOP00000005786	LOC100911110	1	0
ENSRNOP00000005837	Phf5a	1	0
ENSRNOP00000006148	Traf6	1	0
ENSRNOP00000006361	Nsf	1	0
ENSRNOP00000006607	Actr2	1	0
ENSRNOP00000007079	Crebbp	1	0
ENSRNOP00000007351	Snrpf	1	0
ENSRNOP00000007641	Stx17	1	0
ENSRNOP00000007998	Snap25	1	0
ENSRNOP00000008355	Sf3a1	1	0
ENSRNOP00000008492	Aurkb	1	0
ENSRNOP00000008612	Cpsf2	1	0
ENSRNOP00000009261	Wasl	1	0
ENSRNOP00000010419	Ehd3	1	0
ENSRNOP00000010701	Ehd4	1	0
ENSRNOP00000011065	Vamp7	1	0
ENSRNOP00000011499	Arpc3	1	0
ENSRNOP00000011565	Mrps15	1	0
ENSRNOP00000011937	Arpc4	1	0
ENSRNOP00000011948		1	0
ENSRNOP00000012734	Rab11fip2	1	0
ENSRNOP00000012984	Mdm4	1	0
ENSRNOP00000013375	Eif2s1	1	0
ENSRNOP00000013695	Eif5	1	0
ENSRNOP00000014611	Smptb	1	0
ENSRNOP00000014810	Bet1	1	0
ENSRNOP00000014817	Eif3l	1	0
ENSRNOP00000015120	Socs4	1	0
ENSRNOP00000015602	Rbsn	1	0
ENSRNOP00000016204	RGD1559708	1	0
ENSRNOP00000016758	Snrpa1	1	0
ENSRNOP00000017227	Stx12	1	0
ENSRNOP00000017409	Eif3m	1	0
ENSRNOP00000017718	LOC100912445	1	0
ENSRNOP00000018646	Snrpd1	1	0
ENSRNOP00000019126	Sf3b1	1	0
ENSRNOP00000019265	Arpc2	1	0
ENSRNOP00000019465	Stat1	1	0
ENSRNOP00000019910	Prpf4	1	0
ENSRNOP00000020065	Mapkapk3	1	0
ENSRNOP00000020077	Thumpd1	1	0
ENSRNOP00000020346	Socs5	1	0
ENSRNOP00000021017	Eif3f	1	0
ENSRNOP00000021221	Snrpd2	1	0
ENSRNOP00000021639	Polr2c	1	0

ENSRNOP00000021738	Polr2d	1	0
ENSRNOP00000022138	Nsa2	1	0
ENSRNOP00000022437	Eif3j	1	0
ENSRNOP00000023282	Adad1	1	0
ENSRNOP00000023342	Ide	1	0
ENSRNOP00000023786	Eif2s2	1	0
ENSRNOP00000023854	Sf3b3	1	0
ENSRNOP00000023886	Pias2	1	0
ENSRNOP00000024753	Abce1	1	0
ENSRNOP00000025615	Eif1b	1	0
ENSRNOP00000025782	Eif3c	1	0
ENSRNOP00000026202	Sf3a2	1	0
ENSRNOP00000026297	Nudt21	1	0
ENSRNOP00000027986	Eif3g	1	0
ENSRNOP00000028074	Cpsf7	1	0
ENSRNOP00000028807	Rbm8a	1	0
ENSRNOP00000028929	Myo1c	1	0
ENSRNOP00000029696	Upf3b	1	0
ENSRNOP00000033029	Fus	1	0
ENSRNOP00000036466	Dgkq	1	0
ENSRNOP00000036844	Eif5b	1	0
ENSRNOP00000038586	Klhdc10	1	0
ENSRNOP00000038996	LOC688526	1	0
ENSRNOP00000039298	Snrpb	1	0
ENSRNOP00000041459	Eif1	1	0
ENSRNOP00000041576	Actr3b	1	0
ENSRNOP00000042416	Snrpep2	1	0
ENSRNOP00000043202	Srsf11	1	0
ENSRNOP00000044296	Actb	1	0
ENSRNOP00000046345	Eif1a	1	0
ENSRNOP00000049419	Eif4a1	1	0
ENSRNOP00000061066	Eif3k	1	0
ENSRNOP00000032389	Gfap	1	0
ENSRNOP00000028143	Pten	1	0
ENSRNOP00000031764	Slc34a1	1	0
ENSRNOP00000010690	Nf2	1	0
ENSRNOP00000042886	Trpc4	1	0
ENSRNOP00000009400	Trpc5	1	0
ENSRNOP00000004391	Slc4a4	1	0
ENSRNOP00000046593	Ezr	1	0
ENSRNOP00000021270	Slc9a2	1	0
ENSRNOP00000008759	Slc4a7	1	0
ENSRNOP00000020711	Slc9a3	1	0
ENSRNOP00000028435	Pth1r	1	0
ENSRNOP00000020304	Ap2a1	1	0
ENSRNOP00000063136	Mst1r	1	0

ENSRNOP00000009211	Itk	1	0
ENSRNOP00000030928	Cdc42	1	0
ENSRNOP00000060296	Dnm2	1	0
ENSRNOP00000017968	Map3k1	1	0
ENSRNOP00000039940	Bcar1	1	0
ENSRNOP00000012328	Epha2	1	0
ENSRNOP00000009556	LOC103692716	1	0
ENSRNOP00000024922	Wipf1	1	0
ENSRNOP00000036862	Irs2	1	0
ENSRNOP00000059209	Eps15	1	0
ENSRNOP00000020663	Ppp2cb	1	0
ENSRNOP00000045832	Pak1	1	0
ENSRNOP00000023144	Fgfr3	1	0
ENSRNOP00000007472	Frs2	1	0
ENSRNOP00000019014	Blnk	1	0
ENSRNOP00000019404	Frs3	1	0
ENSRNOP00000009028	Sptb	1	0
ENSRNOP00000022179	Pik3cb	1	0
ENSRNOP00000009359	Sos1	1	0
ENSRNOP00000011084	Shc4	1	0
ENSRNOP00000006425	Sos2	1	0
ENSRNOP00000057696	Rapgef1	1	0
ENSRNOP00000041842	Ptpn11	1	0
ENSRNOP00000050879	Lcp2	1	0
ENSRNOP00000031304	Lat2	1	0
ENSRNOP00000012588	Kras	1	0
ENSRNOP00000063226	Cbl	1	0
ENSRNOP00000011219	Ptk2	1	0
ENSRNOP00000040409	Rap1a	1	0
ENSRNOP00000036381	Nras	1	0
ENSRNOP00000036086	Tek	1	0
ENSRNOP00000026358	Csk	1	0
ENSRNOP00000036885	Fgfr1	1	0
ENSRNOP00000026210	Pik3r2	1	0
ENSRNOP00000019579	Irs1	1	0
ENSRNOP00000064264	Vav1	1	0
ENSRNOP00000031615	Ptk2b	1	0
ENSRNOP00000052051	Itga2b	1	0
ENSRNOP00000066894	Khdrbs1	1	0
ENSRNOP00000019267	Igf1r	1	0
ENSRNOP00000050988	Fgfr4	1	0
ENSRNOP00000008210	Sptbn1	1	0
ENSRNOP00000006741	Sh3kbp1	1	0
ENSRNOP00000028038	Shc1	1	0
ENSRNOP00000021223	Arhgap35	1	0
ENSRNOP00000009764	Hgf	1	0

ENSRNOP00000014708	Stambp	1	0
ENSRNOP00000013701	Cd28	1	0
ENSRNOP00000027837	Map4k1	1	0
ENSRNOP00000024390	Gab1	1	0
ENSRNOP00000051849	Hgs	1	0
ENSRNOP00000017369	Epor	1	0
ENSRNOP00000016942	Syk	1	0
ENSRNOP00000017753	Ajuba	1	0
ENSRNOP00000007621	LOC103694903	1	0
ENSRNOP00000059005	Fgfr2	1	0
ENSRNOP00000060141	Insr	1	0
ENSRNOP00000040411	Csf1r	1	0
ENSRNOP00000018960	Eps15l1	1	0
ENSRNOP00000066886	Kdr	1	0
ENSRNOP00000006796	Erbb3	1	0
ENSRNOP00000025687	Pik3r1	1	0
ENSRNOP00000017938	Pik3ap1	1	0
ENSRNOP00000007268	Ngfr	1	0
ENSRNOP00000051781	Dock1	1	0
ENSRNOP00000018961	Ntrk1	1	0
ENSRNOP00000060992	Ap2a2	1	0
ENSRNOP00000059867	Ptpn6	1	0
ENSRNOP00000061371	Inppl1	1	0
ENSRNOP00000013342	Spry2	1	0
ENSRNOP00000006407	Crk	1	0
ENSRNOP00000014309	Ptpn1	1	0
ENSRNOP00000009511	Rap1b	1	0
ENSRNOP00000009893	Vav2	1	0
ENSRNOP00000019442	Shc3	1	0
ENSRNOP00000018492	Tnfrsf14	1	0
ENSRNOP00000040591	Erbb2	1	0
ENSRNOP00000047793	Ret	1	0
ENSRNOP00000040111	Inpp5d	1	0
ENSRNOP00000066048	Sh2b1	1	0
ENSRNOP00000020330	Nck1	1	0
ENSRNOP00000023563	Lat	1	0
ENSRNOP00000024272	Apbb1ip	1	0
ENSRNOP00000010714	Shc2	1	0
ENSRNOP00000022363	Hras	1	0
ENSRNOP00000052657	Ptpra	1	0
ENSRNOP00000032337	Wipf2	1	0
ENSRNOP00000006408	Sirpa	1	0
ENSRNOP00000026920	Hsp90ab1	1	0
ENSRNOP00000011732	Jun	1	0
ENSRNOP00000023741	Ctr9	1	0
ENSRNOP00000035059	Sec63	1	0

ENSRNOP00000026439	Dvl1	1	0
ENSRNOP00000026470	Jund	1	0
ENSRNOP00000051745	Nap1l4	1	0
ENSRNOP00000027057	Xrcc1	1	0
ENSRNOP00000009894	Nfkbia	1	0
ENSRNOP00000012022	Ssrp1	1	0
ENSRNOP00000024348	Dvl2	1	0
ENSRNOP00000046783	Hnrnpu	1	0
ENSRNOP00000041788	RGD1561871	1	0
ENSRNOP00000040086	LOC502176	1	0
ENSRNOP00000067869	RGD1560073	1	0
ENSRNOP00000058953	Vti1a	1	0
ENSRNOP00000054114	Vamp2	1	0
ENSRNOP00000040699	Stx1a	1	0
ENSRNOP00000064401		1	0
ENSRNOP00000048364	Vamp3	1	0
ENSRNOP00000021318	Stx7	1	0
ENSRNOP00000020693	Ykt6	1	0
ENSRNOP00000025664	Stx5	1	0
ENSRNOP00000027666	Stxbp3	1	0
ENSRNOP00000025327	Sec22b	1	0
ENSRNOP00000028535	Stx3	1	0
ENSRNOP00000027760	Cd81	1	0
ENSRNOP00000027305	Eef1g	1	0
ENSRNOP00000025906	Ilk	1	0
ENSRNOP00000065234	Rab10	1	0
ENSRNOP00000025649	Rab14	1	0
ENSRNOP00000040878	Gapdh	1	0
ENSRNOP00000039818	RGD1562758	1	0
ENSRNOP00000050241	Il2rg	1	0
ENSRNOP00000059152	Pias1	1	0
ENSRNOP00000026760	Stat3	1	0
ENSRNOP00000034983	Stat6	1	0
ENSRNOP00000044119	Ghr	1	0
ENSRNOP00000046647	Lepr	1	0
ENSRNOP00000066383	Il2ra	1	0
ENSRNOP00000054982	Socs6	1	0
ENSRNOP00000028814	Pias3	1	0
ENSRNOP00000066184	Lep	1	0
ENSRNOP00000027441	Pias4	1	0
ENSRNOP00000026662	Stat5a	1	0
ENSRNOP00000051977	Aurka	1	0
ENSRNOP00000051863	Tgfb1i1	1	0
ENSRNOP00000057786	Mapkapk2	1	0
ENSRNOP00000045761	RGD1560186	1	0
ENSRNOP00000063449	Mdm2	1	0

ENSRNOP00000063831	Dnmt1	1	0
ENSRNOP00000048598	Snrnp200	1	0
ENSRNOP00000058923	Cdc40	1	0
ENSRNOP00000065463	Lsm2	1	0
ENSRNOP00000055962	Hnrnph1	1	0
ENSRNOP00000052955	Srrm1	1	0
ENSRNOP00000051838	Alyref	1	0
ENSRNOP00000067005	U2af1	1	0
ENSRNOP00000064830	Gtf2f1	1	0
ENSRNOP00000063102	Myo10	1	0
ENSRNOP00000067288		1	0

Table 8. GO enrichment of WAT protein-protein interaction network

Pathway	Total	Expected	Hits	P.Value	FDR
SHT					
Biological Process					
Generation of neurons	17	0.116	7	9.99E-12	6.74E-09
Ras protein signal transduction	63	0.432	9	3.69E-10	1.06E-07
Positive regulation of DNA metabolic process	90	0.616	10	4.72E-10	1.06E-07
Negative regulation of cell migration	389	2.66	16	6.57E-09	1.07E-06
Cell cycle checkpoint	582	3.99	19	9.14E-09	1.07E-06
Regulation of DNA binding	90	0.616	9	9.49E-09	1.07E-06
DNA metabolic process	71	0.486	8	2.56E-08	2.46E-06
Activation of JUN kinase activity	386	2.64	15	4.43E-08	3.73E-06
Cytokine biosynthetic process	151	1.03	10	7.39E-08	5.54E-06
Amine metabolic process	116	0.795	9	8.88E-08	5.99E-06
Carboxylic acid metabolic process	333	2.28	12	2.52E-06	0.000155
Defense response	71	0.486	6	8.60E-06	0.000484
Actin filament polymerization	168	1.15	8	1.87E-05	0.000971
Regulation of organelle organization	51	0.349	5	2.44E-05	0.00118
Cell development	89	0.61	6	3.16E-05	0.00142
Response to external stimulus	10	0.0685	3	3.59E-05	0.00151
Inflammatory response	29	0.199	4	4.26E-05	0.00169
DNA_dependent DNA replication	526	3.6	13	5.37E-05	0.00201
Positive regulation of immune response	860	5.89	17	5.81E-05	0.00206
Regulation of gene expression	32	0.219	4	6.35E-05	0.00214
Embryonic morphogenesis	477	3.27	12	9.06E-05	0.00291
Negative regulation of transcription from RNA polymerase II promoter	16	0.11	3	0.000163	0.00499
Stress_activated protein kinase signaling cascade	41	0.281	4	0.000171	0.00501
Hemostasis	80	0.548	5	0.000214	0.00602
Growth	791	5.42	15	0.000268	0.00724
Organ morphogenesis	49	0.336	4	0.000342	0.00889
Regulation of DNA replication	345	2.36	9	0.000566	0.0141
Monocarboxylic acid transport	160	1.1	6	0.000785	0.0189
Glycoprotein biosynthetic process	33	0.226	3	0.00146	0.0339
Sphingolipid metabolic process	34	0.233	3	0.00159	0.0352
Regulation of cellular protein metabolic process	184	1.26	6	0.00162	0.0352
Xenobiotic metabolic process	191	1.31	6	0.00195	0.0412
Cell division	10	0.0685	2	0.00201	0.0412
Chromatin remodeling	38	0.26	3	0.0022	0.0436
Regulation of cytoskeleton organization	81	0.555	4	0.00228	0.0439
DNA damage response, signal transduction by p53 class mediator	11	0.0753	2	0.00245	0.0447

Amyloid precursor protein metabolic process	11	0.0753	2	0.00245	0.0447
Molecular Function					
Nucleotide binding	273	1.98	16	8.46E-11	2.80E-08
Potassium channel activity	244	1.77	15	1.81E-10	2.99E-08
Exonuclease activity	63	0.456	9	6.01E-10	6.63E-08
DNA binding	840	6.08	24	2.93E-09	2.42E-07
Regulation of DNA_dependent transcription, elongation	41	0.297	7	1.48E-08	9.80E-07
Lipase activity	69	0.499	7	6.04E-07	2.95E-05
Transcription corepressor activity	101	0.731	8	6.25E-07	2.95E-05
Steroid dehydrogenase activity	334	2.42	11	2.68E-05	0.00111
Phosphatase regulator activity	431	3.12	12	5.85E-05	0.00215
Chromatin binding	331	2.39	10	0.000131	0.00434
Nucleoside_triphosphatase activity	477	3.45	12	0.000153	0.00461
Transcription cofactor activity	356	2.58	10	0.000237	0.00653
Protein homodimerization activity	53	0.383	4	0.00057	0.014
Neuropeptide hormone activity	1270	9.21	20	0.000593	0.014
Kinase activity	212	1.53	7	0.000843	0.0183
Exopeptidase activity	103	0.745	5	0.000883	0.0183
Carboxy_lyase activity	29	0.21	3	0.00117	0.0217
Nucleobase_containing compound transmembrane transporter activity	291	2.11	8	0.00118	0.0217
Protein serine/threonine kinase activity	31	0.224	3	0.00142	0.0247
Phospholipase C activity	36	0.26	3	0.0022	0.0363
Protein tyrosine phosphatase activity	259	1.87	7	0.00266	0.0419
Cellular Component					
Nucleus	3830	21.2	65	1.60E-23	2.81E-21
Nucleoplasm	1450	8.07	38	1.99E-17	1.75E-15
Chromosome	4070	22.6	51	7.56E-11	4.43E-09
Apical plasma membrane	122	0.677	9	2.37E-08	1.04E-06
Transcription factor TFIID complex	62	0.344	7	4.85E-08	1.71E-06
Nuclear chromatin	163	0.905	9	2.89E-07	8.48E-06
Clathrin_coated vesicle	85	0.472	6	7.53E-06	0.000189
Chromatin	97	0.539	5	0.000202	0.00445
Histone deacetylase complex	26	0.144	3	0.000391	0.00689
Nuclear chromosome	26	0.144	3	0.000391	0.00689
Integral to organelle membrane	411	2.28	9	0.000449	0.00719
Vesicle membrane	1670	9.26	20	0.000645	0.00946
Microtubule associated complex	50	0.278	3	0.00268	0.0355
DNA_directed RNA polymerase II, core complex	174	0.966	5	0.00282	0.0355
YM-178					
Biological Process					
Chromatin assembly or disassembly	248	5.26	77	9.10E-71	6.14E-68
Regulation of DNA binding	90	1.91	25	1.53E-21	5.16E-19

Cytokine biosynthetic process	151	3.2	25	9.88E-16	2.22E-13
Nucleosome assembly	42	0.891	14	8.17E-14	1.38E-11
Defense response	71	1.51	14	2.15E-10	2.90E-08
Generation of neurons	17	0.361	8	7.59E-10	8.54E-08
Sensory perception of taste	5	0.106	5	4.14E-09	3.99E-07
Transcription, DNA_dependent	21	0.446	8	5.91E-09	4.98E-07
Catabolic process	153	3.25	17	2.46E-08	1.85E-06
Stress_activated protein kinase signaling cascade	41	0.87	9	1.47E-07	9.90E-06
Positive regulation of DNA metabolic process	90	1.91	12	4.06E-07	2.49E-05
Monocarboxylic acid transport	160	3.4	15	1.52E-06	8.55E-05
Activation of JUN kinase activity	386	8.19	24	2.37E-06	0.000123
Ras protein signal transduction	63	1.34	9	6.59E-06	0.000318
Neuron projection development	81	1.72	10	7.76E-06	0.000349
Negative regulation of cell migration	389	8.26	23	8.93E-06	0.000377
Inflammatory response	29	0.616	6	2.71E-05	0.00105
Carboxylic acid metabolic process	333	7.07	20	2.80E-05	0.00105
Amine metabolic process	116	2.46	11	3.48E-05	0.00124
Response to external stimulus	10	0.212	4	3.76E-05	0.00127
Actin filament polymerization	168	3.57	13	5.95E-05	0.00191
Small GTPase mediated signal transduction	104	2.21	10	7.03E-05	0.00216
Apoptotic signaling pathway	68	1.44	8	9.06E-05	0.00266
Protein tetramerization	39	0.828	6	0.000156	0.00439
Chromatin remodeling	38	0.807	5	0.00117	0.0316
Molecular Function					
RNA binding	270	6.21	88	2.35E-80	7.78E-78
RNA helicase activity	49	1.13	17	2.87E-16	4.75E-14
Transcription cofactor activity	356	8.19	35	2.71E-13	2.99E-11
Exonuclease activity	63	1.45	16	5.48E-13	4.54E-11
Deoxyribonuclease activity	23	0.529	11	8.26E-13	5.47E-11
Steroid dehydrogenase activity	334	7.69	32	6.24E-12	3.44E-10
Lipase activity	69	1.59	13	4.64E-09	2.19E-07
Regulation of DNA_dependent transcription, elongation	41	0.944	9	2.91E-07	1.20E-05
Transcription corepressor activity	101	2.32	13	5.08E-07	1.87E-05
Nucleotide binding	273	6.28	21	1.30E-06	4.23E-05
GTPase binding	17	0.391	6	1.40E-06	4.23E-05
Neuropeptide hormone activity	1270	29.3	53	1.17E-05	0.000324
Nucleobase_containing compound transmembrane transporter activity	291	6.7	20	1.28E-05	0.000326
ATPase activity, coupled	10	0.23	4	5.16E-05	0.00122
Transferase activity, transferring acyl groups	253	5.82	17	7.65E-05	0.00169
Organic anion transmembrane transporter activity	65	1.5	8	0.000115	0.00238

Hydrolase activity, acting on glycosyl bonds	25	0.575	5	0.000226	0.00441
Small conjugating protein ligase activity	104	2.39	9	0.000646	0.0119
Hydrolase activity, acting on acid anhydrides	512	11.8	23	0.00168	0.0293
Antiporter activity	24	0.552	4	0.00203	0.0335
Cellular Component					
Microtubule organizing center	109	1.87	28	2.12E-25	3.73E-23
Proteasome complex	44	0.756	15	3.31E-16	2.92E-14
Cell_cell junction	307	5.28	27	3.33E-12	1.96E-10
Spindle	13	0.223	8	8.17E-12	3.59E-10
Endomembrane system	14	0.241	7	1.27E-09	4.45E-08
Vesicle membrane	1670	28.6	62	2.55E-09	7.49E-08
Clathrin_coated vesicle	85	1.46	12	2.23E-08	5.60E-07
Nucleus	3830	65.8	103	2.17E-07	4.78E-06
Chromosome	4070	70	106	7.25E-07	1.42E-05
Transcription factor TFIID complex	62	1.07	9	1.04E-06	1.84E-05
Cytoplasmic vesicle	104	1.79	11	1.70E-06	2.72E-05
Mitochondrial matrix	18	0.309	5	1.03E-05	0.000147
Acetylcholine_gated channel complex	150	2.58	12	1.09E-05	0.000147
Apical junction complex	467	8.03	22	1.94E-05	0.000243
Centrosome	1180	20.3	40	2.59E-05	0.000304
Macromolecular complex	177	3.04	12	5.65E-05	0.000622
Lysosome	186	3.2	12	9.11E-05	0.000943
Microtubule cytoskeleton	227	3.9	13	0.000156	0.00152
Mediator complex	117	2.01	9	0.000187	0.00173
Nucleoplasm	1450	25	43	0.000286	0.00252
Protein serine/threonine phosphatase complex	22	0.378	4	0.000489	0.00409
Immunological synapse	30	0.516	4	0.00164	0.0131
U12_type spliceosomal complex	612	10.5	21	0.00208	0.0159
Anchored to membrane	112	1.92	7	0.0032	0.0235
Actin cytoskeleton	145	2.49	8	0.0036	0.0253
Adherens junction	91	1.56	6	0.0048	0.0324
Integral to organelle membrane	411	7.06	15	0.00508	0.0324
Ruffle	65	1.12	5	0.00515	0.0324
Transport vesicle	96	1.65	6	0.00622	0.0365
Sarcomere	43	0.739	4	0.00622	0.0365
Synapse	23	0.395	3	0.00689	0.0391

Appendix 2

Co-authored papers

Is a reduction in brown adipose thermogenesis responsible for the change in core body temperature at menopause?

Peter Aldiss, Helen Budge and Michael E. Symonds

Cardiovascular Endocrinology 2016, **5**:155–156

The Early Life Research Unit, School of Medicine, Division of Child Health, Obstetrics and Gynaecology, University Hospital, University of Nottingham, Nottingham, UK

Correspondence to Michael Symonds, The Early Life Research Unit, School of Medicine, Division of Child Health, Obstetrics and Gynaecology, University Hospital, University of Nottingham, Nottingham, NG7 2UH, UK
Tel: +44 115 823 06250; fax: +44 115 823 0626;
e-mail: michael.symonds@nottingham.ac.uk

Received 31 May 2016 **Accepted** 24 June 2016

Following menopause, women are at a greater risk of becoming obese and suffering from associated cardiometabolic diseases [1,2]. The transition towards greater visceral adiposity and metabolic dysregulation after menopause is likely to be a consequence of changes in energy metabolism, primarily mediated by a reduction in circulating sex hormones such as estrogen or progesterone [1,2]. In the current issue of cardiovascular endocrinology, Neff *et al.* [3] describe that core body temperature is lower in women who have reached menopause, reaching temperatures similar to that of men. Their observation that the lower core body temperatures in those women who had reached menopause raises the possibility that this little studied factor could itself play a role in the increase in disease risk after this time [1,2], although whether the associated higher BMI and adiposity is an effect of age or the menopause *per se* cannot be determined from their study. Although the researchers acknowledge that the study was an exploratory post-hoc analysis of data synthesized from temporally distinct studies, it is worth further consideration, given current interest in brown adipose tissue (BAT) as a therapeutic target to combat cardiometabolic diseases [4]. BAT is a thermogenic organ located mainly in the supraclavicular regions and in much smaller amounts [5] in other locations such as surrounding the kidneys and heart. Most abundant at birth [6], BAT is responsible for nonshivering thermogenesis and the maintenance of thermal homeostasis. This is achieved

Fig. 1

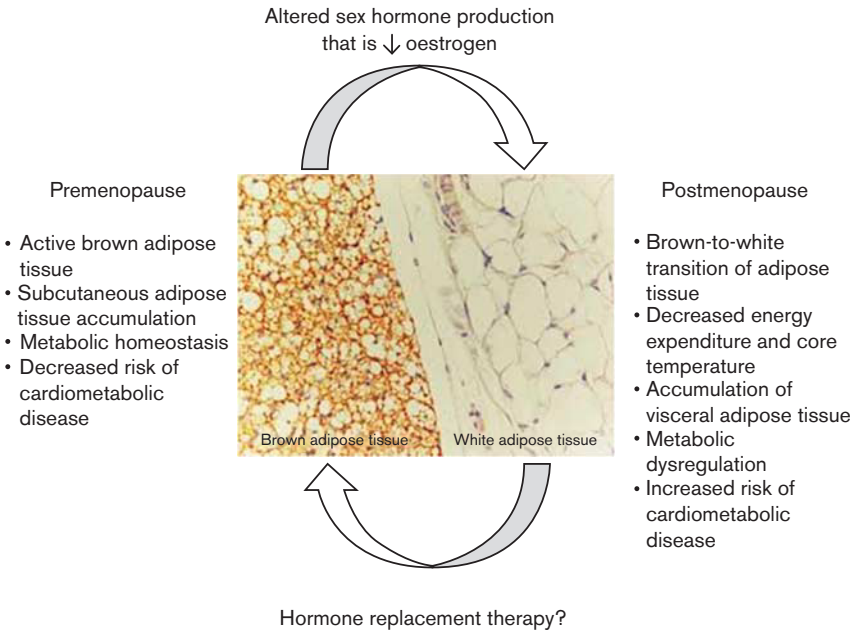

Overview of phenotypic differences between premenopausal/postmenopausal women and possible mechanisms involved. Histological image adapted from Ravussin and Galgani [26].

 DOI: 10.1097/XCE.0000000000000089

through the uncoupling of oxidative metabolism from ATP production through mitochondrial uncoupling protein 1, which dissipates chemical energy as heat [7]. We now know that a majority of adults retain metabolically active BAT into adulthood [8], in declining amounts with age, and that sex hormones such as estrogen are likely to play a key role in the development of brown adipocytes and their function [9,10]. Preclinical research has long demonstrated that exogenous sex hormones play a key role in the metabolic activity of BAT, and more recently it has been shown that cerebroventricular estradiol administration stimulates BAT function, increasing core body and BAT temperatures [11–13].

Another feature of the study by Neff and colleagues is the large variation in body temperatures within women irrespective of age, and this appears to be most marked in the group described as postmenopausal. Although the authors do not define how many of the so-called postmenopausal women in the study were still experiencing hot flushes, a stage already known to be associated with lower body temperature, [14,15] and a truly age-matched group of men is omitted, their observations fit with studies showing that women are more sensitive to cold compared with men [8,16]. This is likely to be a primary factor contributing to their higher incidence of BAT [17]. Moreover, a recent small study in premenopausal women demonstrated a potentially important relationship between salivary cortisol and basal temperature of BAT within the neck [18]. A combination of differences in the hypothalamic–pituitary–adrenal axis, BAT abundance, stress and thermal sensitivity could explain the large variation in body temperatures of healthy women. These relationships may shift after menopause as BAT activity declines.

However, whether a decline in BAT after menopause occurs in humans and, therefore, contributes to greater BMI and fat mass remains to be determined. Given the role of BAT in metabolic homeostasis [19,20] and the recent associations between BAT activity and cardiovascular events [21], investigation of changes in BAT around the menopause and any effects of hormone replacement therapy are warranted. Maintenance of active BAT after the menopause has potential to attenuate the development of adiposity. Future investigations would require well-matched groups as differences in age, body mass and seasonality can all have a significant impact on BAT functionality as highlighted by the authors. Future studies should use additional methods as core body temperature measurements to determine thermal homeostasis and should include supraclavicular skin temperature [22–25] and thermal imaging [22,25] to assess BAT function (Fig. 1).

Acknowledgements

Conflicts of interest

There are no conflicts of interest.

References

1 Rosano GM, Vitale C, Marazzi G, Volterrani M. Menopause and cardiovascular disease: the evidence. *Climacteric* 2007; **10** (Suppl 1): 19–24.
2 Carr MC. The emergence of the metabolic syndrome with menopause. *J Clin Endocrinol Metab* 2003; **88**:2404–2411.
3 Neff LM, Hoffmann ME, Zeiss DM, Lowry K, Edwards M, Rodriguez SM, *et al*. Core body temperature is lower in postmenopausal women than premenopausal women: potential implications for energy metabolism and midlife weight gain. *Cardiovasc Endocrinol* 2016; **5**:154–157.
4 Harms M, Seale P. Brown and beige fat: development, function and therapeutic potential. *Nat Med* 2013; **19**:1252–1263.
5 Sacks H, Symonds ME. Anatomical locations of human brown adipose tissue: functional relevance and implications in obesity and type 2 diabetes. *Diabetes* 2013; **62**:1783–1790.
6 Symonds ME, Pope M, Budge H. The ontogeny of brown adipose tissue. *Annu Rev Nutr* 2015; **35**:295–320.
7 Cannon B, Nedergaard J. Brown adipose tissue: function and physiological significance. *Physiol Rev* 2004; **84**:277–359.
8 Cypess AM, Lehman S, Williams G, Tal I, Rodman D, Goldfine AB, *et al*. Identification and importance of brown adipose tissue in adult humans. *N Engl J Med* 2009; **360**:1509–1517.
9 Velickovic K, Cvoro A, Srdic B, Stokic E, Markelic M, Golic I, *et al*. Expression and subcellular localization of estrogen receptors α and β in human fetal brown adipose tissue. *J Clin Endocrinol Metab* 2014; **99**:151–159.
10 Bloor ID, Symonds ME. Sexual dimorphism in white and brown adipose tissue with obesity and inflammation. *Horm Behav* 2014; **66**:95–103.
11 Kemnitz JW, Glick Z, Bray GA. Ovarian hormones influence brown adipose tissue. *Pharmacol Biochem Behav* 1983; **18**:563–566.
12 Yoshioka K, Yoshida T, Wakabayashi Y, Nishioka H, Kondo M. Reduced brown adipose tissue thermogenesis of obese rats after ovariectomy. *Endocrinol Jpn* 1988; **35**:537–543.
13 Martínez de Morentin PB, González-García I, Martins L, Lage R, Fernández-Mallo D, Martínez-Sánchez N, *et al*. Estradiol regulates brown adipose tissue thermogenesis via hypothalamic AMPK. *Cell Metab* 2014; **20**:41–53.
14 Freedman RR, Subramanian M. Effects of symptomatic status and the menstrual cycle on hot flash-related thermoregulatory parameters. *Menopause* 2005; **12**:156–159.
15 Freedman RR, Norton D, Woodward S, Cornélissen G. Core body temperature and circadian rhythm of hot flashes in menopausal women. *J Clin Endocrinol Metab* 1995; **80**:2354–2358.
16 Au-Yong IT, Thorn N, Ganatra R, Perkins AC, Symonds ME. Brown adipose tissue and seasonal variation in humans. *Diabetes* 2009; **58**:2583–2587.
17 Nedergaard J, Bengtsson T, Cannon B. Three years with adult human brown adipose tissue. *Ann N Y Acad Sci* 2010; **1212**:E20–E36.
18 Robinson LJ, Law JM, Symonds ME, Budge H. Brown adipose tissue activation as measured by infrared thermography by mild anticipatory psychological stress in lean healthy females. *Exp Physiol* 2016; **101**:549–557.
19 Hanssen MJ, Hoeks J, Brans B, van der Lans AA, Schaart G, van den Driessche JJ, *et al*. Short-term cold acclimation improves insulin sensitivity in patients with type 2 diabetes mellitus. *Nat Med* 2015; **21**:863–865.
20 Van der Lans AA, Hoeks J, Brans B, Vijgen GH, Visser MG, Vosselman MJ, *et al*. Cold acclimation recruits human brown fat and increases nonshivering thermogenesis. *J Clin Invest* 2013; **123**:3395–3403.
21 Takx R, Ishai A, Truong QA, MacNabb MH, Scherrer-Crosbie M, Tawakol A. Supraclavicular brown adipose tissue FDG uptake and cardiovascular disease. *J Nucl Med* 2016. [Epub ahead of print].
22 Robinson L, Ojha S, Symonds ME, Budge H. Body mass index as a determinant of brown adipose tissue function in healthy children. *J Pediatr* 2014; **164**:318.
23 Van der Lans AA, Vosselman MJ, Hanssen MJ, Brans B, van Marken Lichtenbelt WD. Supraclavicular skin temperature and BAT activity in lean healthy adults. *J Physiol Sci* 2016; **66**:77–83.
24 Boon MR, Bakker LE, van der Linden RA, Pereira Arias-Bouda L, Smit F, Verberne HJ, *et al*. Supraclavicular skin temperature as a measure of ^{18}F-FDG uptake by BAT in human subjects. *PLoS One* 2014; **9**:e98822.
25 Symonds ME, Henderson K, Elvidge L, Bosman C, Sharkey D, Perkins AC, Budge H. Thermal imaging to assess age-related changes of skin temperature within the supraclavicular region co-locating with brown adipose tissue in healthy children. *J Pediatr* 2012; **161**:892–898.
26 Ravussin E, Galgani JE. The implication of brown adipose tissue for humans. *Annu Rev Nutr* 2011; **31**:33–47.

REVIEW

Brown adipose tissue development and function and its impact on reproduction

Michael E Symonds[1,2], Peter Aldiss[1], Neele Dellschaft[1], James Law[1], Hernan P Fainberg[1], Mark Pope[1], Harold Sacks[3] and Helen Budge[1]

[1]Early Life Research Unit, Division of Child Health, Obstetrics & Gynaecology, School of Medicine, University of Nottingham, Nottingham, UK
[2]Nottingham Digestive Disease Centre and Biomedical Research Centre, School of Medicine, University of Nottingham, Nottingham, UK
[3]VA Endocrinology and Diabetes Division, VA Greater Los Angeles Healthcare System, and Department of Medicine, David Geffen School of Medicine, University of California, Los Angeles, California, USA

Correspondence should be addressed to M E Symonds: michael.symonds@nottingham.ac.uk

Abstract

Although brown adipose tissue (BAT) is one of the smallest organs in the body, it has the potential to have a substantial impact on both heat production as well as fat and carbohydrate metabolism. This is most apparent at birth, which is characterised with the rapid appearance and activation of the BAT specific mitochondrial uncoupling protein (UCP)1 in many large mammals. The amount of brown fat then gradually declines with age, an adaptation that can be modulated by the thermal environment. Given the increased incidence of maternal obesity and its potential transmission to the mother's offspring, increasing BAT activity in the mother could be one mechanism to prevent this cycle. To date, however, all rodent studies investigating maternal obesity have been conducted at standard laboratory temperature (21°C), which represents an appreciable cold challenge. This could also explain why offspring weight is rarely increased, suggesting that future studies would benefit from being conducted at thermoneutrality (~28°C). It is also becoming apparent that each fat depot has a unique transcriptome and show different developmental pattern, which is not readily apparent macroscopically. These differences could contribute to the retention of UCP1 within the supraclavicular fat depot, the most active depot in adult humans, increasing heat production following a meal. Despite the rapid increase in publications on BAT over the past decade, the extent to which modifications in diet and/or environment can be utilised to promote its activity in the mother and/or her offspring remains to be established.

Key Words

- adipose tissue
- diabetes
- metabolism
- obesity
- pregnancy

Journal of Endocrinology (2018) **238**, R53–R62

Introduction

Although brown adipose tissue (BAT) may be one of the smallest fat depots in the adult, it has the potential to have a substantial influence on energy balance, as well as glucose and lipid metabolism (Cannon & Nedergaard 2012*b*). BAT could be considered as the body's natural radiator, which can be rapidly stimulated during thermal or dietary challenges (Symonds *et al.* 2015). Brown fat is able to generate large amounts of heat due to the presence of a unique uncoupling protein (UCP)1 on the inner mitochondrial membrane (Cannon & Nedergaard 2004). When stimulated, UCP1 enables the free flow of protons across the mitochondria, by-passing the usual

http://joe.endocrinology-journals.org
https://doi.org/10.1530/JOE-18-0084

production of ATP, which occurs in the mitochondria of all other organs (Cannon & Nedergaard 2004). At maximal stimulation, brown fat has the capacity to generate up to 300 times more heat per unit mass than any other organ in the body (Symonds *et al.* 2015) and, as such, can account for up to 10% of total daily heat production (Klingenspor & Fromme 2012). In large mammalian species, including humans, brown fat is first activated around the time of birth following cold exposure to the extra-uterine environment and intense endocrine stimulation (Symonds 2013, Symonds *et al.* 2015). The activity of brown fat then gradually declines, with the possible exception of during puberty (Gilsanz *et al.* 2012) when there may be an increase (Symonds *et al.* 2016). Furthermore, many of the more recent findings on brown fat are in accord with those demonstrated nearly 50 years ago following the first comprehensive studies on the distribution and function of brown fat in neonatal (Hull & Segall 1966) and adult humans (Heaton & Nicholls 1977) but which were not always published at the time (Aldiss *et al.* 2017).

Since the rediscovery of brown fat in adult humans in 2009, there has been a steep increase in publications on the subject (Fig. 1). This has been accompanied with the finding that there are three types of fat depots: namely brown, white and beige adipose tissue (Cypess *et al.* 2014). The latter has the largest potential as a therapeutic target in the prevention of obesity and/or diabetes. This is because, from an adult perspective, beige (or recruitable) fat can be present in many white depots as clusters of pre-adipocytes that on differentiation to the mature adipocyte possess UCP1 (Nedergaard & Cannon 2013). Although the relative abundance of UCP1 in beige fat is only c.10% of that found in 'classic' brown fat, that it resides in white fat of much greater abundance confers potential for sustained functional significance (Cannon & Nedergaard 2012*a*). Complementary lineage-tracing studies in mice have also suggested that beige and white adipocytes share a

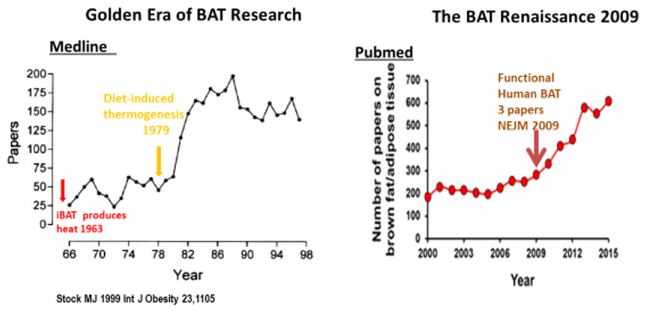

Figure 1
Summary of the number of publications relating to brown fat over the past 50 years.

common developmental lineage, whilst brown adipocytes may originate from the same embryonic precursor as skeletal muscle (Harms & Seale 2013). To date, the primary stimulus of the beiging process appears to be a reduction in ambient temperature, acting through an increase in the activity of the sympathetic nervous system (Cannon & Nedergaard 2012*b*). However, as it becomes clear that the development of each fat depot is unique, a substantial amount of research is still required.

It is now recognised that many of the experimental protocols adopted do not replicate the human environment (Maloney *et al.* 2014), in which cold exposure is the primary stimulus for UCP1 (Chondronikola *et al.* 2014). This is especially the case for many studies in rodents where exposure to the standard housing temperature used of 20–21°C represents an appreciable cool challenge (Fischer *et al.* 2018). Furthermore, rodent models of obesity in which healthy animals are 'simply' switched to a high-energy diet (usually in the form of extra fat) and rapidly become obese is not the typical pathway to obesity in humans (Symonds *et al.* 2011). In humans, excess adiposity is the consequence of a much smaller change in energy balance over a prolonged period of time and is typically accompanied by a range of behavioural adaptations such as reduced activity and more frequent snacking (Weinsier *et al.* 1998, Diaz-Zavala *et al.* 2017). In this context, it is much more likely that enhanced brown or beige fat will provide an additional target to promote weight loss or indeed the maintenance of a healthy weight.

Adipose tissue development and the thermal environment

The development and maturation of adipose tissue varies substantially between large and small mammals. The latter are born with an immature hypothalamic–pituitary axis after a short gestation with very little capacity for independent thermogenesis at birth (Symonds *et al.* 2007) and the abundance of UCP1 increases postnatally in parallel with brain maturation (Symonds & Budge 2009). This contrasts with large mammals, such as humans and sheep, in which parturition and birth are accompanied with intense endocrine stimulation of BAT fully developed at birth and an exponential rise in UCP1 (Symonds 2013, Symonds *et al.* 2015). The magnitude of response is dependent on the thermal environment, the route of delivery (Symonds *et al.* 1995) and can also be modulated by the mother. Prolonged maternal cold

http://joe.endocrinology-journals.org
https://doi.org/10.1530/JOE-18-0084

exposure, for example, promotes overall foetal growth and fat deposition in the foetus and enhances the newborn's capacity to thermoregulate after birth (Symonds *et al.* 1992). Metabolic adaptation around the time of birth is accompanied by rapid mobilisation of lipid and glycogen reserves to meet such a pronounced increase in metabolic rate (Mellor & Cockburn 1986) that is seldom reached at any other time of life (Symonds *et al.* 1989). At the same time, the increase in blood oxygenation following the onset of breathing and exposure to the extra-uterine environment is paralleled by a rise in circulating glucose and free fatty acids (Symonds *et al.* 2015). Concomitantly, plasma short-chain fatty acids, such as acetate, decline (Symonds *et al.* 2015), although the direct impact this has on the subsequent postnatal disappearance of brown fat is unknown.

The impact of temperature on adipose tissue function persists after birth when rearing in a warm temperature accelerates the loss of UCP1 and promotes lipid deposition (Symonds *et al.* 1996). Maternal diet can also modulate the amount of brown fat in the newborn, with an increase in food intake promoting the relative abundance of UCP1 (Budge *et al.* 2000), although the postnatal consequences remain to be explored. The thermal environment also has a modulatory role in determining the metabolic outcomes (Maloney *et al.* 2014): an effect seen in adults as well as during early life. For rodents, both during development and in adulthood, it would appear necessary that they are housed at thermoneutrality (i.e. ~28°C) when the aim is to mimic any effects of deviation from thermal neutrality in humans. As such, standard housing conditions (i.e. c.21°C) adopted in all developmental rodent studies represent an appreciable cool stimulus, which would stimulate thermogenesis in brown fat (Maloney *et al.* 2014). Rearing in a cool temperature also impacts on a wide range of other physiological functions including cardiovascular control and the capacity to replicate metabolic-related diseases in mice as these appear to be housing temperature dependent (e.g. Giles *et al.* 2017). Indeed, epidemiological evidence from the United States suggests that rising environmental temperatures could contribute to enhanced risk of diabetes (Blauw *et al.* 2017), whilst a Canadian study indicated a similar relationship with the onset of gestational diabetes (Booth *et al.* 2017).

To date, the influence of the thermal environment has been ignored in studies examining the impact of the developmental origins of adult disease. This should be rectified and it must be noted that the thermoneutral zone in newborn and young animals is actually closer to their body temperature (Cannon & Nedergaard 2011). Recent studies have suggested that low-birth-weight offspring have raised UCP1 compared to normal-sized litter mates (Dumortier *et al.* 2017). Growth-restricted offspring would be expected to be much more susceptible to cold stress due to their lower body weight, greater surface area to body weight ratio and reduced substrate availability, providing additive stress to increase non-shivering thermogenesis – an effect less likely to be seen if animals were housed at thermoneutrality. Furthermore, the modest perturbations in glucose homeostasis typically seen in offspring born to dams fed low-protein diet (Dumortier *et al.* 2017) may not be present if they were maintained in a thermoneutral environment with its inherently reduced thermogenic stimulus and brown fat activity. This also means that the pre-diabetes phenotype that occurs with ageing in this model would be expected to develop much earlier and provides an example of sub-optimal experimental protocols adopted in these types of studies.

In addition to the confounding effects of the environmental temperature adopted in studies of metabolic activity and brown fat function, common errors include the potentially confounding effects of gender and foetal number and the potential inflation of any effects when the much larger number of offspring are considered the unit of assessment for maternal interventions in place of the mother (Symonds *et al.* 2009). Taken together, it is not surprising that comparatively little progress has been made into elucidating the primary mechanisms by which maternal obesity may programme the offspring, let alone designing, and testing, credible interventions that could impact on obese pregnant women. Such methodologies may also explain why a majority of rodent models of maternal obesity either have no impact on birth weight (Symonds *et al.* 2013*a*) or increase the incidence of intra-uterine growth retardation (Panchenko *et al.* 2016).

Brown fat thermogenesis and the control of body temperature

In accord with anatomical studies conducted in newborn infants nearly 50 years ago (Aherne & Hull 1966), the main depot of brown fat identified from positron emission tomography-CT (PET-CT) studies in adult humans resides within the supraclavicular depot (Au-Yong *et al.* 2009, van Marken Lichtenbelt *et al.* 2009). Due to the relatively close location of this depot to the skin, it has proven feasible to measure changes in its activity using thermal imaging (Law *et al.* 2017). Such studies have shown that

http://joe.endocrinology-journals.org
https://doi.org/10.1530/JOE-18-0084

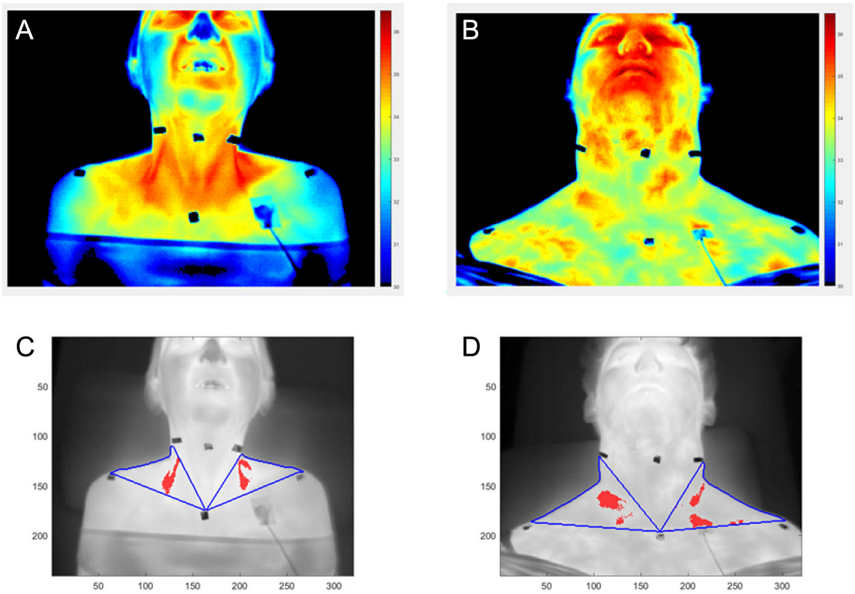

Figure 2
Infrared thermographs of (A) a lean and (B) an obese child showing increased supraclavicular hotspot temperature overlying BAT in the lean individual (35.4°C) compared with obese (34.5°C). Images after analysis to locate the hottest 10% pixels show (C) a centralised hotspot (red) within the supraclavicular region of interest (blue line) in the lean individual and (D) a more dispersed heat signature in the obese. BAT, brown adipose tissue.

the temperature of the supraclavicular region is at least 0.5°C higher than the surrounding area (Fig. 2), whilst the relative difference between this area and adjacent regions increase further when brown fat is activated. There is also a close relationship between body temperature and brown fat function during development so that, in the sheep, for example, body temperature increases immediately after birth to ~1°C higher (Fig. 3A) than would be expected in the adult and then gradually declines as brown fat is lost (Symonds *et al.* 1989). The relationship between body temperature and brown fat function in adult humans indicates that the reduced activity of BAT seen with obesity is accompanied by a lower body temperature (Grimaldi *et al.* 2015). This is particularly noticeable during the day (Fig. 3B), after feeding and is indirect evidence of defective dietary-induced thermogenesis (Symonds 2013), although further studies are required to confirm these findings.

Maternal obesity and BAT as a potential therapeutic target

In the United Kingdom for example, overweight or obesity affects almost half the women of child-bearing age (16–44 years) (Health and Social Care Information Centre 2016), and represents an important health issue for women and their children. Inadequate diet is clearly a factor and could relate to the much greater purchase of processed foods compared with the rest of Europe (Monteiro *et al.* 2018). Maternal obesity during pregnancy can directly influence infant size and metabolic characteristics from conception onward, is one of the main predicting factors of later offspring obesity (Dabelea & Crume 2011) and can have trans-generational effects. With increased BMI and reduced insulin sensitivity, an enhanced trans-placental gradient exposes the foetus to more nutrients, especially glucose (Catalano *et al.* 2009). The consequent increase in

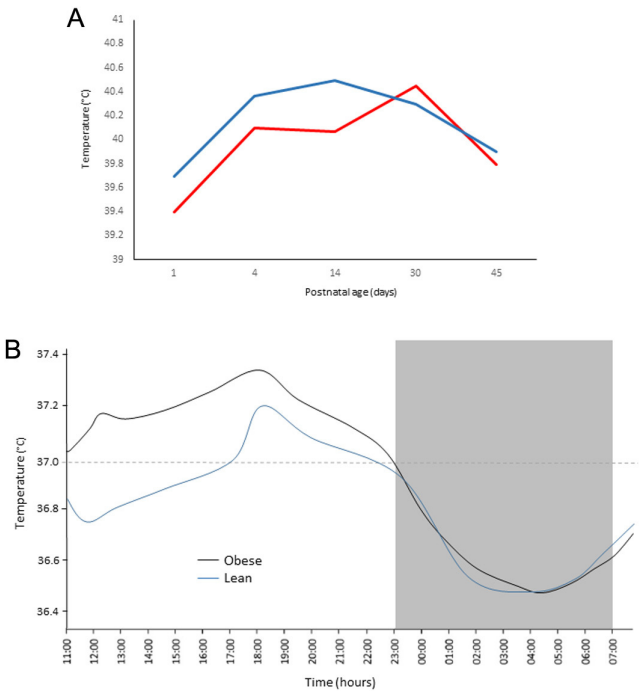

Figure 3
Summary of changes in body temperature over the life cycle and the effect of obesity. (A) Shows the rise in temperature after birth in young sheep when maintained at thermoneutrality (red line) or in the cold (blue line). (B) Shows difference in diurnal temperatures between lean and obese adult humans.

http://joe.endocrinology-journals.org
https://doi.org/10.1530/JOE-18-0084

foetal insulin secretion (Pedersen 1954) stimulates foetal growth and energy storage, increasing fat mass, and birth weight (Modi *et al*. 2011). Longer term adverse effects on the offspring can include the maintenance of a heavier body weight and greater adiposity, thereby increasing the risk of developing heart disease and diabetes in adulthood (Dabelea & Crume 2011, Reynolds *et al*. 2013, Gaillard 2015).

Obesity during pregnancy is particularly resistant to existing lines of treatment, with weight rebound common, suggesting that prevention or amelioration of the development of obesity in women prior to pregnancy is critical (Symonds *et al*. 2013*b*). Reducing hyperglycaemia in obese mothers throughout conception, pregnancy and lactation could interrupt early-life obesity in offspring, reducing their long-term risk of metabolic disease. Consequently, a primary goal in achieving such outcomes could be to target brown fat (Symonds *et al*. 2017). This may be achieved by treating obese females with metformin, a biguanide drug commonly used in diabetes treatment. It primarily decreases circulating glucose by inhibiting hepatic gluconeogenesis, which is insufficiently suppressed in insulin resistance, and by increasing glucose transporter (GLUT)4-dependent glucose uptake into muscle and white fat (Grisouard *et al*. 2010, Turban *et al*. 2012). Metformin lowers body weight, plasma glucose, glycosylated haemoglobin, triglycerides and non-esterified fatty acids, in humans (Diabetes Prevention Program Research Group 2002) and mice (Geerling *et al*. 2014).

Metformin has also been shown to have a direct effect on thermogenic tissues. In cell culture, brown adipocytes show a dose-dependent response (1–100 µmol/L) to metformin, increasing phosphorylation of hormone-sensitive lipase, AMP-activated kinase and acetyl-coA carboxylase, and lipolysis, indicating lipid consumption (Geerling *et al*. 2014). In ApoE3-transgenic mice with diet-induced obesity, metformin administration induces selective uptake of very-low-density lipoproteins triglycerides into brown fat, induces expression of thermogenic genes including peroxisome proliferator-activated receptor gamma, coactivator 1α (PGC1α) and hormone-sensitive lipase and lowers lipid content in brown fat (Geerling *et al*. 2014). These effects are consistent with enhanced thermogenic activity without the need for cold stimulation.

Oral treatment with metformin is routinely used to reduce hyperglycaemia in pregnancy (Hughes & Rowan 2006) with few maternal side effects (Domecq *et al*. 2013) and no reported adverse effects on foetal development (Cassina *et al*. 2014). Metformin is transported across the placenta (Vanky *et al*. 2005, Eyal *et al*. 2010) and is present at low concentrations in breast milk (Hale *et al*. 2002, Eyal *et al*. 2010). In rodents, maternal treatment with metformin during pregnancy has no reported effect on offspring health when weaned to a low-fat diet but offspring are protected from excess body weight gain and the adverse metabolic effects of subsequent exposure to a high-fat diet (Salomäki *et al*. 2014). In a clinical intervention study, giving metformin to obese pregnant women had no apparent effect on their weight gain, glucose tolerance or the weight and adiposity of their newborn infants (Chiswick *et al*. 2015). However, whether the absence of any immediate outcomes in the newborn could mask protective effects at a later time point for these children has not been studied.

Both pre (Salomäki *et al*. 2014) and early postnatal (Liang *et al*. 2016) exposure to metformin has been linked to sustained effects on offspring thermogenic activity through brown and beige fat. When obese pregnant mice were treated with metformin, both their male and female offspring gained less weight and fat when subsequently exposed to a high-fat diet in adulthood (Salomäki *et al*. 2014). The offspring were also protected from the diet-induced onset of glucose intolerance. White adipocyte size was reduced, suggesting an improved secretory profile (Skurk *et al*. 2007), and UCP1 gene expression was raised (Salomäki *et al*. 2014). Metformin treatment of the offspring through lactation further modulated brown fat function in pups whose mothers were fed a high-fat diet post-partum (Liang *et al*. 2016). In this mouse study (Liang *et al*. 2016), the lipid content of milk was raised, as was fat mass. Critically, although metformin had no effect on body weight, it did restore UCP1 abundance and function in vitro (Liang *et al*. 2016). However, only modest effects on rectal temperature were seen, maybe due to the standard (cool) housing temperature adopted and offspring were only examined up to one month of age. Taken together, these studies demonstrate the potential of metformin to protect offspring of mothers fed a high fat diet from adverse effects. They were, however, limited to the effects of short-term metformin administration or acute exposure to an obesogenic diet in pregnancy (in the case of the clinical study (Chiswick *et al*. 2015) omitting conception and early pregnancy), or to lactation, and measured only short-term outcomes. Therefore, it would appear necessary to apply this intervention in a manner more relevant to the clinical situation.

http://joe.endocrinology-journals.org
https://doi.org/10.1530/JOE-18-0084

Depot-specific developmental profiles and their contribution to heat production in adulthood

The most widely studied brown fat depot in rodents is the interscapular one, although in humans, the primary depot resides in the neck i.e. within the supraclavicular region (Cypess *et al.* 2013). A comparable depot has now been identified in mice, which shows a number of similarities to interscapular fat from as early as 18.5 days post conception (Mo *et al.* 2017). This includes some molecular and morphological (e.g. mitochondrial) characteristics, although its postnatal growth is constrained. Furthermore, gene expression of specific putative beige or white markers, were very different in the supraclavicular region compared with interscapular, inguinal and epididymal (i.e. white fat) depots. For example, *HoxC8* and *Zic1* were absent from the supraclavicular depot, which also showed a separate principal component analysis (Mo *et al.* 2017). In sheep, the equivalent depot is found in the sternal region and has a very different postnatal ontogeny to the more widely studied perirenal-abdominal depot (Henry *et al.* 2017). The sternal depot, unlike other fat depots in the sheep, retains UCP1 into adulthood, where it exhibits a pronounced thermogenic response to feeding (Henry *et al.* 2017). In this regard, it is comparable to the supraclavicular depot in humans, which increases in temperature after a meal (Scotney *et al.* 2017). The unique gene profile of supraclavicular fat shown when candidate genes were measured in both mice (Mo *et al.* 2017) and sheep (Henry *et al.* 2017) has recently been extended to the five major fat depots in young sheep when analysed using microarrays (Fainberg *et al.* 2018).

Undertaking microarray analysis at two important time points in early postnatal life of sheep, coincident with the transition of fat from a depot in which brown characteristics dominate (i.e. 7 days of age) to when brown fat is scarce (i.e. 28 days of age) (Symonds *et al.* 2015), has illustrated the unique nature of each depot (Fainberg *et al.* 2018). Machine learning algorithms, in conjunction with weighted gene co-expression network analysis, demonstrated that the five depots examined (i.e. sternal, perirenal, pericardial, subcutaneous, omental) could be segregated into defined sets of modules containing co-expressed genes, indicative of separate functions. The developmental changes markedly differed between depots despite them showing a similar macroscopic morphology (Fainberg *et al.* 2018). This means that, at 28 days when, in sheep, fat is considered primarily white (Symonds *et al.* 2015), each adipose depot kept a distinct gene expression profile (Fainberg *et al.* 2018). Consequently, although adipose tissue has been considered a metabolic organ with important functions beyond lipid storage, this varies between depots, especially during development. Adipose tissue, therefore, has a range of functions depending on location (Macotela *et al.* 2012). This concept was formulated by using a computer-assisted supervised learning algorithm, to demonstrate that, during postnatal development, each fat depot contains a transcriptome which forms dynamic networks with unique sets of genes (Barabasi & Oltvai 2004). Over the first month of life, in sheep, these gene networks are reorganised by accommodating novel members and/or losing some of their original components (Fainberg *et al.* 2018). Dynamic changes in gene regulation with age are rarely examined but do enable the identification of important regulatory relationships. These will have crucial depot-specific roles to enable differentiation and the adaptation necessary to modulate metabolic homeostasis (Macotela *et al.* 2012). Despite recent efforts to elucidate the cellular and transcriptome composition of different fat depots (Lidell *et al.* 2013, Rockstroh *et al.* 2015), the influence of genetic, endocrine or environmental factors on fat development remains largely unknown. It is further likely that these differences are mediated in part by sympathetic innervation that have recently been shown to include dense arborizations within adipose tissue that regulate the beiging process, at least in adult mice (Jiang *et al.* 2017).

Epicardial adipose tissue

One of the more widely studied depots resides within the epicardial region (Aldiss *et al.* 2016) which retains UCP1 into adulthood (Sacks *et al.* 2013) and, as such, is likely to have a role in heat generation and protecting the heart against the cold (Sacks & Symonds 2013). Epicardial adipose tissue may also have additional roles within the heart apart from thermogenesis, such as the regulation of vascular tone and the modulation of inflammation (Antonopoulos & Antoniades 2017). One of the reasons this depot has been widely studied is its accessibility at the time of surgery and the ease with which small amounts can be removed for subsequent analysis. This has enabled a more detailed ontogeny during early life and demonstrated how utilising contemporary systems biology approaches, such as through construction of gene networks, can elucidate the transcriptional function (Ojha *et al.* 2016). Computational methodology, through the development of open source packages (e.g. WGCNA,

http://joe.endocrinology-journals.org
https://doi.org/10.1530/JOE-18-0084

DAVID and Cytoscape), provides a complementary method to understand adipose tissue biology. Such an approach enables the subdivision of genes into regulatory pathways on the basis of their relative expression. By segregating genes into functional groups, changes in the topology of intra-modular networks enabled the identification of biologically important genes within these pathways. For example in the neonatal (i.e. aged between 1 and 22 days) network, high connectivity of hub genes that regulate cellular activities, particularly those associated with cell differentiation and mitochondrial function, were identified (Ojha *et al.* 2016). It also emphasises the intricate co-ordination of multiple processes that control thermogenesis in epicardial adipose tissue of neonates, as well as the manner in which these gene-to-gene interactions shift towards lipogenesis with age (Fig. 3). The same study indicated significant correlations, both positive and negative, between age and negative Z scores for growth (Ojha *et al.* 2016), which could link adipose tissue dysfunction to environmental factors which promote cardiovascular diseases (Ojha *et al.* 2013). Indeed, the concept of specialisation of epicardial fat genes into functional groups, is based not only on maturation through age but also on location in different anatomic sites within the epicardial fat layer per se, namely pericoronary, periatrial and periventricular (Gaborit *et al.* 2015).

Ultimately, the transcriptome in epicardial adipose tissue in early life appears to be sensitive to a longer term reduction of cardiac performance which is not dissimilar to that found in adults with advanced coronary artery disease (McAninch *et al.* 2015).

The structure and architecture of adipose tissue thus differs between the neonate, infant and child with pronounced regulatory effects on UCP1 (Fig. 4). In particular, epicardial adipose tissue retains discrete islands of UCP1 positive cells persisting beyond the neonatal period (Ojha *et al.* 2016). These thermogenic cells exhibit developmental adaptations in their transcriptional architecture, which could modulate cellular function, and this appears to continue throughout life (Chechi *et al.* 2017). Although epicardial fat has limited flexibility and responsiveness in the newborn period, with age and maturation it becomes more responsive to environmental stimuli (Ojha *et al.* 2016). These unique, developmentally-regulated gene interactions and metabolic-related pathways are potential targets for intervention strategies designed to promote BAT function, and potentially reduce the risk of later heart disease.

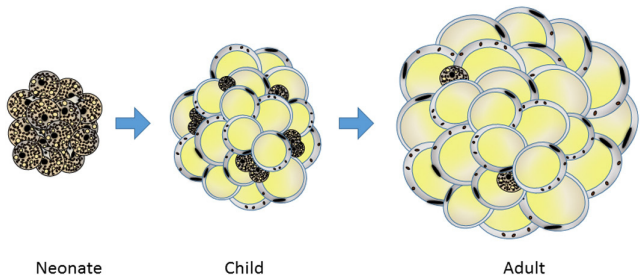

Figure 4
Summary of the changes in epicardial adipose tissue composition through the life cycle.

In conclusion, the study of brown fat has undergone a marked renaissance over the past 10 years, although a majority of studies have adopted cold adapted mice. To make substantial progress over the next decade, focus will need to be on human-relevant studies, together with those which explore the extent to which changes in early life can enhance brown fat function throughout life.

Declaration of interest
The authors declare that there is no conflict of interest that could be perceived as prejudicing the impartiality of this review.

Funding
This work did not receive any specific grant from any funding agency in the public, commercial or not-for-profit sector.

References

Aherne W & Hull D 1966 Brown adipose tissue and heat production in the newborn infant. *Journal of Pathology and Bacteriology* **91** 223–234. (https://doi.org/10.1002/path.1700910126)

Aldiss P, Davies G, Woods R, Budge H, Sacks HS & Symonds ME 2016 'Browning' the cardiac and peri-vascular adipose tissues to modulate cardiovascular risk. *International Journal of Cardiology* **228** 265–274. (https://doi.org/10.1016/j.ijcard.2016.11.074)

Aldiss P, Burton P, Ojha S, Budge H & Symonds ME 2017 Brown adipose tissue and disease: new insights from historical data. *Clinical Medical: Reviews and Case Reports* **4** 182. (https://doi.org/10.23937/22378-23656/1410182)

Antonopoulos AS & Antoniades C 2017 The role of epicardial adipose tissue in cardiac biology: classic concepts and emerging roles. *Journal of Physiology* **595** 3907–3917. (https://doi.org/10.1113/JP273049)

Au-Yong IT, Thorn N, Ganatra R, Perkins AC & Symonds ME 2009 Brown adipose tissue and seasonal variation in humans. *Diabetes* **58** 2583–2587. (https://doi.org/10.2337/db09-0833)

Barabasi AL & Oltvai ZN 2004 Network biology: understanding the cell's functional organization. *Nature Reviews Genetics* **5** 101–113. (https://doi.org/10.1038/nrg1272)

Blauw LL, Aziz NA, Tannemaat MR, Blauw CA, de Craen AJ, Pijl H & Rensen PC 2017 Diabetes incidence and glucose intolerance prevalence increase with higher outdoor temperature. *BMJ Open Diabetes Research and Care* **5** e000317. (https://doi.org/10.1136/bmjdrc-2016-000317)

Booth GL, Luo J, Park AL, Feig DS, Moineddin R & Ray JG 2017 Influence of environmental temperature on risk of gestational diabetes. *Canadian Medical Association Journal* **189** E682–E689. (https://doi.org/10.1503/cmaj.160839)

Budge H, Bispham J, Dandrea J, Evans E, Heasman L, Ingleton PM, Sullivan C, Wilson V, Stephenson T & Symonds ME 2000 Effect of maternal nutrition on brown adipose tissue and its prolactin receptor status in the fetal lamb. *Pediatric Research* **47** 781–786. (https://doi.org/10.1203/00006450-200006000-00017)

Cannon B & Nedergaard J 2004 Brown adipose tissue: function and physiological significance. *Physiological Reviews* **84** 277–359. (https://doi.org/10.1152/physrev.00015.2003)

Cannon B & Nedergaard J 2011 Nonshivering thermogenesis and its adequate measurement in metabolic studies. *Journal of Experimental Biology* **214** 242–253. (https://doi.org/10.1242/jeb.050989)

Cannon B & Nedergaard J 2012*a* Cell biology: neither brown nor white. *Nature* **488** 286–287. (https://doi.org/10.1038/488286a)

Cannon B & Nedergaard J 2012*b* Yes, even human brown fat is on fire! *Journal of Clinical Investigation* **122** 486–489. (https://doi.org/10.1172/JCI60941)

Cassina M, Dona M, Di Gianantonio E, Litta P & Clementi M 2014 First-trimester exposure to metformin and risk of birth defects: a systematic review and meta-analysis. *Human Reproduction Update* **20** 656–669. (https://doi.org/10.1093/humupd/dmu022)

Catalano PM, Presley L, Minium J & Hauguel-de Mouzon S 2009 Fetuses of obese mothers develop insulin resistance in utero. *Diabetes Care* **32** 1076–1080. (https://doi.org/10.2337/dc08-2077)

Chechi K, Voisine P, Mathieu P, Laplante M, Bonnet S, Picard F, Joubert P & Richard D 2017 Functional characterization of the Ucp1-associated oxidative phenotype of human epicardial adipose tissue. *Scientific Reports* **7** 15566. (https://doi.org/10.1038/s41598-017-15501-7)

Chiswick C, Reynolds RM, Denison F, Drake AJ, Forbes S, Newby DE, Walker BR, Quenby S, Wray S, Weeks A, *et al*. 2015 Effect of metformin on maternal and fetal outcomes in obese pregnant women (EMPOWaR): a randomised, double-blind, placebo-controlled trial. *Lancet Diabetes and Endocrinology* **3** 778–786.

Chondronikola M, Volpi E, Borsheim E, Porter C, Annamalai P, Enerback S, Lidell ME, Saraf MK, Labbe SM, Hurren NM, *et al*. 2014 Brown adipose tissue improves whole-body glucose homeostasis and insulin sensitivity in humans. *Diabetes* **63** 4089–4099. (https://doi.org/10.2337/db14-0746)

Cypess AM, White AP, Vernochet C, Schulz TJ, Xue R, Sass CA, Huang TL, Roberts-Toler C, Weiner LS, Sze C, *et al*. 2013 Anatomical localization, gene expression profiling and functional characterization of adult human neck brown fat. *Nature Medicine* **19** 635–639. (https://doi.org/10.1038/nm.3112)

Cypess AM, Haft CR, Laughlin MR & Hu HH 2014 Brown fat in humans: consensus points and experimental guidelines. *Cell Metabolism* **20** 408–415. (https://doi.org/10.1016/j.cmet.2014.07.025)

Dabelea D & Crume T 2011 Maternal environment and the transgenerational cycle of obesity and diabetes. *Diabetes* **60** 1849–1855. (https://doi.org/10.2337/db11-0400)

Diabetes Prevention Program Research Group 2002 Reduction in the incidence of type 2 diabetes with lifestyle intervention or metformin. *New England Journal of Medicine* **2002** 393–403.

Diaz-Zavala RG, Castro-Cantu MF, Valencia ME, Alvarez-Hernandez G, Haby MM & Esparza-Romero J 2017 Effect of the holiday season on weight gain: a narrative review. *Journal of Obesity* **2017** 2085136.

Domecq JP, Prutsky G, Mullan RJ, Sundaresh V, Wang AT, Erwin PJ, Welt C, Ehrmann D, Montori VM & Murad MH 2013 Adverse effects of the common treatments for polycystic ovary syndrome: a systematic review and meta-analysis. *Journal of Clinical Endocrinology and Metabolism* **98** 4646–4654. (https://doi.org/10.1210/jc.2013-2374)

Dumortier O, Roger E, Pisani DF, Casamento V, Gautier N, Lebrun P, Johnston H, Lopez P, Amri EZ, Jousse C, *et al*. 2017 Age-dependent control of energy homeostasis by brown adipose tissue in progeny subjected to maternal diet-induced fetal programming. *Diabetes* **66** 627–639. (https://doi.org/10.2337/db16-0956)

Eyal S, Easterling TR, Carr D, Umans JG, Miodovnik M, Hankins GD, Clark SM, Risler L, Wang J, Kelly EJ, *et al*. 2010 Pharmacokinetics of metformin during pregnancy. *Drug Metabolism and Disposition* **38** 833–840. (https://doi.org/10.1124/dmd.109.031245)

Fainberg HP, Birtwistle M, Alagal R, Alhaddad A, Pope M, Davies G, Woods R, Castellanos M, May ST, Ortori CA, *et al*. 2018 Transcriptional analysis of adipose tissue during post-natal development reveals depot-specific responsiveness to maternal dietary supplementation. *Scientific Reports* [in press].

Fischer AW, Cannon B & Nedergaard J 2018 Optimal housing temperatures for mice to mimic the thermal environment of humans: an experimental study. *Molecular Metabolism* **7** 161–170. (https://doi.org/10.1016/j.molmet.2017.10.009)

Gaborit B, Venteclef N, Ancel P, Pelloux V, Gariboldi V, Leprince P, Amour J, Hatem SN, Jouve E, Dutour A, *et al*. 2015 Human epicardial adipose tissue has a specific transcriptomic signature depending on its anatomical peri-atrial, peri-ventricular, or peri-coronary location. *Cardiovascular Research* **108** 62–73. (https://doi.org/10.1093/cvr/cvv208)

Gaillard R 2015 Maternal obesity during pregnancy and cardiovascular development and disease in the offspring. *European Journal of Epidemiology* **30** 1141–1152. (https://doi.org/10.1007/s10654-015-0085-7)

Geerling JJ, Boon MR, van der Zon GC, van den Berg SA, van den Hoek AM, Lombès M, Princen HM, Havekes LM, Rensen PC & Guigas B 2014 Metformin lowers plasma triglycerides by promoting VLDL-triglyceride clearance by brown adipose tissue in mice. *Diabetes* **63** 880–891. (https://doi.org/10.2337/db13-0194)

Giles DA, Moreno-Fernandez ME, Stankiewicz TE, Graspeuntner S, Cappelletti M, Wu D, Mukherjee R, Chan CC, Lawson MJ, Klarquist J, *et al*. 2017 Thermoneutral housing exacerbates nonalcoholic fatty liver disease in mice and allows for sex-independent disease modeling. *Nature Medicine* **23** 829–838. (https://doi.org/10.1038/nm.4346)

Gilsanz V, Smith ML, Goodarzian F, Kim M, Wren TA & Hu HH 2012 Changes in brown adipose tissue in boys and girls during childhood and puberty. *Journal of Pediatrics* **160** 604.e601–609.e601. (https://doi.org/10.1016/j.jpeds.2011.09.035)

Grimaldi D, Provini F, Pierangeli G, Mazzella N, Zamboni G, Marchesini G & Cortelli P 2015 Evidence of a diurnal thermogenic handicap in obesity. *Chronobiolgy International* **32** 299–302. (https://doi.org/10.3109/07420528.2014.983603)

Grisouard J, Timper K, Radimerski TM, Frey DM, Peterli R, Kola B, Korbonits M, Herrmann P, Krahenbuhl S, Zulewski H, *et al*. 2010 Mechanisms of metformin action on glucose transport and metabolism in human adipocytes. *Biochemical Pharmacology* **80** 1736–1745. (https://doi.org/10.1016/j.bcp.2010.08.021)

Hale TW, Kristensen JH, Hackett LP, Kohan R & Ilett KF 2002 Transfer of metformin into human milk. *Diabetologia* **45** 1509–1514. (https://doi.org/10.1007/s00125-002-0939-x)

Harms M & Seale P 2013 Brown and beige fat: development, function and therapeutic potential. *Nature Medicine* **19** 1252–1263. (https://doi.org/10.1038/nm.3361)

Health and Social Care Information Centre UK 2016 *Health Survey for England 2014*. Colchester, UK: UK Data Service. (available at: https://discover.ukdataservice.ac.uk/series/?sn=2000021)

Heaton GM & Nicholls DG 1977 The structural specificity of the nucleotide-binding site and the reversible nature of the inhibition of proton conductance induced by bound nucleotides in brown-adipose-tissue mitochondria. *Biochemical Society Transactions* **5** 210–212. (https://doi.org/10.1042/bst0050210)

Henry BA, Pope M, Birtwistle M, Loughnan R, Alagal R, Fuller-Jackson J-P, Perry V, Budge H, Clarke IJ & Symonds ME 2017 Ontogeny and thermogenic role for sternal fat in female sheep. *Endocrinology* **158** 2212–2225. (https://doi.org/10.1210/en.2017-00081)

Hughes R & Rowan J 2006 Pregnancy in women with Type 2 diabetes: who takes metformin and what is the outcome? *Diabetic Medicine* **23** 318–322. (https://doi.org/10.1111/j.1464-5491.2006.01750.x)

Hull D & Segall MM 1966 Distinction of brown from white adipose tissue. *Nature* **212** 469–472. (https://doi.org/10.1038/212469a0)

Jiang H, Ding X, Cao Y, Wang H & Zeng W 2017 Dense intra-adipose sympathetic arborizations are essential for cold-induced beiging of mouse white adipose tissue. *Cell Metabolism* **26** 686.e683–692.e683. (https://doi.org/10.1016/j.cmet.2017.08.016)

Klingenspor M & Fromme T 2012 Brown adipose tissue. In *Adipose Tissue Biology*, pp 39–70. Ed ME Symonds. New York: Springer.

Law J, Morris DE, Izzi-Engbeaya C, Salem V, Coello C, Robinson L, Jayasinghe M, Scott R, Gunn R, Rabiner EA, *et al*. 2017 Thermal imaging is a noninvasive alternative to PET-CT for measurement of brown adipose tissue activity in humans. *Journal of Nuclear Medicine* **59** 516–522. (https://doi.org/10.2967/jnumed.117.190546)

Liang X, Yang Q, Zhang L, Maricelli JW, Rodgers BD, Zhu MJ & Du M 2016 Maternal high-fat diet during lactation impairs thermogenic function of brown adipose tissue in offspring mice. *Scientific Reports* **6** 34345. (https://doi.org/10.1038/srep34345)

Lidell ME, Betz MJ, Dahlqvist Leinhard O, Heglind M, Elander L, Slawik M, Mussack T, Nilsson D, Romu T, Nuutila P, *et al*. 2013 Evidence for two types of brown adipose tissue in humans. *Nature Medicine* **19** 631–634. (https://doi.org/10.1038/nm.3017)

Macotela Y, Emanuelli B, Mori MA, Gesta S, Schulz TJ, Tseng YH & Kahn CR 2012 Intrinsic differences in adipocyte precursor cells from different white fat depots. *Diabetes* **61** 1691–1699. (https://doi.org/10.2337/db11-1753)

Maloney SK, Fuller A, Mitchell D, Gordon C & Overton JM 2014 Translating animal model research: does it matter that our rodents are cold? *Physiology* **29** 413–420.

McAninch EA, Fonseca TL, Poggioli R, Panos AL, Salerno TA, Deng Y, Li Y, Bianco AC & Iacobellis G 2015 Epicardial adipose tissue has a unique transcriptome modified in severe coronary artery disease. *Obesity* **23** 1267–1278. (https://doi.org/10.1002/oby.21059)

Mellor DJ & Cockburn F 1986 A comparison of energy metabolism in the new-born infant, piglet and lamb. *Quarterly Journal of Experimental Physiology* **71** 361–379. (https://doi.org/10.1113/expphysiol.1986.sp002995)

Mo Q, Salley J, Roshan T, Baer LA, May FJ, Jaehnig EJ, Lehnig AC, Guo X, Tong Q, Nuotio-Antar AM, *et al*. 2017 Identification and characterization of a supraclavicular brown adipose tissue in mice. *JCI Insight* **2** 93166. (https://doi.org/10.1172/jci.insight.93166)

Modi N, Murgasova D, Ruager-Martin R, Thomas EL, Hyde MJ, Gale C, Santhakumaran S, Doré CJ, Alavi A & Bell JD 2011 The influence of maternal body mass index on infant adiposity and hepatic lipid content. *Pediatric Research* **70** 287–291. (https://doi.org/10.1203/PDR.0b013e318225f9b1)

Monteiro CA, Moubarac JC, Levy RB, Canella DS, Louzada M & Cannon G 2018 Household availability of ultra-processed foods and obesity in nineteen European countries. *Public Health Nutrition* **21** 18–26. (https://doi.org/10.1017/S1368980017001379)

Nedergaard J & Cannon B 2013 UCP1 mRNA does not produce heat. *Biochemica et Biophysica Acta* **1831** 943–949. (https://doi.org/10.1016/j.bbalip.2013.01.009)

Ojha S, Saroha V, Symonds ME & Budge H 2013 Excess nutrient supply in early life and its later metabolic consequences. *Clinical and Experimental Pharmacology and Physiology* **40** 817–823. (https://doi.org/10.1111/1440-1681.12061)

Ojha S, Fainberg HP, Wilson V, Pelella G, Castellanos M, May ST, Lotto AA, Sacks H, Symonds ME & Budge H 2016 Gene pathway development in human epicardial adipose tissue during early life. *JCI Insight* **1** e87460.

Panchenko PE, Voisin S, Jouin M, Jouneau L, Prezelin A, Lecoutre S, Breton C, Jammes H, Junien C & Gabory A 2016 Expression of epigenetic machinery genes is sensitive to maternal obesity and weight loss in relation to fetal growth in mice. *Clinical Epigenetics* **8** 22. (https://doi.org/10.1186/s13148-13016-10188-13143)

Pedersen J 1954 Weight and length at birth of infants of diabetic mothers. *Acta Endocrinologica* **16** 330–342.

Reynolds RM, Allan KM, Raja EA, Bhattacharya S, McNeill G, Hannaford PC, Sarwar N, Lee AJ, Bhattacharya S & Norman JE 2013 Maternal obesity during pregnancy and premature mortality from cardiovascular event in adult offspring: follow-up of 1 323 275 person years. *BMJ* **347** f4539. (https://doi.org/10.1136/bmj.f4539)

Rockstroh D, Landgraf K, Wagner IV, Gesing J, Tauscher R, Lakowa N, Kiess W, Buhligen U, Wojan M, Till H, *et al*. 2015 Direct evidence of brown adipocytes in different fat depots in children. *PLoS ONE* **10** e0117841. (https://doi.org/10.1371/journal.pone.0117841)

Sacks H & Symonds ME 2013 Anatomical locations of human brown adipose tissue: functional relevance and implications in obesity and type 2 diabetes. *Diabetes* **62** 1783–1790. (https://doi.org/10.2337/db12-1430)

Sacks HS, Fain JN, Bahouth SW, Ojha S, Frontini A, Budge H, Cinti S & Symonds ME 2013 Adult epicardial fat exhibits beige features. *Journal of Clinical Endocrinology and Metabolism* **98** E1448–E1455. (https://doi.org/10.1210/jc.2013-1265)

Salomäki H, Heinaniemi M, Vahatalo LH, Ailanen L, Eerola K, Ruohonen ST, Pesonen U & Koulu M 2014 Prenatal metformin exposure in a maternal high fat diet mouse model alters the transcriptome and modifies the metabolic responses of the offspring. *PLoS ONE* **9** e115778.

Scotney H, Symonds ME, Law J, Budge H, Sharkey D & Manolopoulos KN 2017 Glucocorticoids modulate human brown adipose tissue thermogenesis in vivo. *Metabolism* **70** 125–132. (https://doi.org/10.1016/j.metabol.2017.01.024)

Skurk T, Alberti-Huber C, Herder C & Hauner H 2007 Relationship between adipocyte size and adipokine expression and secretion. *Journal of Clinical Endocrinology and Metabolism* **92** 1023–1033. (https://doi.org/10.1210/jc.2006-1055)

Symonds ME 2013 Brown adipose tissue growth and development. *Scientifica* **2013** 14. (https://doi.org/10.1155/2013/305763)

Symonds ME & Budge H 2009 Nutritional models of the developmental programming of adult health and disease. *Proceedings of the Nutrition Society* **68** 173–178. (https://doi.org/10.1017/S0029665109001049)

Symonds ME, Andrews DC & Johnson PJ 1989 The control of thermoregulation in the developing lamb during slow wave sleep. *Journal of Developmental Physiology* **11** 289–298.

Symonds ME, Bryant MJ, Clarke L, Darby CJ & Lomax MA 1992 Effect of maternal cold exposure on brown adipose tissue and thermogenesis in the neonatal lamb. *Journal of Physiology* **455** 487–502. (https://doi.org/10.1113/jphysiol.1992.sp019313)

Symonds ME, Bird JA, Clarke L, Gate JJ & Lomax MA 1995 Nutrition, temperature and homeostasis during perinatal development. *Experimental Physiology* **80** 907–940. (https://doi.org/10.1113/expphysiol.1995.sp003905)

Symonds ME, Andrews DC, Buss DS, Clarke L, Darby CJ & Lomax MA 1996 Effect of rearing temperature on perirenal adipose tissue development and thermoregulation following methimazole treatment of postnatal lambs. *Experimental Physiology* **81** 995–1006. (https://doi.org/10.1113/expphysiol.1996.sp003999)

Symonds ME, Stephenson T, Gardner DS & Budge H 2007 Long-term effects of nutritional programming of the embryo and fetus: mechanisms and critical windows. *Reproduction Fertility and Development* **19** 53–63. (https://doi.org/10.1071/RD06130)

Symonds ME, Sebert SP & Budge H 2009 The impact of diet during early life and its contribution to later disease: critical checkpoints in development and their long-term consequences for metabolic health. *Proceedings of the Nutrition Society* **68** 416–421. (https://doi.org/10.1017/S0029665109990152)

Symonds ME, Sebert S & Budge H 2011 The obesity epidemic: from the environment to epigenetics – not simply a response to dietary manipulation in a thermoneutral environment. *Frontiers in Epigenomics* **2** 24.

Turban S, Stretton C, Drouin O, Green CJ, Watson ML, Gray A, Ross F, Lantier L, Viollet B, Hardie DG, *et al*. 2012 Defining the contribution of AMP-activated protein kinase (AMPK) and protein kinase C (PKC) in regulation of glucose uptake by metformin in skeletal muscle cells. *Journal of Biological Chemistry* **287** 20088–20099. (https://doi.org/10.1074/jbc.M111.330746)

Symonds ME, Budge H & Frazier-Wood AC 2013*a* Epigenetics and obesity: a relationship waiting to be explained. *Human Heredity* **75** 90–97. (https://doi.org/10.1159/000352009)

Symonds ME, Mendez MA, Meltzer HM, Koletzko B, Godfrey K, Forsyth S & van der Beek EM 2013*b* Early life nutritional programming of obesity: mother-child cohort studies. *Annals of Nutrition and Metabolism* **62** 137–145. (https://doi.org/10.1159/000345598)

Symonds ME, Pope M & Budge H 2015 The ontogeny of brown adipose tissue. *Annual Review of Nutrition* **35** 295–320. (https://doi.org/10.1146/annurev-nutr-071813-105330)

Symonds ME, Dellschaft N, Pope M, Birtwistle M, Alagal R, Keisler D & Budge H 2016 Developmental programming, adiposity, and reproduction in ruminants. *Theriogenology* **86** 120–129. (https://doi.org/10.1016/j.theriogenology.2016.04.023)

Symonds ME, Bloor I, Ojha S & Budge H 2017 The placenta, maternal diet and adipose tissue development in the newborn. *Annals of Nutritoin and Metabolism* **70** 232–235.

van Marken Lichtenbelt WD, Vanhommerig JW, Smulders NM, Drossaerts JM, Kemerink GJ, Bouvy ND, Schrauwen P & Teule GJ 2009 Cold-activated brown adipose tissue in healthy men. *New England Journal of Medicine* **360** 1500–1508. (https://doi.org/10.1056/NEJMoa0808718)

Vanky E, Zahlsen K, Spigset O & Carlsen SM 2005 Placental passage of metformin in women with polycystic ovary syndrome. *Fertility and Sterility* **83** 1575–1578. (https://doi.org/10.1016/j.fertnstert.2004.11.051)

Weinsier RL, Hunter GR, Heini AF, Goran MI & Sell SM 1998 The etiology of obesity: relative contribution of metabolic factors, diet, and physical activity. *American Journal of Medicine* **105** 145–150. (https://doi.org/10.1016/S0002-9343(98)00190-9)

Received in final form 18 April 2018
Accepted 22 May 2018
Accepted Preprint published online 22 May 2018

Adipocyte

ISSN: 2162-3945 (Print) 2162-397X (Online) Journal homepage: https://www.tandfonline.com/loi/kadi20

Brown adipose tissue and glucose homeostasis – the link between climate change and the global rise in obesity and diabetes

Michael E. Symonds, Grace Farhat, Peter Aldiss, Mark Pope & Helen Budge

To cite this article: Michael E. Symonds, Grace Farhat, Peter Aldiss, Mark Pope & Helen Budge (2019) Brown adipose tissue and glucose homeostasis – the link between climate change and the global rise in obesity and diabetes, Adipocyte, 8:1, 46-50, DOI: 10.1080/21623945.2018.1551689

To link to this article: https://doi.org/10.1080/21623945.2018.1551689

Accepted author version posted online: 21 Nov 2018.
Published online: 03 Dec 2018.

ADIPOCYTE
2019, VOL. 8, NO. 1, 46–50
https://doi.org/10.1080/21623945.2018.1551689

Taylor & Francis
Taylor & Francis Group

REVIEW

Brown adipose tissue and glucose homeostasis – the link between climate change and the global rise in obesity and diabetes

Michael E. Symonds [a,b], Grace Farhat [c], Peter Aldiss[a], Mark Pope[a], and Helen Budge[a]

[a]Early Life Research Unit, Division of Child Health, Obstetrics & Gynaecology, School of Medicine, University of Nottingham, Nottingham, UK; [b]Nottingham Digestive Disease Centre and Biomedical Research Centre, School of Medicine, University of Nottingham, Nottingham, UK; [c]School of Health Sciences, Liverpool Hope University, Hope Park, Liverpool, UK

ABSTRACT

There is increasing evidence that the global rise in temperature is contributing to the onset of diabetes, which could be mediated by a concomitant reduction in brown fat activity. Brown (and beige) fat are characterised as possessing a unique mitochondrial protein uncoupling protein (UCP)1 that when activated can rapidly generate large amounts of heat. Primary environmental stimuli of UCP1 include cold-exposure and diet, leading to increased activity of the sympathetic nervous system and large amounts of lipid and glucose being oxidised by brown fat. The exact contribution remains controversial, although recent studies indicate that the amount of brown and beige fat in adult humans has been greatly underestimated. We therefore review the potential mechanisms by which glucose could be utilised within brown and beige fat in adult humans and the extent to which these are sensitive to temperature and diet. This includes the potential contribution from the peridroplet and cytoplasmic mitochondrial sub-fractions recently identified in brown fat, and whether a proportion of glucose oxidation could be UCP1-independent. It is thus predicted that as new methods are developed to assess glucose metabolism by brown fat, a more accurate determination of the thermogenic and non-thermogenic functions could be feasible in humans.

ARTICLE HISTORY
Received 26 September 2018
Revised 6 November 2018
Accepted 12 November 2018

KEYWORDS
brown adipose tissue; glucose; mitochondria

There is increasing evidence that the rise in diabetes is partly mediated by the increase in global temperatures over the past 20 years.[1,2] This has been observed across the general population in the USA[3] and, in pregnant women in Canada relative to the onset of gestational diabetes.[4] Moreover, the prevalence of gestational diabetes in Canada is higher in the summer and rising ambient temperatures in the 3–4 weeks prior to third trimester glucose tolerance testing can predict gestational diabetes onset.[5] Consequently as brown fat is highly sensitive to changes in ambient temperature and is normally activated by cold exposure it would be expected to become less active as temperature rises.[6,7] The unique capacity of brown fat to rapidly respond to cold exposure resides within uncoupling protein (UCP)1 that is located on the inner mitochondrial membrane.[8] When activated this results in the free flow of protons across the inner mitochondrial membrane,[8] thereby bypassing the need to convert ADP to ATP, as occurs in the mitochondria of all other tissues.

The presence of brown fat is adult humans was originally identified from positron emission tomography-computed tomography (PET-CT) studies in cancer patients,[9] and has been confirmed across a range of ethnicities including Caucasian,[6] Asian[10] and African[11] populations. This technique is dependent on subjects showing an increase in radio-labelled glucose uptake within their brown fat, a response that can be modulated by season and sensitivity to cold.[12] Consequently the extent to which environmentally induced changes in brown fat function can impact on glucose homeostasis remains a matter of debate.[13] It should be noted that with repeated PET-CT scans on the same subject then brown fat is identifiable in most, if not all, adults,[14] and comparable quantification of brown fat has been shown between PET-CT and thermal imaging.[15] Consequently, it is likely that brown fat is present in all adults,[16] and as shown in rodents its temperature fluctuates appreciably over a 24h period.[17] The acute sensitivity of brown fat to changes in temperature would thus mean that an overall rise in current global temperature (see https://climate.nasa.gov/vital-signs/global-temperature/) would be sufficient to reduce its activity on a population wide basis. Moreover, if the United Nations report on climate breakdown (see

CONTACT Michael E. Symonds michael.symonds@nottingham.ac.uk Division of Child Health, Obstetrics and Gynaecology, School of Medicine, University Hospital, University of Nottingham, Nottingham NG7 2UH, UK

http://www.ipcc.ch/report/sr15/) is not swiftly acted upon then an even greater challenge would present itself.

What is the contribution of brown fat to whole body glucose homeostasis?

The primary factors that determine glucose consumption by brown fat are the total amount of fat, its rate of glucose oxidation and capacity to transport glucose.[18] A number of important recent publications have demonstrated that summary estimates appear to substantially underestimate each of these measures. It is therefore highly likely that current calculations suggesting only 1% of total daily glucose utilisation is partitioned across brown fat are inaccurate.[13] The total contribution of brown fat should therefore be revised due to the following:

(1) The amount of brown fat in adult humans is routinely underestimated, mainly due to the current imaging techniques and the difficulty in measurement because of the mixing of brown and beige fat with other white fat depots in multiple sites in the body.[19] Beige fat is defined as being a discrete region within white fat that possesses UCP1 although at approximately ten-fold lower concentrations than "classic" brown fat,[20]
(2) Brown fat can be activated by diet[21,22] to the same degree as by cold exposure.[21] The extent to which these dual activation pathways may be additive is unknown as current studies on cold exposure have been conducted in fasted subjects.
(3) Brown fat shows appreciable metabolic activity in warm ambient temperatures, effects that remain for at least two hours after removal of cold exposure.[23]

It is now apparent that the total amount of brown and/or beige fat in adult humans could be up to ten-fold higher, even in obese adults.[19] This is based on studies that have been able to conduct repeated PET-CT scans of the same individual,[14] together with further refinements in image analysis.[19] Furthermore, a significant proportion of adipocytes present in brown or beige depots do not appear to be activated by acute cold exposure. Consequently, we suggest that as much as 20% of daily glucose oxidation could be potentially accounted for within brown fat, as a consequence of either diet and/or cold exposure (see Figure 1). This is in accord with the recognition that brown fat has a regulatory role in glucose homeostasis[18] explaining why cold-induced stimulation of brown fat has the potential to improve glucose metabolism in both lean[24] and diabetic[25] subjects. Indeed, it has recently been shown in obese adults, that long term caloric restriction sufficient

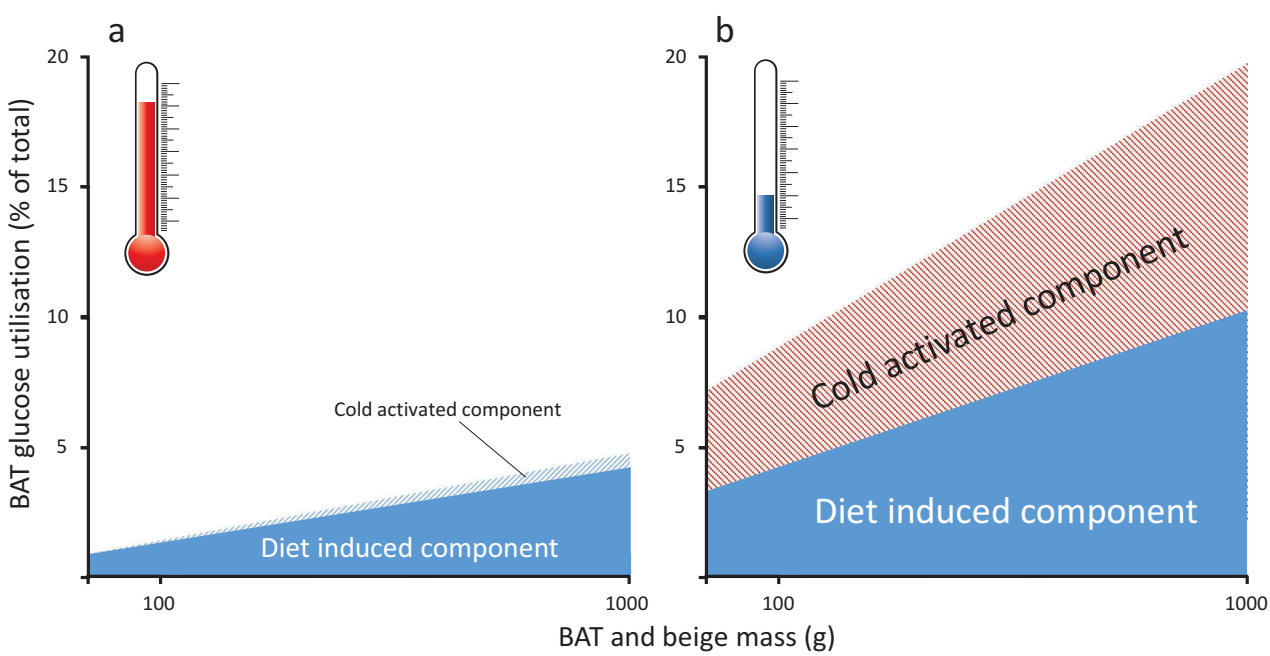

Figure 1. Summary of the potential change in glucose utilisation by brown and beige fat between (A) warm and (B) cool ambient temperature increases. Overall the fraction of whole body-glucose utilisation increases in parallel with an increase in the amount of brown and beige fat, but this is lower in the warm. It is based on calculated estimates of glucose oxidation in adult humans as determined in the cold (e.g.[13]) or after feeding (e.g.[40]).

to reduce body weight by 16.5% (primarily due to fat loss) promoted the brown adipocyte content in subcutaneous fat by 10%.[26] At the same time, fasting blood insulin and glucose were improved. Furthermore, in humans, brown fat appears to exhibit a glucose responsive biorhythm that is disrupted when the abundance of brown fat is low.[27]

Is glucose metabolism by brown fat independent of UCP1 mediated thermogenesis?

Glucose utilisation within UCP1-containing adipocytes in brown and beige fat can occur independently of UCP1-mediated thermogenesis.[18] This would explain the observation of substantial glucose present in brown fat depots,[28] and its appreciable utilisation even at thermoneutrality.[23] Glucose present within brown fat could act, in part, as a reserve to be utilised during cold exposure, as the amount of glucose taken up within supraclavicular brown fat, for example, is closely associated with cold-induced thermogenesis.[28] Cold exposure is also likely to be accompanied by increased uptake of triglycerides which, in murine obesity models, results in improved glucose homeostasis and up to a five-fold rise in glucose uptake within interscapular brown fat.[29] If triglyceride uptake is inhibited pharmacologically, then the uptake of glucose by brown fat is greatly reduced whereas, in other tissues such as skeletal muscle, it is unaffected.[30] Gene deletion studies in mice indicate an increasing number of pathways which can restrict glucose uptake by brown fat.[18] These appear to be linked to glucose transporter 4, e.g. the GAP complex RalGAP which, when inactivated, results in a seven-fold rise in glucose uptake by brown fat.[31] It is likely that other pathways are involved and that these may differ between brown and beige adipocytes. For example, deletion of endonuclease G is associated with increased expression of thermogenic genes in beige, but not brown, adipocytes.[32] This, is turn, is accompanied with improved glucose homeostasis and reduced white fat mass. Indeed, multiple pathways are involved and extend to a wide range of signalling molecules as identified in mice e.g. DJ-1,[33] although these need confirming in humans.

Two types of brown fat mitochondria and their differential roles in energy balance

The concept that the regulation of UCP1 differs between brown and beige adipocytes and that the utilisation of glucose by these different cell populations requires further investigation. Glucose oxidation by beige fat has been shown to be independent of UCP1 and is, therefore, non-classical.[34] The potential divergence in mitochondrial function between dietary and cold-induced thermogenesis could be partly explained by the recent discovery that brown fat contains two different types of mitochondria i.e. the peridroplet and cytoplasmic mitochondrial sub-fractions.[35] It has been suggested that these fractions are functionally different in their bioenergetic capacity and fatty acid oxidation despite both possessing UCP1. One potential consequence is that there is a greater recruitment of lipid-droplets within the peridroplet mitochondrial domain after feeding,[35] and perhaps cytoplasmic mitochondria are dominant with cold exposure (see Figure 2). Such an adaptation to feeding would be in accord with the diurnal rhythm in brown fat activity seen in mice, which is consistent with a lower postprandial lipid response, in the morning compared to evening in humans.[36] The fundamentally different processes between the peridroplet and cytoplasmic mitochondrial sub-fractions[35] have yet to be examined in different human disease states. These types of investigations could determine whether glucose metabolism differs between each domain. They could also start to explain the recent demonstration of considerable heterogeneity in nutrient, including glucose uptake by brown adipocytes.[37]

Future research on the role of brown and/or beige adipocytes on glucose homeostasis

Given the increasing evidence that brown and/or beige fat has a role in both dietary and cold-induced thermogenesis, more focus is now required on the impact of diet especially under thermoneutral conditions.[38] A combined effect of diet and cold exposure could therefore herald ground-breaking approaches to diabetes prevention and/or treatment. The urgent need to make such an intervention is high-lighted by the continued rise in global temperatures, and the increased duration of "summer" (see https://www.metoffice.gov.uk/binaries/content/assets/mohippo/pdf/uk-climate/state-of-the-uk-climate/soc_supplement-002.pdf) which currently appear to be largely unpreventable. Moreover, the impact of ageing needs to be considered as this is accompanied with a "natural" decline in brown fat mass, which could underpin the onset of type 2 diabetes.[39] Critically, more sophisticated assessments (including the potential use of glucose tracers) to accurately assess glucose uptake by brown adipose tissue and of UCP1, both in vivo and in vitro, are required to enable a more accurate partitioning of its thermogenic and non-thermogenic functions.

Disclosure statement

No potential conflict of interest was reported by the authors.

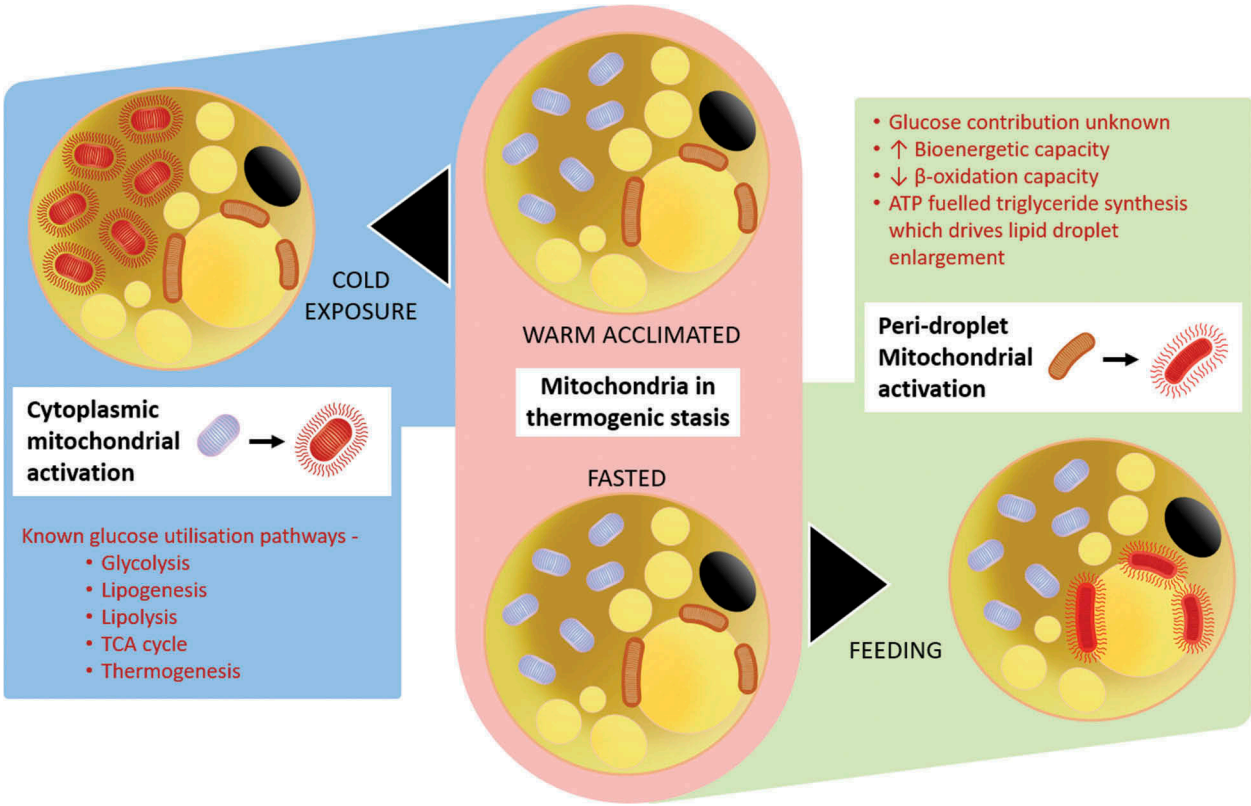

Figure 2. Summary of the potentially different responses between the peridroplet and cytoplasmic mitochondrial fractions within brown (and beige) fat to oxidative metabolism in response to diet or cold-exposure.

ORCID

Michael E. Symonds http://orcid.org/0000-0001-9649-8963
Grace Farhat http://orcid.org/0000-0002-7134-7445

References

1. Symonds ME, Aldiss P, Dellschaft N, Law J, Fainberg HP, Pope M, Sacks H, Budge H. Brown adipose tissue development and function and its impact on reproduction. J Endocrinol. 2018;238(1): R53–R62.
2. Ruiz JR, Martinez-Tellez B, Sanchez-Delgado G, Osuna-Prieto FJ, Rensen PCN, Boon MR. Role of human brown fat in obesity, metabolism and cardiovascular disease: strategies to turn up the heat. Prog Cardiovasc Dis. 2018;61(2):232–245.
3. Blauw LL, Aziz NA, Tannemaat MR, Blauw CA, de Craen AJ, Pijl H, Rensen PC. Diabetes Incidence and glucose intolerance prevalence increase with higher outdoor temperature. BMJ Open Diabetes Res Care. 2017;5(1): e000317.
4. Booth GL, Luo J, Park AL, Feig DS, Moineddin R, Ray JG. Influence of environmental temperature on risk of gestational diabetes. Cmaj. 2017;189(19): E682–E689.
5. Retnakaran R, Ye C, Kramer CK, Hanley AJ, Connelly PW, Sermer M, Zinman B. Impact of daily incremental change in environmental temperature on beta cell function and the risk of gestational diabetes in pregnant women. Diabetologia. 2018;61: 2633–2642.
6. Au-Yong ITH, Thorn N, Ganatra R, Perkins AC, Symonds ME. Brown adipose tissue and seasonal variation in humans. Diabetes. 2009;58(11):2583–2587.
7. Cypess AM, Lehman S, Williams G, Tal I, Rodman D, Goldfine AB, Kuo FC, Palmer EL, Tseng Y-H, Doria A, et al. Identification and importance of brown adipose tissue in adult humans. N Engl J Med. 2009;360(15):1509–1517.
8. Cannon B, Nedergaard J. Brown adipose tissue: function and physiological significance. Physiol Rev. 2004;84(1):277–359.
9. Matsushita M, Yoneshiro T, Aita S, Kameya T, Sugie H, Saito M. Impact of brown adipose tissue on body fatness and glucose metabolism in healthy humans. Int J Obes (Lond). 2014;38(6):812–817.
10. Bakker LE et al. Brown adipose tissue volume in healthy lean south asian adults compared with white caucasians: a prospective, case-controlled observational study. Lancet Diabetes Endocrinol. 2014;2(3): 210–217.
11. Perkins AC, Mshelia DS, Symonds ME, Sathekge M. Prevalence and pattern of brown adipose tissue distribution of 18f-Fdg in patients undergoing Pet-Ct in a subtropical climatic zone. Nucl Med Commun. 2013;34 (2):168–174.
12. Cypess AM, Haft CR, Laughlin MR, Hu HH. Brown fat in humans: consensus points and experimental guidelines. Cell Metab. 2014;20(3):408–415.

13. Carpentier AC, Blondin DP, Virtanen KA, Richard D, Haman F, Turcotte EE. Brown adipose tissue energy metabolism in humans. Front Endocrinol (Lausanne). 2018;9: 447.
14. Gerngross C, Schretter J, Klingenspor M, Schwaiger M, Fromme T. Active brown fat during 18F-FDG PET/CT imaging defines a patient group with characteristic traits and an increased probability of brown fat redetection. J Nucl Med. 2017;58(7): 1104–1110.
15. Law, J., et al. Thermal imaging is a noninvasive alternative to PET/CT for measurement of brown adipose tissue activity in humans. J Nucl Med. 2018;59: 516–522.
16. Law J, Chalmers J, Morris DE, Robinson L, Budge H, Symonds ME. The use of infrared thermography in the measurement and characterization of brown adipose tissue activation. Temp. 2017; 1–15.
17. Ootsuka Y, de Menezes RC, Zaretsky DV, Alimoradian A, Hunt J, Stefanidis A, Oldfield BJ, Blessing WW. Brown adipose tissue thermogenesis heats brain and body as part of the brain-coordinated ultradian basic rest-activity cycle. Neuroscience. 2009;164(2):849–861.
18. Hankir MK, Klingenspor M. Brown adipocyte glucose metabolism: a heated subject. EMBO Rep. 2018;19:9.
19. Leitner BP, Huang S, Brychta RJ, Duckworth CJ, Baskin AS, McGehee S, Tal I, Dieckmann W, Gupta G, Kolodny GM, et al. Mapping of human brown adipose tissue in lean and obese young men. Proc Natl Acad Sci U S A. 2017;114(32):8649–8654.
20. Nedergaard J, Cannon B. Ucp1 Mrna does not produce heat. Biochemi Biophys Acta. 2013;1831(5):943–949.
21. Din, M. U., et al. Postprandial oxidative metabolism of human brown fat indicates thermogenesis. Cell Metab. 2018.
22. Scotney H, Symonds ME, Law J, Budge H, Sharkey D, Manolopoulos KN. Glucocorticoids modulate human brown adipose tissue thermogenesis in vivo. Metabolism. 2017;70: 125–132.
23. Leitner BP, Weiner LS, Desir M, Kahn PA, Selen DJ, Tsang C, Kolodny GM, Cypess AM. Kinetics of human brown adipose tissue activation and deactivation. Int J Obesity. 2018. doi:10.1038/s41366-018-0104-3.
24. Iwen KA, Backhaus J, Cassens M, Waltl M, Hedesan OC, Merkel M, Heeren J, Sina C, Rademacher L, Windjäger A, et al. Cold-induced brown adipose tissue activity alters plasma fatty acids and improves glucose metabolism in men. J Clin Endocrinol Metab. 2017;102(11):4226–4234.
25. Hanssen MJW, Hoeks J, Brans B, van der Lans AAJJ, Schaart G, van Den Driessche JJ, Jörgensen JA, Boekschoten MV, Hesselink MKC, Havekes B, et al. Short-term cold acclimation improves insulin sensitivity in patients with type 2 diabetes mellitus. Nat Med. 2015;21(8):863–865.
26. Perdikari A, Leparc GG, Balaz M, Pires ND, Lidell ME, Sun W, Fernandez-Albert F, Müller S, Akchiche N, Dong H, et al. Batlas: deconvoluting brown adipose tissue. Cell Rep. 2018;25(3):784–97 e4.
27. Lee P, Bova R, Schofield L, Bryant W, Dieckmann W, Slattery A, Govendir MA, Emmett L, Greenfield JR. Brown adipose tissue exhibits a glucose-responsive thermogenic biorhythm in humans. Cell Metab. 2016;23(4):602–609.
28. Weir, G., et al. Substantial metabolic activity of human brown adipose tissue during warm conditions and cold-induced lipolysis of local triglycerides. Cell Metab. 2018;27:1348–1355.e4.
29. Bartelt A, Bruns OT, Reimer R, Hohenberg H, Ittrich H, Peldschus K, Kaul MG, Tromsdorf UI, Weller H, Waurisch C, et al. Brown adipose tissue activity controls triglyceride clearance. Nat Med. 2011;17(2):200–205.
30. Blondin DP, Frisch F, Phoenix S, Guérin B, Turcotte ÉE, Haman F, Richard D, Carpentier AC. Inhibition of intracellular triglyceride lipolysis suppresses cold-induced brown adipose tissue metabolism and increases shivering in humans. Cell Metab. 2017;25(2):438–447.
31. Skorobogatko Y, Dragan M, Cordon C, Reilly SM, Hung C-W, Xia W, Zhao P, Wallace M, Lackey DE, Chen X-W, et al. Rala controls glucose homeostasis by regulating glucose uptake in brown fat. Proc Natl Acad Sci U S A. 2018;115(30):7819–7824.
32. Pardo R, Blasco N, Vilà M, Beiroa D, Nogueiras R, Cañas X, Simó R, Sanchis D, Villena JA. Endog knockout mice show increased brown adipocyte recruitment in white adipose tissue and improved glucose homeostasis. Endocrinology. 2016;157(10):3873–3887.
33. Wu R, Liu X-M, Sun J-G, Chen H, Ma J, Dong M, Peng S, Wang J-Q, Ding J-Q, Li D-H, et al. Dj-1 maintains energy and glucose homeostasis by regulating the function of brown adipose tissue. Cell Discov. 2017;3:16054.
34. Ikeda K, Kang Q, Yoneshiro T, Camporez JP, Maki H, Homma M, Shinoda K, Chen Y, Lu X, Maretich P, et al. Ucp1-independent signaling involving serca2b-mediated calcium cycling regulates beige fat thermogenesis and systemic glucose homeostasis. Nat Med. 2017;23 (12):1454–1465.
35. Benador, I. Y., et al. mitochondria bound to lipid droplets have unique bioenergetics, composition, and dynamics that support lipid droplet expansion. Cell Metab. 2018;27(4): 869–885.e6.
36. van Den Berg R, Kooijman S, Noordam R, Ramkisoensing A, Abreu-Vieira G, Tambyrajah LL, Dijk W, Ruppert P, Mol IM, Kramar B, et al. A diurnal rhythm in brown adipose tissue causes rapid clearance and combustion of plasma lipids at wakening. Cell Rep. 2018;22(13):3521–3533.
37. He, C., et al. Nanosims imaging reveals unexpected heterogeneity in nutrient uptake by brown adipocytes. Biochem Biophys Res Commun. 2018;504:899–902.
38. Symonds ME, Aldiss P, Pope M, Budge H. Recent advances in our understanding of brown and beige adipose tissue: the good fat that keeps you healthy. F1000Res. 2018;7.
39. Blondin DP, Labbé SM, Noll C, Kunach M, Phoenix S, Guérin B, Turcotte ÉE, Haman F, Richard D, Carpentier AC. Selective impairment of glucose but not fatty acid or oxidative metabolism in brown adipose tissue of subjects with type 2 diabetes. Diabetes. 2015;64(7):2388–2397.
40. Gerich JE. Role of the kidney in normal glucose homeostasis and in the hyperglycaemia of diabetes mellitus: therapeutic implications. Diabet Med. 2010;27(2):136–142.